

USE OF BIOFUNCTIONAL HYDROGEL MATRICES FOR CHONDROCYTE TRANSPLANTATION APPLICATIONS

by

Balaji V. Sridhar

B.S., Massachusetts Institute of Technology, 2009

A thesis submitted to the

Faculty of the Graduate School of the

University of Colorado in partial fulfillment

of the requirement for the degree of

Doctor of Philosophy

Department of Chemical and Biological Engineering

2015

This thesis entitled:

Use of Biofunctional Hydrogel Matrices for Chondrocyte Transplantation Applications

written by Balaji V. Sridhar

has been approved for the Department of Chemical and Biological Engineering

Kristi S. Anseth, Ph.D.

Stephanie J. Bryant, Ph.D.

Date: _____

The final copy of this thesis has been examined by the signatories, and we find that both the content and the form meet acceptable presentation standards of scholarly work in the above mentioned discipline.

ABSTRACT

Sridhar, Balaji V. (Ph.D., Chemical and Biological Engineering)

Use of Biofunctional Hydrogel Matrices for Chondrocyte Transplantation Applications

Thesis directed by Professor Kristi S. Anseth

Healing joint articular cartilage is a significant clinical challenge because it lacks self-healing properties. Focal defects that do not heal properly tend to progress to debilitating osteoarthritis that affects millions of people worldwide. Tissue engineering strategies that utilize biofunctional scaffolds as chondrocyte carriers present a promising treatment option to regenerate cartilage tissue. Autologous chondrocytes are a good cell source since they regulate cartilage extracellular matrix (ECM) production in the tissue. Cells can be combined with photopolymerizable scaffolds, which permit control over network formation and can be modified to present biological cues. Current treatment options for cartilage regeneration have generally yielded unsatisfactory long-term results, thus making it necessary to engineer alternate methods that could easily stimulate chondrocyte ECM production and potentially be used to heal joint defects.

In this thesis, we present the development of biofunctional scaffolds that promote cartilage ECM deposition for potential use as cartilage implants. Initial work focused on presenting TGF- β 1 in a local and persistent manner to encapsulated chondrocytes by tethering the growth factor into the scaffold network. Results revealed that this method of growth factor delivery enhances tissue production over 28 days; however, since the scaffold was non-

degradable, the matrix was limited to the pericellular space. Subsequent work focused on the development of an enzymatically-sensitive peptide-linked scaffold that continued to provide a local growth factor signal, but was also cellularly degradable. We found that cell-mediated degradation permitted wide-spread matrix production and increased the bulk mechanical properties of constructs over 14 days. In this particular system, we needed to utilize mesenchymal stem cells (MSCs) to assist the chondrocytes in degrading the scaffold, which motivated the development of a full-length protein-linked scaffold that could locally degrade readily in response to chondrocyte-mediated enzymes. We crosslinked gelatin with a synthetic linker using a photopolymerization reaction and found that this hybrid scaffold promotes increased cellularity of chondrocytes as well as permits wide-spread cartilage ECM via cell-mediated degradation. In summary, this thesis demonstrated that a biofunctional scaffold for cartilage engineering applications should present promotive cues to encapsulated chondrocytes as well as locally degrade in response to cells to facilitate tissue generation.

DEDICATION

To my parents V.A. & Hema Sridhar and my brother Ananth Sridhar for continually supporting me and being the best family I could ask for. Also to my friends who have stayed by my side through both the good and bad times and believing in me.

ACKNOWLEDGEMENTS

Graduate school has been an amazing experience that I will cherish forever. I have gained valuable insights that will help me in my future endeavors as a clinician, researcher, and an entrepreneur. First and foremost, I would like to thank Prof. Kristi Anseth for her mentorship and for believing in me. I came into her lab with the goal of utilizing polymer scaffolds to regenerate cartilage tissue since my father had sports-related cartilage deterioration in both of his knees. Although no one else in the lab was working on cartilage regeneration when I entered, she was able to tap into her amazing network and rekindle a scientific collaboration with Mark Randolph of Massachusetts General Hospital, so that I could pursue this specific project. I am grateful that she was able to arrange this for me since it made me extra motivated to develop strategies to attack this problem. I have become a better at generating hypotheses, creating experiments to test them, writing, and presenting my work more clearly because of her guidance. I am extremely grateful and I know that I am lucky to have her as an advisor, mentor, and role model.

I would also like to thank Mark Randolph for collaborating with me. He has amazing insights into cartilage regeneration and sent me chondrocytes so that I could develop scaffolds for cartilage repair. His help and expertise pushed this project forward. I would also like to thank my committee members: Dr. Stephanie Bryant, Dr. Virginia Ferguson, Dr. John Kisiday, and Dr. Jeffrey Stansbury. The insight and expertise among these members is immense and their feedback on my thesis project was extremely valuable to my development as a scientist. Furthermore, I would like to thank my undergraduate research advisor, Prof. Robert Langer of MIT for recommending that I join Professor Anseth's lab in my home state of Colorado.

I am grateful for the funding sources that have supported my research efforts throughout graduate school at the University of Colorado. These include grants from the Department of Defense (W81XWH-10-1-0791) and the National Institutes of Health (R01 DE016523-10) as well as funding from the Howard Hughes Medical Institute.

Moreover, I would like to thank the University of Colorado Medical Scientist Training Program for giving me the opportunity to pursue my Ph.D. in chemical and biological engineering in Boulder. I would like to thank Dr. Arthur Gutierrez-Hartmann for his mentorship and guidance through both medical school classes as well as the Ph.D. portion. I would also like to thank Dr. Angie Ribera and Jodi Cropper for their support during my studies at the University of Colorado. I am grateful that I have the opportunity to be both a physician and a scientist with this program.

I would not have been able to accomplish research in the lab without the help of a very supportive and collaborative environment in the department of chemical engineering. Former members of the Bryant lab, particularly Drs. Justine Roberts and Stacey Skaalure were very helpful with experimental design since they had experience with working on cartilage regeneration. I would also like to thank members of the Anseth lab including Dr. Josh McCall for his initial help with the TGF- β studies, Dr. Sharon Wang for her expertise on navigating graduate studies, Dr. Malar Azagarsamy for his help with chemical synthesis and interpretation of NMR, Dr. William Wan for his help with statistical analysis, Prof. Jennifer Leight, Dr. Emi Tokuda, Dr. Kyle Kyburz, Dr. Chun Yang, Prof. Daniel Alge, and Dr. Eric Dailing for his help with the GPC studies. Catherine Chierotti was helpful along the way, ordering many materials and dealing with journal publishing payments. Additionally, I would like to thank Dr. Magnus Ølderoy from the Brinchmann lab in Norway who performed second harmonic generation microscopy on some

of the samples. My lab work was also made more successful and fulfilling with the contributions of several students (both undergraduate and graduate) that I had the privilege to mentor, which include Nicholas Doyle, Jason Silver, and Logan Brock. Their positive attitude, willingness to learn, and variety of personalities were a pleasure to be around and work alongside!

Last, but not least, I would like to thank my family and friends who supported me through graduate school. My parents made sure that I was well-fed with healthy food every week, and would call every day to make sure I was on track. I truly appreciate their support. I would also like to thank my friends who play squash, basketball, and lift with me. They would work out with me every day and in doing so, they helped me relax so that I could stay focused on the thesis project when I came into work. I could not have finished this Ph.D. without the help and support of my friends and family.

TABLE OF CONTENTS

CHAPTER I - INTRODUCTION AND BACKGROUND.....	1
1.1. Cartilage Tissue: Its Cellularity, Composition, and the Effects of Growth Factors....	1
1.1.1. Development of cartilage tissue.....	2
1.1.2. Cartilage cells.....	2
1.1.3. Cartilage matrix.....	4
1.1.4. Matrix metabolism.....	9
1.1.5. Effects of growth factors.....	14
1.2. Etiology of Cartilage Damage.....	16
1.3. Current Treatment Options for Cartilage Lesions.....	17
1.3.1. Conservative treatment of defects.....	18
1.3.2. Operative treatment options.....	19
1.3.3. Acellular scaffold therapies.....	20
1.3.4. Cell-only based therapies.....	21
1.4. Cartilage Tissue Engineering Approach.....	22
1.4.1. Cell source.....	23
1.4.2. Biomaterial scaffolds.....	26

1.4.2.1. Natural materials.....	27
1.4.2.2. Synthetic biomaterials.....	28
1.4.2.3. Synthetic-natural material hybrid scaffolds.....	32
1.4.3. Bioactive factors and their incorporation.....	33
1.5. Current Challenges in Cartilage Tissue Engineering.....	35
1.6. Research Summary.....	37
1.7. References.....	38
CHAPTER II – OBJECTIVES.....	54
2.1. Overview.....	54
2.2. Aim 1: Determine the effect of covalently tethered TGF- β 1 on chondrocyte proliferation and ECM production in non-degradable PEG hydrogels.....	55
2.3. Aim 2: Develop a cellularly degradable PEG hydrogel with tethered growth factor to promote articular cartilage extracellular matrix deposition.....	56
2.4. Aim 3: Develop and investigate use of a PEG-gelatin hybrid gel as a scaffold for cartilage engineering.....	57
2.5. References.....	59
CHAPTER III – COVALENTLY TETHERED TGF- β 1 WITH ENCAPSULATED CHONDROCYTES IN A PEG HYDROGEL SYSTEM ENHANCES EXTRACELLULAR MATRIX PRODUCTION.....	62
3.1. Abstract.....	62
3.2. Introduction.....	63
3.3. Materials and Methods.....	65
3.3.1. PEG monomer synthesis.....	65

3.3.2. Cell harvest and expansion.....	66
3.3.3. PEG hydrogel polymerization and growth factor incorporation.....	66
3.3.4. Quantifying growth factor incorporation.....	68
3.3.5. TGF- β 1 bioactivity and cellular signaling.....	69
3.3.6. Chondrocyte encapsulation in PEG thiol-ene hydrogels.....	69
3.3.7. Biochemical analysis of cell-hydrogel constructs.....	70
3.3.8. Histological and immunohistochemical analysis.....	70
3.3.9. Statistical analyses.....	71
3.4. Results.....	71
3.4.1. Distribution of thiolated TGF- β 1 in PEG hydrogels.....	71
3.4.2. Bioactivity and concentration of tethered TGF- β 1 in 3D culture.....	72
3.4.3. Proliferation of chondrocytes exposed to TGF- β 1.....	74
3.4.4. Matrix deposition as a function of TGF- β 1 presentation and culture time..	76
3.4.5. Matrix organization.....	77
3.5. Discussion.....	80
3.6. Conclusion.....	83
3.7. Acknowledgements.....	83
3.8. Supplementary Figures.....	84
3.9. References.....	85
 CHAPTER IV – DEVELOPMENT OF A CELLULARLY DEGRADABLE PEG HYDROGEL TO PROMOTE ARTICULAR CARTILAGE EXTRACELLULAR MATRIX DEPOSITION..	
4.1. Abstract.....	89
4.2. Introduction.....	90
4.3. Results.....	93

4.3.1. Chondrocyte cleavage of MMP-degradable sequences in 3D monoculture.....	93
4.3.2. Utilization of co-culture to aid in degradation of the MMP-sensitive sequence.....	95
4.3.3. Viability of cells and morphology of MSCs in co-culture scaffolds.....	97
4.3.4. Effect of local degradation on cartilage-specific matrix production and distribution.....	98
4.3.5. Effect of cell-mediated degradation on the mechanical properties of the scaffold.....	101
4.3.6. Quality of composition of ECM in co-culture scaffolds.....	103
4.3.7. Effect of inhibition of MMP activity on cartilage-specific matrix production and distribution.....	105
4.4. Discussion.....	105
4.5. Conclusion.....	109
4.6. Experimental Section	109
4.6.1. PEG monomer synthesis.....	109
4.6.2. Cell harvest and expansion.....	110
4.6.3. Hydrogel formation and cell encapsulation.....	111
4.6.4. In situ confirmation of MMP cleavage in a 3D environment.....	112
4.6.5. Wet weight, compressive modulus, and biochemical analysis.....	113
4.6.6. Histology and immunofluorescent analysis.....	114
4.6.7. Statistical Analysis.....	115
4.7. Acknowledgements.....	115
4.8. Supplementary Figures.....	115
4.9. References.....	119
CHAPTER V – A BIOSYNTHETIC SCAFFOLD THAT FACILITATES CHONDROCYTE-MEDIATED DEGRADATION AND PROMOTES ARTICULAR CARTILAGE EXTRACELLULAR MATRIX DEPOSITION.....	125
5.1. Abstract.....	125
5.2. Introduction.....	126

5.3. Materials and Methods.....	129
5.3.1. Functionalization of gelatin with norbornene.....	129
5.3.2. Characterization of degradation of functionalized gelatin.....	130
5.3.3. PEG-Gelatin network formation and mechanical measurements.....	130
5.3.4. Cell harvest and expansion.....	131
5.3.5. Chondrocyte encapsulation and viability assessment.....	132
5.3.6. Biochemical assays of cell-hydrogel constructs.....	132
5.3.7. Histology and immunofluorescence analysis.....	132
5.3.8. Statistical analysis.....	133
5.4. Results.....	134
5.4.1. Modifying PEG-gelatin network properties.....	134
5.4.2. Verification of degradation of modified gelatin by chondrocyte-secreted enzymes.....	137
5.4.3. Chondrocyte viability, cellularity, and morphology.....	138
5.4.4. ECM production and deposition in scaffolds.....	140
5.4.5. Quality of collagen generated by chondrocytes in the scaffold.....	143
5.5. Discussion.....	144
5.6. Conclusion.....	147
5.7. Acknowledgments.....	148
5.8. Supplementary Figures.....	149
5.7. References.....	151
CHAPTER VI – CONCLUSIONS AND RECOMMENDATIONS.....	156
6.1. Conclusions.....	156
6.2. Recommendations.....	161

6.2.1. Alternate methods to design scaffolds that locally degrade in response to chondrocyte-secreted enzymes.....	162
6.2.2. Use of a covalently adaptable network as a biofunctional scaffold for cartilage tissue engineering.....	164
6.2.3. Alternate cell sources for cartilage tissue engineering.....	165
6.2.4. In vivo studies with hydrogel matrices.....	166
6.3. References.....	167
CHAPTER VII – REFERENCES.....	172
7.1. CHAPTER I.....	172
7.2. CHAPTER II.....	187
7.3. CHAPTER III.....	189
7.4. CHAPTER IV.....	192
7.5. CHAPTER V.....	197
7.6. CHAPTER VI.....	201

LIST OF TABLES

Table 1.1. Extracellular matrix (ECM) composition of human cartilage tissue.....	5
Table 1.2. Collagen composition of human articular cartilage.....	8
Table 1.3. Common MMPs and TIMPs found in cartilage.....	12
Table 4.1. Percentage of cells that stain positive for type I or type II collagen in gels at day 14.....	103
Table 5.1. Material properties of acellular hybrid scaffolds (n=5).....	136

LIST OF FIGURES

Figure 1.1. Masson's trichrome stain of porcine articular cartilage to reveal collagen distribution. Lacunae are cavities in the tissue from which isogenous groups consisting of primary chondrocyte cells produce cartilage tissue. Nuclei are stained violet and collagen is stained blue. Scale bar represents 100 μm4

Figure 1.2. Schematic of cartilage ECM and aggrecan a) Cartilage ECM with predominant type II collagen fibers (green) intertwined by aggrecan molecules (black) that attach to hyaluronic acid (blue) by link proteins (yellow). This network of macromolecules works together to help retain water in the tissue to give cartilage robust mechanical properties. b) Aggrecan is a high molecular weight molecule that contains highly branched, negatively charged chondroitin sulfate and keratan sulfate molecules. Aggrecan helps retain water in the cartilage ECM with its predominantly negative charge.....10

Figure 1.3. Schematic of the breakdown of type II collagen. Type II collagen contains three $\alpha 1$ chains and is initially cleaved by collagenase MMPs (-1,-8,-13) at physiologic conditions. After cleavage of the fiber, neoepitopes (red dots) like C1,2C and C2C are revealed. Furthermore, the collagen degradation by-products, in excess, can upregulate collagenase expression, while TIMPs can repress its production. Image modified from http://www.ibex.ca/DX_C12C.htm.....14

Figure 1.4. Schematic of TGF- β signaling to chondrocyte. First convertases cleave the precursor latency associated peptide (LAP) so that TGF- β can be activated and bind to the dimer receptor found on the chondrocyte (yellow) membrane. The binding event initiates phosphorylation (red circle) of Smad. The phosphorylated Smad complex enters the nucleus (grey), and influences transcription to increase chondrocyte ECM production and proliferation.....16

Figure 1.5. Schematic for MACT in which autologous chondrocytes are isolated from non-weight bearing portions of the knee and expanded *in vitro*. The cells are encapsulated in a biomaterial scaffold (either synthetic or natural) and then directly injected into the defect site wherein the cell-laden scaffold can be polymerized by a variety of schemes including a photoinitiation reaction to mold the gel to fill the defect site.24

Figure 1.6. Thiol Norbornene Photopolymerization (A) Mechanism of thiol-ene polymerization. An initiator abstracts a hydrogen atom from a thiol group, the resulting thiyl radical propagates across the norbornene double bond and the resulting norbornene radical abstracts a hydrogen atom from another thiol completing the bond formation and regenerating a thiyl radical. Image modified from Fairbanks, B. D. *et al.* A Versatile Synthetic Extracellular Matrix Mimic via Thiol-Norbornene Photopolymerization. *Adv. Mater.* (B) Example of step-growth photopolymerization between multi-arm PEG-norbornene and a dithiol linker. Light-activated initiation results in the formation of homogeneous networks.....30

Scheme 3.1. Pre-polymerization scheme with thiolated TGF- β 1. Initially thiolated TGF- β 1 is phototethered into the 8-arm 10 kDa PEG norbor-nene network, then the 3.5 kDa dithiol crosslinker is added in with chondrocytes to complete the encapsulation process. Growth factor is not drawn to scale. In featured experiments, there is a lower amount of growth factor attached to the monomer end. Chondrocytes seeded at 40 million cells/mL retain a rounded morphology similar to cells in native tissue. Scale bar represents 50 μ m.....67

Figure 3.1. TGF- β 1 is homogenously distributed throughout the PEG hydrogel. Section ELISA of tethered gels without cells show detection of TGF- β at similar levels to theoretical values with graphic on top depicting slice areas. Each section ~20 mm thickness. Theoretical values indicated by dashed lines (0.1 ng for 10 nM, 0.5 ng for 50 nM, and 0.9 ng for 90 nM gels). 0 nM value is subtracted out of all conditions. Results are presented as mean activity \pm SD (n=2). Solid lines indicate p values with one way ANOVA analysis to confirm sections of each gel are not statistically different from each other.....72

Figure 3.2. Determining TGF- β 1 concentration that yields maximal response. (a) PE-25s were encapsulated at 40 million cells/mL with varying concentrations of tethered TGF- β and 50 nM yielded a maximal response. * indicates statistically significant difference between 50 nM and the other concentrations with $p < 0.001$. Results are presented as mean activity \pm SD (n=4). (b) PE-25 cells encapsulated at 40 million cells/mL were transiently exposed to varying concentrations of TGF- β in the media. The 0.3 nM output is higher on average than the other concentrations. Results are presented as mean activity \pm SD (n=4).....74

Figure 3.3. Increased proliferation of chondrocytes exposed to TGF- β 1. (a) Live/dead staining of 50 nM gels seeded at 40 million cells/mL on day 1 and day 28 shows chondrocytes retain a spherical morphology, have high viability, and increase in number. Scale bars represent 50 μ m. (b) DNA content of chondrocytes encapsulated at 40 million cells/ mL that were exposed to 0 nM, 0.3 nM which was delivered through the media, or 50 nM which was tethered into the gel. Over a 28-day period, the cells in the 50 nM condition show a steady rate of increase of DNA content.+ indicates significant difference between the 0.3 nM and 0 nM case ($p < 0.001$), ++ indicates significant difference between 50 nM and 0 nM case ($p < 0.001$), * indicates significant difference between 0.3 nM and 0 nM($p < 0.001$), ** indicates significant difference between 50 nM and 0.3 nM case at day 28 ($p < 0.001$), and *** indicates significant difference between 50 nM and 0 nM for day 28 ($p < 0.001$). Results are presented as mean \pm SD (n=3).....76

Figure 3.4. Enhanced matrix production of encapsulated chondrocytes exposed to TGF- β . (a) GAG production was normalized per cell. * indicates significant difference between 50 nM and 0.3 nM condition at day 28 ($p < 0.05$), ** indicates significant difference between 50 nM and 0

nM at day 28 ($p < 0.001$). Data presented as mean \pm SD ($n=3$). (b) Collagen production was normalized per cell. + indicates significant difference between 50 nM and 0.3 nM at day 28 ($p < 0.01$) and ++ indicates significant difference between 50 nM and 0 nM at day 28 ($p < 0.001$). Data presented as mean \pm SD ($n=3$).....77

Figure 3.5. Matrix protein distribution in gels. At day 28, gels seeded with chondrocytes at 40 million cells/mL were sectioned and stained for matrix distribution. (a) 0 nM gel stained for collagen, (b) 0 nM gel stained for GAG, (c) 0.3 nM (soluble) gel stained for collagen, (d) 0.3 nM (soluble) gel stained for GAG, (e) 50 nM (tethered) gel stained for collagen, (f) 50 nM (tethered) gel stained for GAG. Blue indicates collagen and red indicates GAG. Scale bars represent 100 μ m.....78

Figure 3.6. Collagen I versus collagen II distribution in constructs. Gels seeded with chondrocytes at 40 million cells/mL were cryosectioned at day 28. Immunohistochemistry analysis reveals collagen type distribution in scaffolds. (a) 0 nM with collagen I, (b) 0 nM with collagen II, (c) 0.3 nM (soluble) with collagen I, (d) 0.3 nM (soluble) with collagen II, (e) 50 nM (tethered) with collagen I, (f) 50 nM (tethered) with collagen II. Sections were stained red for both anti-collagen I and anti-collagen II antibodies and were counterstained with DAPI (blue) for cell nuclei. Scale bars represent 50 μ m.....79

Figure 3.S1. (a) Type I collagen immune staining of porcine meniscus (b) Type II collagen staining of porcine hyaline articular cartilage. Sections were stained red for both anti-collagen I and anti-collagen II antibodies and were counterstained with DAPI (blue) for cell nuclei. Scale bars represent 50 μ m.....84

Figure 4.1. Effect of chondrocytes encapsulated in an MMP-degradable gel. (a) Schematic of 4-arm 20 kDa PEG norbornene network with tethered MMP fluorescent sensor (Dab-GGPQG↓IWGQK-FI-AhxC), and TGF- β 1. The macromer solution, containing tethered peptides, is combined with chondrocytes at 40 million cells/mL. Resultant networks are either crosslinked by an MMP-degradable peptide sequence (KCGPQG↓IWGQCK) or non-degradable (3.5 kDa PEG dithiol) linker for *in situ* cleavage experiments. (b) Measurement of *in situ* cleavage of fluorescent sensor by chondrocytes. Over 3 days, acellular and chondrocyte-laden non-degradable gels had similar normalized fluorescent activity, but in a degradable gel, chondrocytes had higher fluorescent activity (where A.U. stands for arbitrary units) suggesting cleavage of the sequence. Results are presented as mean \pm SD ($n=3$). (c) GAG staining of sections obtained at day 28 with chondrocytes seeded in degradable gels at 40 million cells/mL with nuclei stained black and GAGs stained red. (d) Collagen staining of sections obtained at day 28 with chondrocytes seeded in degradable gels at 40 million cell/mL with nuclei stained black and collagen stained blue. Scale bars represent 100 μ m.....94

Figure 4.2. Effect of co-culture of chondrocytes and MSCs on degradation of MMP-sensitive sequence. (a) Schematic of 4-arm 20 kDa PEG norbornene network with tethered TGF- β 1, RGD, and MMP fluorescent sensor (Dab-GGPQG↓IWGQK-FI-AhxC) crosslinked by an MMP degradable peptide sequence (KCGPQG↓IWGQCK). Chondrocytes were encapsulated at a fixed seeding density of 40 million cell/mL, and the density of MSCs varied from 1.7 to 5 million cells/ mL during the co-encapsulation process for *in situ* cleavage experiments to measure the effect of co-culture on local degradation. (b) After 3 days, chondrocytes, at 40 million cells/mL, have a lower fluorescent signal than MSCs, at 5 million cells/mL, in degradable gels. Fluorescent signal is highest from day 1 to 3 when cells are co-encapsulated at a ratio of 24:1 chondrocytes: MSCs (40×10^6 chondrocytes/mL + 1.67×10^6 MSCs/mL). (c) By varying the ratio of chondrocytes to MSCs, and keeping the chondrocyte seeding density constant at 40 million cells/mL, it was found after 3 days, 8:1 yielded the highest amount of degradation out of the tested conditions and was used for subsequent matrix deposition experiments. The MMP activity of each group is significantly different from each other at each timepoint ($p < 0.05$) with the 8:1 condition generating the highest MMP activity. Results are presented as mean \pm SD ($n=3$).....96

Figure 4.3. Viability, morphology and cellularity of co-culture system. (a) Viability at day 1 with degradable 8:1 co-culture gels with live cells (gray), dead cells (red), MSCs labeled with CellTracker™ Violet (blue), and all 3 images merged together. Viability was quantified at $93 \pm 3\%$. Scale bars represent 100 μ m. (b) DNA content of degradable and non-degradable 8:1 co-culture gels assessed at day 1, 7, and 14. Both degradable and non-degradable conditions show similar DNA content at each time point, but they increase over the 14 day period. Results are presented as mean \pm SD ($n=3$).....98

Figure 4.4. Glycosaminoglycan distribution and production in non-degradable and degradable 8:1 co-culture constructs. (a) Non-degradable gel section stained for GAGs at day 14. (b) Degradable gel stained for GAGs at day 14 with nuclei stained black and GAGs stained red. Scale bars represent 100 μ m. (c) GAG content expressed as a percentage of the respective construct wet weight assessed at day 1, 7, and 14. * indicates a statistically significant difference in GAG content at day 7 between degradable and non-degradable gels ($p < 0.01$), and ** indicates a statistically significant difference in GAG content at day 14 between degradable and non-degradable gels ($p < 0.001$). Results are presented as mean \pm SD ($n=3$).....100

Figure 4.5. Collagen distribution, production, and scaffold compressive modulus in non-degradable and degradable 8:1 co-culture constructs. (a) Non-degradable gel section stained for collagen at day 14. (b) Degradable gel stained for collagen at day 14 with nuclei stained black or violet and collagen stained blue. Scale bars represent 100 μ m. (c) Total collagen content expressed as a percentage of the respective construct wet weight assessed at day 1, 7, and 14. + indicates a statistically significant difference in collagen content at day 7 between degradable and non-degradable gels ($p < 0.05$), and ++ indicates a statistically significant difference in

collagen content at day 14 between degradable and non-degradable gels ($p < 0.001$). Results are presented as mean \pm SD ($n=3$).....101

Figure 4.6. Compressive modulus of constructs assessed at day 1, 7, and 14. # indicates a statistically significant difference in modulus value at day 7 between degradable and non-degradable gels ($p < 0.05$) and ## indicates a statistically significant difference in modulus value at day 14 between degradable and non-degradable gels ($p < 0.001$). The line with ### indicates a statistically significant difference between day 1 and day 14 in moduli values for degradable gels only ($p < 0.001$). Results are presented as mean \pm SD ($n=3$).....102

Figure 4.7. Type I collagen vs. type II collagen distribution assessed by immunofluorescence in non-degradable and degradable 8:1 co-culture constructs. (a) Non-degradable gel section stained for type I collagen at day 14, (b) non-degradable gel section stained for type II collagen at day 14, (c) degradable gel section stained for type I collagen at day 14, (d) degradable gel stained for type II collagen at day 14. Sections were stained for both anti-collagen type I and anti-collagen type II antibodies (red) and were counterstained with DAPI (blue) for cell nuclei. Scale bars represent 50 μm104

Figure 4.S1. Effect of MMP inhibitor on degradable 8:1 co-culture construct ECM production. (a) Evaluation of MMP cleavage rate reveals that the addition of MMP inhibitor (100 μM) to co-culture gel media decreases the degradation rate of the degradable gel to a similar fluorescent signal as non-degradable and acellular constructs at day 3. Unadulterated co-culture gels continue to degrade the sequence at a high level. Results are presented as mean \pm SD ($n=3$). (b) GAG distribution in degradable gel sections treated with MMP inhibitor at day 14 with nuclei stained black and GAGs stained red. (c) Collagen distribution in degradable gel sections treated with MMP inhibitor at day 14 with nuclei stained black and collagen stained blue. Scale bars represent 100 μm116

Figure 4.S2. Early culture time points for matrix deposition of chondrocytes in degradable systems. (a) GAG distribution in degradable gel sections with chondrocytes seeded at 40 million cells/mL at day 7 with nuclei stained black and GAGS stained red. (b) Collagen distribution in degradable gel sections with chondrocytes seeded at 40 million cells/mL at day 7 with nuclei stained black and collagen stained blue. Scale bars represent 100 μm117

Figure 4.S3. Live/dead stain of an 8:1 co-culture degradable gel at day 14 with live cells (green), and dead cells (red). Non-degradable viability results are similar. Cells maintain $96 \pm 2\%$ viability in the degradable gel at day 14 ($n=3$). Scale bars represent 100 μm117

Figure 4.S4. Gel total content as a function of time. (a) Wet weight values shown for non-degradable and degradable 8:1 co-culture constructs at day 1, 7, and 14. Results are presented as mean \pm SD (n=3). (b) GAG content per gel at day 1, 7, and 14 for degradable and non-degradable constructs. (c) Total collagen content at day 1, 7, and 14 for degradable and non-degradable constructs. Results are presented as mean \pm SD (n=3).....118

Figure 4.S5. ECM staining of native tissue.(a) Type I collagen (red) distribution in porcine meniscus with cell nuclei counterstained with DAPI (blue) as a positive control to confirm the antibody is working as expected. Scale bars represent 50 μ m. (b) Type II collagen (red) distribution in porcine articular cartilage with cell nuclei counterstained with DAPI (blue) as a positive control to confirm the antibody is working as expected. Scale bars represent 50 μ m. (c) GAG (red) distribution in porcine articular cartilage with cell nuclei stained black or violet. Scale bars represent 100 μ m. (d) Collagen (blue) distribution in porcine meniscus with cell nuclei stained violet or black. Scale bars represent 100 μ m.....119

Figure 5.1. Gelatin functionalization with norbornene and photopolymerization with PEG. a) Depiction of the reaction of gelatin with varying molar amounts of norbornene succinimidyl ester. The reaction proceeded for 1 h at 37°C and the amount of functionalization on the product was measured by TNBSA. The estimated amount of norbornenes per gelatin molecule is shown below based on functionalization efficiency calculations. b) Photopolymerization scheme between 2 wt% norbornene-functionalized gelatin with varying amounts of norbornene [1.1-4.5 mM] and 0.1 wt% 3.5 kDa PEG dithiol with [0.6 mM] thiol to form a covalently-crosslinked hybrid scaffold.....135

Figure 5.2. GPC chromatogram of gelatin functionalized with norbornene at 1:1 NB:gelatin amine that is either untreated (A), treated with 20 U/mL collagenase for 1 h at 37°C (B) or treated with day 3 chondrocyte-conditioned media for 1 h at 37°C (C). The untreated gelatin peak that is found at 18 min elution disappears after treatment with either collagenase or chondrocyte-conditioned media suggesting degradation of gelatin to smaller byproducts by the enzymes.....138

Figure 5.3. Viability, morphology, and cellularity of 1:1 NB:gelatin amine hybrid scaffold. a) Live(green)/dead (red) stains of encapsulated chondrocytes. Viability is calculated to be greater than 95% at all the time points. Insets highlight single cells changing in morphology from rounded to more spread over time. Scale bars represent 50 μ m. b) Degree of circularity between 0 (not rounded) and 1(rounded) of the encapsulated cells. # with a line indicates a statistically significant difference in circularity value between day 1 and day 7 (p=0.02). Results are presented as mean \pm SD (n=3). c) DNA content (μ g/gel) as measured by Picogreen assay over 14 days. * with a line indicates a statistically significant difference between day 1 and day 14 in DNA content (p=0.01). Results are presented as mean \pm SD (n=3).....140

Figure 5.4. Glycosaminoglycan distribution and production in a 1:1 NB:gelatin amine hybrid scaffold. a) Section with encapsulated chondrocytes at day 14 stained for GAGs with nuclei stained black and GAGs stained red. b) Acellular section stained for GAGs at day 14. Scale bars represent 100 μ m. c) Total GAG content expressed as a percentage of the respective construct wet weight assessed at day 1, 7, and 14. + with a line indicates a statistically significant difference in GAG content between day 1 and day 14 ($p=0.0004$), and ++ with a line indicates a statistically significant difference in GAG content between day 7 and day 14 ($p=0.001$). Results are presented as mean \pm SD ($n=3$).....142

Figure 5.5. Collagen and ECM distribution in a 1:1 NB:gelatin amine hybrid scaffold. a) Section with encapsulated chondrocytes at day 14 stained for collagen with nuclei stained violet and collagen stained blue. b) Acellular section stained for collagen at day 14. Scale bars represent 100 μ m. c) Gross image of a transparent acellular scaffold at day 1. d) Gross image of a translucent scaffold with encapsulated chondrocytes at day 1. e) Gross image of an opaque scaffold with encapsulated chondrocytes at day 14 that has a cartilaginous appearance.....143

Figure 5.6. Type I collagen versus type II collagen distribution assessed by immunofluorescence in a 1:1 NB:gelatin amine hybrid construct with encapsulated chondrocytes at day 14. a) Gel section stained for type I collagen. b) Gel section stained for type II collagen. Sections were stained for both anti-collagen type I and anti-collagen type II antibodies (red) and were counterstained with DAPI (blue) for cell nuclei. Scale bars represent 50 μ m.....144

Figure 5.S1. Gel permeation chromatography chromatograms to assess degradation of gelatin functionalized with norbornene. a) GPC chromatogram of unmodified and gelatin functionalized with varying ratios of norbornene in buffer. b) Unmodified and functionalized gelatin treated with 20 U/mL collagenase type II for 1 h at 37°C with disappearance of peak found at 18 min. c) Unmodified and functionalized gelatin treated with chondrocyte-conditioned medium for 1 h at 37°C with disappearance of peak at 18 min.....149

Figure 5.S2. Staining of native tissue. a) Type I collagen (red) distribution in porcine meniscus with cell nuclei counterstained with DAPI (blue) as a positive control to confirm the antibody is working as expected. Scale bar represents 50 μ m. b) Type II collagen (red) distribution in porcine articular cartilage with cell nuclei counterstained with DAPI (blue) as a positive control to confirm the antibody is working as expected. Scale bar represents 50 μ m. c) GAG (red) distribution in porcine articular cartilage with cell nuclei stained black and GAGs stained red. Scale bar represents 100 μ m. d) Collagen (blue) distribution in porcine cartilage with cell nuclei stained violet and collagen stained blue. Scale bar represents 100 μ m.....150

Figure 5.S3. a) Wet weight values (g) shown for 1:1 NB: gelatin amine hybrid scaffold collected at day 1,7, and 14. Results are presented as mean \pm SD (n=3). b) GAG content per gel (μ g) at day 1, 7, and 14 for constructs with encapsulated chondrocytes. Results are presented as mean \pm SD (n=3).....150

Figure 6.1. Second harmonic generation signal of collagen generated from chondrocytes encapsulated in a covalently adaptable network (15:9 HZ:ALD) after 49 days of culture. This data suggests that covalently adaptable scaffolds could be used to help promote functional tissue production from cells in lieu of cellularly degradable constructs. Blue represents cell nuclei and white fibers represent organized collagen fibers. Scale bar is 10 μ m. Image courtesy of Dr. Magnus Ølderoy.....165

CHAPTER I

INTRODUCTION AND BACKGROUND

1.1. Cartilage Tissue: Its Cellularity, Composition, and the Effects of Growth Factors

Hyaline articular cartilage is present on the surface of articulating joints such as the knee, hip, and shoulder. This tissue provides an elastic, load-bearing surface that increases contact area between bones, lubricates the joint space, and reduces friction during articulation.¹ One of the main functions of cartilage is to act as a cushion between the ends of bone to prevent pain and loss of mobility during joint movement and weight-bearing activities.² Cartilage is primarily composed of interstitial fluid and cross-linked extracellular matrix (ECM) molecules.³ The primary cells residing in cartilage are chondrocytes, specialized cells that produce and maintain the surrounding ECM that is composed of collagen, proteoglycans, and multi-adhesive glycoproteins.⁴ While chondrocytes are responsible for maintaining the structure of the tissue through regulating matrix molecules, there is a balance between anabolic (matrix-producing) and catabolic (matrix-destructive) processes in healthy tissue.⁵ Tissue homeostasis can be disrupted due to traumatic injuries and from constant wear and tear of the surface, which can eventually lead to the onset of pathologies like osteoarthritis and resultant destruction of cartilage.⁶ If cartilage tissue is unaltered and maintained in a healthy state, it shows no signs of wear over a lifetime.⁴ Unfortunately, cartilage is under constant stress in a human lifespan that oftentimes leads to tissue damage. The problem is exacerbated by the fact that cartilage has a very limited capacity for self-repair since it is an avascular tissue that lacks innervation, and thus does not have a supply of growth factors when they are needed.⁷ Because of its critical function and the fact that cartilage is currently difficult to repair, there is huge demand to treat symptomatic

cartilage lesions by an increasingly aging population afflicted by joint pain. The premise of this thesis is that in order to repair or regenerate damaged cartilage in patients, it is first helpful to understand the development, biochemical composition, and function of cartilage tissue when engineering a treatment option.

1.1.1. Development of cartilage tissue

During human embryogenesis, cartilage of the skeletal system is derived from the mesoderm germ layer of the embryo. At the end of the fourth week of development, progenitor cells aggregate to form a connective tissue called mesenchyme. Mesenchyme is comprised of mesenchymal cells which receive cues from the body in the form of gene signals in order to direct differentiation of these cells into bone-forming osteoblast or cartilage-forming chondrocytes; this process is called condensation.⁸ Cartilage development begins in the fifth week in which bone structure is laid out with the mesenchyme tissue as the scaffold. The mesenchyme contains mesenchymal stem cells (MSCs), which receive chemical cues from compounds like transforming growth factor β (TGF- β) or β -catenin in the canonical Wnt signaling pathway. MSCs differentiate to form primary cartilage cells, which eventually produce the matrix molecules that compromise cartilage tissue.⁹

1.1.2. Cartilage cells

The resident cells in articular cartilage are mainly of one type, and they are sparsely distributed relative to cells in other tissues of the body (e.g., muscle satellite cells account for 30-35% of muscle while chondrocytes only account for roughly 5% of cartilage).¹⁰ Chondrocytes are primary cells, and as a simplified description means that multipotent stem cells, in this case MSCs, differentiated into this cell type, and chondrocytes are limited to producing cartilage

tissue. Chondrocytes that occupy hyaline cartilage all have similar gene and protein expression levels, as well as surface markers and metabolism rates.¹¹ These cells are located within spaces of the hyaline tissue matrix, also known as lacunae, and occupy only 3-5% of the total tissue mass, and all matrix components in cartilage are synthesized by chondrocytes.¹² After development of the bone is complete, and the epiphyseal gap closes, chondrocytes lose their mitotic and metabolic activity, and degenerated cells are not replaced, which partly explains why cartilage has a low intrinsic healing capacity.¹³ Chondrocytes have a low metabolic activity, as they reside in a hypoxic environment, but this also renders them a more robust cell type that can withstand this somewhat supraphysiologic environments. For example, chondrocytes express high levels of hypoxia-inducible factor-1 (HIF-1), which regulates glycolytic enzymes and helps the cells generate ATP in a low-oxygen environment.¹⁴

Chondrocytes are sparsely populated within cartilage tissue, and are present either singularly or in clusters called isogenous groups. Figure 1.1. shows a typical histology section of cartilage tissue stained for collagen with Masson's Trichrome. Chondrocytes that are found in the less common isogenous groups have recently divided, and new cells produce and disperse ECM material. Cavities formed in the tissue from which isogenous groups produce cartilage tissue are known as lacunae. Cells in isogenous groups also secrete matrix metalloproteinase (MMP) enzymes that can degrade the surrounding cartilage matrix, thereby allowing cells to expand and reposition themselves within the tissue matrix.¹⁵ Chondrocytes receive nutrients and discard waste through joint movement, which permits diffusion of synovial (a viscous fluid found in the joint capsule) and interstitial fluid.¹⁶ These fluids are highly pressurized under normal cyclic mechanical loading, inducing fluid flow throughout the highly hydrated tissue.¹² In

brief summary, chondrocytes are integral to creating and maintaining joint function, especially the complex tissue matrix, which is described in the next section.

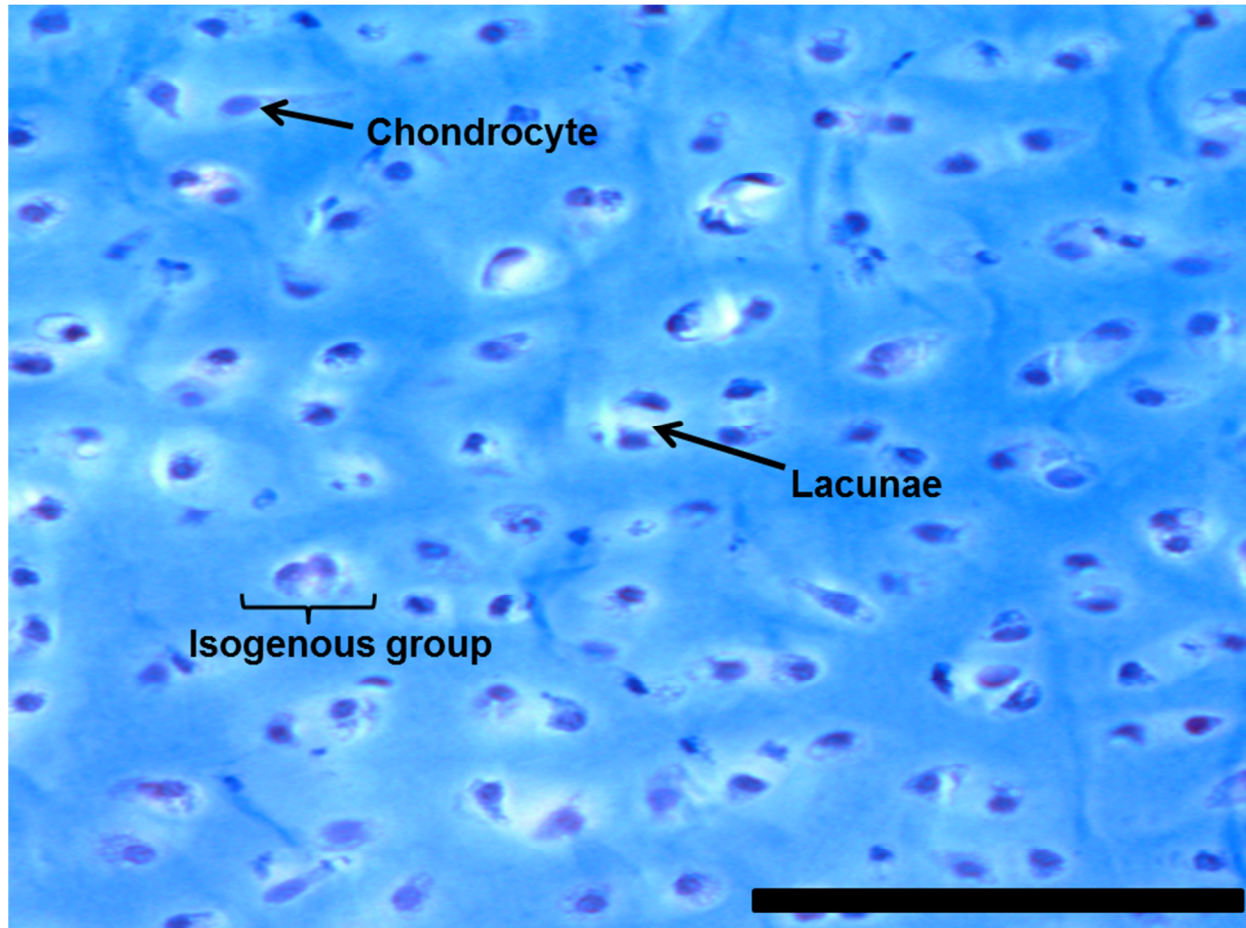


Figure 1.1. Masson's trichrome stain of porcine articular cartilage to reveal collagen distribution. Lacunae are cavities in the tissue from which isogenous groups consisting of primary chondrocyte cells produce cartilage tissue. Nuclei are stained violet and collagen is stained blue. Scale bar represents 100 μm .

1.1.3. Cartilage matrix

Chondrocytes are embedded in a matrix composed mainly of intercellular water. In mature articular cartilage, 65-85% of its composition is water. This interstitial fluid contains

various ions and salts such as sodium and potassium, which act to regulate osmotic pressure and dynamic loads placed on the tissue. Part of the reason that cartilage can withstand prolonged compressive loads, with a Young's modulus that ranges from 450-800 kPa,¹⁷ is because of the presence of this interstitial fluid.¹⁸

Table 1.1. Extracellular matrix (ECM) composition of human cartilage tissue	
<u>ECM component</u>	<u>Percentage of cartilage tissue (by weight)</u>
Interstitial Fluid	65-85%
Collagen	10-30%
Proteoglycans (aggrecan, decorin, biglycan)	3-10%
Noncollagenous glycoproteins (annexin V)	1-3%

References: Interstitial fluid,¹⁸ collagen,¹⁹ proteoglycans,²⁰ noncollagenous glycoproteins.²¹

In addition to water, the solid phase of cartilage is comprised of various types of collagen fibers, which can range from 10-30% of the cartilage wet weight depending on its zonal location with respect to the subchondral bone and joint surface. Proteoglycans make up 3-10% of the cartilage wet weight.¹⁹ The remaining extracellular matrix consists of proteins such as link protein, lubricin, cartilage oligomeric protein, and superficial zone protein as well as lipids, salts, and glycoproteins like decorin and biglycan, which facilitate attachment to chondrocytes.²⁰ The components are summarized in Table 1.1. Collagen fibers create an elastic meshwork that entraps proteoglycans and other large biomacromolecules in the tissue. The most common type of collagen found in cartilage is collagen type II, which accounts for 90-95% of the total collagen

content and imparts tensile strength to cartilage.²² Additionally, the most common proteoglycan, and hence other highly prevalent ECM macromolecule in cartilage, is aggrecan, which when aggregated, is indirectly responsible for maintaining compressive strength of cartilage.²³

Collagen fibers in cartilage tissue exhibit unique characteristics. These fibers provide the structural framework that is responsible for the tissue biomechanical properties, such as resistance to pressure, torsion, and tension.²⁴ In vertebrates, there are 27 genetically distinct collagen types with diverse structural and biochemical features that have been identified, but only about half of these isoforms are present in hyaline cartilage.^{25,26} Collagens indirectly regulate essential cell biological functions, including proliferation, cytoskeletal organization, differentiation and many others via transmembrane receptors of integrin and syndecan families.²⁷ A structural requirement for the assembly of polypeptide chains into a collagen triple helix is the occupation of every third position by a glycine residue, resulting in the (Gly-X-Y)_n repeat structure with X and Y being amino acids such as proline.²⁸ Sometimes, the prolines in the Y-position are converted to 4-hydroxyproline by the enzyme prolyl-4-hydroxylase.²⁹ This specific amino acid can be detected in a colorimetric assay to quantify the total collagen in tissue.³⁰ Collagens are synthesized as procollagen molecules that first align to form a cross-linked triple helix with the help of the enzyme lysyloxidase³¹ and are then cleaved and activated by specific proteinases after release from the cell.³² Variants of collagen molecules are similar in structure, but differ in gene sequences due to alternative splicing events, as well as polyadenylation at the 3' end of most collagen genes.³³

Type II collagen, the predominant form of collagen in articular cartilage, is a homotrimeric molecule composed of 3 poly-peptide α -chains or helices that crosslink with other type II collagen triple helices to form fibrils, which can be up to 400 nm in width.³⁴ Type II

collagen is integral in the development of cartilage; studies on mutations in the COL2A1 gene, which leads to downstream type II collagen fiber formation, can lead to cartilage malformation disorders like chondrodysplasia.³⁵ Compared to antibodies against other fibrillar collagens, the type II collagen antibody can cross-react between species relatively easily, indicating highly conserved epitopes.³⁶ The way that type II collagen fibrils are aligned in the tissue can play a major role in the macroscopic mechanical properties of cartilage. The alignment of fibers varies based upon which region of tissue the collagen resides. In the superficial zone of cartilage, a region that experiences the most mechanical stress since it is at the articulating surface, collagen II fibers are arranged parallel to each other in order to withstand constant compression.³⁷ Directional dependence of type II collagen fibers, also known as anisotropy, plays a huge role in the macroscopic mechanical properties of the tissue, and its signal can be found by a microscopy technique known as second harmonic generation.³⁸

In addition to type II collagen, there are other collagens that play important roles in maintaining cartilage structure and strength. Namely, types VI, IX, and XI are involved with transducing mechanical signals to inhabitant chondrocytes, as well as stabilizing the surrounding type II collagen mesh.^{26,39} On the other hand, type X and type I collagen molecules tend to be present in diseased cartilage. Types of collagen fiber and their relative abundance in cartilage tissue are summarized in Table 1.2. Type X collagen is a short-chain molecule that plays a role in cartilage mineralization at the osteochondral interface and is a marker for hypertrophy of chondrocytes.⁴⁰ Type I collagen is a 300 kDa molecule and is the most abundant collagen in the body, especially in tissues with high tensile strength like bone. It also acts as a substrate for cell adhesion and proliferation.^{41,42} However when found in cartilage, type I collagen indicates the presence of a mechanically inferior (relative to articular cartilage) fibrocartilage, generated by

the body in an attempt to repair damaged tissue.⁴³ It is interesting to note that type I collagen is very similar to type II collagen; it can self-assemble to form fibrillar structures and is only differentiated from type II by having less hydroxylysine-linked disaccharides.²⁵ In fact, it is because of their similarities that type I fibrils can reassemble into type II fibrils in the presence of chondrogenic factors.⁴⁴

Table 1.2. Collagen composition of human articular cartilage	
<u>Collagen Type</u>	<u>Percentage of cartilage tissue collagen content</u>
Type II collagen (structural backbone of ECM)	90-95% of total cartilage collagen content
Types III, VI, IX, XI, XII, and XV collagen (facilitate fibril interactions with the ECM)	5-10% of total cartilage collagen content
Type I (fibrocartilage), Type X (hypertrophic)	Trace amounts in healthy tissue

References: Type II,²² Types I-XV.²⁶

In addition to collagen, proteoglycans are present in the cartilage ECM, and these biomacromolecules interact with the collagen mesh and contribute to the tissue's structure and properties. A common aggregating proteoglycan in the tissue is known as aggrecan, and it is entrapped within the collagen network with the assistance of hyaluronic acid (HA).⁴⁵ Aggrecans introduce fixed-charge groups that can create an osmotic environment in cartilage, immobilizing and restricting water flow such that mechanical loads are distributed over the tissue area. The retention of water places tension on the collagen mesh and with these combined properties, cartilage can have high compressive resistance properties.⁴⁶ A schematic of the collagen network linked with aggrecan, and a more detailed view of aggrecan is shown in Figure 1.2.

Aggrecan is a linear core protein of high molecular weight with multiple globular domains and is highly glycosylated. The unbranched carbohydrate chains, or sulfated glycosaminoglycans (sGAG), that attach to the aggrecan surface are negatively charged and contribute significantly to helping aggrecan maintain an osmotic gradient to retain water.⁴⁷ The predominant sGAG found on aggrecan is chondroitin sulfate with keratan sulfate being less abundant.⁴⁸ Aggrecan is stabilized by a link protein that binds to a long, linear glycosaminoglycan hyaluronan (HA) chain, which can have up to 100 different aggrecans per molecule.⁴⁹ HA binds to the CD-44 receptor on chondrocytes, thereby helping to retain aggrecan in the cartilage ECM.⁵⁰ Maintenance of ECM is important to ensure long-term stability of the tissue, and chondrocytes do this by a unique homeostatic process.

1.1.4. Matrix metabolism

After it has developed into mature tissue, cartilage undergoes a homeostasis of matrix anabolism and catabolism that is regulated by cell-secreted proteases. This natural tissue remodeling is necessary to transport ECM molecules from the chondrocyte pericellular space to the extracellular space and replace the resultant void with newer matrix molecules.⁵¹ In a healthy environment, the rate of matrix turnover is a slow process; the half-lives of aggrecan and collagen molecules are on the order of 15-100 days and 100 years respectively.^{52,53}

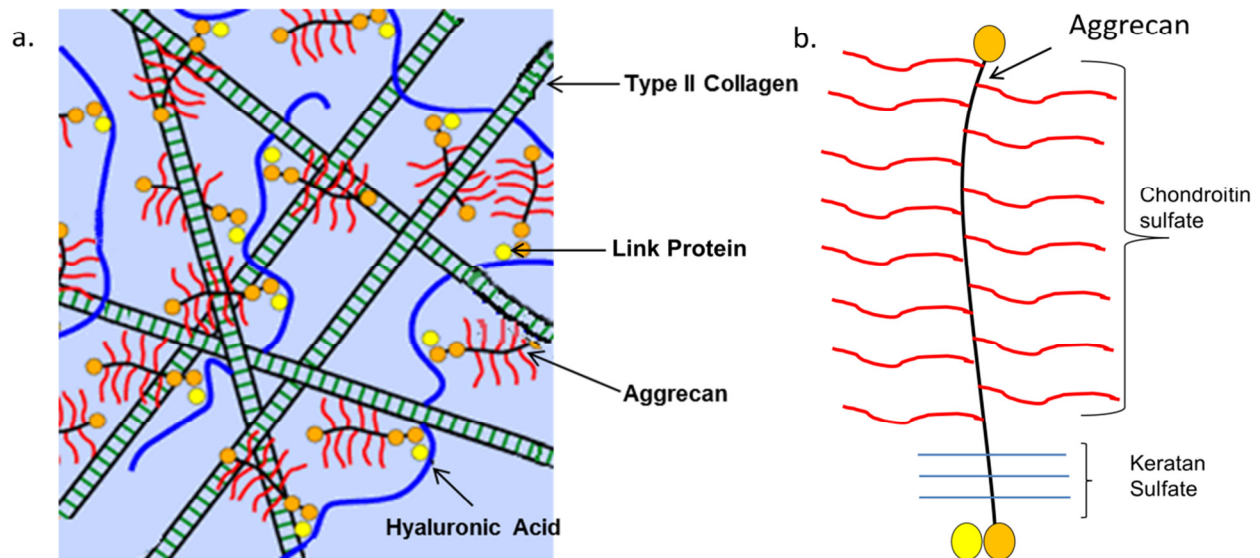


Figure 1.2. Schematic of cartilage ECM and aggrecan a) Cartilage ECM with predominant type II collagen fibers (green) intertwined by aggrecan molecules (black) that attach to hyaluronic acid (blue) by link proteins (yellow). This network of macromolecules works together to help retain water in the tissue to give cartilage robust mechanical properties. b) Aggrecan is a high molecular weight molecule that contains highly branched, negatively charged chondroitin sulfate and keratan sulfate molecules. Aggrecan helps retain water in the cartilage ECM with its predominantly negative charge.

This slow turnover is partly due to the cells in the joint being exposed to an hypoxic environment with an oxygen tension level as low as 1-3%, compared to closer to 15% in normoxic conditions of the body.⁵⁴ To maintain a healthy cartilage tissue, the rate of matrix degradation (catabolism) should not exceed the rate of matrix synthesis (anabolism); however, in a diseased state, this is not the case and cartilage degeneration occurs.⁵⁵

Proteolysis of the ECM is regulated through various cell-secreted proteinases of which MMPs have the most ubiquitous role in matrix turnover.⁵⁶ There are 23 known human variants of these zinc-dependent enzymes, and they are grouped based on their targets of cleavage. Some MMPs belong to a group that can specifically cleave aggrecan molecules and are known as “aggrecanases” or stromelysins. MMP-1, MMP-8 and MMP-13 are known as “collagenases”

since they have the specific ability to degrade fibrillar collagens within a triple helix that has been processed and digested by enzymes such as MMP-3.²⁶ MMP-13 is the most effective at cleaving collagen, especially type II collagen in a diseased state.^{57,58} Chondrocytes are known to primarily secrete MMP-1, MMP-3, MMP-8, and the gelatinases (MMP-2 & MMP-9) in healthy tissue, and primarily MMP-13 in an osteoarthritic state.^{59,60,61} This activity makes sense as collagens, and their degradation product gelatins, are the predominant proteins found in the ECM, and hence, good molecules to target when designing degradable scaffolds, which are susceptible to MMP cleavage, for cartilage tissue engineering applications.

Since the balance of catabolism and anabolism can sometimes be tipped in favor of catabolism even in a healthy state,⁶² the body has a group of specific inhibitors of MMPs known as tissue inhibitors of metalloproteinases (TIMPs), to ensure that equilibrium is maintained. There are four known variants of TIMPs and most bind to the catalytic site of the enzyme where MMP-3 and MMP-9 are their primary targets.⁶³ TIMPs can be induced and repressed by the same growth factors to ensure proper remodeling of tissue takes place. For example, TGF- β can act as a stimulator of TIMP-1 and TIMP-3, which tend to inactivate MMP-9 (a gelatinase which cleaves the inactivated form of collagen known as gelatin).⁶⁴ However, TGF- β is also known to inactivate TIMP-2, which acts on MMP-3 (stromelysin that prepares collagen to be degraded by collagenases), thereby ensuring that the active collagen matrix can be remodeled while the denatured collagen can be degraded and disposed.⁶⁵ A list of the common MMPs and TIMPs found in cartilage and their actions are summarized in Table 1.3.

Table 1.3. Common MMPs and TIMPs found in cartilage	
<u>MMP or TIMP Number</u>	<u>Other names and actions</u>
MMP-1, MMP-8, & MMP-13	Collagenases I, II, and III respectively, specifically cleave fibrillar collagens as well as denatured collagens (gelatins).
MMP-2 & MMP-9	Gelatinase A and B respectively are secreted by chondrocytes and actively degrade gelatin molecules found in the tissue.
MMP-3	Stromelysin that cleaves a number of matrix components, notably aggrecan, and fibronectin. Also prepares collagen molecules for subsequent cleavage by collagenases.
TIMP-1 & TIMP-3	Inactivate gelatinase B and are stimulated by TGF- β .
TIMP-2	Inactivate MMP-3, and is inhibited by TGF- β .

References MMP-1,-2-8,-9, -13,^{59,60,61} MMP-3,²⁶ TIMP-1,-3,⁶⁴ TIMP-2.⁶⁵

Degraded matrix byproducts can act on chondrocytes in both positive and negative ways to affect matrix output. Degradation of type II collagen is a rate-limiting step in cartilage remodeling because it is the most abundant component of the collagenous meshwork (90-95% of the total collagen content).¹ Some degradation products of type II collagen may act in a positive-feedback mechanism to stimulate further collagen gene expression and promote the differentiation of cartilage cells.⁶⁶ On the other hand, too many degraded byproducts of type II collagen can induce chondrocytes to produce high levels of MMP-1, MMP-13, and pro-inflammatory cytokines like interleukin-1(IL-1) and tumor necrosis factor (TNF- α), which can lead to chondrocyte hypertrophy and de-differentiation.⁶⁷ Therefore, in engineering a cartilage

implant, it is important to maintain a degradation rate that is regulated by the local cells to prevent excess inflammation and tissue damage.

When the collagen molecule is cleaved by proteinases, neoepitopes arise on the newly degraded molecule and can be detected by immunoassays. Once the procollagen telopeptides have been cleaved by proteases, the triple-helical domain in the middle is exposed to cleavage by collagenases. Once the helical domain is cleaved, it unwinds to reveal neoepitopes that are not normally detected in the native triple-helix form.⁶⁸ The neoepitopes that are not destroyed by subsequent collagenase-mediated cleavage and are released into the surrounding body fluids include COL2-3/4C_{long} (C2C), and COL2-3/4C_{short} (C1,2C), which are derived from the carboxy-terminus end of the N-terminal α chain of the degraded type II collagen molecule and can be detected by antibodies.⁶⁸ Furthermore, a neoepitope generated during initial cleavage of the C-terminal telopeptide from procollagen known as CTX-II, can also be reliably detected by antibodies and is a strong sign that collagen is being degraded.⁶⁹ A schematic of the breakdown process of collagen is shown in Figure 1.3.

Another breakdown byproduct of collagen found in cartilage is gelatin. Gelatin is regulated in the tissue by gelatinases generated by chondrocytes. Gelatin can be easily produced commercially by thermal denaturation and hydrolysis of type I collagen.⁷⁰ Gelatin is an assembly of the decoupled alpha chain strands of collagen, which renders it more susceptible to cleavage by most proteases compared to the special collagenases required for collagen enzyme hydrolysis.⁷¹ Beyond bioactive signals arising from matrix degradation by-products, cell-secreted growth factors also play a major role in regulating chondrocyte activity.

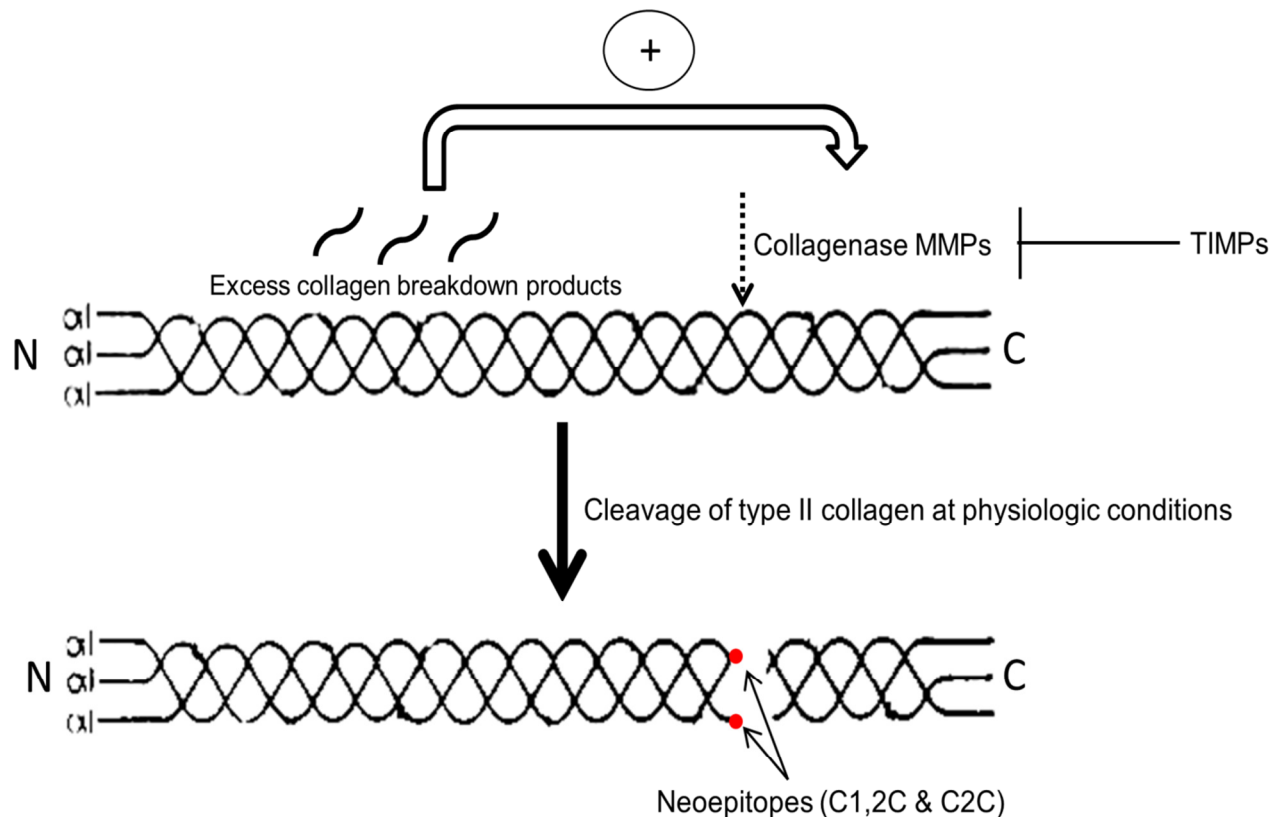


Figure 1.3. Schematic of the breakdown of type II collagen. Type II collagen contains three $\alpha 1$ chains and is initially cleaved by collagenase MMPs (-1,-8,-13) at physiologic conditions. After cleavage of the fiber, neoepitopes (red dots) like C1,2C and C2C are revealed. Furthermore, the collagen degradation by-products, in excess, can upregulate collagenase expression, while TIMPs can repress its production. Image modified from http://www.ibex.ca/DX_C12C.htm

1.1.5. Effects of growth factors

Cartilage growth factors are secreted proteins that are generally produced in the local joint microenvironment and act in a paracrine or autocrine fashion to regulate growth and repair of the tissue. These proteins can stimulate cell growth, as well as enhance differentiated function. Growth factors can be sequestered to extracellular matrix components of the tissue for long-term storage until release during matrix remodeling.⁷² Growth factors that assist in cartilage

development include basic fibroblast growth factor (bFGF), hepatocyte growth factor (HGF), and platelet-derived growth factor (PDGF), transforming growth factor-beta (TGF- β) and insulin-like growth factors (IGF) playing major roles in tissue growth.^{73,74}

In this research, IGF was used to stimulate growth of chondrocytes on tissue culture plates prior to encapsulation. The two isoforms of IGF (IGF-I and II) are polypeptide hormones structurally related to insulin and synthesized in the liver. IGF-I helps prevent chondrocyte differentiation into a fibroblastic or osteoblastic phenotype during culture on tissue culture plastic styrene (TCPS),⁷⁵ and induces chondrocytes to produce more ECM molecules.⁷⁶

This thesis research focuses on the local presentation of TGF- β to influence chondrocytes embedded in hydrogel matrices. The TGF- β family consists of three mammalian isoforms (TGF- β 1-3). Each isoform is 25 kDa and they share greater than 70% of their amino acid sequence.⁷⁷ TGF- β is produced as a 100 kDa precursor latent complex that can then be activated with convertases once in the chondrocyte periphery.⁷⁸ The TGF receptor is a serine/threonine kinase that operates as a heterodimer in that one part of the receptor is required for binding to the ligand, while the other part has to dimerize with the bound receptor to initiate a signaling cascade.⁷⁹ All three isoforms can bind to the same receptor and elicit similar responses in chondrocytes.⁸⁰ The signaling cascade initiated by the ligand binding event leads to downstream Smad signaling. When the Smad molecules translocate to the cell nucleus, they can either directly bind to DNA or form complexes with transcription factors to influence protein expression.⁸¹ Activated TGF- β is known to be highly conserved (>99% amino acid sequence identity) throughout mammalian species.⁸² TGF- β 1 in particular is known to direct differentiation of mesenchymal stem cells to chondrocytes and repress adipogenesis.⁸³ TGF- β 1 also plays an essential role in maintaining mature articular cartilage thickness,⁸⁴ as well as

increasing chondrocyte proliferation rates.⁸⁵ A schematic of TGF signaling is shown in Figure 1.4.

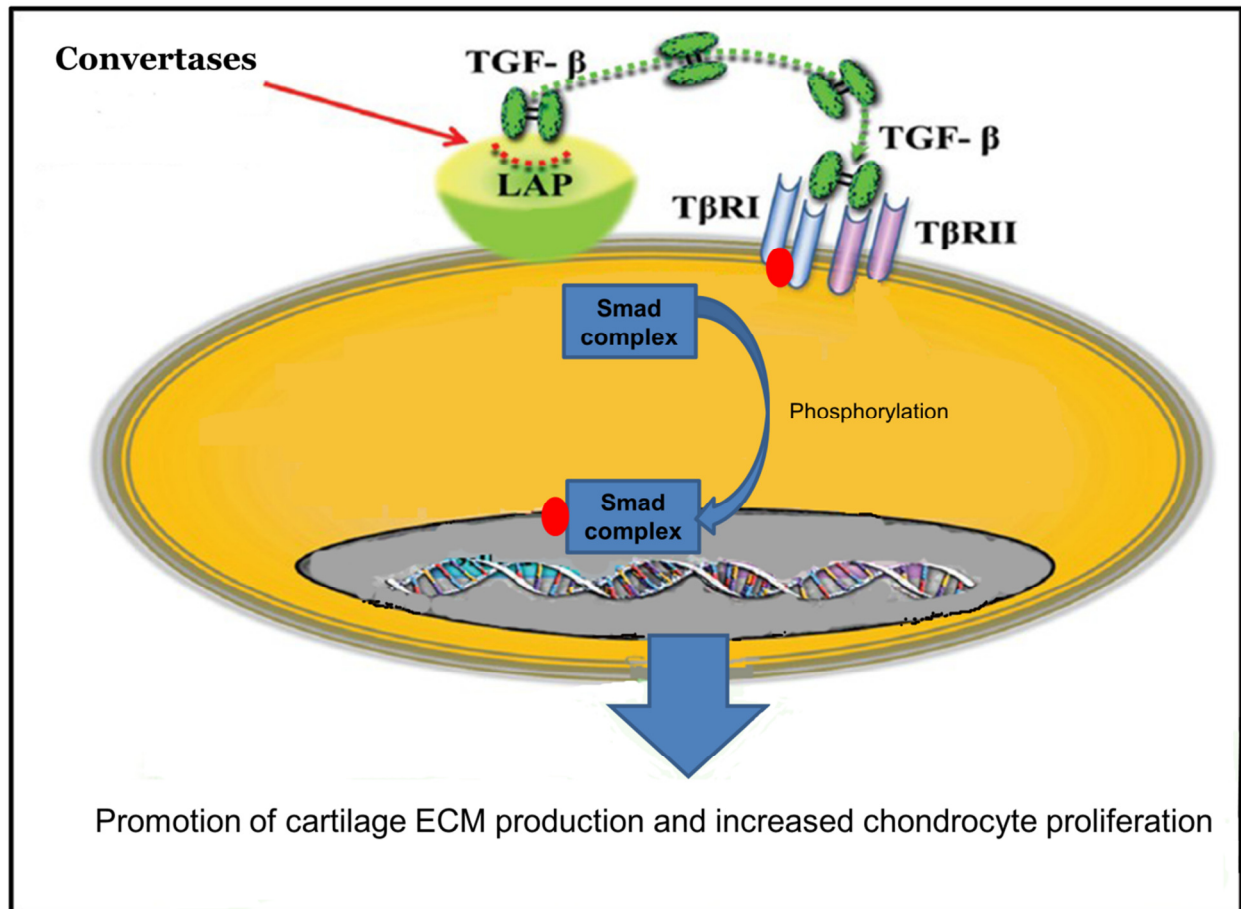


Figure 1.4. Schematic of TGF- β signaling to chondrocyte. First convertases cleave the precursor latency associated peptide (LAP) so that TGF- β can be activated and bind to the dimer receptor found on the chondrocyte (yellow) membrane. The binding event initiates phosphorylation (red circle) of Smad. The phosphorylated Smad complex enters the nucleus (grey), and influences transcription to increase chondrocyte ECM production and proliferation.

1.2 Etiology of Cartilage Damage

Tissues in articulating joints of large weight-bearing bones, like the knees and hips, experience constant stress due to motion that the human body places on them. A common culprit

for initiating cartilage injury is traumatic impact due to events ranging from sports activities, to motor vehicle accidents, to direct falls.⁸⁶ Other causes of traumatic injuries include mal-alignment of the bones above and below the joint, unrepaired meniscal and ligament tears which lead to instability of the joint, osteochondrosis dissecans (OCD): in which there is a slow, symptomless separation of cartilage from the subchondral bone, and microtrauma from repeated stress which can include walking.⁸⁷ These incidents can form focal defects that range in depth: from those limited to the superficial area in microtrauma cases to full osteochondral defects that penetrate cartilage layers to the underlying subchondral bone. Superficial lacerations due to microtrauma do not heal, although some proliferation of chondrocytes may occur.⁸⁸ In osteochondral defects, since the defect penetrates all the way to the subchondral bone, progenitor cells can be recruited from the bone, like MSCs, to repair to defect. However, the repair tissue that is created, fibrocartilage, is composed primarily of type I collagen and has a much lower mechanical integrity compared to healthy articular cartilage.⁸⁹

Because cartilage is an avascular and aneural tissue, it has a limited ability to repair damaged tissue; thus, there is a major risk of focal defects developing into osteoarthritis (OA) if they are untreated.^{90,91} Osteoarthritis is believed to have an inflammatory pathology in which pro-inflammatory cytokines are released into the joint space and alter tissue homeostasis in favor of cartilage catabolism, which can result in destruction of the entire cartilage surface.⁹² The disease is characterized by increased pain, a loss of mobility, and is one of the leading causes of disability in the US.⁹³ It is important to prevent the onset of osteoarthritis, which currently has no cure, by treating focal defects when they are first detected. Some of the current interventions used to treat cartilage defects are summarized in the following section.

1.3. Current Treatment Options for Cartilage Lesions

Patients with articular cartilage defects commonly present with knee pain often exacerbated by impact of weight-bearing activities. The spectrum of chondral pathologies seen in practice are osteochondral traumatic injuries, focal defects, and early OA.⁹⁴ Chondral defects can be differentiated from early OA, and this is imperative in managing treatment options appropriately.⁹⁵ Surgeons will diagnose and grade the extent of a cartilage injury using imaging techniques like x-ray and MRI with arthroscopy being the gold standard for assessing the grade of a lesion.⁹⁶ Treatment options should be individualized based on lesion etiology, size, location, duration of symptoms, state of the subchondral bone, and the number of previous interventions.⁹⁷ Additionally, patient characteristics such as activity level, smoking history, demographics, body mass index, and rehabilitation compliance need to be assessed prior to intervention, since they play a significant role in treatment outcomes.⁹⁸ Once the cartilage lesion and patient are well-understood, the following treatment options are used.

1.3.1. Conservative treatment of defects

One of most common treatment methods for patients with joint pain is simply relieving the symptoms in order to prolong the need for surgery to repair the underlying cartilage damage. Temporary options to mask the pain include non-steroidal anti-inflammatory drugs (NSAIDs) or neuroceuticals, like glucosamines in which a glycosaminoglycan (e.g., chondroitin sulfate) is ingested with the hope that it will replenish aggrecan-related structural deficiencies in the damaged cartilage.⁹⁹ For longer term relief, doctors can administer intra-articular cortisone, a glucocortical steroid, to decrease inflammation and pain; however, long-term effects of cortisone administration have been shown to degrade articular cartilage.⁹⁹ Hyaluronic acid, another glycosaminoglycan found in the cartilage matrix that plays a role in lubricating the tissue, is directly injected into the damaged joint at a high molecular weight formulation in a process

called viscosupplementation. Viscosupplementation tends to help in preventing further degeneration of cartilage, but multiple injections are required to maintain a symptom-free knee rendering it a temporary solution in pain management.¹⁰⁰ If conservative management does not help abate the symptoms, the next treatment option is usually surgery.

1.3.2. Operative treatment options

In contrast to conservative therapies, surgical interventions attempt to remove the defect and prevent the recurrence of joint pain for longer periods of time. A simple and commonly used technique is arthroscopic debridement of localized defects, also known as chondroplasty. In chondroplasty, damaged cartilage flaps are removed so that the defect area can be smoothed and reshaped to more easily permit joint articulation. Chondroplasty has a decent success rate in improving pain and mechanical symptoms;¹⁰¹ however, the regenerated tissue is mechanically inferior fibrocartilage and long-term effects have not been well-studied.¹⁰²

For lesions with subchondral bone loss, autologous osteochondral (both cartilage and subchondral bone) plugs can be harvested from non-weight bearing portions of the knee and inserted into the defect site in a technique called mosaicplasty.¹⁰³ There are high success rates of restoring hyaline articular cartilage in small defect areas ($< 2 \text{ cm}^2$) with mosaicplasty.¹⁰⁴ However, challenges with mosaicplasty include plugs not fully covering the defect, donor site morbidity, and if placed incorrectly, healed tissue can form irregular surfaces.^{105,106}

Marrow stimulation is based on the principle of exposing the chondral defect to bone marrow, thus trying to create an environment for fibrocartilage healing. The technique was developed by Pridie in 1959.¹⁰⁷ A common marrow stimulation technique is microfracture in which multiple, small perpendicular perforations are made to the subchondral plate to stimulate

infiltration of MSCs and growth factors to promote healing in the cartilage defect.¹⁰⁸ However, a main limitation of this technique is the generation of fibrocartilage repair tissue with inferior mechanics. A study of 3000 patients showed that the effectiveness of microfracture usually diminishes as the thin fibrocartilage degenerates, resulting in a recurrent loss of function.¹⁰⁹ Thus, to improve upon this outcome, microfracture has been more recently combined with scaffolds.^{110,111}

In cases where there is severely damaged cartilage that is beyond repair, surgeons will perform full joint arthroplasty, in which the entire joint is replaced by a prosthetic. This prosthetic device restores knee joint function, but can limit physical activity. The procedure is highly invasive, and the prosthetics tend to wear out or loosen over time, which makes this treatment a difficult option for younger patients.^{55,112} Alternative technologies to treat cartilage lesions aim to prevent the need for full joint replacement therapy, since this is not an ideal solution. Many of the newer and emerging technologies focus on recapitulating the native structure and composition of articular cartilage to better match the function of hyaline tissue.

1.3.3. Acellular scaffold therapies

Numerous acellular products have been developed to treat cartilage defects that use a biomaterial matrix to either augment techniques like microfracture or provide mechanical support. These synthetic replacements are attractive because of their ease of handling, modification, and the ability for patients to delay full joint replacement procedures.¹¹³ Some scaffolds attempt to directly mimic the high compressive and low friction properties of native articular cartilage without the use of cells. For example, synthetic poly-(vinyl alcohol) networks interwoven with gelatin strands¹¹⁴ and polyurethane plugs like Chondrocushion

(Advanced Bio Surfaces, Inc.)⁹⁷ have been engineered for these purposes. Other biomaterials are designed to permit cell infiltration and gradual replacement of the material with tissue as it degrades. As an example, products like Trufit plug (Smith and Nephew), Chondromimetic (Tigenix), and BST Cargel (Biosyntech Canada) have combined synthetic and naturally-derived biomaterials to augment marrow stimulation techniques.¹¹⁵ Though early results with MRI show repair fill, there is concern that the repair is fibrous tissue with foreign body giant cells identified at revision surgery.⁹⁶ While the acellular scaffolds provide a unique approach to cartilage regeneration, biomaterials alone may not be able to fully recapitulate native tissue properties over long periods of time since there are generally no cells to provide regenerative capacity.

1.3.4. Cell-only based therapies

Since the aforementioned operational techniques tend to lead to fibrocartilage formation, and in the large part are temporary solutions, many current research directions are focused on cell-based strategies to regenerate tissue that is hyaline-like in its biochemical composition and mechanical properties, with the goal of providing a longer-term solution to joint pain. Cell-only based techniques involve delivering chondrocytes (either autologous, allogenic, or xenogenic) to cartilage lesions without a scaffold to promote formation of new tissue.

Autologous chondrocyte transplantation (ACT) is a two-stage process which involves isolating and expanding chondrocytes, and then implanting them at a later time into a debrided defect site. The site is covered with a periosteal patch (most commonly obtained from the tibial head) or a collagen membrane to retain the cells.^{116,117} In this procedure, the surgeon removes cartilage from a non-load bearing region, enzymatically digests the tissue, expands the isolated chondrocytes *in vitro* until there are a sufficient number of cells to re-implant into the damaged

area in a subsequent surgery.¹¹⁸ The only FDA-approved ACT product is Carticel®, which does result in cartilage containing predominantly type II collagen in younger patients,^{119,120} but does not fully replicate the mechanical properties of the surrounding cartilage because of a lack of integration and alignment with the surrounding native tissue.¹²¹

Another cell-only based approach involves isolating chondrocytes from an autologous, allogenic, or xenogenic source, because it is perceived that cartilage is immune-privileged due to its avascular properties.¹¹ Avoiding patient-specific autologous cells simplify the clinical procedure, potential cost of the product, and could minimize variations in tissue regeneration related to age, sex, et cetera. In this approach, isolated cells are centrifuged to form a pellet, and then shaped to the size of the defect.¹²² This scaffoldless approach relies on the principle of enhancing cell-cell interactions that are seen early in development, by placing many cells in close proximity to promote matrix production. Currently, scaffoldless technologies are undergoing clinical trials with limited quality of clinical evidence,¹²³ and similar to ACT, integration with the host tissue remains a problem.¹²⁴ While the acellular and cell-only based techniques show promise, the cells lack a foundation to facilitate placement and retention in a joint defect site. This limitation has led to the advent of cartilage tissue engineering, a term used to describe strategies where cells are encapsulated in or seeded on biomaterial scaffolds.

1.4. Cartilage Tissue Engineering Approach

A goal of cartilage tissue engineering is to prevent the onset of osteoarthritis after cartilage injury by regenerating or replacing the damaged tissue. To date, technological advances have led to a third-generation ACT that uses a biomaterial scaffold seeded with chondrocytes as a carrier to support cell growth. The composite “all-in-one” tissue-engineered

approach combines cultured chondrocytes with 3-D biocompatible scaffolds for the purpose of generating new functional articular tissue, which is also known as matrix-assisted autologous chondrocyte transplantation (MACT).¹²⁵ After debridement of the defect, biomaterials with seeded cells are shaped to match the defect size via *in-situ* polymerization schemes and implanted without the use of a periosteal flap or fixing stitches as shown in Figure 1.5. A wide variety of cell sources, scaffolds, and bioactive factors have been investigated to improve upon MACT or similar techniques involving a combination of cells and scaffolds.

1.4.1. Cell source

Some of the considerations when identifying an appropriate cell source for cartilage tissue engineering applications include the ease of isolation, and the ability of the cells to synthesize abundant cartilage-specific ECM, particularly collagen II and aggrecan. Primary chondrocytes and progenitor stem cells have been extensively investigated as cell sources; however, each cell source provides its own distinct challenges towards creating a single option because of cell variability between patients and alterations of cell metabolism with aging.¹²⁶ Primary chondrocytes are most commonly used, because they have a well-known capacity to produce cartilage-specific matrix.

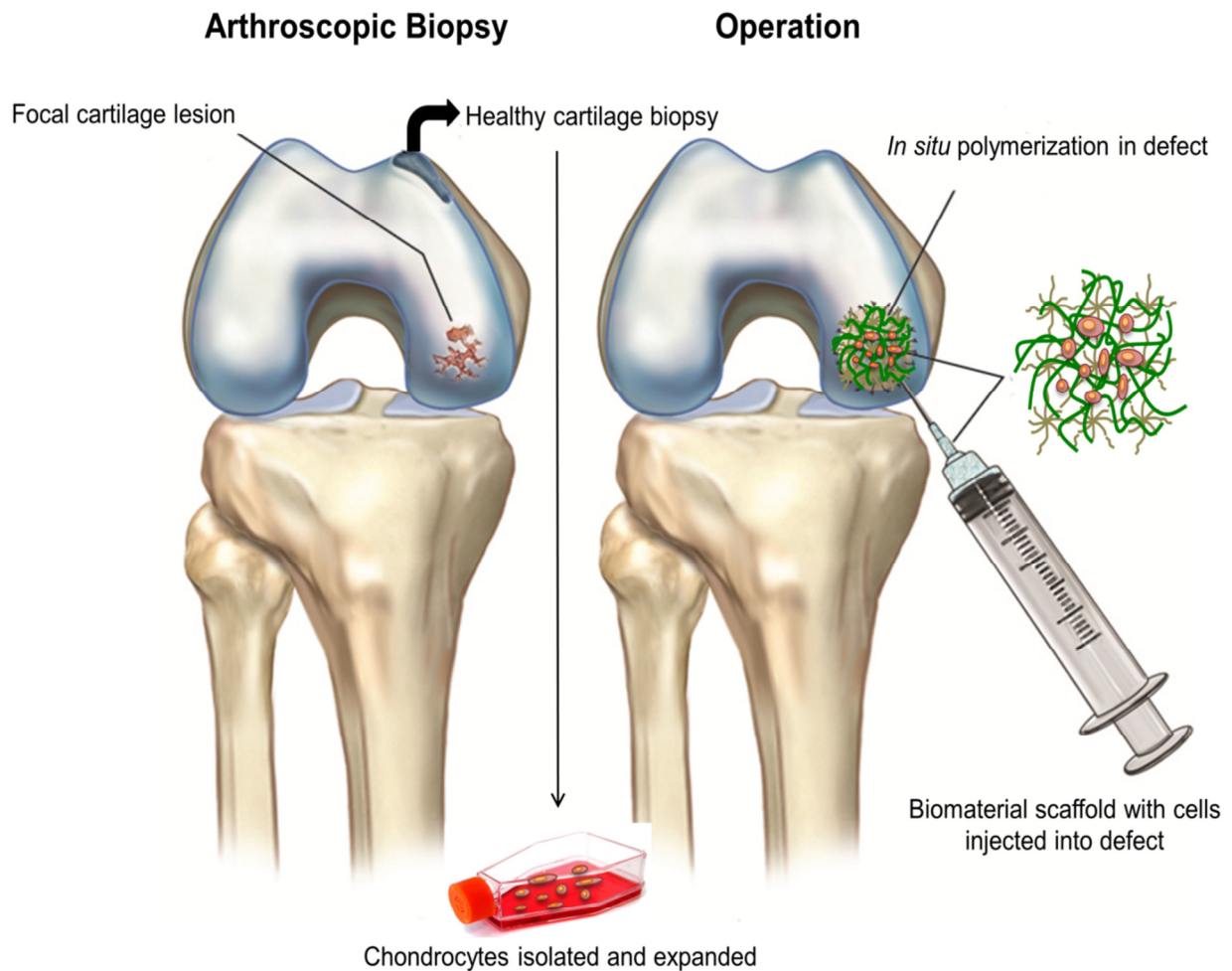


Figure 1.5. Schematic for MACT in which autologous chondrocytes are isolated from non-weight bearing portions of the knee and expanded *in vitro*. The cells are encapsulated in a biomaterial scaffold (either synthetic or natural) and then directly injected into the defect site wherein the cell-laden scaffold can be polymerized by a variety of schemes including a photoinitiation reaction to mold the gel to fill the defect site.

However, one of the main problems with chondrocytes is that the harvested cell number tends to be quite low, necessitating expansion in 2-D culture. This expansion can result in de-differentiation away from the chondrocyte phenotype if cultured for multiple passages.¹²⁷

Mesenchymal stem cells (MSCs) can be derived from adult tissue, typically bone marrow, and can be harvested fairly easily with low donor-site morbidity relative to

chondrocytes. MSCs can be easily expanded in 2-D culture and chemically coaxed to differentiate into a variety of cell types including chondrocytes.¹²⁸ However, MSC-laden scaffolds generally have reduced matrix accumulation and weaker mechanical properties compared to chondrocyte-laden constructs.^{129,130} Another limitation of MSCs, is that when stimulated down a chondrogenic pathway, they tend to terminally differentiate into hypertrophic chondrocytes that express large quantities of type I¹³¹ and type X¹³² collagen, which leads to fibrocartilage formation and calcification of tissue, respectively. Thus, one of the main challenges of using MSCs alone is that they can hypertrophy relatively easily, which makes it difficult to obtain a stable cartilage phenotype.¹³³

In addition to bone marrow-derived MSCs, adipose-derived adult stem cells (ADSCs) harvested from subcutaneous adipose tissue can be differentiated into chondrocytes, but also have a similar hypertrophic differentiation limitation.¹³⁴ Embryonic stem cells, which are sometimes obtained from cord blood, have been differentiated into chondrocytes,¹³⁵ but these cells still present challenges due to poorly controlled cell proliferation, immunogenicity potential, and teratoma formation.¹³⁶ Induced pluripotent stem cells (iPSCs) are somatic cells that have been reprogrammed to have properties similar to pluripotent stem cells. iPSCs have been differentiated into chondrocytes, but require extensive manipulation of the cells, and more work needs to be done to characterize the quality of cartilage tissue generated.¹³⁷ Interestingly, neonatal chondrocytes (NChons) have been recently utilized as a cell source, since only a small amount of NChons is required to greatly influence adult chondrocyte secretory properties in co-culture.¹³⁸

In general, all of the progenitor stem cells, when used as monoculture in constructs, tend to form poor quality tissue. One tissue engineering approach to circumvent this issue is to co-

culture chondrocytes and stem cells to synergize and maximize the benefits that both cell types provide. A common co-culture tissue engineering technique is to seed at a high MSC: chondrocyte ratio since it is easier to isolate MSCs, and chondrocytes produce high quality cartilage. Multiple studies have shown that this co-culture technique with engineered implant produces tissue that more closely resembles hyaline cartilage, without cell hypertrophy, than monoculture constructs both *in vitro*^{139,140} and *in vivo*.^{141,142} Co-culture has also been performed with ADSCs and chondrocytes, with a similarly beneficial synergistic response with respect to cartilage production.¹⁴³ This thesis research focuses primarily on strategies that use primary chondrocytes for cartilage regeneration, as it is widely known that chondrocytes in monoculture produce hyaline-like tissue, but aspects exploit co-culture with MSCs to stimulate chondrocyte activity, bioscaffold degradation, and matrix deposition.

1.4.2. Biomaterial scaffolds

The use of a biomaterial scaffold in conjunction with cells is intended to stimulate cells to synthesize a cartilage-specific matrix and temporarily replace the function of the native ECM while the tissue is regenerating. When selecting or designing scaffolds for this purpose, engineers consider several factors, such as whether or not the initial scaffold structure can support cells in the joint environment, allow for diffusion of nutrients and waste, promote cell viability and ECM production, permit integration of ECM molecules with the host tissue, and biodegrade in a way that corresponds with tissue deposition so that applied loads in the joint transitions from the construct to tissue over time. Scaffolds tend to be important for culturing chondrocytes because a rounded cell morphology, and hence chondrocyte phenotype, can be better maintained in 3-D culture compared to 2-D.¹⁴⁴ A wide variety of natural and synthetic materials have been investigated as cartilage tissue engineering scaffolds, where some of the

most promising scaffolds have characteristics of both natural and synthetic materials. These scaffold materials are summarized briefly below.

1.4.2.1 Natural materials

Natural biomaterials are attractive as cell carriers because they can form viscoelastic gels, are derived from cartilage ECM of biologic sources, and their biological derivation renders them biocompatible and biodegradable. Some advantages of natural material scaffolds include eliciting a minimal immune response if processed appropriately, providing bioactive signals, and the ability to design them as an injectable liquid that can solidify in the defect.

Protein-based natural materials used for cartilage tissue-engineering include fibrin,¹⁴⁵ gelatin,¹⁴⁶ and collagen (type I and/or type II).¹⁴⁷ Collagen is one of the most commonly studied materials and is advantageous because of its ability to mimic the native ECM chemistry, as it is a major matrix component. Collagen has been shown to enhance ECM production of encapsulated chondrocytes, as well as have the ability to be injected and solidified in the defect *in situ*.¹⁴⁸ Cell-mediated degradation can occur in natural materials, like collagen, but it is difficult to form reproducible or mechanically robust hydrogels since there is great batch-to-batch variation¹⁴⁹ and the gels do not form densely cross-linked networks without some chemical modification.¹⁵⁰

Carbohydrate-based natural materials include hyaluronic acid,¹⁵¹ agarose,¹⁵² alginate,¹⁵³ and chitosan.¹⁵⁴ Hyaluronic acid is an attractive material to use in scaffolds due to its function in keeping the ECM intact, but it typically must undergo chemical functionalization to permit crosslinking.¹⁵⁵ Agarose has been extensively studied as a natural biomaterial, particularly in experiments that include mechanical loading and studying the effect of mechanical stimuli on chondrocytes.^{156,157} While agarose allows tailoring a wide range of moduli, including those

closer to that of cartilage tissue, a major limitation of agarose gels for cartilage tissue engineering is that it cannot be degraded by chondrocytes.¹⁵⁶

1.4.2.2. Synthetic biomaterials

Synthetic chemistries typically allow customization of well-defined chemical, mechanical, and structural properties of scaffolds that are simple to manufacture and can be processed reproducibly. The flexibility of synthesis allows for the design of scaffolds with known degradation rates, mechanical characteristics, and incorporation of covalently tethered bioactive molecules. Some well-known synthetic polymers used to create scaffolds include poly(lactic acid) (PLA), poly(glycolic acid) (PGA), and polycaprolactone (PCL), which all have been commonly used for biomedical applications,^{158,159} because they are biodegradable and are approved by the US Food and Drug Administration (FDA) for specific clinical applications.¹⁶⁰ However, these materials produce acidic degradation products that can be cytotoxic at high concentration,⁵⁵ and they are often processed as macroporous materials (pores $\gg 10\ \mu\text{m}$ diameter) to allow cell seeding. Unfortunately, chondrocytes seeded in these macroporous scaffolds often alter their phenotype, since their rounded morphology cannot be maintained in such large pores.¹⁶¹

To capture the microenvironment of many soft tissues, especially cartilage, numerous groups began exploring hydrogel scaffolds. In its basic sense, hydrogels are a network of large, hydrophilic macromolecules that would typically dissolve in water, but are rendered insoluble by physical or chemical crosslinks between them. Some of the most common synthetic hydrogels used as cell scaffolds are based on poly(ethylene glycol) (PEG), poly(vinyl alcohol) (PVA), and poly(2-hydroxyethyl methacrylate) (PHEMA). Their high hydrophilicity allows for the

absorption and retention of water to better simulate the native ECM environment, while also permitting nutrient diffusion.^{162,163}

There have been a multitude of synthetic hydrogels that have been explored in tissue engineering applications. Since this thesis work focuses on PEG hydrogels, the discussion that follows is limited to common methods of tailoring PEG hydrogels for cartilage regeneration purposes. PEG hydrogels have been employed extensively in cartilage tissue engineering due to their ability to maintain chondrocyte phenotype and permit cartilaginous tissue formation.^{164,165} Covalently-crosslinked PEG hydrogels can be synthesized by first chemically modifying the ends of PEG macromolecules with groups like acrylates, maleimides, vinylsulfones, azides, alkynes, norbornenes, and thiols. These versatile chemistries allow for a variety of reactions, including bioorthogonal “click” conjugations.¹⁶⁶ There are numerous ways to initiate polymerization of gels, which include temperature¹⁶⁷ and Michael-type addition;¹⁶⁸ however, this thesis work utilizes light to trigger crosslinking of PEG, so the discussion will focus on photo-initiated polymerization of hydrogels.

Photoinitiation of hydrogels often involves the use free radicals that are generated when an initiator species is exposed to light. With certain end functionalities, free radicals can propagate through un-saturated end groups, leading to the evolution of network formation with multifunctional macromolecular monomers as shown in Figure 1.6.A.¹⁶⁹ Photopolymerization is desirable from an application standpoint, as the reaction is controlled in both time and space, the polymerizations are typically rapid, and can be performed under cytocompatible conditions.¹⁷⁰ One of the most common photochemical approaches to synthesizing PEG hydrogels is via a chain-growth mechanism using (meth)acrylated PEGs.¹⁷¹ PEG macromers can also be photopolymerized via a controlled, bioorthogonal step-growth mechanism (i.e., thiol-ene

reaction). The step-growth mechanism leads to a more homogenous network, and allows facile incorporation of thiol-containing biofunctional groups (e.g. peptides, and proteins) as shown in Figure 1.6.B.^{172,173} Furthermore, a recent study with a step-growth polymerization scheme of thiol-norbornene monomers with a non-degradable linker showed reduced radical damage to encapsulated chondrocytes and enhanced cartilage regeneration relative to cells in diacrylate, chain-growth polymerized gels.¹⁷⁴

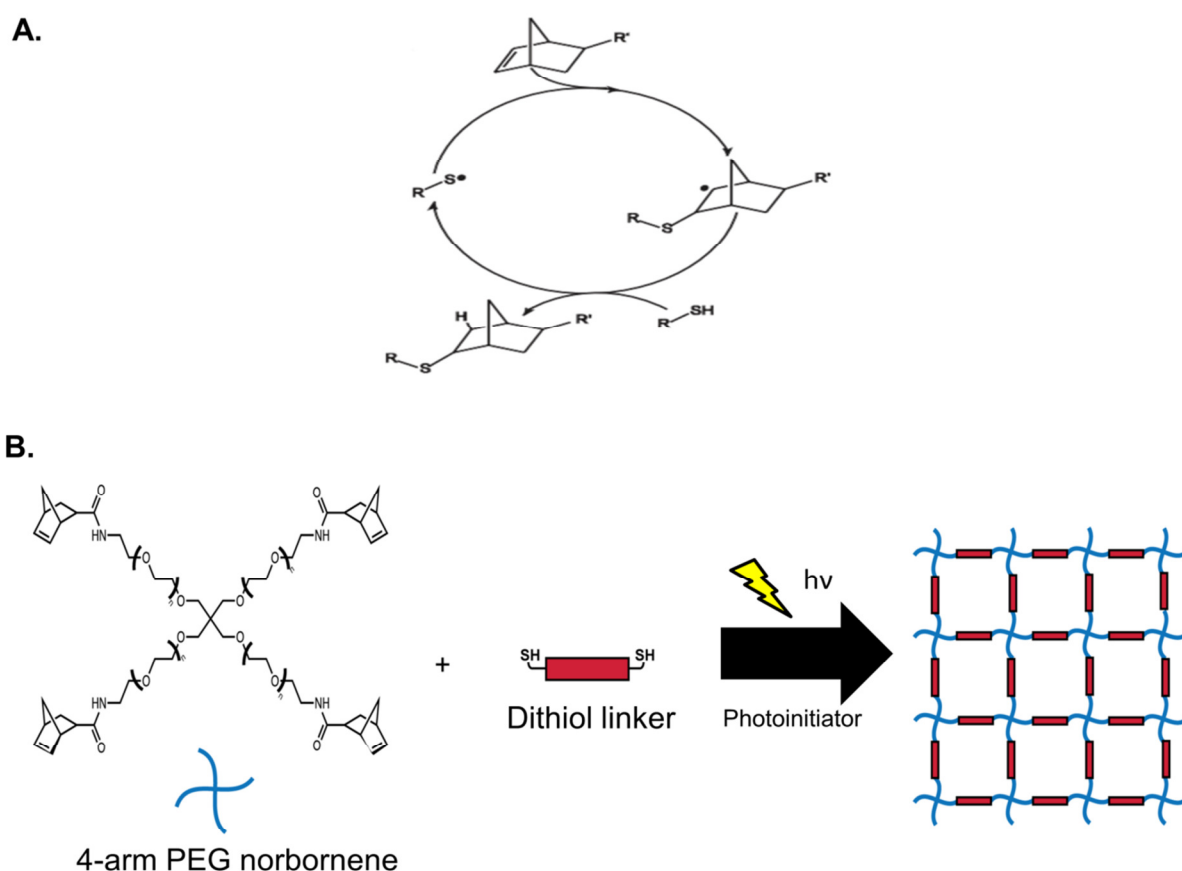


Figure 1.6. Thiol Norbornene Photopolymerization (A) Mechanism of thiol-ene polymerization. An initiator abstracts a hydrogen atom from a thiol group, the resulting thiyl radical propagates across the norbornene double bond and the resulting norbornene radical abstracts a hydrogen atom from another thiol completing the bond formation and regenerating a thiyl radical. Image modified from Fairbanks, B. D. *et al.* A Versatile Synthetic Extracellular Matrix Mimic via Thiol-Norbornene Photopolymerization. *Adv. Mater.* (B) Example of step-growth photopolymerization between multi-arm PEG-norbornene and a dithiol linker. Light-activated initiation results in the formation of

homogeneous networks.

A potential problem with long-term presence of PEG hydrogel in the body is that it can induce a foreign body reaction, which initiates an adverse inflammatory response,¹⁷⁵ and can then inhibit ECM deposition.¹⁷⁶ Therefore, approaches have evolved to render PEG gels degradable.

A common approach to degrading PEG hydrogels is to incorporate hydrolytically-degradable linkers, especially those that cleave at physiological pH. PLA is often grafted from linear PEGs, and subsequently end-functionalized with reaction groups, to create hydrogels with hydrolytically cleavable crosslinks.¹⁶³ The rate of degradation in the gel can be tuned, to a degree, by varying the number PLA repeats in the starting macromere (e.g. PLA-b-PEG-b-PLA), and has been shown to influence ECM deposition.¹⁷⁷ However, the gels degrade via a bulk mechanism with a rate that is engineering a priori. Bulk degradation correlates with an exponentially decaying modulus and increasing swelling,^{178,179} without enough gel erosion to allow collagen assembly. This renders the process of engineering the material for cartilage regeneration, a delicate trial and error process. Thus, recent work established in the Anseth group, exploits thiol-ene chemistry to create cellularly-degradable hydrogels.

Synthetic PEG hydrogels that can be degraded by a local and cell-mediated process provides numerous advantages for a chondrocyte carrier. Enzymatically-sensitive peptide sequences derived from natural materials, like collagen, can be modified so that they can be incorporated as crosslinks into PEG hydrogels. Hubbell *et al.* investigated one of the first PEG hydrogel system that incorporated a collagenase-sensitive linkers,¹⁸⁰ which eventually led to improved tissue engineering outcomes with encapsulated cells.^{181,182} However, research towards designing these types of hydrogels for chondrocytes has been limited. Park *et al.* encapsulated

bovine chondrocytes in a PEG scaffold crosslinked with an MMP-sensitive peptide that increased type II collagen and aggrecan gene expression, but matrix deposition was restricted to the pericellular space.¹⁸³ Other naturally-derived peptides can be used as linkers in this system in an attempt to match MMP secretion by chondrocytes to other cell types. In the case of the PEG-thiol-ene reaction, the peptide linkers are simply designed to include bis-cysteines (dithiol) so they can cross-link multi-arm PEG norbornene monomers. The gel degradation can be tailored to respond to the appropriate cell type at an appreciable rate by varying the sequence composition, or the connectivity of the network.¹⁸⁴ Peptide linkers are often advantageous since they are short sequences that can be easily incorporated into hydrogels; however, the efficiency and accessibility of the degradation site can be a confounding factor. For this reason, full-length proteins such as collagen, or its denatured form gelatin have multiple degradation sites and sequences, which can provide a compliment to peptide linkers.

1.4.2.3. Synthetic-natural material hybrid scaffolds

An advantage of synthetic materials is that their physical properties can be controlled to match the needs of a tissue type, but their synthetic nature renders them with a limited capacity to present bioactive signals to cells. On the other hand, natural materials derived from the ECM provide numerous biological cues to promote cell function, but are often inferior in terms of their mechanical properties and reproducibility. Hence, tissue engineering scaffolds that integrate the desired control of synthetic polymers with the biological activity of natural ECM are favorable. Ultimately, such hybrid gel should be able to promote ECM-like interactions between cells and the matrix, be susceptible to cell-mediated degradation, and provide improved control over structural and mechanical properties.

Seliktar *et al.* provided one of the early examples of protein-polymer conjugates to form hydrogels for tissue engineering purposes using PEGylated collagen.^{185,186} To date, combinations of hybrid gels have been investigated for tissue engineering purposes including PEG-collagen,¹⁸⁷ PEG-proteoglycan,¹⁸⁸ PEG-fibrinogen,¹⁸⁹ and PEG-albumin.¹⁸⁶ Additionally, gelatin, a partial derivative of collagen, has relatively low antigenicity compared to its precursor, yet still retain signals that promote adhesion, and proliferation.¹⁹⁰ It is also far less expensive to manufacture than collagen.¹⁹¹ PEG-gelatin has been implemented in tissue engineering applications,^{192,193} and appears to be a good candidate scaffold to use in cartilage engineering. Collectively, studies have revealed that hybrid materials impart more user control of network formation compared to purely natural materials.

Numerous hydrogel scaffolds have been synthesized from natural matrix components and rendered biofunctional by including both synthetic and natural materials. But biological cues extend beyond the matrix, and numerous growth factors are sequestered in the ECM or secreted by cells. Thus, methods to introduce biologic cues in scaffolds also include those that locally present diffusible signals in a variety of ways.

1.4.3. Bioactive factors and their incorporation

Many synthetic hydrogels have well-defined chemical and mechanical properties; however, they contain no epitopes for biorecognition or must rely on non-specific protein adsorptions for signaling. Bioactive molecules of interest for cartilage regeneration include growth factors, adhesion peptides, or any entity that binds to cells or cell-secreted ECM to create a biological response. *In vitro* investigations typically deliver soluble growth factors as a media additive when culturing cell-laden constructs,¹⁹⁴ but this approach has limited applicability *in*

vivo, as one does not have local control of the fluid surrounding the implant. Thus, a variety of ways have evolved to incorporate biological factors into scaffolds, localizing their presentation and sustaining the signaling.

Since most hydrogels used for encapsulating chondrocytes have a relatively large mesh size, this often leads to rapid diffusion of many bioactive signals (e.g., <10 kDa in size) and not a sustained presentation. Thus, one approach to delivering bioactive molecules in hydrogel scaffolds is to entrap growth factors in polymeric carriers, such as PLGA microspheres, which can steadily release its payload over time to neighboring cells when co-encapsulated in a gel.¹⁹⁵ Other strategies involve covalently binding bioactive molecules throughout the hydrogel in a manner that allows cell signaling. This approach leads to local and persistent signaling, and also mimics aspects of how growth factors are sequestered in the native ECM. Numerous synthetic scaffolds are amenable to chemical modifications to tether protein or peptide signaling molecules. For example, the fibronectin derived adhesion peptide, CRGDS, is routinely incorporated into gel networks. RGDS facilitates cell adhesion through integrin binding, which typically promotes cell survival and function.^{196,197} A second example involves tethering of a full protein. PEG gels with covalently tethered TGF- β 1 and encapsulated MSCs,¹⁹⁸ or chondrocytes¹⁹⁹ displayed enhanced levels of cartilage matrix synthesis. However, a limitation to covalent conjugation is that one must ensure that the activity and availability of the signal are not compromised. As a result, more recent work has utilized affinity binding systems. Here, biotinylated basic fibroblast growth factor (bFGF) immobilized to PEG can react with diffusible streptavidin to control how the peptide signal is presented to encapsulated cells,²⁰⁰ or bFGF can be directly incorporated into the network and bind to diffusible bFGF-specific peptides.²⁰¹

The strategy of controllably presenting growth factors is particularly attractive because it can greatly decrease the quantity of growth factors required, and allow for local presentation in a clinical setting. With a wide variety of cell sources, scaffolds, and bioactive factors available, the potential combinations are numerous, and this section has served as a general overview of the various strategies and directions that have been reported in the literature related to the broad field of cartilage tissue engineering research.

1.5. Current Challenges in Cartilage Tissue Engineering

While many advances have been made in the field of cartilage tissue engineering, there are still a number of design challenges to overcome before these techniques can be successfully employed in the clinic. One of the major challenges in designing a scaffold is that it should have a high enough compressive and shear modulus to withstand forces found in the joint. However, in tissue-engineered constructs, the best cartilaginous matrix deposition has typically occurred in relatively soft hydrogels. Studies investigating the effect of gel crosslink density on matrix production by encapsulated cells found that scaffolds with lower crosslinking densities, and correspondingly weaker mechanical properties, best supported ECM deposition in both PEG gels^{165,202} and HA gels.²⁰³ Part of the reason this occurs is because there is not as much physical restriction placed in the pericellular space of loosely crosslinked networks to limit large matrix molecule transport. A potential solution to this problem is to shoulder the implant into the cartilage defect, by placing it in such a way that it does not experience the majority of the mechanical impact, at least initially. Another potential approach is to encapsulate cells in a degradable gel with a high initial modulus that can withstand mechanical forces, but would degrade over time to permit matrix deposition.¹⁷⁷ However, this approach requires a difficult optimization and one that depends on the cell source, age of the cells, cell type, size of the defect,

et cetera. This is part of the reason that cellularly degradable matrices have gained traction in the field, as the bulk gel properties are somewhat independent of the local cellular environment and its degradational remodeling. However, challenges still exist in understanding the complex dynamics of protease secretion, how it is elevated and inhibited, and knowing which linkers will be most susceptible to cleavage, or at least at a rate that coordinates with matrix deposition.

Another challenge with designing scaffolds for cartilage regeneration is that chondrocytes have low metabolic activity and secrete lower amounts of ECM in constructs compared to native tissue equivalents over long periods of time. Some studies have shown that the collagen content in engineered constructs only reaches 15-35% of healthy levels after 5-12 weeks of culture.^{204,205} This issue warrants special consideration as to whether or not the scaffold functionality could be altered to stimulate the secretory properties of chondrocytes. Furthermore, scaffolds need to be modified to sequester cell-secreted matrix components, as some studies have shown that significant amounts of sulfated GAGs can be lost from the construct and into the culture medium.^{206,207} Some ways to address this issue have been to incorporate large biomimetic molecules, such as collagen or hyaluronan, into scaffolds to bind other ECM components, but these have had limited success.²⁰⁸ In a joint environment, this issue may not be relevant, as some of the matrix molecules from the construct might integrate with the host tissue and a significant fraction of the scaffold would be surrounded by dense cartilage tissue. But, experiments have not been performed to address this issue, and it remains a challenge to the field. In summary, much progress has been made in tissue engineering cartilage, but several key hurdles remain to be addressed. This section has highlighted a few major factors with the goal of providing an overview of the key design challenges. These design challenges helped provide insight into the specific aims and approach to this thesis research.

1.6. Research Summary

The advent of matrix-assisted autologous chondrocyte transplantation (MACT) brings the opportunity to tailor biomaterial scaffolds to introduce bioactive cues that might direct implanted autologous chondrocytes.²⁰⁹ The ultimate goal is to develop a scaffold that would improve upon current MACT constructs to facilitate cartilage regeneration and improve clinical outcomes for patients. In this thesis, PEG-based scaffolds are used, not only because they have been used to improve cartilage regeneration outcomes in human trials,²¹⁰ but also because this chemistry can be tuned readily to incorporate bioactive molecules, introduce degradable linkers, and even incorporate large protein molecules; all of which can be modified to alter the chondrocyte microenvironment in beneficial ways.

Chapter 2 outlines the global hypothesis and specific objectives that will be addressed in this thesis. Briefly, the first objective focuses on comparing the effect of presenting a chondro-inductive growth factor, TGF- β 1, into PEG hydrogels via covalent tethering or soluble delivery method (Chapter 3). The ability of local TGF- β 1 presentation to signal to encapsulated chondrocytes by influencing proliferation and matrix production will be investigated. The second objective then examines the development of multifunctional PEG gels (Chapter 4). A cellularly degradable crosslinker is introduced into the PEG hydrogels, along with tethered TGF- β 1, and the production of the matrix molecules is quantified while distribution of the ECM is qualitatively and quantitatively assessed. The third objective then investigates the degradation behavior of full-length gelatin molecules, which have been crosslinked with PEG, in response to chondrocyte-secreted enzymes and its effect on ECM distribution (Chapter 5). It is important to engineer a hydrogel that degrades in response to local, cell-mediated cues so that bulk scaffold mechanical properties are kept intact while also permitting cartilage-specific ECM secretion.

Future directions to improve cartilage engineering scaffolds would focus on tailoring the hydrogel to degrade more effectively in response to chondrocyte-secreted enzymes. Chapter 6 summarizes the overall conclusions from the work presented in the thesis, and provides future recommendations that may further aid in developing tunable hydrogels for cartilage tissue engineering and their ultimate adaptation for clinical use.

1.7. References

1. Manicourt, D. H., Devogelaer, J. P. & Thonar, E. J. in *Dyn. Bone Cartil. Metab.* (Seibel, M., Robins, S. P. & Bilezikian, J. P.) 421–439 (Elsevier Science, 2006).
2. Buckwalter, J. A. *et al.* Soft-tissue aging and musculoskeletal function. *J. Bone Joint Surg. Am.* **75**, 1533–48 (1993).
3. Robins, S. P. in *Dyn. Bone Cartil. Metab.* (Seibel, Markus J. Robins, Simon P, Bilezikian, J. P.) 41–51 (Elsevier Science, 2006).
4. Ross, M. & Wojciech, P. *Histology: A Text and Atlas.* (Lippincott, Williams, & Wilkins, 2010).
5. Mueller, Michael B. Tuan, R. S. Anabolic/Catabolic Balance in Pathogenesis of Osteoarthritis: Identifying Molecular Targets. *PM&R* **3**, S3–S11 (2011).
6. Hootman, J. M. & Helmick, C. G. Projections of US prevalence of arthritis and associated activity limitations. *Arthritis Rheum.* **54**, 226–9 (2006).
7. Hunziker, E. B. Articular cartilage repair: basic science and clinical progress. A review of the current status and prospects. *Osteoarthr. Cartil.* **10**, 432–63 (2002).
8. Hall, B. K. Earliest evidence of cartilage and bone development in embryonic life. *Clin. Orthop. Relat. Res.* 255–72 (1987).
9. Moore, K. L., Persaud, T. V. N. & Torchia, M. G. in *Dev. Hum. Clin. Oriented Embryol.* (Elsevier, 2011).
10. Yin, H., Price, F. & Rudnicki, M. A. Satellite cells and the muscle stem cell niche. *Physiol. Rev.* **93**, 23–67 (2013).
11. Athanasiou, K., Darling, E. & Hu, J. Articular Cartilage Tissue Engineering. *Synth. Lect. Tissue Eng.* **1**, 1–182 (2009).

12. Ateshian, G. A. & Hung, C. T. in *Funct. Tissue Eng.* (Guliak, F Butler, DL Goldstein, SA Mooney, D.) 46–68 (Springer-Verlag, 2003).
13. Erggelet, C. & Mandelbaum, B. R. in *Princ. Cartil. Repair* 1–5 (Springer-Verlag, 2008).
14. Coimbra, I. B., Jimenez, S. A., Hawkins, D. F., Piera-Velazquez, S. & Stokes, D. G. Hypoxia inducible factor-1 alpha expression in human normal and osteoarthritic chondrocytes. *Osteoarthritis Cartilage* **12**, 336–45 (2004).
15. Ng, S. S. *et al.* Biomechanical study of the edge outgrowth phenomenon of encapsulated chondrocytic isogenous groups in the surface layer of hydrogel scaffolds for cartilage tissue engineering. *Acta Biomater.* **8**, 244–52 (2012).
16. Archer, C., McDowell, J., Bayliss, M., Stephens, M. & Bentley, G. Phenotypic modulation in sub-populations of human articular chondrocytes in vitro. *J. Cell Sci.* **97**, 361–371 (1990).
17. Mansour, J. M. in *Kinesiol. Mech. Pathomechanics Hum. Mov.* (Oatis, C. A.) 66–75 (Lippincott, Williams, & Wilkins, 2003).
18. Ateshian, G. A., Lai, W. M., Zhu, W. B. & Mow, V. C. An asymptotic solution for the contact of two biphasic cartilage layers. *J. Biomech.* **27**, 1347–1360 (1994).
19. Sabatini, M., Pastoureau, P. & Ceuninck De, F. *Cartilage and Osteoarthritis*. (Humana Press, 2004).
20. Guilak, F., Setton, L. & Kraus, V. in *Princ. Pract. Orthop. Sport. Med.* (Garrett, W., Speer, K. & Kirkendall, D.) 1057–1064 (Lippincott, Williams, & Wilkins, 2000).
21. Sophia Fox, A. J., Bedi, A. & Rodeo, S. A. The basic science of articular cartilage: structure, composition, and function. *Sports Health* **1**, 461–8 (2009).
22. Martel-Pelletier, J., Boileau, C., Pelletier, J.-P. & Roughley, P. J. Cartilage in normal and osteoarthritis conditions. *Best Pract. Res. Clin. Rheumatol.* **22**, 351–84 (2008).
23. Hardingham, T. & Fosang, A. Proteoglycans: many forms and many functions. *FASEB J* **6**, 861–870 (1992).
24. Boskey, A. L., Wright, T. M. & Blank, R. D. Collagen and bone strength. *J. Bone Miner. Res.* **14**, 330–5 (1999).
25. Bruckner, P. & van der Rest, M. Structure and function of cartilage collagens. *Microsc. Res. Tech.* **28**, 378–84 (1994).
26. Eyre, D. Collagen of articular cartilage. *Arthritis Res.* **4**, 30–5 (2002).

27. Von der Mark, K. & Sorokin, L. M. in *Connect. Tissue its Heritable Disord.* (Royce, P. M. & Steinmann, B.) 293–328 (Wiley-Liss, 2002).
28. Berg, R. A. & Prockop, D. J. The thermal transition of a non-hydroxylated form of collagen. Evidence for a role for hydroxyproline in stabilizing the triple-helix of collagen. *Biochem. Biophys. Res. Commun.* **52**, 115–120 (1973).
29. Kivirikko, K. I. & Myllyharju, J. Prolyl 4-hydroxylases and their protein disulfide isomerase subunit. *Matrix Biol.* **16**, 357–368 (1998).
30. Edwards, C. A. & O'Brien, W. D. Modified assay for determination of hydroxyproline in a tissue hydrolyzate. *Clin. Chim. Acta* **104**, 161–167 (1980).
31. Smith-Mungo, L. I. & Kagan, H. M. Lysyl oxidase: Properties, regulation and multiple functions in biology. *Matrix Biol.* **16**, 387–398 (1998).
32. Tuderman, L. & Prockop, D. J. Procollagen N-Proteinase. Properties of the Enzyme Purified from Chick Embryo Tendons. *Eur. J. Biochem.* **125**, 545–549 (1982).
33. Olsen, B. R. in *Cell Biol. Extracell. Matrix* (Hay, E. D.) 139–177 (Plenum Press, 1981).
34. Mayne, R. Cartilage collagens. What Is Their Function, and Are They Involved in Articular Disease? *Arthritis Rheum.* **32**, 241–246 (1989).
35. Byers, P. H. Molecular genetics of chondrodysplasias, including clues to development, structure, and function. *Curr. Opin. Rheumatol.* **6**, 345–350 (1994).
36. Von der Mark, K. Localization of collagen types in tissues. *Int. Rev. Connect. Tissue Res.* **9**, 265–324 (1981).
37. De Visser, S. K. *et al.* Anisotropy of collagen fibre alignment in bovine cartilage: comparison of polarised light microscopy and spatially resolved diffusion-tensor measurements. *Osteoarthritis Cartilage* **16**, 689–97 (2008).
38. Zipfel, W. R. *et al.* Live tissue intrinsic emission microscopy using multiphoton-excited native fluorescence and second harmonic generation. *Proc. Natl. Acad. Sci. U. S. A.* **100**, 7075–80 (2003).
39. Guilak, F. *et al.* The pericellular matrix as a transducer of biomechanical and biochemical signals in articular cartilage. *Ann. N. Y. Acad. Sci.* **1068**, 498–512 (2006).
40. Aigner, T. *et al.* Type X collagen expression in osteoarthritic and rheumatoid articular cartilage. *Virchows Arch. B Cell Pathol. Incl. Mol. Pathol.* **63**, 205–211 (1993).
41. Von der Mark, K. in *Dyn. Bone Cartil. Metab.* (Seibel, M. ., Robins, S. P. & Bilezikian, J. P.) 3–40 (Elsevier, 2006).

42. Hay, E. D. in *Cell Biol. Extracell. Matrix* (Hay, E. D.) 379–409 (Plenum Press, 1981).
43. Mandelbaum, B. R. *et al.* Articular Cartilage Lesions of the Knee. *Am. J. Sport. Med.* **26**, 853–861 (1998).
44. Aigner, T., Bertling, W., Stöss, H., Weseloh, G. & von der Mark, K. Independent expression of fibril-forming collagens I, II, and III in chondrocytes of human osteoarthritic cartilage. *J. Clin. Invest.* **91**, 829–37 (1993).
45. Heinegard, D., Lorenzo, P. & Saxne, T. in *Dyn. Bone Cartil. Metab.* (Seibel, M., Robins, S. P. & Bilezikian, J. P.) 71–73 (Elsevier, 2006).
46. Mow, V. & Setton, L. in *Osteoarthritis* (Brandt, K. D., Doherty, M. & Lohmander, L. S.) 108–122 (Oxford University Press Inc., 1998).
47. Hall, A., Horwitz, E. & Wilkins, R. The cellular physiology of articular cartilage. *Exp Physiol* **81**, 535–545 (1996).
48. Knudson, C. B. & Knudson, W. Cartilage proteoglycans. *Semin. Cell Dev. Biol.* **12**, 69–78 (2001).
49. Buckwalter, J. A. & Rosenberg, L. C. Electron Microscopic Studies of Cartilage Proteoglycans. *J. Biol. Chem.* 9830–9839 (1981).
50. Knudson, C. B. Hyaluronan Receptor-Directed Assembly of Chondrocyte Pericellular Matrix. *J. Cell Biol.* 825–834 (1993).
51. Forsyth, C. B. *et al.* Increased matrix metalloproteinase-13 production with aging by human articular chondrocytes in response to catabolic stimuli. *J. Gerontol. A. Biol. Sci. Med. Sci.* **60**, 1118–24 (2005).
52. Mok, S. S., Masuda, K., Hauselmann, H. J., Aydelotte, M. B. & Thonar, E. J. M. A. Aggrecan Synthesized by Mature Bovine Chondrocytes Suspended in Alginate associated matrix and the further removed matrix. *J. Biol. Chem.* **269**, 33021–33027 (1994).
53. Häuselmann, H. J. *et al.* Adult human chondrocytes cultured in alginate form a matrix similar to native human articular cartilage. *Am. J. Physiol.* **271**, C742–52 (1996).
54. Grimshaw, M. J. & Mason, R. M. Modulation of bovine articular chondrocyte gene expression in vitro by oxygen tension. *Osteoarthritis Cartilage* **9**, 357–64 (2001).
55. Nesic, D. *et al.* Cartilage tissue engineering for degenerative joint disease. *Adv. Drug Deliv. Rev.* **58**, 300–22 (2006).
56. Clark, I. M. & Murphy, G. in *Dyn. Bone Cartil. Metab.* (Seibel, M. J., Robins, S. P. & Bilezikian, J. P.) 181–198 (Elsevier, 2006).

57. Wu, W. *et al.* Sites of collagenase cleavage and denaturation of type II collagen in aging and osteoarthritic articular cartilage and their relationship to the distribution of matrix metalloproteinase 1 and matrix metalloproteinase 13. *Arthritis Rheum.* **46**, 2087–94 (2002).
58. Knauper, V., Lopez-Otin, C., Smith, B., Knight, G. & Murphy, G. Biochemical Characterization of Human Collagenase-3. *J. Biol. Chem.* **271**, 1544–1550 (1996).
59. Mehraban, F., Lark, M. W., Ahmed, F. N., Xu, F. & Moskowitz, R. W. Increased secretion and activity of matrix metalloproteinase-3 in synovial tissues and chondrocytes from experimental osteoarthritis. *Osteoarthritis Cartilage* **6**, 286–94 (1998).
60. Chubinskaya, S. Chondrocyte Matrix Metalloproteinase-8. *J. Biol. Chem.* **271**, 11023–11026 (1996).
61. Stanton, H., Ung, L. & Fosang, A. The 45 kDa collagen-binding fragment of fibronectin induces matrix metalloproteinase-13 synthesis by chondrocytes and aggrecan degradation by aggrecanases. *Biochem. J.* **364**, 181–190 (2002).
62. Baker, A. H., Edwards, D. R. & Murphy, G. Metalloproteinase inhibitors: biological actions and therapeutic opportunities. *J. Cell Sci.* 3719–3727 (2002).
63. Goldberg, G. I., Strongin, A., Collier, I. E., Genrich, L. T. & Marmer, B. L. Interaction of 92-kDa type IV collagenase with the tissue inhibitor of metalloproteinases prevents dimerization, complex formation with interstitial collagenase, and activation of the proenzyme with stromelysin. *J. Biol. Chem.* **267**, 4583–4591 (1992).
64. Murphy, G. *et al.* The N-terminal domain of tissue inhibitor of metalloproteinases retains metalloproteinase inhibitory activity. *Biochemistry* **30**, 8097–8102 (1991).
65. Edwards, D. R. *et al.* in *Inhib. Met. Dev. Dis.* (Hawkes, S. P., Edwards, D. R. & Khokha, R.) 13–25 (Harwood Academic Press, 2000).
66. Poole, A. *et al.* Proteolysis of the collagen fibril in osteoarthritis. *Biochem. Soc. Symp.* 115–123 (2003).
67. Hashimoto, S., Ochs, R. L., Komiya, S. & Lotz, M. Linkage of chondrocyte apoptosis and cartilage degradation in human osteoarthritis. *Arthritis Rheum.* **41**, 1632–8 (1998).
68. Billingham, R. C., Mwale, F., Hollander, A., Ionescu, M. & Poole, A. R. Immunoassays for collagens in chondrocyte and cartilage explant cultures. *Methods Mol. Med.* **100**, 251–74 (2004).
69. Eyre, D. R. *et al.* in *Chem. Biol. Miner. Tissues* (Goldber, M., Boskey, A. & Robinson, C.) 347–350 (American Academy of Orthopedic Surgeons, 2000).

70. Gómez-Guillén, M. C. *et al.* Fish gelatin: a renewable material for developing active biodegradable films. *Trends Food Sci. Technol.* **20**, 3–16 (2009).
71. Cole, B. Gelatin. *Encycl. Food Sci. Technol.* (1999).
72. Masters, K. S. Covalent growth factor immobilization strategies for tissue repair and regeneration. *Macromol. Biosci.* **11**, 1149–63 (2011).
73. Darling, E. M. & Athanasiou, K. A. in *Biomed. Technol. devices handbook*. (Moore, J. E. & Zouridakis, G.) (CRC Press, 2004).
74. Reddi, A. H. Role of morphogenetic proteins in skeletal tissue engineering and regeneration. *Nat. Biotechnol.* **16**, 247–52 (1998).
75. Takigawa, M., Kimura, Y. & Takahashi, K. The basic effect of IGF on chondrocytes. *Clin. Pediatr. Endocrinol.* (1997).
76. Vanosch, G., Vandenberg, W., Hunziker, E. & Hausselmann, H. Differential effects of IGF-1 and TGFbeta-2 on the assembly of proteoglycans in pericellular and territorial matrix by cultured bovine articular chondrocytes. *Osteoarthr. Cartil.* **6**, 187–195 (1998).
77. Hulley, P., Russell, G. & Croucher, P. in *Dyn. Bone Cartil. Metab.* (Seibel, M. J., Robins, S. P. & Bilezikian, J. P.) 99–107 (Elsevier, 2006).
78. Lyons, R. M. Mechanism of activation of latent recombinant transforming growth factor beta 1 by plasmin. *J. Cell Biol.* **110**, 1361–1367 (1990).
79. Bassing, C. *et al.* A transforming growth factor beta type I receptor that signals to activate gene expression. *Science (80-.)*. **263**, 87–89 (1994).
80. Alevizopoulos, A. & Mermoud, N. Transforming growth factor-beta: the breaking open of a black box. *Bioessays* **19**, 581–91 (1997).
81. Nakao, A. *et al.* TGF-beta receptor-mediated signalling through Smad2, Smad3 and Smad4. *EMBO J.* **16**, 5353–62 (1997).
82. Derynck, R. *et al.* Human transforming growth factor-beta complementary DNA sequence and expression in normal and transformed cells. *Nature* **316**, 701–5 (1985).
83. Zhou, S., Eid, K. & Glowacki, J. Cooperation between TGF-beta and Wnt pathways during chondrocyte and adipocyte differentiation of human marrow stromal cells. *J. Bone Miner. Res.* **19**, 463–70 (2004).
84. Scharstuhl, A., Vitters, E. L., van der Kraan, P. M. & van den Berg, W. B. Reduction of osteophyte formation and synovial thickening by adenoviral overexpression of

- transforming growth factor beta/bone morphogenetic protein inhibitors during experimental osteoarthritis. *Arthritis Rheum.* **48**, 3442–51 (2003).
85. Li, T., O’Keefe, R. & Chen, D. TGF- β signaling in chondrocytes. *Front. Biosci.* 681–688 (2005).
 86. Buckwalter, J. A. Articular Cartilage Injuries. *Clin. Orthop. Relat. Res.* 21–37 (2002).
 87. Erggelet, C. & Mandelbaum, B. R. in *Princ. Cartil. Repair* 7–17 (Springer-Verlag, 2008).
 88. Reddy, A. S. & Frederick, R. W. Evaluation of the Intraosseous and Extraosseous Blood Supply to the Distal Femoral Condyles. *Am. J. Sport. Med.* **26**, 415–419 (1998).
 89. Furukawa, T., Eyre, D. R., Koide, S. & Glimcher, M. J. Biochemical Studies on Repair Cartilage Resurfacing Experimental Defects in the Rabbitt Knee. *J. Bone Jt. Surgery-American Vol.* **1**, 79–89 (1980).
 90. Buckwalter, J. A., Mankin, H. J. & Grodzinsky, A. J. Articular cartilage and osteoarthritis. in *AAOS Instr. Course Lect.* 465–480 (2005).
 91. Gelber, A. C. Joint Injury in Young Adults and Risk for Subsequent Knee and Hip Osteoarthritis. *Ann. Intern. Med.* **133**, 321 (2000).
 92. Dean, D. D., Martel-Pelletier, J., Pelletier, J. P., Howell, D. S. & Woessner, J. F. Evidence for metalloproteinase and metalloproteinase inhibitor imbalance in human osteoarthritic cartilage. *J. Clin. Invest.* **84**, 678–85 (1989).
 93. Lawrence, R. C. *et al.* Estimates of the prevalence of arthritis and selected musculoskeletal disorders in the United States. *Arthritis Rheum.* **41**, 778–99 (1998).
 94. O’Driscoll, S. W. The healing and regeneration of articular cartilage. *J. Bone Joint Surg. Am.* **80**, 1795–812 (1998).
 95. Oei, E. H. G., van Tiel, J., Robinson, W. H. & Gold, G. E. Quantitative radiological imaging techniques for articular cartilage composition: Towards early diagnosis and development of disease-modifying therapeutics for osteoarthritis. *Arthritis Care Res. (Hoboken)*. (2014). doi:10.1002/acr.22316
 96. Gomoll, A. H. *et al.* Surgical treatment for early osteoarthritis. Part I: cartilage repair procedures. *Knee Surg. Sports Traumatol. Arthrosc.* **20**, 450–66 (2012).
 97. Rambani, R. & Venkatesh, R. Current concepts in articular cartilage repair. *J. Arthrosc. Jt. Surg.* (2014). doi:10.1016/j.jajs.2014.06.003
 98. Pascual-Garrido, C., Moran, C. J., Green, D. W. & Cole, B. J. Osteochondritis dissecans of the knee in children and adolescents. *Curr. Opin. Pediatr.* 46–51 (2013).

99. Erggelet, C. & Mandelbaum, B. R. in *Princ. Cartil. Repair* 29–36 (Springer-Verlag, 2008).
100. Goldberg, V. M. & Buckwalter, J. A. Hyaluronans in the treatment of osteoarthritis of the knee: evidence for disease-modifying activity. *Osteoarthritis Cartilage* **13**, 216–24 (2005).
101. Lu, Y. *et al.* Thermal chondroplasty with bipolar and monopolar radiofrequency energy. *Arthrosc. J. Arthrosc. Relat. Surg.* **18**, 779–788 (2002).
102. Levy, A. S., Lohnes, J., Sculley, S., LeCroy, M. & Garrett, W. Chondral Delamination of the Knee in Soccer Players. *Am. J. Sports Med.* **24**, 634–639 (1996).
103. Mollon, B., Kandel, R., Chahal, J. & Theodoropoulos, J. The clinical status of cartilage tissue regeneration in humans. *Osteoarthritis Cartilage* 1–10 (2013).
104. Marcacci, M. *et al.* Arthroscopic autologous osteochondral grafting for cartilage defects of the knee: prospective study results at a minimum 7-year follow-up. *Am. J. Sports Med.* **35**, 2014–21 (2007).
105. Wood, J. J. *et al.* Autologous cultured chondrocytes: adverse events reported to the United States Food and Drug Administration. *J. Bone Joint Surg. Am.* **88**, 503–7 (2006).
106. Vanlauwe, J. *et al.* Repair of symptomatic cartilage lesions of the knee: the place of autologous chondrocyte implantation. *Acta Orthop. Belgium* 145–158 (2007).
107. Pridie, K. & Gordon, G. A method of resurfacing osteoarthritic knee joints. *J. Bone Jt. Surgery-British Vol.* **41**, 618–9 (1959).
108. Steadman, J. R. *et al.* Outcomes of microfracture for traumatic chondral defects of the knee: average 11-year follow-up. *Arthroscopy* **19**, 477–84 (2003).
109. Mithoefer, K., McAdams, T., Williams, R. J., Kreuz, P. C. & Mandelbaum, B. R. Clinical efficacy of the microfracture technique for articular cartilage repair in the knee: an evidence-based systematic analysis. *Am. J. Sports Med.* **37**, 2053–63 (2009).
110. Hoemann, C. D. *et al.* Chitosan-glycerol phosphate/blood implants improve hyaline cartilage repair in ovine microfracture defects. *J. Bone Joint Surg. Am.* **87**, 2671–86 (2005).
111. Erggelet, C. *et al.* Formation of cartilage repair tissue in articular cartilage defects pretreated with microfracture and covered with cell-free polymer-based implants. *J. Orthop. Res.* **27**, 1353–60 (2009).
112. Fortin, P. R. *et al.* Outcomes of total hip and knee replacement: preoperative functional status predicts outcomes at six months after surgery. *Arthritis Rheum.* **42**, 1722–8 (1999).

113. McNickle, A., Provencher, M. & Cole, B. Overview of existing cartilage repair technology. *Sports Med. Arthrosc.* **4**, 196–201 (2008).
114. Liao, I.-C., Moutos, F. T., Estes, B. T., Zhao, X. & Guilak, F. Tissue Engineering: Composite Three-Dimensional Woven Scaffolds with Interpenetrating Network Hydrogels to Create Functional Synthetic Articular Cartilage. *Adv. Funct. Mater.* **23**, 5825–5825 (2013).
115. Gomoll, A. H. *et al.* Surgical treatment for early osteoarthritis. Part II: allografts and concurrent procedures. *Knee Surg. Sports Traumatol. Arthrosc.* **20**, 468–86 (2012).
116. Richardson, J. B., Caterson, B., Evans, E. H., Ashton, B. A. & Roberts, S. Repair of human articular cartilage after implantation of autologous chondrocytes. *J Bone Jt. Surg Br* **81-B**, 1064–1068 (1999).
117. Gillogly, S. D. & Myers, T. H. Treatment of full-thickness chondral defects with autologous chondrocyte implantation. *Orthop. Clin. North Am.* **36**, 433–46 (2005).
118. Brittberg, M. & Lindahl, A. Treatment of deep cartilage defects in the knee with autologous chondrocyte transplantation. *N. Engl. J. Med.* **331**, 889–895 (1994).
119. Roberts, S., McCall, I. & Darby, A. Autologous chondrocyte implantation for cartilage repair: monitoring its success by magnetic resonance imaging and histology. *Arthritis Res. Ther.* **5**, 60–73 (2003).
120. Kurkijärvi, J. E. *et al.* Evaluation of cartilage repair in the distal femur after autologous chondrocyte transplantation using T2 relaxation time and dGEMRIC. *Osteoarthritis Cartilage* **15**, 372–8 (2007).
121. Peterson, L., Brittberg, M., Kiviranta, I., Akerlund, E. L. & Lindahl, A. Autologous Chondrocyte Transplantation: Biomechanics and Long-Term Durability. *Am. J. Sport. Med.* **30**, 2–12 (2002).
122. Huey, D., Hu, J. & Athanasiou, K. Unlike Bone, Cartilage Regeneration Remains Elusive. *Science (80-.)*. **6933**, 917–921 (2012).
123. Worthen, J., Waterman, B. R., Davidson, P. A. & Lubowitz, J. H. Limitations and sources of bias in clinical knee cartilage research. *Arthroscopy* **28**, 1315–25 (2012).
124. Adkisson, H. D. *et al.* The potential of human allogeneic juvenile chondrocytes for restoration of articular cartilage. *Am. J. Sports Med.* **38**, 1324–33 (2010).
125. Marlovits, S., Zeller, P., Singer, P., Resinger, C. & Vécsei, V. Cartilage repair: generations of autologous chondrocyte transplantation. *Eur. J. Radiol.* **57**, 24–31 (2006).

126. Barbero, A. *et al.* Age related changes in human articular chondrocyte yield, proliferation and post-expansion chondrogenic capacity. *Osteoarthr. Cartil.* **12**, 476–84 (2004).
127. Schnabel, M. *et al.* Dedifferentiation-associated changes in morphology and gene expression in primary human articular chondrocytes in cell culture. *Osteoarthr. Cartil.* **10**, 62–70 (2002).
128. Tuan, R. S. Stemming cartilage degeneration: adult mesenchymal stem cells as a cell source for articular cartilage tissue engineering. *Arthritis Rheum.* **54**, 3075–8 (2006).
129. Mauck, R. L., Byers, B. A., Yuan, X. & Tuan, R. S. Regulation of cartilaginous ECM gene transcription by chondrocytes and MSCs in 3D culture in response to dynamic loading. *Biomech. Model. Mechanobiol.* **6**, 113–25 (2007).
130. Erickson, I. E. *et al.* Differential maturation and structure-function relationships in mesenchymal stem cell- and chondrocyte-seeded hydrogels. *Tissue Eng. Part A* **15**, 1041–52 (2009).
131. Steck, E. *et al.* Induction of intervertebral disc-like cells from adult mesenchymal stem cells. *Stem Cells* **23**, 403–11 (2005).
132. Koga, H., Engebretsen, L., Brinchmann, J. E., Muneta, T. & Sekiya, I. Mesenchymal stem cell-based therapy for cartilage repair: a review. *Knee Surg. Sports Traumatol. Arthrosc.* **17**, 1289–97 (2009).
133. Richardson, S. M. *et al.* Mesenchymal stem cells in regenerative medicine: opportunities and challenges for articular cartilage and intervertebral disc tissue engineering. *J. Cell. Physiol.* **222**, 23–32 (2010).
134. Guilak, F., Awad, H. A., Fermor, B., Leddy, H. A. & Gimple, J. A. Adipose-derived adult stem cells for cartilage tissue engineering. *Biorheology* 389–399 (2004).
135. Koay, E. J., Hoben, G. M. B. & Athanasiou, K. A. Tissue engineering with chondrogenically differentiated human embryonic stem cells. *Stem Cells* **25**, 2183–90 (2007).
136. Drukker, M. & Benvenisty, N. The immunogenicity of human embryonic stem-derived cells. *Trends Biotechnol.* **22**, 136–41 (2004).
137. Diekman, B. O. *et al.* Cartilage tissue engineering using differentiated and purified induced pluripotent stem cells. *Proc. Natl. Acad. Sci.* **109**, (2012).
138. Saha, S., Kirkham, J., Wood, D., Curran, S. & Yang, X. Comparative study of the chondrogenic potential of human bone marrow stromal cells, neonatal chondrocytes and adult chondrocytes. *Biochem. Biophys. Res. Commun.* **401**, 333–8 (2010).

139. Bian, L., Zhai, D. Y., Mauck, R. L. & Burdick, J. A. Coculture of Human Mesenchymal Stem Cells and Enhances Functional Properties of Engineered Cartilage Reverse primer. *Tissue Eng. Part A* **17**, 1137–1145 (2011).
140. Tsuchiya, K., Chen, G., Ushida, T., Matsuno, T. & Tateishi, T. The effect of coculture of chondrocytes with mesenchymal stem cells on their cartilaginous phenotype in vitro. *Mater. Sci. Eng. C* **24**, 391–396 (2004).
141. Dahlin, R. L. *et al.* Articular chondrocytes and mesenchymal stem cells seeded on biodegradable scaffolds for the repair of cartilage in a rat osteochondral defect model. *Biomaterials* **35**, 7460–7469 (2014).
142. Hubka, K. M., Dahlin, R. L., Meretoja, V. V., Kasper, K. & Mikos, A. G. Enhancing Chondrogenic Phenotype for Cartilage Tissue Engineering: Monoculture and Co-culture of Articular Chondrocytes and Mesenchymal Stem Cells. *Tissue Eng. Part B* 1–50 (2014).
143. Lai, J. H., Kajiya, G., Smith, R. L., Maloney, W. & Yang, F. Stem cells catalyze cartilage formation by neonatal articular chondrocytes in 3D biomimetic hydrogels. *Sci. Rep.* **3**, 1–9 (2013).
144. Darling, E. M. & Athanasiou, K. A. Retaining zonal chondrocyte phenotype by means of novel growth environments. *Tissue Eng.* **11**, 395–403 (2005).
145. Hunter, C. Dynamic compression of chondrocyte-seeded fibrin gels: effects on matrix accumulation and mechanical stiffness. *Osteoarthr. Cartil.* **12**, 117–130 (2004).
146. Liu, Y., Shu, X. Z. & Prestwich, G. D. Osteochondral defect repair with autologous bone marrow-derived mesenchymal stem cells in an injectable, in situ, cross-linked synthetic extracellular matrix. *Tissue Eng.* **12**, 3405–16 (2006).
147. Nehrer, S. *et al.* Canine chondrocytes seeded in type I and type II collagen implants investigated in vitro. *J. Biomed. Mater. Res.* **38**, 95–104 (1997).
148. Omobono, M. A. *et al.* Enhancing the stiffness of collagen hydrogels for delivery of encapsulated chondrocytes to articular lesions for cartilage regeneration. *J. Biomed. Mater. Res. Part A* 1–7 (2014). doi:10.1002/jbm.a.35266
149. Zhao, W., Jin, X., Cong, Y., Liu, Y. & Fu, J. Degradable natural polymer hydrogels for articular cartilage tissue engineering. *J. Chem. Technol. Biotechnol.* **88**, 327–339 (2013).
150. Nicodemus, G. D. & Bryant, S. J. Cell encapsulation in biodegradable hydrogels for tissue engineering applications. *Tissue Eng. Part B. Rev.* **14**, 149–65 (2008).
151. Burdick, J. A., Chung, C., Jia, X., Randolph, M. A. & Langer, R. Controlled degradation and mechanical behavior of photopolymerized hyaluronic acid networks. *Biomacromolecules* **6**, 386–91 (2005).

152. Buschmann, M. D., Gluzband, Y. A., Grodzinsky, A. J., Kimura, J. H. & Hunziker, E. B. Chondrocytes in agarose culture synthesize a mechanically functional extracellular matrix. *J. Orthop. Res.* **10**, 745–58 (1992).
153. Augst, A. D., Kong, H. J. & Mooney, D. J. Alginate hydrogels as biomaterials. *Macromol. Biosci.* **6**, 623–33 (2006).
154. Hong, Y. *et al.* Covalently crosslinked chitosan hydrogel: properties of in vitro degradation and chondrocyte encapsulation. *Acta Biomater.* **3**, 23–31 (2007).
155. Burdick, J. A. & Prestwich, G. D. Hyaluronic acid hydrogels for biomedical applications. *Adv. Mater.* **23**, H41–56 (2011).
156. Mauck, R. L. *et al.* Functional Tissue Engineering of Articular Cartilage Through Dynamic Loading of Chondrocyte-Seeded Agarose Gels. *J. Biomech. Eng.* **122**, 252–260 (2000).
157. Kelly, T.-A. N., Ng, K. W., Wang, C. C.-B., Ateshian, G. A. & Hung, C. T. Spatial and temporal development of chondrocyte-seeded agarose constructs in free-swelling and dynamically loaded cultures. *J. Biomech.* **39**, 1489–97 (2006).
158. Athanasiou, K. Sterilization, toxicity, biocompatibility and clinical applications of polylactic acid/ polyglycolic acid copolymers. *Biomaterials* **17**, 93–102 (1996).
159. Athanasiou, K., Agrawal, C., Barber, F. & Burkhart, S. Orthopaedic applications for PLA-PGA biodegradable polymers. *Arthrosc. J. Arthrosc. Relat. Surg.* **14**, 726–737 (1998).
160. Yoon, D. . & Fisher, J. P. Chondrocyte signaling and artificial matrices for articular cartilage engineering. *Adv. Exp. Med. Biol.* **585**, 67–86 (2006).
161. Chen, G. *et al.* The use of a novel PLGA fiber/collagen composite web as a scaffold for engineering of articular cartilage tissue with adjustable thickness. *J. Biomed. Mater. Res. A* **67**, 1170–80 (2003).
162. Slaughter, B. V, Khurshid, S. S., Fisher, O. Z., Khademhosseini, A. & Peppas, N. A. Hydrogels in regenerative medicine. *Adv. Mater.* **21**, 3307–29 (2009).
163. Ifkovits, J. L. & Burdick, J. A. Review: photopolymerizable and degradable biomaterials for tissue engineering applications. *Tissue Eng.* **13**, 2369–85 (2007).
164. Bryant, S. J., Durand, K. L. & Anseth, K. S. Manipulations in hydrogel chemistry control photoencapsulated chondrocyte behavior and their extracellular matrix production. *J. Biomed. Mater. Res. A* **67**, 1430–6 (2003).

165. Bryant, S. J. & Anseth, K. S. Hydrogel properties influence ECM production by chondrocytes photoencapsulated in poly(ethylene glycol) hydrogels. *J. Biomed. Mater. Res.* **59**, 63–72 (2002).
166. Azagarsamy, M. A. & Anseth, K. S. Bioorthogonal Click Chemistry: An Indispensable Tool to Create Multifaceted Cell Culture Scaffolds. *ACS Macro Lett.* **2**, 5–9 (2013).
167. Sanborn, T. J., Messersmith, P. B. & Barron, A. E. In situ crosslinking of a biomimetic peptide-PEG hydrogel via thermally triggered activation of factor XIII. *Biomaterials* **23**, 2703–2710 (2002).
168. Lutolf, M. P. & Hubbell, J. A. Synthesis and physicochemical characterization of end-linked poly(ethylene glycol)-co-peptide hydrogels formed by Michael-type addition. *Biomacromolecules* **4**, 713–22 (2003).
169. Lin, C.-C., Sawicki, S. M. & Metters, A. T. Free-radical-mediated protein inactivation and recovery during protein photoencapsulation. *Biomacromolecules* **9**, 75–83 (2008).
170. Nguyen, K. T. & West, J. L. Photopolymerizable hydrogels for tissue engineering applications. *Biomaterials* **23**, 4307–14 (2002).
171. Nuttelman, C. R. *et al.* Macromolecular Monomers for the Synthesis of Hydrogel Niches and Their Application in Cell Encapsulation and Tissue Engineering. *Prog. Polym. Sci.* **33**, 167–179 (2008).
172. Kloxin, A. M., Kloxin, C. J., Bowman, C. N. & Anseth, K. S. Mechanical properties of cellularly responsive hydrogels and their experimental determination. *Adv. Mater.* **22**, 3484–94 (2010).
173. Fairbanks, B. D. *et al.* A Versatile Synthetic Extracellular Matrix Mimic via Thiol-Norbornene Photopolymerization. *Adv. Mater.* **21**, 5005–5010 (2009).
174. Roberts, J. J. & Bryant, S. J. Comparison of photopolymerizable thiol-ene PEG and acrylate-based PEG hydrogels for cartilage development. *Biomaterials* (2013).
175. Lynn, A. D., Blakney, A. K., Kyriakides, T. R. & Bryant, S. J. Temporal progression of the host response to implanted poly(ethylene glycol)-based hydrogels. *J. Biomed. Mater. Res. A* **96**, 621–31 (2011).
176. Nicodemus, G. D., Skaalure, S. C. & Bryant, S. J. Gel structure has an impact on pericellular and extracellular matrix deposition, which subsequently alters metabolic activities in chondrocyte-laden PEG hydrogels. *Acta Biomater.* **7**, 492–504 (2011).
177. Bryant, S. J., Bender, R. J., Durand, K. L. & Anseth, K. S. Encapsulating chondrocytes in degrading PEG hydrogels with high modulus: engineering gel structural changes to facilitate cartilaginous tissue production. *Biotechnol. Bioeng.* **86**, 747–55 (2004).

178. Metters, A. T., Anseth, K. S. & Bowman, C. N. Fundamental studies of a novel, biodegradable PEG-b-PLA hydrogel. *Polymer (Guildf)*. **41**, 3993–4004 (2000).
179. Anseth, K. S. *et al.* In situ forming degradable networks and their application in tissue engineering and drug delivery. *J. Control. Release* **78**, 199–209 (2002).
180. West, J. L. & Hubbell, J. A. Polymeric Biomaterials with Degradation Sites for Proteases Involved in Cell Migration. *Macromolecules* **32**, 241–244 (1999).
181. Lutolf, M. P. *et al.* Synthetic matrix metalloproteinase-sensitive hydrogels for the conduction of tissue regeneration: engineering cell-invasion characteristics. *Proc. Natl. Acad. Sci. U. S. A.* **100**, 5413–8 (2003).
182. Lutolf, M. P., Raeber, G. P., Zisch, A. H., Tirelli, N. & Hubbell, J. A. Cell-Responsive Synthetic Hydrogels. *Adv. Mater.* **15**, 888–892 (2003).
183. Park, Y., Lutolf, M. P., Hubbell, J. A., Hunziker, E. B. & Wong, M. Bovine Primary Chondrocyte Culture in Synthetic Matrix Hydrogels as a Scaffold for Cartilage Repair. *Tissue Eng.* **10**, 515–522 (2004).
184. Patterson, J. & Hubbell, J. A. Enhanced proteolytic degradation of molecularly engineered PEG hydrogels in response to MMP-1 and MMP-2. *Biomaterials* **31**, 7836–45 (2010).
185. Mironi-Harpaz, I., Wang, D. Y., Venkatraman, S. & Seliktar, D. Photopolymerization of cell-encapsulating hydrogels: crosslinking efficiency versus cytotoxicity. *Acta Biomater.* **8**, 1838–48 (2012).
186. Gonen-Wadmany, M., Oss-Ronen, L. & Seliktar, D. Protein-polymer conjugates for forming photopolymerizable biomimetic hydrogels for tissue engineering. *Biomaterials* **28**, 3876–86 (2007).
187. Singh, R. K., Seliktar, D. & Putnam, A. J. Capillary morphogenesis in PEG-collagen hydrogels. *Biomaterials* **34**, 9331–40 (2013).
188. Appelman, T. P., Mizrahi, J., Elisseeff, J. H. & Seliktar, D. The influence of biological motifs and dynamic mechanical stimulation in hydrogel scaffold systems on the phenotype of chondrocytes. *Biomaterials* **32**, 1508–16 (2011).
189. Almany, L. & Seliktar, D. Biosynthetic hydrogel scaffolds made from fibrinogen and polyethylene glycol for 3D cell cultures. *Biomaterials* **26**, 2467–77 (2005).
190. Ito, A. *et al.* Transglutaminase-mediated gelatin matrices incorporating cell adhesion factors as a biomaterial for tissue engineering. *J. Biosci. Bioeng.* **95**, 196–199 (2003).

191. Lien, S.-M., Ko, L.-Y. & Huang, T.-J. Effect of pore size on ECM secretion and cell growth in gelatin scaffold for articular cartilage tissue engineering. *Acta Biomater.* **5**, 670–9 (2009).
192. Mazaki, T. *et al.* A novel, visible light-induced, rapidly cross-linkable gelatin scaffold for osteochondral tissue engineering. *Sci. Rep.* **4**, 4457 (2014).
193. Daniele, M. A., Adams, A. A., Naciri, J., North, S. H. & Ligler, F. S. Interpenetrating networks based on gelatin methacrylamide and PEG formed using concurrent thiol click chemistries for hydrogel tissue engineering scaffolds. *Biomaterials* **35**, 1845–56 (2014).
194. Byers, B. A., Mauck, R. L., Chiang, I. E. & Tuan, R. S. Transient exposure to transforming growth factor beta 3 under serum-free conditions enhances the biomechanical and biochemical maturation of tissue-engineered cartilage. *Tissue Eng. Part A* **14**, 1821–34 (2008).
195. Park, H., Temenoff, J. S., Holland, T. A., Tabata, Y. & Mikos, A. G. Delivery of TGF-beta1 and chondrocytes via injectable, biodegradable hydrogels for cartilage tissue engineering applications. *Biomaterials* **26**, 7095–103 (2005).
196. Salinas, C. N. & Anseth, K. S. The influence of the RGD peptide motif and its contextual presentation in PEG gels on human mesenchymal stem cell viability. *J. Tissue Eng. Regen. Med.* **2**, 296–304 (2008).
197. Salinas, C. N. & Anseth, K. S. The enhancement of chondrogenic differentiation of human mesenchymal stem cells by enzymatically regulated RGD functionalities. *Biomaterials* **29**, 2370–7 (2008).
198. McCall, J. D., Luoma, J. E. & Anseth, K. S. Covalently tethered transforming growth factor beta in PEG hydrogels promotes chondrogenic differentiation of encapsulated human mesenchymal stem cells. *Drug Deliv. Transl. Res.* **2**, 305–312 (2012).
199. Sridhar, B. V, Doyle, N. R., Randolph, M. A. & Anseth, K. S. Covalently tethered TGF- β 1 with encapsulated chondrocytes in a PEG hydrogel system enhances extracellular matrix production. *J. Biomed. Mater. Res. A* **102**, 4464–4472 (2014).
200. Lin, C.-C. & Anseth, K. S. Controlling Affinity Binding with Peptide-Functionalized Poly(ethylene glycol) Hydrogels. *Adv. Funct. Mater.* **19**, 2325 (2009).
201. Lin, C.-C. & Anseth, K. S. PEG hydrogels for the controlled release of biomolecules in regenerative medicine. *Pharm. Res.* **26**, 631–43 (2009).
202. Bryant, S. J., Chowdhury, T. T., Lee, D. A., Bader, D. L. & Anseth, K. S. Crosslinking Density Influences Chondrocyte Metabolism in Dynamically Loaded Photocrosslinked Poly(ethylene glycol) Hydrogels. *Ann. Biomed. Eng.* **32**, 407–417 (2004).

203. Chung, C., Beecham, M., Mauck, R. L. & Burdick, J. A. The influence of degradation characteristics of hyaluronic acid hydrogels on in vitro neocartilage formation by mesenchymal stem cells. *Biomaterials* **30**, 4287–96 (2009).
204. Eyrich, D. *et al.* In vitro and in vivo cartilage engineering using a combination of chondrocyte-seeded long-term stable fibrin gels and polycaprolactone-based polyurethane scaffolds. *Tissue Eng.* **13**, 2207–18 (2007).
205. Miot, S. *et al.* Cartilage tissue engineering by expanded goat articular chondrocytes. *J. Orthop. Res.* **24**, 1078–85 (2006).
206. Villanueva, I., Klement, B. J., von Deutsch, D. & Bryant, S. J. Cross-linking density alters early metabolic activities in chondrocytes encapsulated in poly(ethylene glycol) hydrogels and cultured in the rotating wall vessel. *Biotechnol. Bioeng.* **102**, 1242–50 (2009).
207. Kisiday, J. D., Jin, M., DiMicco, M. A., Kurz, B. & Grodzinsky, A. J. Effects of dynamic compressive loading on chondrocyte biosynthesis in self-assembling peptide scaffolds. *J. Biomech.* **37**, 595–604 (2004).
208. Roberts, J. J., Nicodemus, G. D., Giunta, S. & Bryant, S. J. Incorporation of biomimetic matrix molecules in PEG hydrogels enhances matrix deposition and reduces load-induced loss of chondrocyte-secreted matrix. *J. Biomed. Mater. Res. A* **97**, 281–91 (2011).
209. Kon, E. *et al.* Matrix-assisted autologous chondrocyte transplantation for the repair of cartilage defects of the knee: systematic clinical data review and study quality analysis. *Am. J. Sports Med.* **37**, 1565–665 (2009).
210. Sharma, B. *et al.* Human cartilage repair with a photoreactive adhesive-hydrogel composite. *Sci. Transl. Med.* **5**, 167–173 (2013).

OBJECTIVES

2.1. Overview

Cartilage tissue defects remain an elusive challenge to repair in a clinical setting. Healing focal cartilage lesions when they are found early is paramount to preventing the onset of osteoarthritis and the resulting debilitating joint pain in an increasingly aging population. Autologous cell-based tissue engineering treatment options seem promising for regenerating cartilage in defects; however, techniques like autologous chondrocyte transplantation (ACT) have yielded unsatisfactory long-term results.¹ As detailed in Chapter 1, newer techniques have emerged to improve upon current cartilage lesion treatment options. One example is matrix-assisted autologous chondrocyte transplantation (MACT), which involves encapsulating chondrocytes into scaffolds that provide a nurturing microenvironment and influence primary cells to produce a native tissue equivalent. A 5-year clinical study with collagen as a MACT scaffold showed symptom relief in 8 out of 11 patients,² but natural material constructs have batch variability and low biomechanical integrity.³ Hence, there is room for improvement on cartilage tissue engineering scaffold design to create a less variable, tunable, and longer-term solution that generates better clinical outcomes.

Synthetic poly-(ethylene glycol) (PEG) based hydrogels have been widely investigated within the field of regenerative medicine for cell encapsulation and delivery. They provide structured networks and spatiotemporally tunable properties that can be incorporated to improve upon current MACT techniques.^{4,5} Chondrocytes can generate cartilage-specific extracellular matrix (ECM) macromolecules, but since native tissue is avascular and aneural, there are no

bioactive signals to stimulate the regenerative capacity of these cells in a defect site.⁶ Thus, the focus of this thesis research is to utilize the easily tunable PEG hydrogel system to introduce bioactive cues to encapsulated cells, tailor their presentation, and ultimately create a scaffold that mimics the cartilage microenvironment to facilitate ECM deposition. Rationally chosen strategies to create bioactive PEG hydrogels are evaluated quantitatively and qualitatively *in vitro* to determine their utility as biofunctional MACT scaffolds. With the global objective of engineering a better scaffold in mind, three specific aims are outlined below to determine which formulations would permit and promote cartilage-specific ECM formation of encapsulated chondrocytes. The specific aims of this thesis are as follows:

2.2. Aim 1: Determine the effect of covalently tethered TGF- β 1 on chondrocyte proliferation and ECM production in non-degradable PEG hydrogels

PEG hydrogels permit sequestration of growth factors via covalent tethering, which can provide advantages compared to other forms of protein delivery.^{7,8} In particular, growth factors are typically cross-reactive with multiple cell types and can have short serum half-lives *in vitro*, limitations that often necessitate localized presentation.⁹ Therefore, strategies to immobilize growth factors in a bioactive, physiologically relevant context are a complementary and important step towards directing cells to regenerate cartilage tissue. Previously, transforming growth factor β isoform 1 (TGF- β 1) has been shown to increase chondrocyte proliferation and cartilage ECM production in both three-dimensional¹⁰ and two-dimensional studies.¹¹ Building from this work, the primary goal of Aim 1 is to demonstrate that local presentation of TGF- β 1 can stimulate encapsulated chondrocyte proliferation and ECM production.

In accordance to this objective, we will use a robust thiol-ene chemistry to incorporate thiolated proteins in PEG hydrogels. We will quantify the effects of covalently attaching the

chondro-inductive TGF- β 1 into a homogenous PEG thiol-ene system and its efficacy on stimulating chondrocytes compared to soluble delivery. Confirmation that TGF- β 1 is conjugated in the PEG network and distributed homogeneously will be performed via section ELISA. We further will confirm that the tethered protein is bioactive and investigate a range of concentrations in both delivery forms that yields maximal bioactivity using a cell reporter system. Subsequently, we study the long-term effects of localized tethered growth factor presentation on chondrocyte cellularity with a combination of DNA content quantification and viability studies. Finally, long-term ECM production will be characterized using quantitative biochemical assays for sGAG and collagen, immunofluorescent staining for collagen typing, and histological staining for overall ECM distribution.

2.3. Aim 2: Develop a cellularly degradable PEG hydrogel with tethered growth factor to promote articular cartilage extracellular matrix deposition

A limitation with most MACT scaffolds is the resorption rate of the surrounding network does not necessarily match the rate of matrix deposition by encapsulated chondrocytes like what is observed in native tissue during the matrix turnover process.¹² In the case of many synthetic scaffolds, non-degradable constructs pericellularly limit matrix deposition.¹³ Hydrolytically degradable scaffolds permit tissue deposition in physiologically relevant environments, but bulk degradation decreases the mechanics of the network too rapidly where the inhabitant cell may not have enough time to generate tissue before the scaffold degrades.^{13,14} Therefore, a scaffold that can maintain its bulk mechanical properties and permit cell-mediated local degradation should facilitate ECM deposition of encapsulated cells.

Expanding upon the findings of Aim 1, the focus of Aim 2 is to develop a cell-specific enzyme-sensitive degradable platform with tethered TGF- β 1 to enhance ECM production of

chondrocytes compared to cells in non-degradable gels of the same formulation. We plan to demonstrate that encapsulated chondrocytes degrade the collagen-derived matrix metalloproteinase (MMP)-cleavable peptide crosslinker, KCGPQG↓IWGQCK (where the arrow denotes the cleavage site), by using a fluorescent peptide sensor comprised of the same sequence that can be tethered into the gel to monitor *in situ* cleavage.¹⁵ Further, we seek to utilize mesenchymal stem cells (MSCs), at smaller amounts, in co-culture with chondrocytes to aid in local degradation of the network, since MSCs have previously been shown to cleave this sequence at a relatively rapid rate.^{16,17} Cleavage of the sequence in co-culture will be measured using the fluorescent peptide sensor. We will verify that MSCs retain a rounded, chondrogenic phenotype in three-dimensional co-culture by tracking the cells and observing their morphology. Additionally, we will examine the cellularity in the gels by quantifying DNA content and assessing cell viability. Cartilage-specific ECM (sGAG and collagen) outputs of constructs will be quantified using conventional biochemical assays. ECM distribution will be observed by histological staining techniques, and functional mechanical properties of the scaffold will be monitored over time by measuring scaffold compressive modulus values. Finally, the collagen generated by the constructs will be qualitatively typed using immunofluorescent staining to verify that the ECM contains a more mechanically robust articular cartilage phenotype.

2.4. Aim 3: Develop and investigate use of a PEG-gelatin hybrid gel as a scaffold for cartilage engineering

Peptides derived from full-length proteins can be advantageous for tissue engineering because they are readily synthesized, short amino acid sequences that can be easily incorporated into a PEG backbone. Usually the sequences are designed to contain functional aspects of a native full protein (e.g., a specific site that is susceptible to enzyme cleavage, an integrin-binding

domain). However, in the case of the collagen-derived MMP-degradable linker used in Aim 2, encapsulated chondrocytes do not cleave this sequence at an appreciable rate, possibly because of its limited susceptibility to degradation by collagenases or the activity of the chondrocytes in secreting enzymes that specifically target MMPs. Therefore, a linker with a larger number of different cleavable sites may create more opportunities for chondrocyte-secreted enzymes to locally degrade the surrounding network and permit ECM expansion.

In Aim 3, we plan to combine the beneficial effects of synthetic and natural materials by forming a hybrid gel, which incorporates both PEG and a full-length gelatin molecule. This could make tethering growth factors unnecessary since gelatin also provides a nurturing environment with multiple sites to bind and present cell-secreted proteins.¹⁸ Furthermore, hybrid gels can form consistently under user-defined conditions with enhanced mechanical integrity compared to purely natural materials as shown in previous studies.^{19,20} We intend to measure the degradation properties of a full-length protein with the hypothesis that the protein-linked constructs permit chondrocyte-mediated cleavage of the network and lead to cartilage-specific ECM deposition.

We propose to use gelatin as part of the scaffold since it has been shown to degrade more readily than collagen in response to collagenase and has been previously used as a chondrocyte carrier for cartilage tissue engineering applications.²¹ Primary amines on gelatin will be modified to include norbornene functionalities, and utilizing a radical-initiated thiol-ene mechanism, PEG dithiol will be used to crosslink the gelatin-norbornene molecules to form a hydrogel network under cytocompatible conditions. Initially, the extent of norbornene functionalization of the gelatin will be measured using a TNBSA colorimetric assay that produces a color change when it reacts to primary amines. We will look into the ability to tune the macroscopic properties of the

scaffold by varying the norbornene functionality on gelatin and measuring the shear modulus of the resulting constructs. Degradation of the norbornene-functionalized gelatin in response to collagenases and chondrocyte-secreted enzymes will be assessed using gel permeation chromatography. Subsequently, chondrocytes will be encapsulated in selected hybrid gelatin formulations to permit facile local matrix degradation in response to chondrocyte-secreted enzymes. We plan to monitor chondrocyte cellularity, viability and morphology over time. Furthermore, production and deposition of chondrocyte-specific matrix macromolecules will be quantified by biochemical assays and assessed histologically to support the hypothesis that increased local degradation will permit diffuse ECM distribution. Finally, immunofluorescent staining will be used to type collagen in the cell-laden gels.

2.5. References

1. Bentley, G. *et al.* A prospective, randomized comparison of autologous chondrocyte implantation versus mosaicplasty for osteochondral defects in the knee. *J. Bone Jt. Surg.* **85**, 223–230 (2003).
2. Behrens, P., Bitter, T., Kurz, B. & Russlies, M. Matrix-associated autologous chondrocyte transplantation/implantation (MACT/MACI)--5-year follow-up. *Knee* **13**, 194–202 (2006).
3. Malafaya, P. B., Silva, G. A. & Reis, R. L. Natural-origin polymers as carriers and scaffolds for biomolecules and cell delivery in tissue engineering applications. *Adv. Drug Deliv. Rev.* **59**, 207–33 (2007).
4. Nguyen, K. T. & West, J. L. Photopolymerizable hydrogels for tissue engineering applications. *Biomaterials* **23**, 4307–14 (2002).
5. Elisseeff, J. *et al.* Photoencapsulation of chondrocytes in poly(ethylene oxide)-based semi-interpenetrating networks. *J. Biomed. Mater. Res.* **51**, 164–71 (2000).
6. Hunziker, E. B. Articular cartilage repair: basic science and clinical progress. A review of the current status and prospects. *Osteoarthr. Cartil.* **10**, 432–63 (2002).
7. Hume, P. S., He, J., Haskins, K. & Anseth, K. S. Strategies to reduce dendritic cell activation through functional biomaterial design. *Biomaterials* **33**, 3615–25 (2012).

8. Aimetti, A. A., Machen, A. J. & Anseth, K. S. Poly(ethylene glycol) hydrogels formed by thiol-ene photopolymerization for enzyme-responsive protein delivery. *Biomaterials* **30**, 6048–54 (2009).
9. Lee, S. J. Cytokine delivery and tissue engineering. *Yonsei Med. J.* **41**, 704–719 (2000).
10. Park, H., Temenoff, J. S., Holland, T. A., Tabata, Y. & Mikos, A. G. Delivery of TGF- β 1 and chondrocytes via injectable, biodegradable hydrogels for cartilage tissue engineering applications. *Biomaterials* **26**, 7095–103 (2005).
11. Li, T., O’Keefe, R. & Chen, D. TGF- β signaling in chondrocytes. *Front. Biosci.* 681–688 (2005).
12. Forsyth, C. B. *et al.* Increased matrix metalloproteinase-13 production with aging by human articular chondrocytes in response to catabolic stimuli. *J. Gerontol. A. Biol. Sci. Med. Sci.* **60**, 1118–24 (2005).
13. Nicodemus, G. D., Skaalure, S. C. & Bryant, S. J. Gel structure has an impact on pericellular and extracellular matrix deposition, which subsequently alters metabolic activities in chondrocyte-laden PEG hydrogels. *Acta Biomater.* **7**, 492–504 (2011).
14. Bryant, S. J. & Anseth, K. S. Hydrogel properties influence ECM production by chondrocytes photoencapsulated in poly(ethylene glycol) hydrogels. *J. Biomed. Mater. Res.* **59**, 63–72 (2002).
15. Leight, J. L., Alge, D. L., Maier, A. J. & Anseth, K. S. Direct measurement of matrix metalloproteinase activity in 3D cellular microenvironments using a fluorogenic peptide substrate. *Biomaterials* **34**, 7344–7352 (2013).
16. Kyburz, K. A. & Anseth, K. S. Three-dimensional hMSC motility within peptide-functionalized PEG-based hydrogels of varying adhesivity and crosslinking density. *Acta Biomater.* **9**, 6381–92 (2013).
17. Anderson, S. B., Lin, C.-C., Kuntzler, D. V & Anseth, K. S. The performance of human mesenchymal stem cells encapsulated in cell-degradable polymer-peptide hydrogels. *Biomaterials* **32**, 3564–74 (2011).
18. Zhao, W., Jin, X., Cong, Y., Liu, Y. & Fu, J. Degradable natural polymer hydrogels for articular cartilage tissue engineering. *J. Chem. Technol. Biotechnol.* (2012).
19. Fu, Y. *et al.* 3D cell entrapment in crosslinked thiolated gelatin-poly(ethylene glycol) diacrylate hydrogels. *Biomaterials* **33**, 48–58 (2012).
20. Daniele, M. A., Adams, A. A., Naciri, J., North, S. H. & Ligler, F. S. Interpenetrating networks based on gelatin methacrylamide and PEG formed using concurrent thiol click chemistries for hydrogel tissue engineering scaffolds. *Biomaterials* **35**, 1845–56 (2014).

21. Gorgieva, S. & Kokol, V. in *Biomater. Appl. Nanomedicine* (Pignatello, R.) 17–52 (InTech, 2011).

CHAPTER III

COVALENTLY TETHERED TGF- β 1 WITH ENCAPSULATED CHONDROCYTES IN A PEG HYDROGEL SYSTEM ENHANCES EXTRACELLULAR MATRIX PRODUCTION

As appearing in the Journal of biomedical materials research Part A 2014

3.1. Abstract

Healing articular cartilage defects remains a significant clinical challenge because of its limited capacity for self-repair. While delivery of autologous chondrocytes to cartilage defects has received growing interest, combining cell-based therapies with growth factor delivery that can locally signal cells and promote their function is often advantageous. We have previously shown that PEG thiol-ene hydrogels permit covalent attachment of growth factors. However, it is not well known if embedded chondrocytes respond to tethered signals over a long period. Here, chondrocytes were encapsulated in PEG hydrogels functionalized with transforming growth factor-beta 1 (TGF- β 1) with the goal of increasing proliferation and matrix production. Tethered TGF- β 1 was found to be distributed homogenously throughout the gel, and its bioactivity was confirmed with a TGF- β 1 responsive reporter cell line. Relative to solubly delivered TGF- β 1, chondrocytes presented with immobilized TGF- β 1 showed significantly increased DNA content and GAG and collagen production over 28 days, while maintaining markers of articular cartilage. These results indicate the potential of thiol-ene chemistry to covalently conjugate TGF- β 1 to PEG to locally influence chondrocyte function over 4 weeks. Scaffolds with other or multiple tethered growth factors may prove broadly useful in the design of chondrocyte delivery vehicles for cartilage tissue engineering applications.

3.2. Introduction

Healing articular cartilage defects remains a significant clinical challenge because of its limited capacity for self-repair and mechanical properties that are difficult to emulate.¹ Articular cartilage is an avascular tissue with a sparse population of cells surrounded by an extracellular matrix (ECM) that is regulated by numerous growth factors.² Therefore, tissue engineering strategies involving chondrocytes and growth factor delivery may help to improve the treatment of articular cartilage lesions.^{3,4}

There is growing interest in the regenerative medicine community in methods to sequester and present bioactive therapeutic proteins to chondrocytes immobilized in three-dimensional matrices.⁵ Cytokines are attractive targets for tissue engineering since, at low concentrations, they can regulate cellular functions, such as proliferation and matrix production.⁶ Many of these proteins are commonly introduced as soluble factors in culture media during *in vitro* experiments; however, *in vivo*, growth factors tend to be sequestered in the extracellular matrix, allowing local presentation to cells.⁵

A variety of natural and synthetic materials have been examined as potential cell carriers or as therapeutic agents for cartilage repair.^{7,8,9} Hydrogel scaffolds appear to be one promising class of materials, due to their high water content which mimics native tissue microenvironments.¹⁰ Furthermore, poly-(ethylene glycol) (PEG) hydrogels have been used to improve micofracture cartilage regeneration outcomes in human trials.¹¹

Hydrogel systems permit sequestration of growth factors via covalent tethering, which can provide advantages compared to other forms of protein delivery. In particular, growth factors are typically cross-reactive with multiple cell types and can have short serum half-lives *in vivo*,

limitations that often necessitate localized presentation.¹² Since diffusion of lower molecular weight proteins in hydrogels can be quite rapid, some researchers have used microparticles for controlled release presentation of growth factors to encapsulated chondrocytes.¹³ While this approach is quite useful, the process can increase the complexity of scaffold preparation and design. Variability can result from differences in protein loading, release kinetics, as well as the size distribution of loaded microparticles. Therefore, strategies to immobilize growth factors in a bioactive, physiologically relevant context are a complementary and important step towards directing cells to regenerate cartilage tissue.

As one robust method to create protein functionalized materials, we used thiol-ene chemistry to incorporate thiolated proteins in PEG hydrogels. Previously, PEG systems have been broadly explored for cell delivery applications.^{14,15,16,17} Specifically, we formed PEG hydrogels through a photoinitiated step-growth polymerization, by reacting norbornene-terminated PEG macromolecules with a dithiol PEG crosslinker.¹⁸ This photopolymerizable system allows for precise spatial and temporal control over polymer formation, as well as facile encapsulation of cells and biologics. The resulting crosslinked PEG hydrogel has been employed to encapsulate numerous primary cells with high survival rates following photoencapsulation.^{10,19}

Previously, our group has successfully incorporated thiolated TGF- β 1 in a chain-growth polymerized PEG diacrylate system and showed enhanced chondrogenesis of human mesenchymal stem cells (MSC).²⁰ Here, we encapsulated chondrocytes in step-growth polymerized PEG thiol-ene hydrogels, and we hypothesized that local presentation of TGF- β 1 would influence chondrocyte secretory properties and improve the system's application for cartilage regeneration. Step-growth polymerization leads to more ideal network structures than chain-growth polymerization, and the thiol-ene chemistry has also been shown to be more

compatible for coupling proteins and maintaining their activity.²¹ In contrast to other cell types, primary chondrocytes are a versatile cell source since they deposit a matrix more similar to articular cartilage. For example, MSC derived fibrocartilage is biomechanically inferior.²² Additionally, a recent comparison study revealed that encapsulating chondrocytes in a PEG thiol-ene system yielded more hyaline-like cartilage than cells encapsulated in a PEG diacrylate system.²³

In this work TGF- β 1 was thiolated and incorporated into a PEG thiol-ene hydrogel. We selected TGF- β 1 because it has been shown to increase chondrocyte proliferation and cartilage ECM production in both 3D¹³ and 2D studies.²⁴ We confirmed the presence of tethered TGF- β 1 in the gel by ELISA and investigated its bioactivity using a PE-25 cell reporter assay for SMAD2 signaling.²⁵ We also found that tethering growth factors to a scaffold results in increased cell proliferation and ECM production *in vitro*. These results suggest that a step-growth PEG hydrogel system is capable of tunable control of local bioactive signals. Chondrocytes encapsulated in this system are presented with a local and sustained delivery of TGF- β 1, resulting in enhanced cartilage tissue regeneration.

3.3. Materials and Methods

3.3.1. PEG monomer synthesis

8-arm polyethylene glycol (PEG) amine norbornene M_n 10,000 was synthesized as previously described.¹⁶ Briefly, 5-norbornene-2-carboxylic acid (predominantly endo isomer, Sigma Aldrich) was first converted to a dinorbornene anhydride using N,N'-dicyclohexylcarbodiimide (0.5 molar eq. to norbornene, Sigma Aldrich) in dichloromethane. The 8-arm PEG monomer (JenKem Technology USA) was then reacted overnight with the norbornene anhydride (5 molar eq. to PEG hydroxyls) in dichloromethane. Pyridine (5 molar eq.

to PEG hydroxyls) and 4-dimethylamino pyridine (0.05 molar eq. to PEG hydroxyls) were also included. The reaction was conducted at room temperature under argon. End group functionalization was verified by ^1H NMR to be >90%. ^1H NMR (500 MHz, CDCl_3) δ 6.30-5.80 (m, 16H), 4.0-3.0 (m, 1010H), 2.5-1.2 (m, 100H). The photoinitiator lithium phenyl-2,4,6-trimethylbenzoylphosphinate (LAP) was synthesized as described.¹⁹ The 3.5 kDa PEG dithiol linker was purchased from JenKem Technology.

3.3.2. Cell harvest and expansion

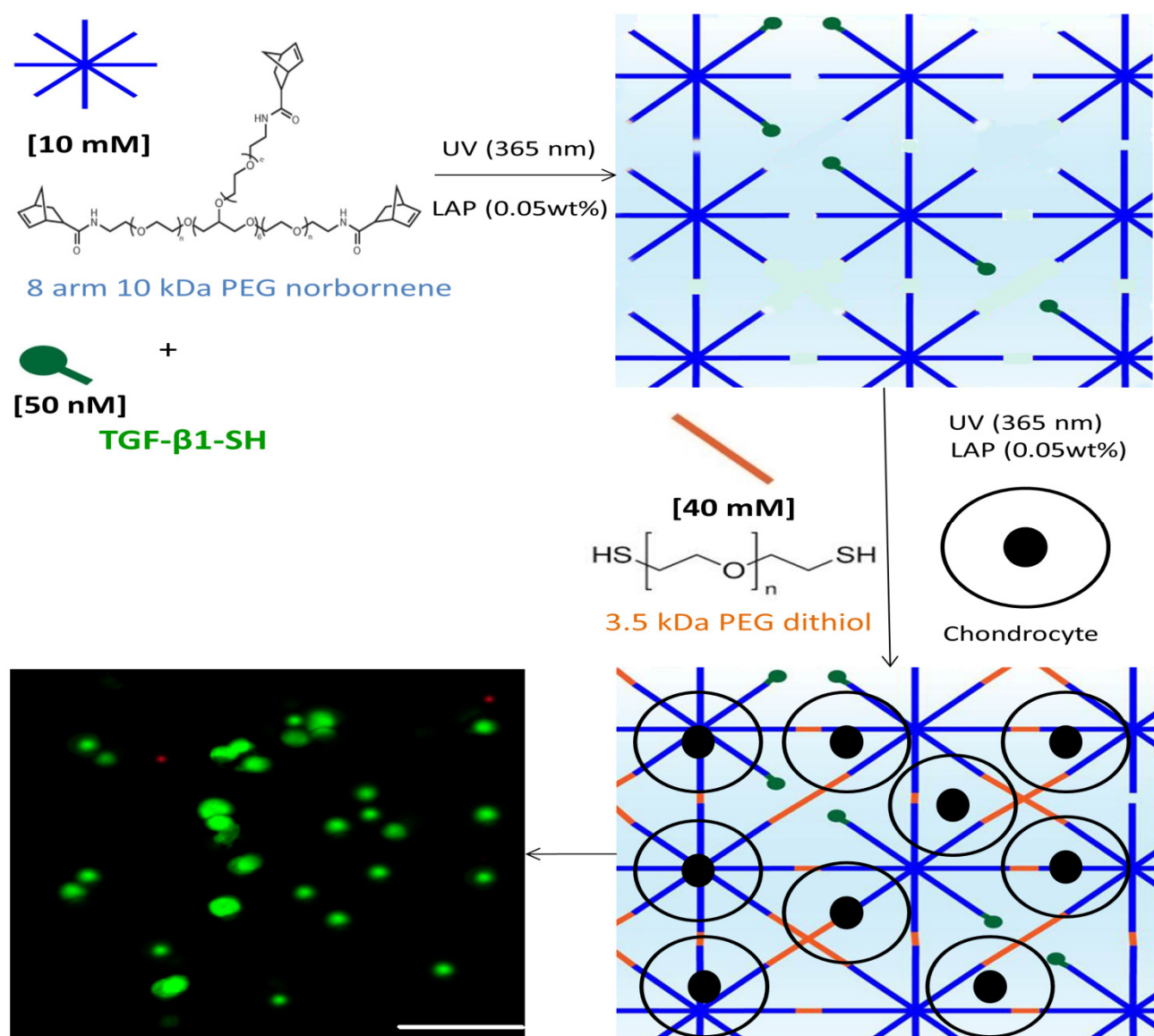
Primary chondrocytes were isolated from articular cartilage of the femoral-patellar groove of 6 month old Yorkshire swine as detailed previously.²⁶ Cells were grown in a culture flask in media as previously described.²⁷ Briefly, cells were grown in DMEM growth medium (phenol red, high glucose DMEM supplemented with ITS+Premix 1% v/v (BD Biosciences), 50 $\mu\text{g/mL}$ L-ascorbic acid 2-phosphate, 40 $\mu\text{g/mL}$ L-proline, 0.1 μM dexamethasone, 110 $\mu\text{g/mL}$ pyruvate, and 1% penicillin-streptomycin-fungizone with the addition of 10 ng/mL IGF-1 (Peprotech) to maintain cells in de-differentiated state. ITS promotes formation of hyaline cartilage over serum.²⁸ Cultures were maintained at 5% CO_2 and 37 °C.

Mink lung epithelial PE-25 cells containing a stably transfected luciferase reporter gene for TGF- β 1 were cultured in low glucose DMEM supplemented with 10% fetal bovine serum, and 1% penicillin-streptomycin-fungizone. Cells that were passaged three times were used in encapsulation experiments.

3.3.3. PEG hydrogel polymerization and growth factor incorporation

2-Iminothiolane (Pierce) was used to thiolate human TGF- β 1 (Peprotech). Briefly, 2-Iminothiolane was reacted at a 4:1 molar ratio to TGF β for 1 hour at RT. Thiolated TGF β was pre-reacted at various concentrations with PEG norbornene monomer solution prior to cross-

linking via photoinitiated polymerization with UV light ($I_0 \sim 3.5 \text{ mW/cm}^2$ at $\lambda = 365 \text{ nm}$) and 0.05 wt% LAP for 30 s. The monomer solution was then crosslinked with a 3.5 kDa PEG dithiol at a stoichiometric ratio of [40 mM dithiol]: [80 mM Norbornene] in a 10 wt% PEG solution using longwave ultraviolet light ($I_0 \sim 3.5 \text{ mW/cm}^2$ at $\lambda = 365 \text{ nm}$) for 30 s. (Scheme 3.1.)



Scheme 3.1. Pre-polymerization scheme with thiolated TGF-β1. Initially thiolated TGF-β1 is phototethered into the 8-arm 10 kDa PEG norbornene network, then the 3.5 kDa dithiol crosslinker is added in with chondrocytes to complete the encapsulation process. Growth factor is not drawn to scale. In featured experiments, there is a lower amount of growth factor attached to the monomer end. Chondrocytes seeded at 40 million cells/mL retain a rounded morphology similar to cells in native

tissue. Scale bar represents 50 μm .

3.3.4. Quantifying growth factor incorporation

10 wt% hydrogels were synthesized with tethered TGF- β 1 at 0, 10, 50, or 90 nM and prepared for cryosectioning as previously described.²⁹ Briefly, hydrogels were flash frozen in liquid nitrogen and placed in HistoPrep (Fisher Scientific) in cryomolds. 20 μm cross-sections along the plane of the construct were collected on SuperFrost® Plus Gold slides (Fisher Scientific).

40 μL disc-shaped gels (O.D. \sim 5 mm, thickness \sim 2 mm) without encapsulated cells and with varying concentrations of tethered growth factor were also prepared and sectioned. 20 μm sections were collected from the top, middle, and bottom of gel. To quantify the TGF- β concentration in each section, a modified ELISA was used as previously described.¹⁴ Briefly, sections were blocked for 1 hour at RT in 5% bovine serum albumin (BSA). Sections were washed 3x in ELISA buffer (0.01% BSA, & 0.05% Tween-20 in PBS) prior to incubation with a mouse anti-human TGF- β 1 antibody (Peprotech) at 1:100 dilution overnight at 4 $^{\circ}\text{C}$. Sections were washed again, then incubated with goat anti mouse-HRP (eBioscience) for 1 hour at RT and washed again. Sections were incubated with 100 μL of peroxidase and 3,3',5,5' tetramethylbenzidine substrate until color developed then the reaction was stopped using 100 μL 2 N sulfuric acid. The absorbance was measured at 450 nm using a Bio-Tek H1 spectrophotometer.

To calculate the theoretical loading of growth factor in each section, the volume was determined assuming the section was a thin disc with a 5 mm diameter and 20 μm height. Using $V = \pi r^2 h$ and the molecular weight of TGF- β 1 (M_n =25,000 g/mol), the amount of growth factor

per section was calculated in nanograms. For instance, a 50 nM 40 μ L gel section is expected to have 0.5 ng of TGF- β 1 per 20 μ m section assuming ideal conditions.

Finally, a standard curve was made simultaneously by prepping 96 well high binding clear plates with known amounts of TGF- β 1. The 0 nM value at 450 nm absorbance was subtracted out from all values in the curve.

3.3.5. TGF- β 1 bioactivity and cellular signaling

PE-25 cells were encapsulated in 10 wt% gels functionalized with a 1 mM Cys-Arg-Gly-Asp-Ser (CRGDS) peptide to promote survival. Thiolated TGF- β 1 was incorporated into the gel at 0, 12.5, 25, 50, or 100 nM. Additionally, cells encapsulated in PEG gels without tethered growth factor were exposed to soluble TGF- β 1 at concentrations of 0, 0.2, 0.3, 1, or 2 nM. Cells were photo-encapsulated at a density of 40 million cells/mL, and cell-laden hydrogels were formed in syringe tips at a volume of 40 μ L. Following encapsulation, hydrogels were placed into DMEM growth medium in 48 well plates and incubated overnight at 37 $^{\circ}$ C, 5% CO₂. Afterwards, hydrogels were incubated in Glo-Lysis buffer (Promega) for 10 min at 37 $^{\circ}$ C; the samples were centrifuged for 10 min (13,400 rpm, 4 $^{\circ}$ C), and the lysate was transferred to white 96 well plates (50 μ L per well). 50 μ L luciferase substrate (Promega) was added to the lysate for 5 min and luminescence was quantified between 300-700 nm.

3.3.6. Chondrocyte encapsulation in PEG thiol-ene hydrogels

Chondrocytes were encapsulated at 40 million cells/mL in 10 wt% monomer solution and thiolated TGF- β 1 at concentrations of 0 or 50 nM. 40 μ L cell-laden gels were immediately placed in 1 mL DMEM growth medium (without phenol red) in 48 well non-treated tissue culture plates. As a positive control, a subset group of gels without tethered growth factor was exposed to 0.3 nM (7.5 ng/mL) soluble TGF- β 1. Media was changed every 3 days. Samples were

collected at days 1, 14, and 28 for analysis of ECM production and chondrocyte proliferation. At day 1 and 28 cell viability was assessed using a LIVE/DEAD[®] membrane integrity assay and confocal microscopy.

3.3.7. Biochemical analysis of cell-hydrogel constructs

Cell-laden hydrogels were collected at specified time points, snap frozen in LN₂, and stored at -70 °C until analysis. Hydrogels were digested in enzyme buffer (125 µg/mL papain [Worthington Biochemical], and 10 mM cysteine) and homogenized using 5 mm steel beads in a TissueLyser (Qiagen). Homogenized samples were digested overnight at 60 °C.

DNA content was measured using a Picogreen assay (Invitrogen). Cell number was determined by assuming each cell produced 7.7 pg DNA per chondrocyte.³⁰ Sulfated glycosaminoglycan (GAG) content was assessed using a dimethyl methylene blue assay as previously described with results presented in equivalents of chondroitin sulfate.³¹ Collagen content in the gels was measured using a hydroxyproline assay, where hydroxyproline is assumed to make up 10% of collagen.³² DNA content was normalized per gel while GAG and collagen content were normalized per cell.

3.3.8. Histological and immunohistochemical analysis

On day 28, constructs (n=2) were fixed in 10% formalin for 30 min at RT, then snap frozen and cryosectioned. Sections were stained for safranin-O or masson's trichrome on a Leica autostainer XL and imaged in bright field (40X objective) on a Nikon inverted microscope.

For immunostaining, sections were blocked with 10% goat serum, then analyzed by anti-collagen type II (1:50, US Biologicals) and anti-collagen type I (1:50). Sections were treated with appropriate enzymes for 1 hour at 37 °C: hyaluronidase (2080 U) for collagen II, and pepsin A (4000 U) with Retrieagen A (BD Biosciences) treatment for collagen I to help expose the

antigen. Sections were probed with AlexaFluor 568-conjugated secondary antibodies and counterstained with DAPI for cell nuclei. All samples were processed at the same time to minimize sample-to-sample variation. Images were collected on a Zeiss LSM710 scanning confocal microscope with a 20X objective using the same settings and post-processing for all images. The background gain was set to negative controls on blank sections that received the same treatment. Positive controls were performed on porcine hyaline cartilage for collagen type II and porcine meniscus for collagen type I (Figure 3.S1.).

3.3.9. Statistical analyses

Data are shown as mean \pm standard deviation. Two way analysis of variance (ANOVA) with Bonferroni posttest for pairwise comparisons was used to evaluate the statistical significance of data. One way ANOVA was used to assess differences within specific conditions. $p < 0.05$ was considered to be statistically significant.

3.4. Results

3.4.1. Distribution of thiolated TGF- β 1 in PEG hydrogels

We confirmed that TGF- β 1 was homogeneously distributed within the gel after the thiol-ene tethering process, using a modified section ELISA.¹⁴ The results presented in Figure 3.1. show TGF- β 1 incorporation throughout the gel, and its relatively homogeneous distribution among gel regions. We further showed that experimentally measured values were similar to theoretically calculated levels (0.1 ng for 10 nM, 0.5 ng for 50 nM, and 0.9 ng for 90 nM).

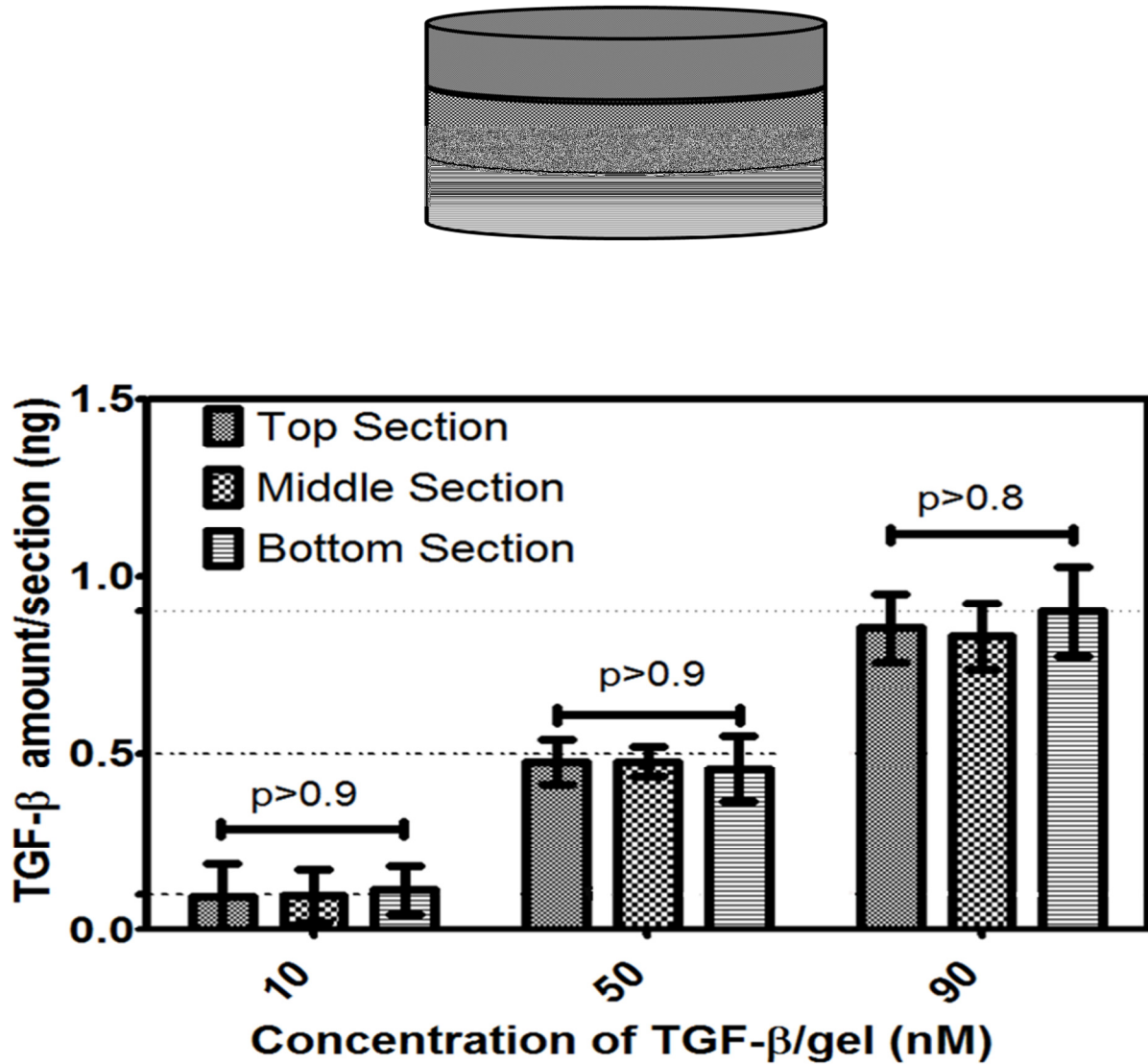
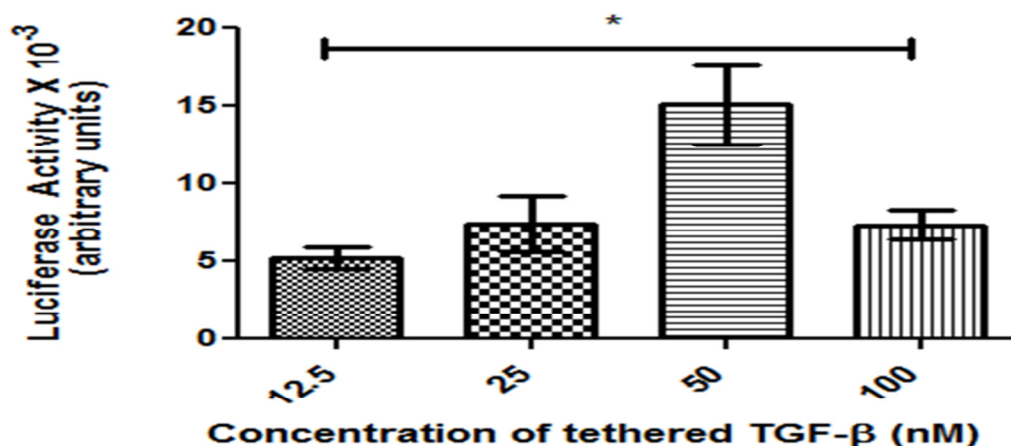


Figure 3.1. TGF- β 1 is homogenously distributed throughout the PEG hydrogel. Section ELISA of tethered gels without cells show detection of TGF- β at similar levels to theoretical values with graphic on top depicting slice areas. Each section ~20 mm thickness. Theoretical values indicated by dashed lines (0.1 ng for 10 nM, 0.5 ng for 50 nM, and 0.9 ng for 90 nM gels). 0 nM value is subtracted out of all conditions. Results are presented as mean activity \pm SD (n=2). Solid lines indicate p values with one way ANOVA analysis to confirm sections of each gel are not statistically different from each other.

3.4.2. Bioactivity and concentration of tethered TGF- β 1 in 3D culture

We investigated the bioactivity of tethered TGF- β 1 in 3D culture using a reporter cell line. Briefly, it was shown that tethered proteins typically maintain high levels of bioactivity when conjugated using thiol-ene reactions.²⁰ We further determined concentrations of soluble and tethered TGF- β 1 that yielded a maximal response in PE-25 cells at a seeding density of 40 million cells/mL. In Figure 3.2. a, there was a significant difference in luciferase output of 50 nM gels compared to other conditions. In Figure 3.2. b, 0.3 nM via soluble delivery elicited a maximal cellular response. Interestingly, when we dosed 50 nM of soluble TGF β -1 to encapsulated PE-25s at 40 million cells/mL, the average luciferase response was ~ 6,510 arbitrary units (n=4), which is a 3-fold lower response than for the same concentration of tethered TGF- β 1. Based on these results, we elected to dose soluble TGF- β 1 at the magnitude of 0.3 nM. Overall, these results suggest that tethered TGF- β 1 is bioactive, and at 40 million cells/mL, the conditions that elicited the highest response to TGF- β 1 were 0.3 nM (soluble) and 50 nM (tethered).

a.



b.

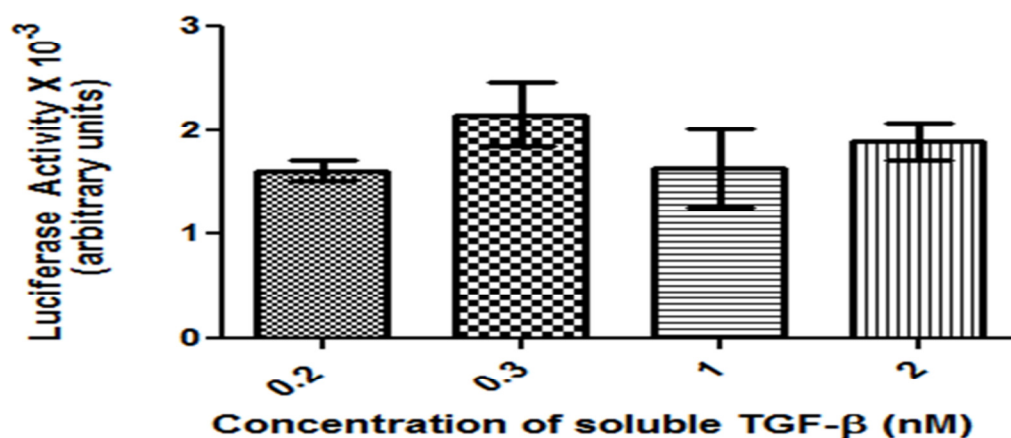
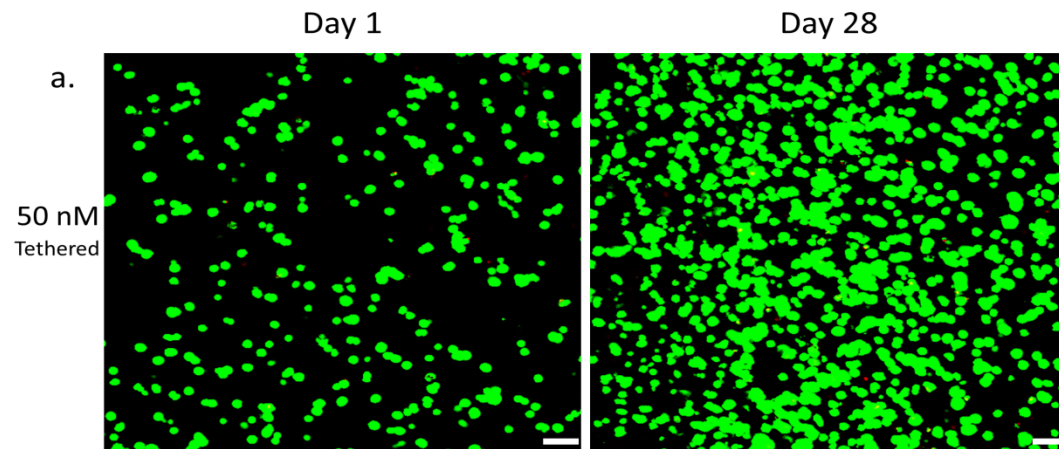


Figure 3.2. Determining TGF-β1 concentration that yields maximal response. (a) PE-25s were encapsulated at 40 million cells/mL with varying concentrations of tethered TGF-β and 50 nM yielded a maximal response. * indicates statistically significant difference between 50 nM and the other concentrations with $p < 0.001$. Results are presented as mean activity \pm SD ($n=4$). (b) PE-25 cells encapsulated at 40 million cells/mL were transiently exposed to varying concentrations of TGF-β in the media. The 0.3 nM output is higher on average than the other concentrations. Results are presented as mean activity \pm SD ($n=4$).

3.4.3. Proliferation of chondrocytes exposed to TGF-β1

Cell viability for all encapsulation and culture conditions was between 80%-90% assessed by live/dead membrane integrity assay at both days 1 and 28. Figure 3.3. a shows the rounded shape of encapsulated cells; there was significant increase in number of cells in the 50 nM TGF-β1 tethered gels. To further quantify this proliferation, we harvested samples at day 1, 14, and 28 and assayed for DNA content (Figure 3.3. b). There was a statistically significant

increase in DNA content, at day 28, for cells encapsulated in 50 nM TGF- β 1 containing gels. Further, there was significantly more DNA in the day 28 50 nM condition than either the 0.3 nM or 0 nM gel condition ($p<0.001$). Combined with the viability results, these data suggest an increase in chondrocyte proliferation in response to tethered growth factor presentation.



b.

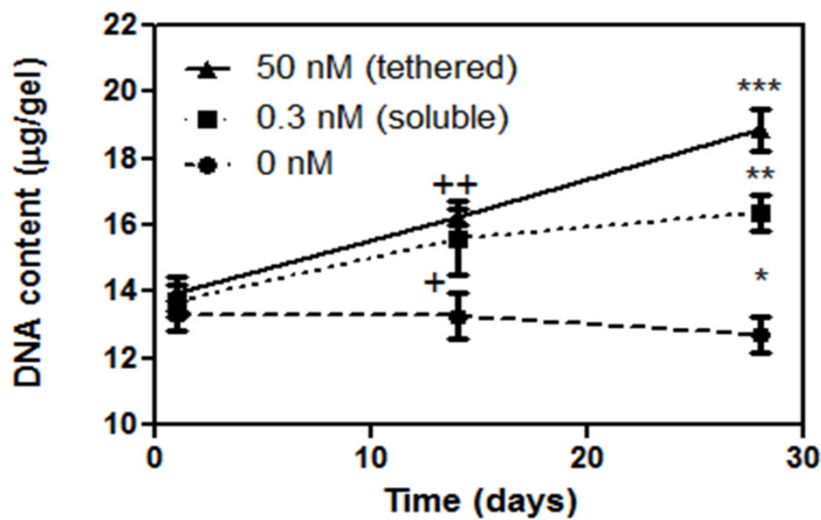


Figure 3.3. Increased proliferation of chondrocytes exposed to TGF- β 1. (a) Live/dead staining of 50 nM gels seeded at 40 million cells/mL on day 1 and day 28 shows chondrocytes retain a spherical morphology, have high viability, and increase in number. Scale bars represent 50 μ m. (b) DNA content of chondrocytes encapsulated at 40 million cells/ mL that were exposed to 0 nM, 0.3 nM which was delivered through the media, or 50 nM which was tethered into the gel. Over a 28-day period, the cells in the 50 nM condition show a steady rate of increase of DNA content.+indicates significant difference between the 0.3 nM and 0 nM case ($p<0.001$), ++ indicates significant difference between 50 nM and 0 nM case ($p<0.001$), * indicates significant difference between 0.3 nM and 0 nM($p<0.001$), ** indicates significant difference between 50 nM and 0.3 nM case at day 28 ($p<0.001$), and *** indicates significant difference between 50 nM and 0 nM for day 28 ($p<0.001$). Results are presented as mean \pm SD (n=3).

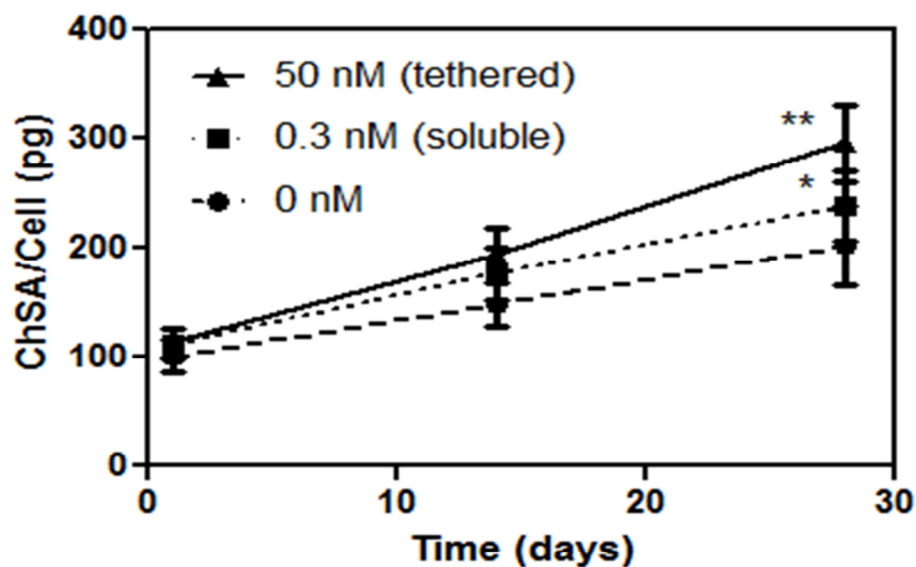
3.4.4. Matrix deposition as a function of TGF- β 1 presentation and culture time

We assessed glycosaminoglycan (GAG) and total collagen content of gels at day 1, 14, and 28. Encapsulated chondrocytes were either exposed to 0 nM, 0.3 nM solubly or 50 nM tethered TGF- β 1. Measured quantities were normalized to cell content in the respective hydrogel formulations.

In Figure 3.4. a, GAG production per cell on day 28 for the tethered construct was significantly higher than non-treated groups ($p<0.001$). There was also a significant difference at day 28 between constructs that presented tethered TGF- β 1 compared to solubly delivered TGF- β 1 ($p<0.05$), suggesting that the tethered growth factor enhanced ECM production over soluble growth factor delivered in the media.

In Figure 3.4. b, total collagen production per cell was highest at day 28 from the construct with tethered TGF- β 1. Further, there was a significant difference between the tethered and soluble TGF- β 1 conditions ($p<0.01$) at day 28, and the tethered group was significantly increased from the 0 nM group ($p<0.001$), indicating that collagen content is highest in the tethered protein constructs.

a.



b.

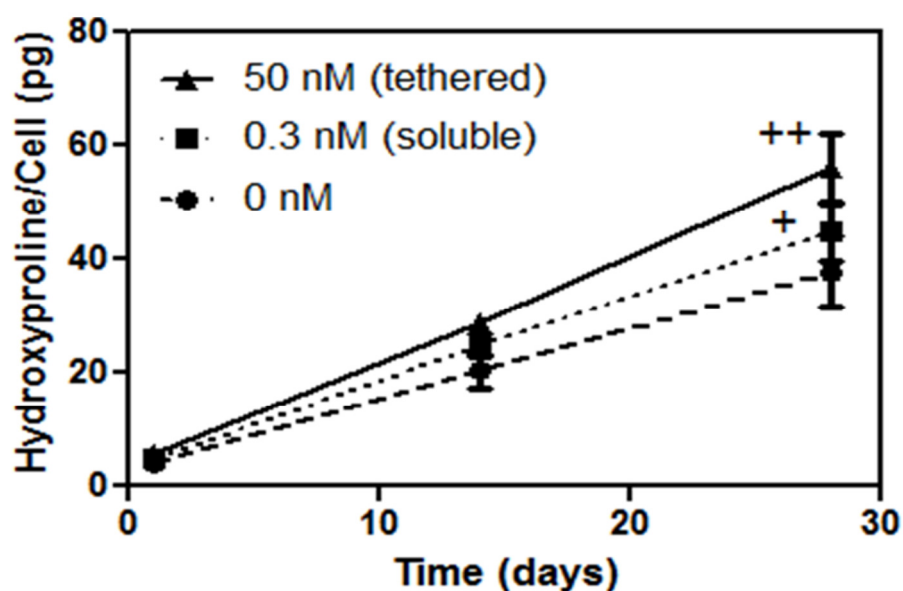


Figure 3.4. Enhanced matrix production of encapsulated chondrocytes exposed to TGF- β . (a) GAG production was normalized per cell. * indicates significant difference between 50 nM and 0.3 nM condition at day 28 ($p < 0.05$), ** indicates significant difference between 50 nM and 0 nM at day 28 ($p < 0.001$). Data presented as mean \pm SD ($n=3$). (b) Collagen production was normalized per cell. + indicates significant difference between 50 nM and 0.3 nM at day 28 ($p < 0.01$) and ++ indicates significant difference between 50 nM and 0 nM at day 28 ($p < 0.001$). Data presented as mean \pm SD ($n=3$).

3.4.5. Matrix organization

We examined the distribution and deposition of extracellular matrix molecules by histological and immunofluorescence techniques. Masson's trichrome staining (Figure 3.5. a,c,e) revealed collagen deposition increased in the pericellular space of encapsulated chondrocytes

with both tethered and soluble TGF- β 1 gels on day 28 compared to 0 nM gels. Overall, it appears that most of the pericellular collagen deposition occurs in the 50 nM gels at day 28. In a similar fashion, safranin-O (Figure 3.5. b,d,f) staining revealed that GAG deposition localized in the pericellular region with increased deposition per cell in the presence of TGF- β 1. These results support the data that tethered TGF- β increases ECM secretion.

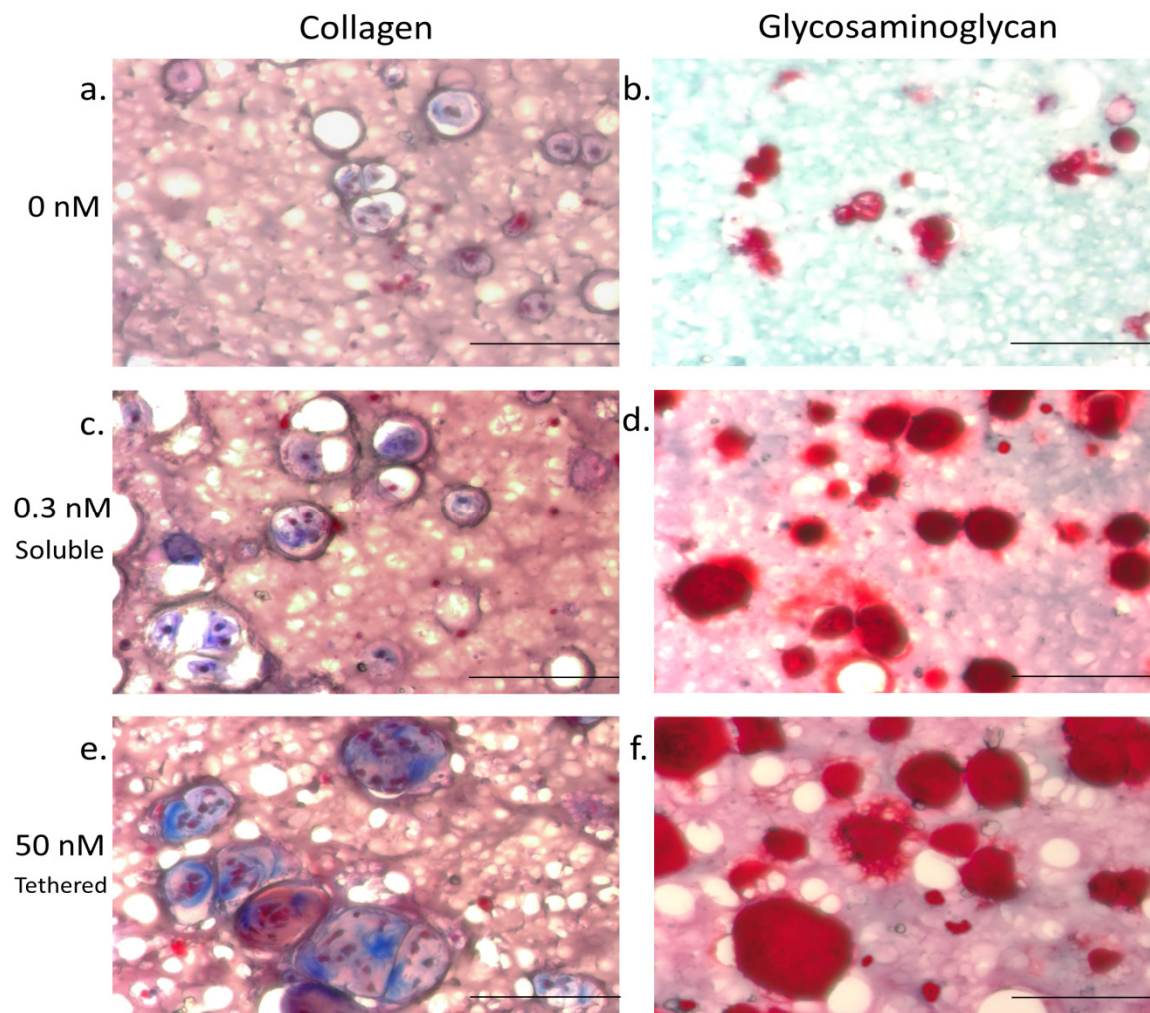


Figure 3.5. Matrix protein distribution in gels. At day 28, gels seeded with chondrocytes at 40 million cells/mL were sectioned and stained for matrix distribution. (a) 0 nM gel stained for collagen, (b) 0 nM gel stained for GAG, (c) 0.3 nM (soluble) gel stained for collagen, (d) 0.3 nM (soluble) gel stained for GAG, (e) 50 nM (tethered) gel stained for collagen, (f) 50 nM (tethered) gel stained for GAG. Blue indicates collagen and red indicates GAG. Scale bars represent 100 μm.

Immunofluorescence staining revealed that by day 28, there was a scarce amount of collagen I throughout all samples (Figure 3.6. a,c,e) and that collagen II was prevalent in the growth factor treated samples (Figure 3.6. d,f) compared to the 0 nM sample (Figure 3.6. b). A high collagen II and low collagen I signal is indicative of articular cartilage, and the constructs maintained that phenotype over 28 days of culture.³³

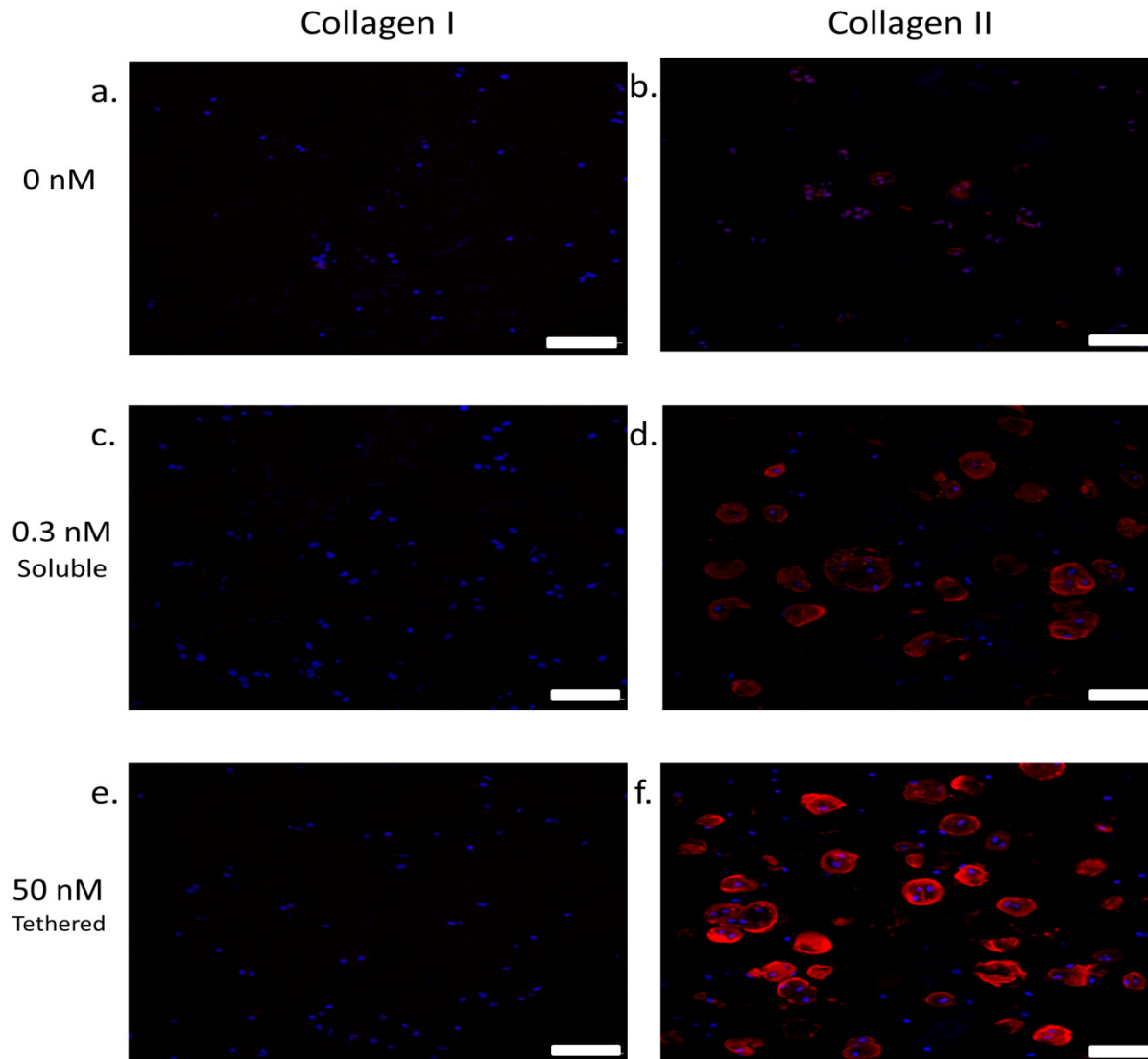


Figure 3.6. Collagen I versus collagen II distribution in constructs. Gels seeded with chondrocytes at 40 million cells/mL were cryosectioned at day 28. Immunohistochemistry analysis reveals collagen type distribution in scaffolds. (a) 0 nM with collagen I, (b) 0 nM with collagen II, (c) 0.3 nM (soluble) with collagen I, (d) 0.3 nM (soluble) with collagen II, (e) 50 nM

(tethered) with collagen I, (f) 50 nM (tethered) with collagen II. Sections were stained red for both anti-collagen I and anti-collagen II antibodies and were counterstained with DAPI (blue) for cell nuclei. Scale bars represent 50 μ m.

3.5. Discussion

Engineering a clinically viable scaffold for chondrocyte delivery and promotion of cartilage regeneration is challenging, partly because of the time required for chondrocytes to generate a robust matrix. By encapsulating chondrocytes in a PEG thiol-ene system with localized presentation of a growth factor, we have shown quantitatively and qualitatively, *in vitro*, that cells survive, proliferate, and generate cartilage specific ECM molecules at a higher rate than without the growth factor. Tethering growth factors into a synthetic material scaffold integrates the promoting effects of a protein cross-linked gel without gel to gel variability. A cell delivery system with such properties can provide certain advantages for clinical applications in techniques such as matrix assisted autologous chondrocyte transplantation (MACT).

There are many advantages to tethering growth factors into a gel system for tissue engineering purposes. Localized presentation precludes growth factors from activating unnecessary cell targets in an *in vivo* setting. Additionally, it requires a lower amount of growth factor. In this 28 day study, TGF- β 1 is dosed in 1 mL media every 3 days at 0.3 nM that results in ~ 70 ng of protein delivered to the cell-laden gel. For the same time period and experimental conditions, a 50 nM tethered gel corresponds to ~50 ng of TGF- β 1/gel, yet led to higher matrix production and DNA content at day 28. When using an expensive and/or potent growth factor to promote tissue regeneration, a tethered system can potentially provide a more efficient and effective delivery system for long time periods appropriate for clinical settings.

In these studies, we chose to look specifically at chondrocytes encapsulated at 40 million cells/mL, since this cell density has been previously shown to be an optimal choice for *in vivo* studies with hydrogel delivery systems.^{34,35,36} We used a cellular assay, based on PE-25 cells as a reporter system with a luciferase output, to determine that an effective concentration of growth factor to deliver to cells was 50 nM (Figure 3.2. a.) for tethered TGF- β 1 and 0.3 nM for soluble TGF- β 1 (Figure 3.2. b.) We chose the initial concentrations of TGF- β 1 for the PE-25 experiments based on previous work for promoting chondrogenesis of hMSCs.²⁰ We hypothesized that encapsulated cells may not respond as well to higher concentrations of soluble TGF- β 1 than tethered TGF- β 1, because PE-25s may internalize the factor, and seeding at high density may reduce the cellular response. Related studies with Mv1Lu cells showed that they internalized TGF- β 1, so it is reasonable to consider this explanation for the PE-25 experiments.³⁷

We speculate that for gels presenting 100 nM of tethered TGF- β 1, the PE-25s encapsulated at 40 million cells/mL showed less activity compared to 50 nM gels (Figure 3.2. a) because growth factors can have pleiotropic effects that may lead to a negative feedback loop. Additionally, since TGF- β binds to a dimer receptor, which requires two receptor subtypes to join to initiate the signaling cascade, it is possible that the orientation of growth factors around the cell prevents complete binding since both subtype receptors may be occupied by separate ligands when only one is required for signaling activation.³⁸

We chose to use human TGF- β 1 with porcine chondrocytes because the PE-25 system has already been established with human TGF- β 1,²⁵ and porcine chondrocytes will be used in future pre-clinical animal studies. We believe that this is unlikely to affect the outcomes of our studies, since mature TGF- β 1 is known to be highly conserved (>99% amino acid sequence identity) throughout mammalian species.³⁹

The data presented in this study suggest that the PEG thiol-ene platform with tethered TGF- β represents a bioactive scaffold with potential tissue engineering applications for chondrocyte delivery. Chondrocytes maintained a spherical morphology, similar to native chondrocytes, in the gel over a 28 day period, as shown in Figure 3.3. a, which suggests the cells are less likely to de-differentiate and generate hyaline-like cartilage.⁴⁰ Chondrocytes also increased in cell number when cultured in PEG thiol-ene gels as shown in Figure 3.3. b, and especially when TGF- β 1 is presented, which is known to induce proliferation.²⁴ Porcine chondrocyte doubling time in 2D culture is around 6.4 ± 0.3 days in serum-containing media.⁴¹ We speculate that part of the reason the cells did not double at a similar rate when encapsulated in the PEG gels is that the selected gel formulations are non-degradable. Thus, the polymer network limited the amount of space available for chondrocytes to grow, and the media did not contain serum. This result was confirmed by a study with rat chondrocytes grown in a non-degradable 3D scaffold which had a longer doubling time (10.04 ± 0.9 days) than cells grown in 2D (2.94 ± 0.3 days).⁴²

Extracellular matrix production data revealed that over 28 days, the tethered-protein gel stimulated chondrocytes to produce more GAGs and collagen, as quantified in Figure 3.4. The cells maintained a high rate of ECM production even though matrix proteins accumulate around the cell after 28 days. This phenomenon implies that TGF- β 1 may maintain activity and interact with the chondrocytes, despite the increased pericellular matrix. Furthermore, when compared to a tethered TGF β study investigating MSC chondrogenesis,²⁰ chondrocytes maintained a similar level of GAG production and also express collagen type II on a similar time scale.

A study with juvenile and adult chondrocytes encapsulated in degradable gels had higher GAG and collagen outputs per cell over a 28 day period compared to the ones in this study.⁴³ We

expected that a degradable gel allows for greater ECM deposition as posited by various groups.^{44,45} Additionally, histology and immunofluorescence staining confirmed that matrix was primarily deposited pericellularly in all conditions, but at a higher level in gels with tethered TGF- β 1. While the secreted matrix was primarily confined to the pericellular region, there were some areas where the ECM molecules, especially GAGs, were more dispersed between cells (Figure 3.5.). These data suggest the need for tethering TGF- β 1 to a degradable PEG thiol-ene system to enhance ECM production and elaboration, with the potential to better capture biochemical and biomechanical properties of native hyaline tissue.

3.6. Conclusion

We confirmed that thiol-ene reactions allow conjugation of TGF- β 1 into PEG gels, while maintaining bioactivity and signaling to encapsulated cells. We showed that tethered TGF- β 1 increased the proliferation rate and ECM production of chondrocytes over a 28 day period, at levels exceeding that of cells in gels where TGF- β 1 was dosed in the culture medium or those that were untreated. The tethered TGF- β hydrogels utilized a lower total protein dosage while still promoting high levels of proliferation and matrix production of chondrocytes. Furthermore, chondrocytes maintained a spherical morphology in the thiol-ene PEG gels with high viability and a phenotype that resembles articular cartilage (i.e. high collagen II and low collagen I levels). Collectively, these results demonstrate the feasibility of delivering bioactive protein signals in a 3D culture platform to enhance matrix production of chondrocytes. This platform may have further applications as a scaffold for *in vivo* cartilage regeneration.

3.7. Acknowledgments

The authors would like to acknowledge Dr. Xuedong Liu for the PE-25 cells. We would also like to acknowledge Dr. William Wan, Dr. Huan Wang, Dr. Justine Roberts, and Stacey

Skaalure for assistance on experimental design, as well as Dr. Malar Azagarsamy for help with NMR characterization of the macromolecules. This research was sponsored by the Howard Hughes Medical Institute and Department of Defense award number W81XWH-10-1-0791. The US Army Medical Research Acquisition Activity, 820 Chandler Street, Fort Detrick MD 21702-5014 is the awarding and administering acquisition office.

3.8. Supplementary Figures

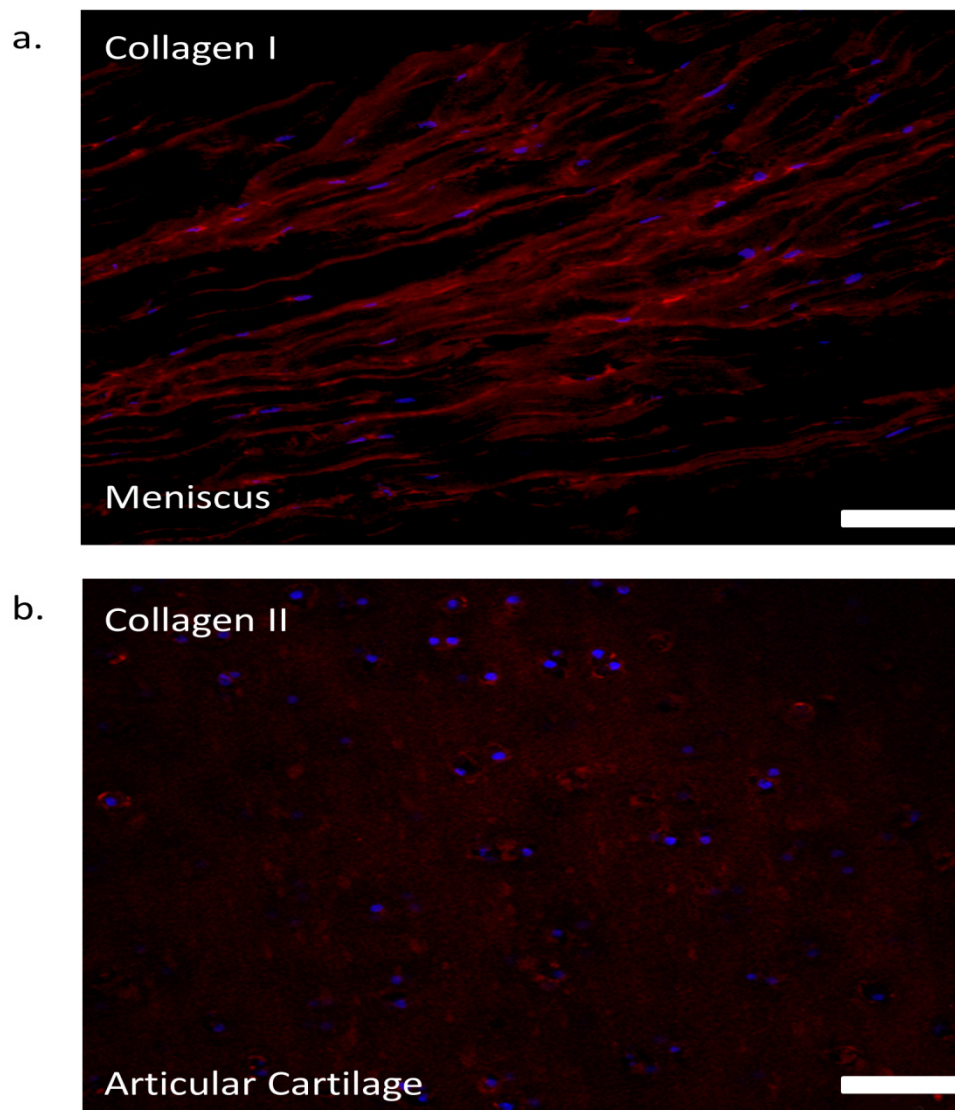


Figure 3.S1. (a) Type I collagen immune staining of porcine meniscus (b) Type II collagen staining of porcine hyaline articular cartilage. Sections were stained red for both anti-collagen I

and anti-collagen II antibodies and were counterstained with DAPI (blue) for cell nuclei. Scale bars represent 50 μ m.

3.9. References

1. Hunziker, E. B. Articular cartilage repair: basic science and clinical progress. A review of the current status and prospects. *Osteoarthr. Cartil.* **10**, 432–63 (2002).
2. Holland, T. A. & Mikos, A. G. Advances in drug delivery for articular cartilage. *J. Control. Release* **86**, 1–14 (2003).
3. Chen, F. H., Rousche, K. T. & Tuan, R. S. Technology Insight: adult stem cells in cartilage regeneration and tissue engineering. *Nat. Clin. Pract. Rheumatol.* **2**, 373–82 (2006).
4. Jackson, D. W. & Simon, T. M. Tissue engineering principles in orthopaedic surgery. *Clin. Orthop. Relat. Res.* S31–45 (1999).
5. Masters, K. S. Covalent growth factor immobilization strategies for tissue repair and regeneration. *Macromol. Biosci.* **11**, 1149–63 (2011).
6. Tayalia, P. & Mooney, D. J. Controlled growth factor delivery for tissue engineering. *Adv. Mater.* **21**, 3269–85 (2009).
7. Zhao, W., Jin, X., Cong, Y., Liu, Y. & Fu, J. Degradable natural polymer hydrogels for articular cartilage tissue engineering. *J. Chem. Technol. Biotechnol.* **88**, 327–339 (2013).
8. Kock, L., van Donkelaar, C. C. & Ito, K. Tissue engineering of functional articular cartilage: the current status. *Cell Tissue Res.* **347**, 613–27 (2012).
9. Spiller, K. L., Maher, S. A. & Lowman, A. M. Hydrogels for the Repair of Articular Cartilage Defects. *Tissue Eng. Part B* **17**, 281–299 (2011).
10. Bryant, S. J. & Anseth, K. S. Hydrogel properties influence ECM production by chondrocytes photoencapsulated in poly(ethylene glycol) hydrogels. *J. Biomed. Mater. Res.* **59**, 63–72 (2002).
11. Sharma, B. *et al.* Human cartilage repair with a photoreactive adhesive-hydrogel composite. *Sci. Transl. Med.* **5**, 167–173 (2013).
12. Lee, S. J. Cytokine delivery and tissue engineering. *Yonsei Med. J.* **41**, 704–719 (2000).

13. Park, H., Temenoff, J. S., Holland, T. A., Tabata, Y. & Mikos, A. G. Delivery of TGF-beta1 and chondrocytes via injectable, biodegradable hydrogels for cartilage tissue engineering applications. *Biomaterials* **26**, 7095–103 (2005).
14. Hume, P. S., He, J., Haskins, K. & Anseth, K. S. Strategies to reduce dendritic cell activation through functional biomaterial design. *Biomaterials* **33**, 3615–25 (2012).
15. Deforest, C. A. & Anseth, K. S. Photoreversible Patterning of Biomolecules within Click-Based Hydrogels. *Angew. Chem. Int. Ed. Engl.* **124**, 1852–1855 (2012).
16. Aimetti, A. A., Machen, A. J. & Anseth, K. S. Poly(ethylene glycol) hydrogels formed by thiol-ene photopolymerization for enzyme-responsive protein delivery. *Biomaterials* **30**, 6048–54 (2009).
17. Benton, J. A., Fairbanks, B. D. & Anseth, K. S. Characterization of valvular interstitial cell function in three dimensional matrix metalloproteinase degradable PEG hydrogels. *Biomaterials* **30**, 6593–603 (2009).
18. Fairbanks, B. D. *et al.* A Versatile Synthetic Extracellular Matrix Mimic via Thiol-Norbornene Photopolymerization. *Adv. Mater.* **21**, 5005–5010 (2009).
19. Fairbanks, B. D., Schwartz, M. P., Bowman, C. N. & Anseth, K. S. Photoinitiated polymerization of PEG-diacrylate with lithium phenyl-2,4,6-trimethylbenzoylphosphinate: polymerization rate and cytocompatibility. *Biomaterials* **30**, 6702–7 (2009).
20. McCall, J. D., Luoma, J. E. & Anseth, K. S. Covalently tethered transforming growth factor beta in PEG hydrogels promotes chondrogenic differentiation of encapsulated human mesenchymal stem cells. *Drug Deliv. Transl. Res.* **2**, 305–312 (2012).
21. McCall, J. D. & Anseth, K. S. Thiol-ene photopolymerizations provide a facile method to encapsulate proteins and maintain their bioactivity. *Biomacromolecules* **13**, 2410–7 (2012).
22. Huey, D., Hu, J. & Athanasiou, K. Unlike Bone, Cartilage Regeneration Remains Elusive. *Science (80-.).* **6933**, 917–921 (2012).
23. Roberts, J. J. & Bryant, S. J. Comparison of photopolymerizable thiol-ene PEG and acrylate-based PEG hydrogels for cartilage development. *Biomaterials* (2013).
24. Li, T., O’Keefe, R. & Chen, D. TGF- β signaling in chondrocytes. *Front. Biosci.* 681–688 (2005).
25. Clarke, D. C., Brown, M. L., Erickson, R. A., Shi, Y. & Liu, X. Transforming growth factor beta depletion is the primary determinant of Smad signaling kinetics. *Mol. Cell. Biol.* **29**, 2443–55 (2009).

26. Yoo, J. J., Bichara, D. A., Zhao, X., Randolph, M. A. & Gill, T. J. Implant-assisted meniscal repair in vivo using a chondrocyte-seeded flexible PLGA scaffold. *J. Biomed. Mater. Res. A* **99**, 102–8 (2011).
27. Byers, B. A., Mauck, R. L., Chiang, I. E. & Tuan, R. S. Transient exposure to transforming growth factor beta 3 under serum-free conditions enhances the biomechanical and biochemical maturation of tissue-engineered cartilage. *Tissue Eng. Part A* **14**, 1821–34 (2008).
28. Chua, K. H., Aminuddin, B. S., Fuzina, N. H. & Ruszymah, B. H. I. Insulin-transferrin-selenium prevent human chondrocyte dedifferentiation and promote the formation of high quality tissue engineered human hyaline cartilage. *Eur. Cell. Mater.* **9**, 58–67 (2005).
29. Ruan, J.-L. *et al.* An Improved Cryosection Method for Polyethylene Glycol Hydrogels Used in Tissue Engineering. *Tissue Eng. Part C. Methods* **19**, 794–801 (2013).
30. Kim, Y.-J., Sah, R. L. Y., Doong, J.-Y. H. & Grodzinsky, A. J. Fluorometric assay of DNA in cartilage explants using Hoechst 33258. *Anal. Biochem.* **174**, 168–176 (1988).
31. Farndale, R. W., Sayers, C. A. & Barrett, A. J. A direct spectrophotometric microassay for sulfated glycosaminoglycans in cartilage cultures. *Connect. Tissue Res.* **9**, 247–8 (1982).
32. Woessner, J. F. The determination of hydroxyproline in tissue and protein samples containing small proportions of this imino acid. *Arch. Biochem. Biophys.* **93**, 440–7 (1961).
33. Ballock, R. T. & O’Keefe, R. J. The Biology of the Growth Plate. *J. Bone Jt. Surg.* **85**, 715–726 (2003).
34. Passaretti, D. & Silverman, R. P. Huang, W Kirchhoff, C.H. Ashiku, S. Randolph, M.A. Yaremchuk, M. J. Cultured chondrocytes produce injectable tissue-engineered cartilage in hydrogel polymer. *Tissue Eng.* **7**, 805–15 (2001).
35. Burdick, J. A., Chung, C., Jia, X., Randolph, M. A. & Langer, R. Controlled degradation and mechanical behavior of photopolymerized hyaluronic acid networks. *Biomacromolecules* **6**, 386–91 (2005).
36. Ibusuki, S. *et al.* Engineering Cartilage in a Photochemically Crosslinked Collagen Gel. *J. Knee Surg.* **22**, 72–81 (2010).
37. Zwaagstra, J. C., El-Alfy, M. & O’Connor-McCourt, M. D. Transforming growth factor (TGF)-beta 1 internalization: modulation by ligand interaction with TGF-beta receptors types I and II and a mechanism that is distinct from clathrin-mediated endocytosis. *J. Biol. Chem.* **276**, 27237–45 (2001).

38. Shi, Y. & Massagué, J. Mechanisms of TGF-beta signaling from cell membrane to the nucleus. *Cell* **113**, 685–700 (2003).
39. Derynck, R. *et al.* Human transforming growth factor-beta complementary DNA sequence and expression in normal and transformed cells. *Nature* **316**, 701–5 (1985).
40. Lin, Z., Willers, C., Xu, J. & Zheng, M.-H. The chondrocyte: biology and clinical application. *Tissue Eng.* **12**, 1971–84 (2006).
41. Jin, R. L., Park, S. R., Choi, B. H. & Min, B.-H. Scaffold-free cartilage fabrication system using passaged porcine chondrocytes and basic fibroblast growth factor. *Tissue Eng. Part A* **15**, 1887–95 (2009).
42. Baghaban Eslaminejad, M., Taghiyar, L. & Falahi, F. Quantitative analysis of the proliferation and differentiation of rat articular chondrocytes in alginate 3D culture. *Iran. Biomed. J.* **13**, 153–60 (2009).
43. Skaalure, S. C., Milligan, I. L. & Bryant, S. J. Age impacts extracellular matrix metabolism in chondrocytes encapsulated in degradable hydrogels. *Biomed. Mater.* **7**, 1–13 (2012).
44. Park, Y., Lutolf, M. P., Hubbell, J. A., Hunziker, E. B. & Wong, M. Bovine Primary Chondrocyte Culture in Synthetic Matrix Hydrogels as a Scaffold for Cartilage Repair. *Tissue Eng.* **10**, 515–522 (2004).
45. Roberts, J. J., Nicodemus, G. D., Greenwald, E. C. & Bryant, S. J. Degradation improves tissue formation in (un)loaded chondrocyte-laden hydrogels. *Clin. Orthop. Relat. Res.* **469**, 2725–34 (2011).

CHAPTER IV

DEVELOPMENT OF A CELLULARLY DEGRADABLE PEG HYDROGEL TO PROMOTE ARTICULAR CARTILAGE EXTRACELLULAR MATRIX DEPOSITION

As appearing in Advanced Healthcare Materials 2015

4.1. Abstract

Healing articular cartilage remains a significant clinical challenge because of its limited self-healing capacity. While delivery of autologous chondrocytes to cartilage defects has received growing interest, combining cell-based therapies with scaffolds that capture aspects of native tissue and promote cell-mediated remodeling could improve outcomes. Currently, scaffold-based therapies with encapsulated chondrocytes permit matrix production; however, resorption of the scaffold does not match the rate of production by cells leading to generally low ECM outputs. Here, a poly (ethylene glycol) (PEG) norbornene hydrogel was functionalized with thiolated transforming growth factor (TGF- β 1) and cross-linked by an MMP-degradable peptide. Chondrocytes were co-encapsulated with a smaller population of mesenchymal stem cells, with the goal of stimulating matrix production and increasing bulk mechanical properties of the scaffold. The co-encapsulated cells cleave the MMP-degradable target sequence more readily than either cell population alone. Relative to non-degradable gels, cellularly degraded materials showed significantly increased glycosaminoglycan and collagen deposition over just 14 days of culture, while maintaining high levels of viability and producing a more widely-distributed matrix. These results indicate the potential of an enzymatically-degradable, peptide-functionalized PEG hydrogel to locally influence and promote cartilage matrix production over a short period. Scaffolds that permit cell-mediated remodeling may be useful in designing treatment options for cartilage tissue engineering applications.

4.2. Introduction

Articular cartilage has limited self-healing properties, in part due to its lack of innervation and vascularization, and cartilage repair remains a significant clinical challenge. Cartilage is composed primarily of specialized extracellular matrix (ECM) components that absorb water and maintain the structure of the tissue. Chondrocytes are the sole, differentiated resident cells found in mature articular cartilage and are responsible for the generation and maintenance of this ECM.¹

As a result of its low cellularity and absence of stimulating growth factors provided by vasculature, cartilage exhibits a low rate of regeneration; hence, focal lesions caused by trauma or joint disorders can lead to debilitating osteoarthritis.² Matrix-assisted autologous chondrocyte transplantation (MACT) involves encapsulating autologous chondrocytes into a tunable scaffold to promote increased matrix synthesis, which is then implanted into a cartilage defect of a patient.^[3] A variety of natural and synthetic materials have been examined as potential cell carriers and as therapeutic agents for cartilage repair.^{4,5,6,7}

Despite advances in MACT, a limitation with many of the scaffold carriers is that their resorption rates do not necessarily match the rate of matrix deposition by encapsulated cells (i.e., what is observed in healthy native tissue).⁸ In the case of hydrogel carriers, synthetic materials often limit deposition of chondrocyte secreted matrix molecules to the space around the cell, also known as the pericellular space.⁹ In order to overcome this issue, current synthetic hydrogels are engineered to hydrolytically degrade at physiologic pH, and while bulk degradation is readily engineered and controlled, numerous material properties are highly coupled to this degradation. For example, high extents of degradation must occur before collagen can assemble throughout hydrogel scaffolds, but this often coincides with a precipitous drop in gel mechanics.^{[9],[10]}

Alternatively, hydrogels derived from native matrix components (e.g., collagen, hyaluronan) can be degraded by cells, and this leads to a local degradation mechanism where the rate is dictated by the cells. However, it is often more challenging to control the degradation and mechanical properties of these materials, which can necessitate synthetic modification to these materials to control their time varying properties.^{11,12} As a result, recent efforts in the field have focused on hybrid synthetic ECM-mimics that can capture the tunability of synthetic scaffolds while integrating the properties of a cell-dictated local degradation.

In this work, we explored the application of a peptide and protein functionalized poly-(ethylene glycol) hydrogel for chondrocyte encapsulation and cartilage regeneration. PEG is a hydrophilic polymer that has been broadly explored for cell delivery applications.^{13,14,15,16} We formed biologically active PEG hydrogels through a photoinitiated step-growth polymerization scheme, by reacting 4-arm norbornene terminated PEG macromolecules with a non-degradable PEG dithiol linker or a bis-cysteine collagenase-sensitive peptide crosslinker, KCGPQG↓IWGQCK (where the arrow indicates cleavage site).¹⁷ This thiolene photopolymerization allows for precise spatial and temporal control over polymer formation, as well as facile encapsulation of cells and biologics.¹⁸ Multiple studies have shown the resulting crosslinked PEG hydrogel can encapsulate numerous primary cells with high survival rates (>90%) following photoencapsulation.^{19,20}

Previous work in our group further demonstrated that chondrocyte ECM production is enhanced in the presence of locally tethered TGF- β 1 in a non-degradable PEG network; however, matrix deposition was limited to the pericellular space.²¹ These results motivated the experiments reported herein, where we study how tethered TGF- β 1 in concert with a cellularly degradable peptide crosslinker influences cartilage ECM production and its distribution. Since

degradation of collagen is a rate-limiting step in cartilage remodeling, as it is the most abundant component of the ECM,²² we selected a peptide linker derived from collagen, KCGPQG↓IWGQCK. Previously, the Hubbell group²³ encapsulated chondrocytes in a PEG gel linked with this peptide and found increased gene expression of cartilage matrix molecules compared to non-degradable gels; however, matrix deposition was pericellularly restricted,²⁴ suggesting that proper degradation did not occur to permit wide-spread ECM deposition. As chondrocytes release both MMP-8²⁵ and MMP-13,²⁶ which are known to cleave this sequence, they are not highly metabolically active.²⁷ We hypothesize that when these primary cells differentiate from their stem cell origin, their low metabolic activity translates to very slow degradation of MMP-cleavable scaffolds.

To catalyze this pericellular degradation process, we examine the MMP activity of chondrocytes and explore the co-encapsulation of chondrocytes with mesenchymal stem cells (MSCs) to aid in scaffold remodeling. In complementary migration experiments, MSCs have been shown to readily degrade the KCGPQG↓IWGQCK sequence when encapsulated in similar PEG gels.²⁸ Furthermore, Bahney *et al.*, incorporated a collagen-derived peptide linker into PEG hydrogels to encourage chondrogenesis of MSCs.²⁹ In addition to catalyzing degradation of the target peptide linker, MSCs co-encapsulated with chondrocytes can also stimulate matrix deposition and reduce hypertrophy of chondrocytes.³⁰ Furthermore, in clinical settings, a low density of MSCs have the potential to migrate into a PEG MACT scaffold when combined with a procedure like microfracture surgery, which stimulates MSC migration.³¹

In this work, we report the development of a MMP-sensitive PEG based hydrogel that employs co-culture of MSCs and chondrocytes to suggest that local degradation facilitates diffuse ECM deposition. This multifunctional scaffold is further engineered to present TGF- β 1 to

encourage matrix deposition by both chondrocytes²¹ and MSCs.³² MSCs are seeded at a low density to facilitate degradation of the linker, while allowing us to design experiments focused on ECM secretion by co-encapsulated chondrocytes. Other common co-culture studies utilize much higher ratios of MSCs to chondrocytes.^{30,33} Additionally, we demonstrate *in situ* degradation by encapsulated cells utilizing a fluorogenic peptide, assess construct matrix deposition both qualitatively and quantitatively, and show increased scaffold mechanical integrity over 14 days.

4.3. Results

4.3.1. Chondrocyte cleavage of the MMP-degradable sequence in 3D monoculture

We confirmed *in situ* degradation of the peptide linker sequence (KCGPQG↓IWGQCK) utilizing a fluorogenic peptide sensor (Dab-GGPQG↓IWGQK-Fl-AhxC)³⁴ that was covalently tethered to the gel network. Figure 4.1.(a) shows a 4-arm PEG-NB hydrogel formulation, which includes tethered TGF-β1 [50 nM], and fluorogenic peptide sensor [0.5 mM], for experiments used to determine the amount of cleavage of the MMP-sensitive sequence. We chose the chondrocyte seeding density of 40 million cells/mL, because chondrocytes have been studied at this density and shown to produce native-like tissue at this concentration in 3D experiments.^{35,36,37} Over a 3 day period, we found that chondrocytes seeded at this density degrade the MMP-degradable sequence at a higher rate than either a chondrocyte-laden non-degradable or acellular gel of the same formulation as shown in Figure 4.1.(b). However, when chondrocytes were encapsulated and cultured long term in this formulation, GAG [Figure 4.1.(c)] and collagen [Figure 4.1.(d)] distribution was limited to the pericellular space in degradable, cell-laden constructs, even after 28 days. Even at a shorter culture time of 7 days, the

chondrocytes alone do not significantly degrade the surrounding network, which restricts matrix deposition to the pericellular spaces [Figure 4.S2.].

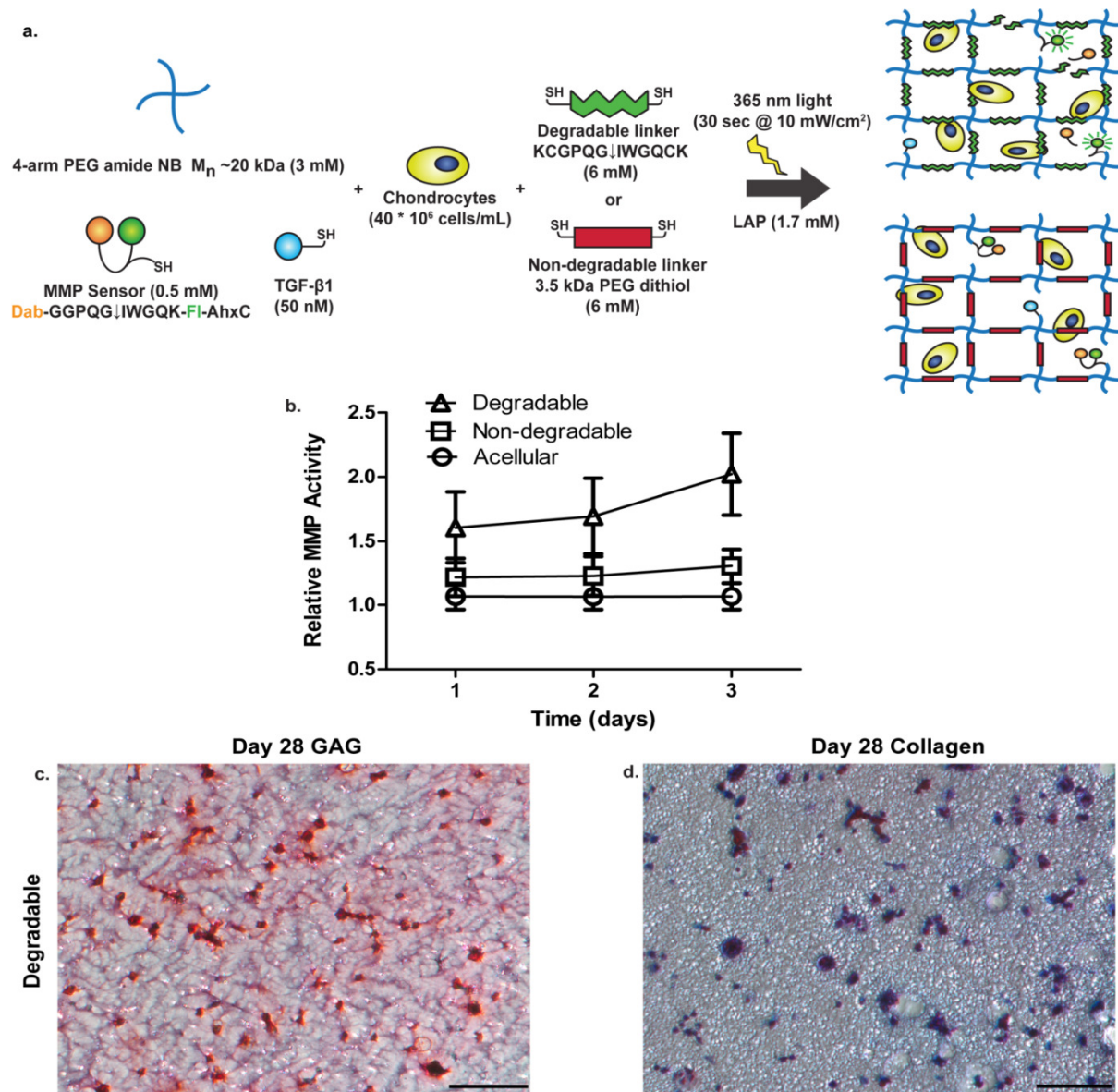


Figure 4.1. Effect of chondrocytes encapsulated in an MMP-degradable gel. (a) Schematic of 4-arm 20 kDa PEG norbornene network with tethered MMP fluorescent sensor (Dab-GGPQG↓IWGQK-FI-Ahx), and TGF-β1. The macromer solution, containing tethered peptides, is combined with chondrocytes at 40 million cells/mL. Resultant networks are either crosslinked by an MMP-degradable peptide sequence (KCGPQG↓IWGQCK) or non-degradable (3.5 kDa PEG dithiol) linker for *in situ* cleavage experiments. (b) Measurement of *in situ* cleavage of fluorescent sensor by chondrocytes. Over 3 days, acellular and chondrocyte-laden non-degradable gels had similar normalized fluorescent activity, but in a degradable gel, chondrocytes had higher fluorescent activity (where A.U. stands for arbitrary units) suggesting

cleavage of the sequence. Results are presented as mean \pm SD (n=3). (c) GAG staining of sections obtained at day 28 with chondrocytes seeded in degradable gels at 40 million cells/mL with nuclei stained black and GAGs stained red. (d) Collagen staining of sections obtained at day 28 with chondrocytes seeded in degradable gels at 40 million cell/mL with nuclei stained black and collagen stained blue. Scale bars represent 100 μ m.

4.3.2. Utilization of co-culture to aid in degradation of the MMP-sensitive sequence

Since chondrocytes alone could not cleave this particular MMP-degradable sequence at a rate that permitted diffuse matrix production, we investigated the use of co-culture with MSCs, as we had previous experience with high levels of degradation of this sequence over shorter time scales.^{28,38} Figure 4.2.(a) shows a 4-arm PEG-NB hydrogel formulation, which includes tethered TGF- β 1 [50 nM], RGD [1 mM], and the fluorogenic peptide sensor [0.5 mM] with varying amounts of encapsulated MSCs and a fixed density of chondrocytes, for experiments used to determine cleavage of the MMP-sensitive sequence. Using the same hydrogel formulation over a 3 day period, we found that not only do MSCs seeded at a lower density than chondrocytes degrade the sequence at a faster rate, but there also seems to be a synergistic effect between MSCs and chondrocytes to degrade the sequence at a significantly higher rate. As shown in Figure 4.2.(b), MSCs seeded at 5 million cells/mL cleaved the target sequence faster than chondrocytes seeded at 40 million cells/mL with increasing relative fluorescent activity. Interestingly, when encapsulated in co-culture with a 24:1 chondrocyte: MSC ratio, with chondrocytes held constant at a density of 40 million cells/mL, the cells increased the amount of cleavage of the target sequence compared to either cell type alone. At each time point, the co-culture (8:1) gel [40 million chondrocytes/mL + 5 million MSCs/mL] MMP activity value was significantly higher than a simple additive effect (from the single cell cultures), suggesting there is indeed a synergistic effect of the co-culture on MMP activity.

In order to determine an appropriate seeding density of MSCs to use in co-culture with chondrocytes in the matrix deposition experiments, we varied the encapsulation ratio of chondrocytes to MSCs. In Figure 4.2.(c), we show that when chondrocytes are held constant at 40 million cells/mL and the concentration of MSCs is increased in the scaffold incrementally, there is a resultant increase in cleavage of the target sequence. There is a statistically significant difference between each of the co-culture groups in Figure 4.2.(c) at each time point ($p < 0.05$) with the 8:1 gel generating the highest MMP activity. Since the lowest ratio of 8:1 chondrocyte:MSC condition yielded the highest fluorescent signal over 3 days, we decided to use this cell ratio for all subsequent experiments.

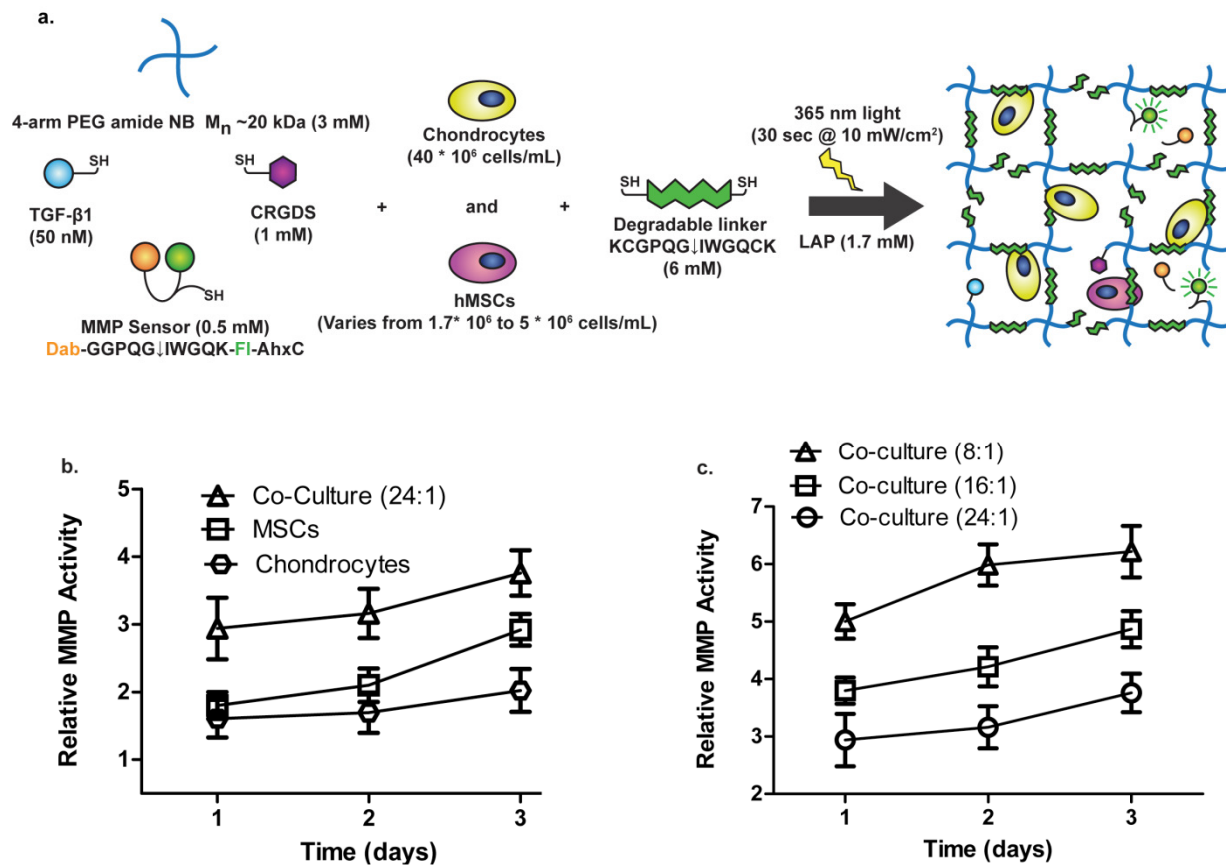


Figure 4.2. Effect of co-culture of chondrocytes and MSCs on degradation of MMP-sensitive sequence. (a) Schematic of 4-arm 20 kDa PEG norbornene network with tethered TGF- β 1, RGD, and MMP fluorescent sensor (Dab-GGPQG↓IWGQCK-Fl-Ahx) crosslinked by an MMP

degradable peptide sequence (KCGPQG↓IWGQCK). Chondrocytes were encapsulated at a fixed seeding density of 40 million cell/mL, and the density of MSCs varied from 1.7 to 5 million cells/ mL during the co-encapsulation process for *in situ* cleavage experiments to measure the effect of co-culture on local degradation. (b) After 3 days, chondrocytes, at 40 million cells/mL, have a lower fluorescent signal than MSCs, at 5 million cells/mL, in degradable gels. Fluorescent signal is highest from day 1 to 3 when cells are co-encapsulated at a ratio of 24:1 chondrocytes: MSCs (40×10^6 chondrocytes/mL + 1.67×10^6 MSCs/mL). (c) By varying the ratio of chondrocytes to MSCs, and keeping the chondrocyte seeding density constant at 40 million cells/mL, it was found after 3 days, 8:1 yielded the highest amount of degradation out of the tested conditions and was used for subsequent matrix deposition experiments. The MMP activity of each group is significantly different from each other at each timepoint ($p < 0.05$) with the 8:1 condition generating the highest MMP activity. Results are presented as mean \pm SD ($n=3$).

4.3.3. Viability of cells and morphology of MSCs in co-culture scaffolds

Cell viability for both non-degradable and degradable co-culture gel conditions was assessed by a live/dead membrane integrity assay at both day 1 [Figure 4.3.(a)] and 14 [Figure 4.S3.]. Non-degradable gels had a viability of $92 \pm 2\%$ at day 1 and $95 \pm 4\%$ at day 14. Degradable gels had a viability of $93 \pm 3\%$ at day 1 and $96 \pm 2\%$ at day 14 as determined by image quantification where results are presented as mean \pm SD ($n=3$). Since both conditions looked very similar, only the viability results of the degradable condition are shown in this article. In addition to assessing viability, we observed the morphology of MSCs present in the scaffold to see if they maintained a rounded shape to suggest a more chondrogenic phenotype^[27] as opposed to an osteogenic phenotype with a more fibroblastic appearance.³⁸ As shown in Figure 4.3.(a), viability of both chondrocytes and MSCs was high on day 1. Furthermore, MSCs, which have been labeled with Cell Tracker™ Violet prior to encapsulation (blue), retained a spherical morphology in spite of being in a degradable system with integrin-binding epitopes. Moreover, DNA content was assessed at day 1, 7, and 14 [Figure 4.3.(b)]. There was no statistically significant difference in cellularity between degradable and non-degradable

conditions, as measured by the amount of DNA present, but there was a steady increase in DNA content from day 1 to 14 in both conditions.

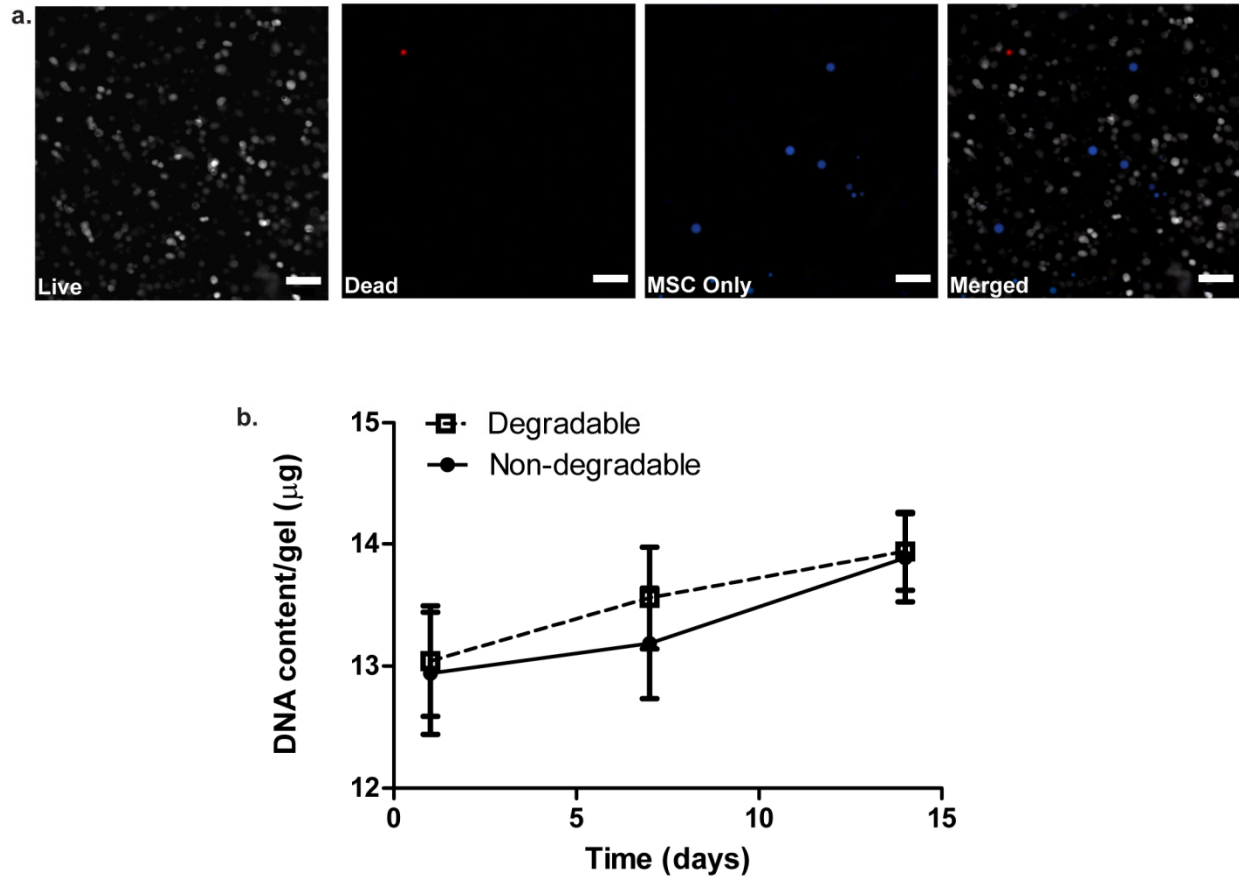


Figure 4.3. Viability, morphology and cellularity of co-culture system. (a) Viability at day 1 with degradable 8:1 co-culture gels with live cells (gray), dead cells (red), MSCs labeled with CellTracker™ Violet (blue), and all 3 images merged together. Viability was quantified at $93 \pm 3\%$. Scale bars represent $100 \mu\text{m}$. (b) DNA content of degradable and non-degradable 8:1 co-culture gels assessed at day 1, 7, and 14. Both degradable and non-degradable conditions show similar DNA content at each time point, but they increase over the 14 day period. Results are presented as mean \pm SD ($n=3$).

4.3.4. Effect of local degradation on cartilage-specific matrix production and distribution

We assessed GAG and total collagen content of gels at day 1, 7, and 14 and further examined the distribution of these molecules throughout the network by staining sections with safranin-O (GAG) and Masson's trichrome (collagen). Measured quantities of either non-degradable or degradable co-culture scaffolds were normalized to the wet weight [wet weight values shown in Figure 4.S4.(a)] of the respective hydrogel formulations. In Figure 4.4.(a) and Figure 4.5.(a), at day 14, GAG and collagen distribution was restricted to the pericellular space in non-degradable gels. On the other hand, in Figure 4.4.(b) and Figure 4.5.(b), at day 14, GAG and collagen were diffusely distributed throughout the gel and connected with other molecules generated by nearby cells. Not only is the visual difference in distribution striking, but it was further confirmed by quantitative analysis. In Figure 4.4.(c) and Figure 4.5.(c), the sGAG and total collagen production as a percentage of the wet weight of the gel on day 7 and 14 for the degradable construct was significantly higher than the non-degradable gel ($p < 0.01$). While cartilage-specific ECM production increases in both conditions over 14 days, it does so at a significantly higher amount in a locally degradable system.

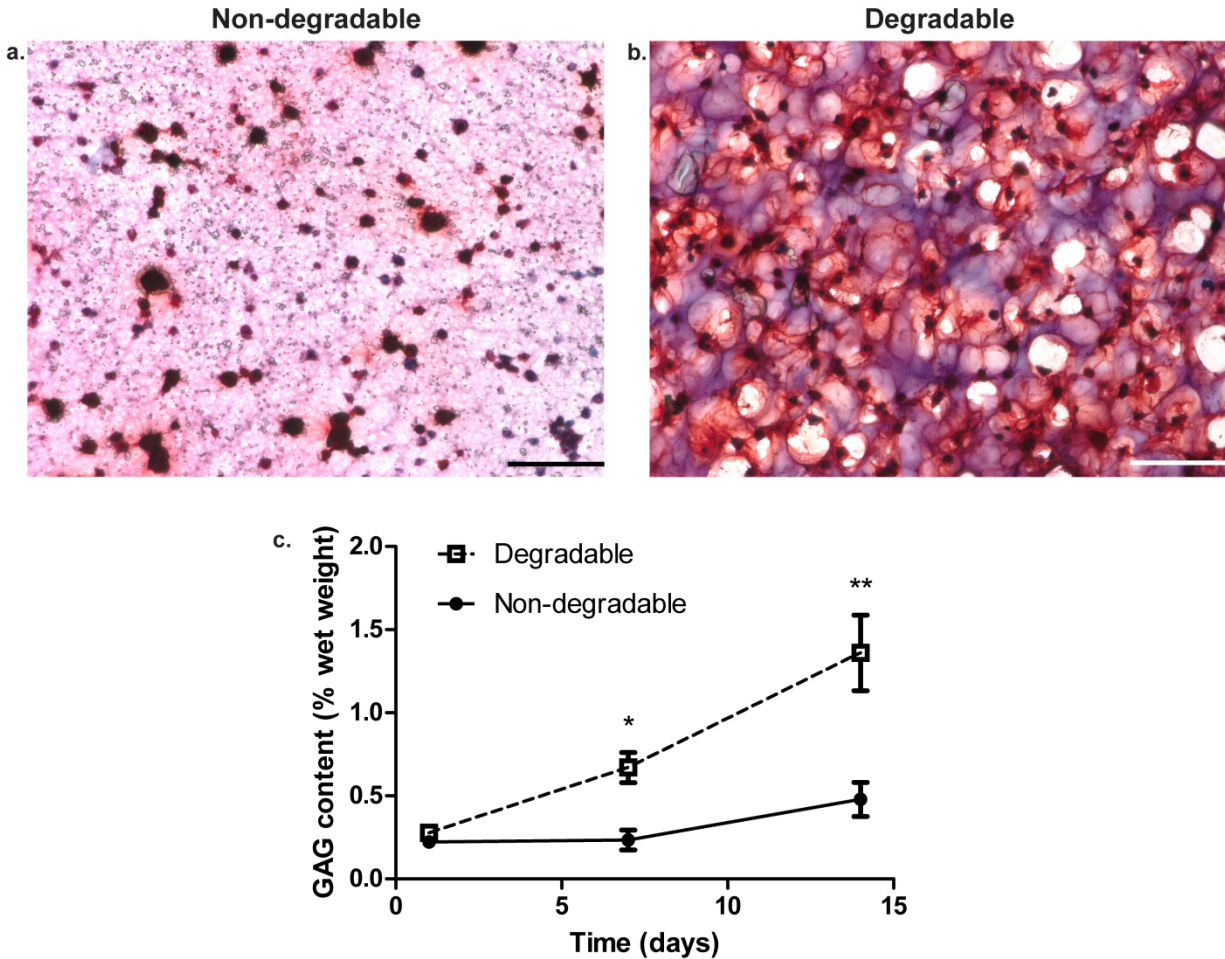


Figure 4.4. Glycosaminoglycan distribution and production in non-degradable and degradable 8:1 co-culture constructs. (a) Non-degradable gel section stained for GAGs at day 14. (b) Degradable gel stained for GAGs at day 14 with nuclei stained black and GAGs stained red. Scale bars represent 100 μ m. (c) GAG content expressed as a percentage of the respective construct wet weight assessed at day 1, 7, and 14. * indicates a statistically significant difference in GAG content at day 7 between degradable and non-degradable gels ($p<0.01$), and ** indicates a statistically significant difference in GAG content at day 14 between degradable and non-degradable gels ($p<0.001$). Results are presented as mean \pm SD ($n=3$).

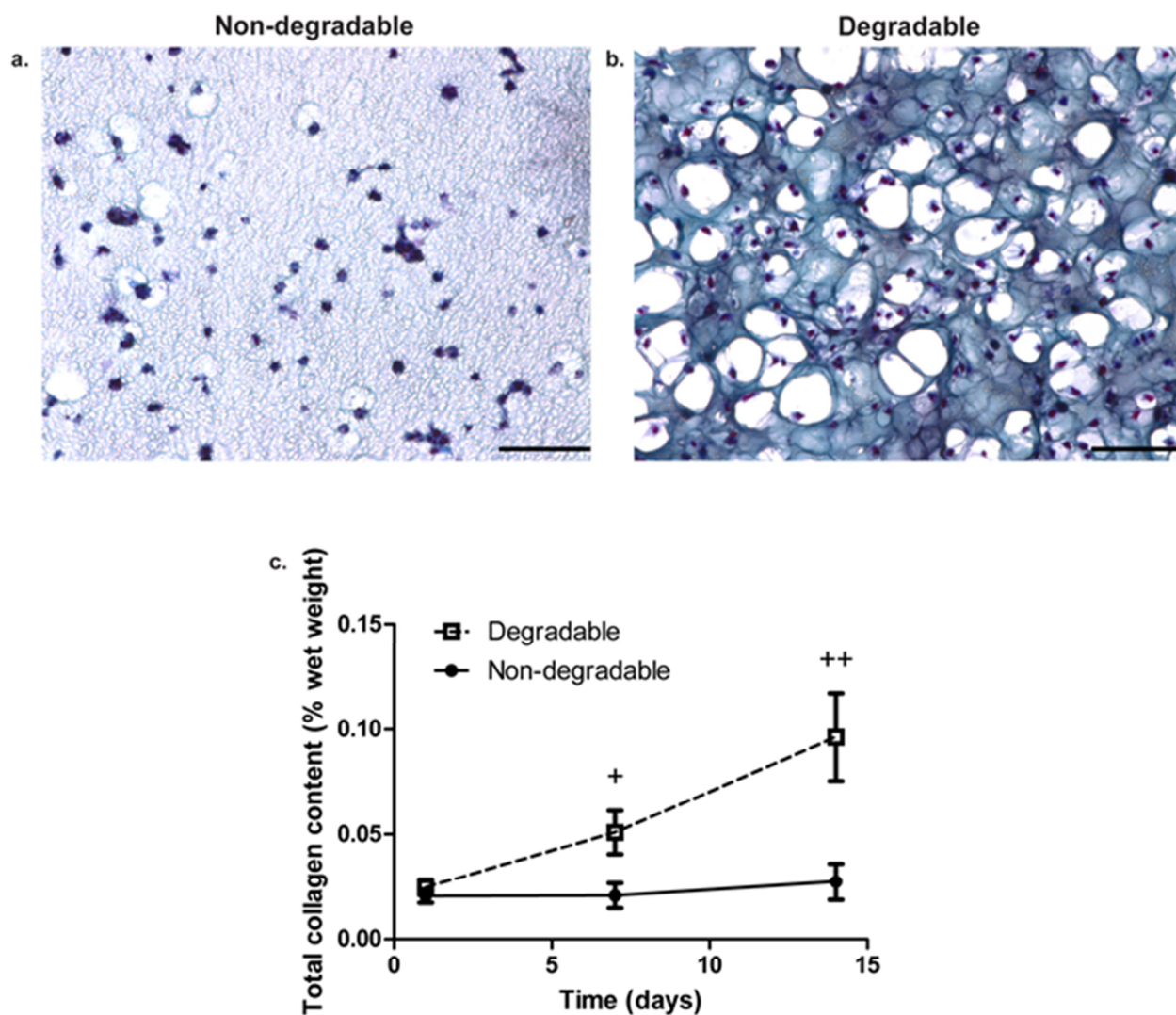


Figure 4.5. Collagen distribution, production, and scaffold compressive modulus in non-degradable and degradable 8:1 co-culture constructs. (a) Non-degradable gel section stained for collagen at day 14. (b) Degradable gel stained for collagen at day 14 with nuclei stained black or violet and collagen stained blue. Scale bars represent 100 μm . (c) Total collagen content expressed as a percentage of the respective construct wet weight assessed at day 1, 7, and 14. + indicates a statistically significant difference in collagen content at day 7 between degradable and non-degradable gels ($p < 0.05$), and ++ indicates a statistically significant difference in collagen content at day 14 between degradable and non-degradable gels ($p < 0.001$). Results are presented as mean \pm SD ($n=3$).

4.3.5. Effect of cell-mediated, local degradation on the mechanical properties of the scaffold

To confirm that our degradable system produced functional, cartilage-specific matrix molecules and increased its mechanical properties over time while permitting ECM expansion, we assessed the bulk compressive modulus of cell-laden non-degradable and degradable gels at day 1, 7, and 14. In Figure 4.6., at day 7, and 14, the value of the compressive modulus of the degradable construct was significantly higher than of the non-degradable gel ($p<0.001$). Furthermore, there was a significant increase ($p<0.001$) between day 1 and 14 of the compressive modulus in degradable scaffolds while the values between day 1 and 14 were not statistically different ($p>0.75$) with non-degradable gels even though both conditions have similar values of compressive elastic modulus initially.

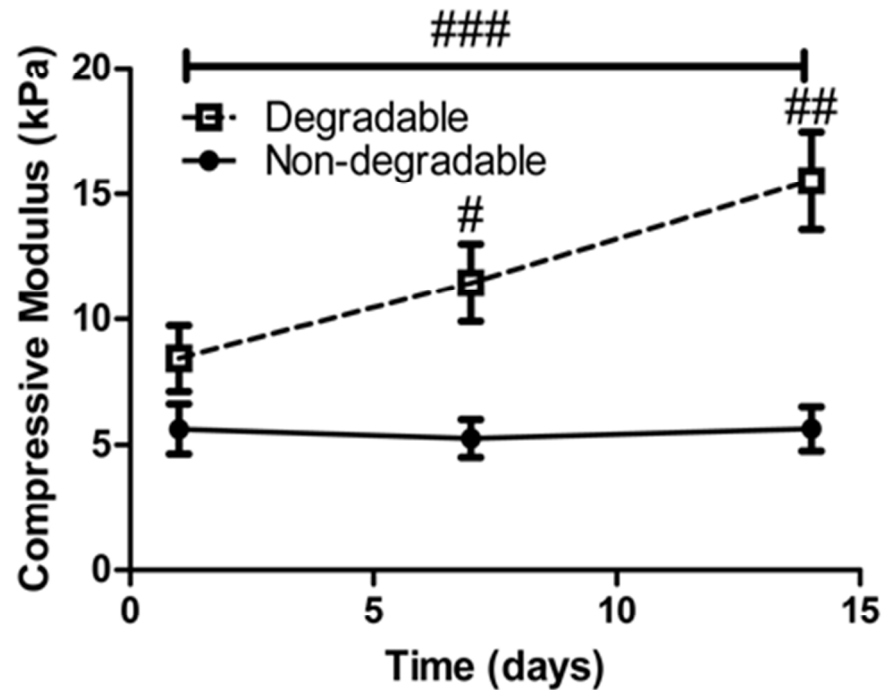


Figure 4.6. Compressive modulus of constructs assessed at day 1, 7, and 14. # indicates a statistically significant difference in modulus value at day 7 between degradable and non-degradable gels ($p<0.05$) and ## indicates a statistically significant difference in modulus value at day 14 between degradable and non-degradable gels ($p<0.001$). The line with ### indicates a statistically significant difference between day 1 and day 14 in moduli values for degradable gels

only ($p < 0.001$). Results are presented as mean \pm SD ($n=3$).

4.3.6. Quality of composition of ECM in co-culture scaffolds

To verify that the ECM produced had an articular cartilage phenotype, we qualitatively assessed the qualitative ratio of type II collagen to type I collagen on gel immunostained sections. Images revealed that at day 14 there was a scarce amount of type I collagen throughout all samples [Figure 4.7.(a,c)]. In contrast, type II collagen was more diffusely distributed in the degradable construct [Figure 4.7.(d)] than in the non-degradable sample, where it was pericellularly restricted and less prevalent [Figure 4.7.(b)]. Quantification of the amount of cells that stained positive for type I and type II collagen with image analysis revealed similar conclusions. As shown in Table 4.1., more cells stained positive for type II collagen in the degradable than the non-degradable sample, and the number of cells staining positive for type II collagen was dramatically higher than type I positive cells for both.

Table 4.1. Percentage of cells that stained positive for different types of collagen. There is a higher amount of cells that stained positive for type II collagen than type I collagen in both systems. In the degradable system, there is a significantly higher amount of cells that stained positive for type II collagen than there is in the non-degradable system ($p < 0.01$). Results are presented as mean \pm SD ($n=3$).

Percentage of cells that stain positive for type I or type II collagen in gels at day 14			
Non-degradable		Degradable	
Type I collagen	Type II collagen	Type I collagen	Type II collagen
26 \pm 6 %	53 \pm 7%	48 \pm 6%	84 \pm 4%

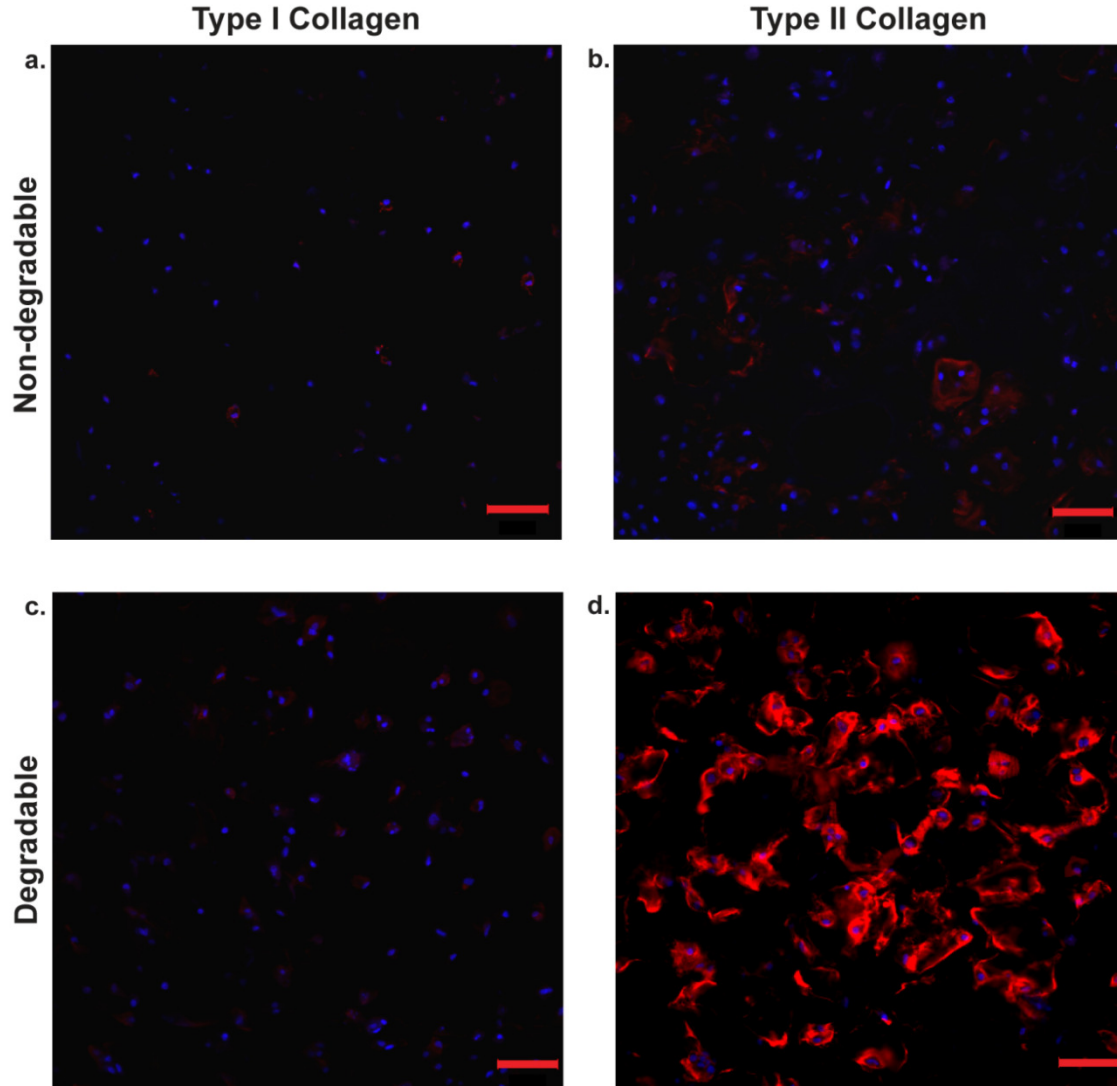


Figure 4.7. Type I collagen vs. type II collagen distribution assessed by immunofluorescence in non-degradable and degradable 8:1 co-culture constructs. (a) Non-degradable gel section stained for type I collagen at day 14, (b) non-degradable gel section stained for type II collagen at day 14, (c) degradable gel section stained for type I collagen at day 14, (d) degradable gel stained for type II collagen at day 14. Sections were stained for both anti-collagen type I and anti-collagen type II antibodies (red) and were counterstained with DAPI (blue) for cell nuclei. Scale bars represent 50 μm .

4.3.7. *Effect of inhibition of MMP activity on cartilage-specific matrix production and distribution*

We sought to test the effect of inhibiting MMP secretion by encapsulated cells and observe if the resulting matrix production was similar to non-degradable gels. Figure 4.S1.(a) shows how the addition of the MMP inhibitor to a co-culture system led to a fluorescent activity level similar to non-degradable gels. Live/Dead staining of gels at day 1 and 14 showed viability greater than 90% (data not shown). Histology staining at day 14 revealed that the co-culture degradable gels treated with the MMP inhibitor had a similar appearance to non-degradable gels with pericellularly limited matrix distribution [Figure 4.S1.(b,c)]. These data show how MMP secretion specifically plays a major role in matrix deposition and remodeling within this system, even more so than TGF- β 1 or the co-culture synergistic effects.

4.4. Discussion

Engineering a clinically viable scaffold for promotion of cartilage regeneration is challenging, partly because of the time required to generate a robust matrix by encapsulated cells, especially chondrocytes in monoculture. By utilizing an enzymatically degradable PEG-peptide system with localized presentation of TGF- β 1 and co-culture of chondrocytes with MSCs, we have shown quantitatively and qualitatively, *in vitro*, that encapsulated cells generate highly distributed and elaborate cartilage-specific ECM molecules at a higher rate than in a non-degradable scaffold. This system that responds to cell-mediated cues permits cells to secrete and distribute large matrix molecules that pervade throughout the scaffold and ultimately, should lead to mechanically robust constructs. Furthermore, since the construct utilized the synergistic

effects of co-culture (to promote scaffold remodeling) along with the benefits of a tethered growth factor, it expedited ECM generation by encapsulated cells relative to other common cartilage tissue engineering scaffolds.^{39,40}

When chondrocytes were encapsulated in PEG gels linked with an MMP-cleavable peptide at 40 million cells/mL, they produced cartilage tissue that was limited to the pericellular space [Figure 4.1.(b & c)]. This suggests that chondrocytes alone may not sufficiently degrade this particular peptide linker. Chondrocytes have relatively low metabolic activity since they reside in a hypoxic and hyperosmotic environment.⁴¹ This may be part of the reason that the chondrocytes were not observed to secrete MMPs at an appreciable rate in 3D culture.

On the other hand, when encapsulated alone, even at a lower seeding density of 5 million cells/mL, MSCs degraded the sequence at a higher rate than chondrocytes at 40 million cells/mL. This is likely because MSCs are more metabolically active than chondrocytes, as MSCs remodel their environments more frequently during development. There appears to be a synergistic effect between encapsulated MSCs and chondrocytes to degrade the sequence as shown in Figure 4.2.(b) and Figure 4.2.(c). The enhancing effect may be from paracrine signaling between cells to boost each other's activity.⁴² This may be more reflective of the native, developing cartilaginous environment, where MSCs and chondrocytes co-exist before all the MSCs differentiate into chondrocytes.⁴³ Furthermore, MSCs may play a role in cell number in the system, as they are known to drive chondrocyte proliferation in co-culture.³⁰ Future experiments could delve deeper into the signaling effects as to why there is increased MMP activity in co-culture between MSCs and chondrocytes. Additionally, studies could look for alternate ways to permit cell-mediated local degradation, which include investigating other peptide linker sequences that are more amenable to cleavage by chondrocyte-secreted enzymes.

In these experiments, a 4-arm 20 kDa PEG backbone at 6 wt% was used for co-culture experiments, since this formulation was studied in the aforementioned MSC experiments to assist in degradation of the peptide linker.^{28,38} Other studies investigating the gel crosslink density on matrix production by encapsulated cells found that scaffolds with a lower crosslinking density, like our monomer formulation, best supported ECM deposition in hydrogels.^{[10],[44]}

Extracellular matrix production data revealed that over just 14 days, the cell-mediated degradable gels permitted greater and widely distributed matrix production than non-degradable gels as revealed in Figures 4.4., 4.5., & 4.6. Furthermore, compressive modulus measurements confirmed that degradable constructs had superior mechanical properties relative to non-degradable gels as shown in Figure 6. There is a steadily increasing trend in modulus values over a short period of time which suggests that the matrix macromolecules generated in the degradable construct assemble in an appropriate fashion to stiffen the mechanical properties of the scaffold.⁴⁵ It is interesting to note that there are pockets of space around the cells in the degradable gel histology images, while only a few are present in non-degradable histology images. These pockets have a similar appearance to lacunae found in cartilage and could be due to pericellular degradation of the network. It is evident that cartilage ECM molecule distribution is wide-spread throughout the degradable scaffold, which likely led to the superior functional mechanical properties of the gel while the pericellularly restricted matrix in the non-degradable gels did not lead to an increased modulus.

The rate at which cartilage matrix molecules are produced and assembled in the locally-degradable constructs is substantial. Compared to the bulk degradation mechanism of hydrolytically cleavable PEG-PLA gels that use chondrocytes at 75 million cells/mL,¹¹ our system produces greater than 2.5 fold increase in GAGs (% wet weight) after 2 weeks while also

increasing modulus over time. Furthermore, when compared to a PEG/Chondroitin sulfate copolymer gel with encapsulated chondrocytes at 75 million cells/mL,⁴⁰ our system produces greater than 6 fold increase in total collagen content (% wet weight) over 2 weeks. Since matrix production is relatively rapid in these constructs, long culture times may not be necessary like they are in conventional cartilage tissue engineering experiments.

There was a concern that encapsulated MSCs in the co-culture system could lead to fibrocartilage formation as they do in monoculture in scaffolds.⁴⁶ However, past studies of co-culture scaffolds with higher amounts of MSCs have confirmed that the neotissue generated is not of fibrocartilagenous nature.³³ Furthermore, after a day, MSCs maintain a spherical morphology in co-culture, which could indicate a chondrogenic phenotype as shown in Figure 3(a). Additionally, collagen typing (high type II: type I collagen ratio by immunofluorescence) revealed an articular cartilage phenotype with type II collagen being diffusely distributed in degradable gels [Figure 4.7.]. Future studies could track the long-term fate of the MSCs in this co-culture system to ensure they maintain a chondrogenic phenotype and do not revert to generating fibrocartilage or bone.

In a potential clinical application as a MACT scaffold, this system could be advantageous due to the low amount of MSCs needed for co-culture. The subchondral bone under the cartilage defect could be stimulated by a technique like microfracture to recruit MSCs into the environment. The chondrocyte-laden PEG construct could then be implanted into the defect and the MSCs could migrate into the gel. Because only a small quantity of MSCs is required to initiate degradation of the target sequence, there is clinical potential with this technique. Furthermore, it is known that increased age of encapsulated chondrocytes can lead to increased MMP activity of the cells.⁸ Future studies should focus on optimizing the chondrocyte: MSC

seeding ratio and the monomer formulation to further tune the local degradation and enhance ECM production. Additional studies could confirm whether older chondrocytes might degrade this system without the aid of MSCs, and one could test the influence of various localized growth factors (e.g., TGF- β , Insulin-like growth factor) on promoting the secretory properties and ECM deposition by aged cells. It would also be interesting to see how matrix production is affected as the length of culture time is extended, especially in an *in vivo* environment.

4.5. Conclusion

A cell-mediated degradable hydrogel system based on peptide and protein functionalized PEG hydrogels was designed to allow local cell degradation in a manner that promotes diffuse cartilage ECM production, which ultimately leads to constructs with improved mechanical properties over just 14 days. The approach exploited the synergistic effects of co-culture between MSCs and chondrocytes to facilitate degradation of a collagen-derived, MMP-degradable peptide sequence (KCGPQG↓IWGQCK) as well as to promote cartilage ECM production in the presence of tethered TGF- β 1. Results confirmed that both encapsulated cell types maintained a high viability and a spherical morphology in the gels. Furthermore, the generated ECM resembles articular cartilage with respect to collagen typing by immunofluorescent staining (high type II collagen: type I collagen ratio). Local degradation seems to play a critical role in matrix elaboration with tissue engineering constructs, and non-degradable constructs of the same formulation had significantly less ECM production and lower moduli values over 14 days. This PEG hydrogel system may prove useful in applications as a scaffold for *in vivo* cartilage regeneration.

4.6. Experimental Section

4.6.1. PEG monomer synthesis

4-arm poly (ethylene glycol) (PEG) amine ($M_n \sim 20,000$) was modified with norbornene end groups as previously described.¹⁵ Briefly, 5-norbornene-2-carboxylic acid (predominantly endo isomer, Sigma Aldrich) was first converted to a dinorbornene anhydride using N,N'-dicyclohexylcarbodiimide (0.5 molar eq. to norbornene, Sigma Aldrich) in dichloromethane. 4-arm PEG amine (JenKem Technology) was then reacted overnight with the norbornene anhydride (5 molar eq. to PEG amines) in dichloromethane. Pyridine (5 molar eq. to PEG amines) and 4-dimethylamino pyridine (0.05 molar eq. to PEG amines) were also included. The reaction was conducted at room temperature under argon. End group functionalization was verified by ¹H NMR (Varian 400 MHz) to be >90%. The photoinitiator lithium phenyl-2,4,6-trimethylbenzoylphosphinate (LAP) was synthesized as described.²⁰ Peptides were purchased from American Peptide Company, Inc., which included a MMP-degradable crosslinker (KCGPQG↓IWGQCK) and a pendant adhesion peptide sequence derived from fibronectin (CRGDS). The non-degradable 3.5 kDa PEG dithiol linker was purchased from JenKem Technology.

4.6.2. Cell harvest and expansion

Primary chondrocytes were isolated from articular cartilage of the femoral-patellar groove of 6-month-old Yorkshire swine as detailed previously.⁴⁷ Cells were grown in a T-75 culture flask with media as previously described.⁴⁸ Briefly, chondrocytes were grown in growth medium (high glucose DMEM supplemented with ITS+ Premix 1% v/v (BD Biosciences), 50 mg/mL L-ascorbic acid 2-phosphate, 40 µg/mL L-proline, 0.1 µM dexamethasone, 110 µg/mL pyruvate, and 1% penicillin-streptomycin-fungizone) with the addition of 10 ng/mL IGF-1 (Peprotech) to maintain cells in a de-differentiated state. ITS was used because it promotes formation of articular cartilage over serum.⁴⁹ Cultures were maintained at 5% CO₂ and 37 °C.

Human mesenchymal stem cells (hMSCs) were isolated from bone marrow aspirates (Lonza) as previously described.^[28] Cells were grown in low glucose DMEM supplemented with 10% fetal bovine serum (FBS), 1% penicillin-streptomycin-fungizone, and 1 ng/mL recombinant human fibroblast growth factor (FGF-2, Peprotech). MSCs that were passaged two times were used for encapsulation experiments.

4.6.3. Hydrogel formulation and cell encapsulation

Human TGF- β 1 (Peprotech) was thiolated using 2-iminothiolane (Pierce) as previously described.³² Briefly 2-iminothiolane was reacted at a 4:1 molar ratio of TGF- β 1 for 1 h at RT. Thiolated TGF- β 1 was pre-reacted with a PEG norbornene monomer solution prior to cross-linking in the hydrogel formulations at a predetermined concentration of 50 nM. This concentration was selected based on previous work, demonstrating a maximal response from chondrocytes seeded at 40 million cells/mL.²¹ Additionally, 1 mM CRGDS was added to promote survival of the encapsulated MSCs.⁵⁰ RGD was not added to the chondrocyte-only system as it has previously been shown to have no impact on chondrocyte metabolic activity.⁵¹ Both growth factors were coupled to PEG norbornene via photoinitiated thiolene polymerization with 1.7 mM LAP and light ($I_0 \sim 3.5 \text{ mW/cm}^2$ at $\lambda=365 \text{ nm}$, ThorLabs M365L2-C2) for 30 seconds. Subsequently, the monomer solution was crosslinked using a degradable MMP linker (KCGPQG↓IWGQCK, MW~1800 kDa) or 3.5 kDa PEG dithiol at a 1:1 [thiol: ene] stoichiometric ratio of [12 mM thiol in either bis-cysteine peptide, or dithiol]: [12 mM norbornene] in a 6 wt% PEG solution using additional light ($I_0 \sim 3.5 \text{ mW/cm}^2$ at $\lambda=365 \text{ nm}$, ThorLabs M365L2-C2) for 30 seconds. For all experiments, 40 μL cylindrical gels (O.D. $\sim 5 \text{ mm}$, height $\sim 2 \text{ mm}$) were formed in the cut end of a 1 mL syringe. Since the degradable MMP

linker is synthesized in an acidic solution, the pH of the final solution was adjusted to 7, so as to not interfere with the bioactivity of the tethered TGF- β or the viability of encapsulated cells.

Unless otherwise specified, chondrocytes were co-encapsulated at 40 million cells/mL along with MSCs at 5 million cells/mL at an 8:1 chondrocyte: MSC ratio in 6 wt% monomer solution with tethered TGF- β and RGD. After gel formation, the cell-laden constructs were immediately placed in 48-well non-treated tissue culture plates with 1 mL DMEM growth medium (without phenol red). Media was changed every 3 days. For viability and morphology studies, MSCs were labeled with CellTracker™ Violet BMQC dye (Life Technologies) prior to encapsulation. At day 1 and 14, cell viability was assessed using a LIVE/DEAD® (Life Technologies) membrane integrity assay and confocal microscopy. Cell viability was quantified by image analysis using ImageJ software.

4.6.4. In situ confirmation of MMP cleavage in a 3D microenvironment

To determine whether the specific variant of the collagen-derived MMP degradable linker sequence used in the experiments (KCGPQG↓IWGQCK) was being cleaved by encapsulated cells, a fluorescently labeled peptide sensor of the same sequence was tethered in the gel. Leight *et al.*, developed the fluorogenic peptide substrate Dab-GGPQG↓IWGQK-Fl-AhxC using solid phase peptide synthesis (Tribute Peptide Synthesizer, Protein Technologies, Inc.) as previously described.³⁴ When the MMP-sensitive sequence is cleaved, it separates the quencher dabyl (Dab) from the fluorophore, fluorescein (Fl), permitting excitation. This fluorescent peptide was tethered into the gel at 0.5 mM along with TGF- β 1 [50 nM] and RGD [1mM] prior to crosslinking as depicted in Figure 4.2.(a).

Various ratios of co-culture seeding densities were used to determine which formulation degraded the sequence at an appreciable rate. As a control, the fluorescence of an acellular gel

was measured over 4 days. For chondrocytes in monoculture, cells were encapsulated at 40 million cells/mL, and for MSCs in monoculture, cells were seeded at 5 million cells/mL. For co-culture experiments, cells were seeded at 8:1, 16:1, and 24:1 (chondrocyte: MSC) where the chondrocyte cell seeding density was held constant at 40 million cells/mL. For MMP inhibitor experiments, the inhibitor GM 6001 (Millipore) was added at a concentration of 100 μ M to the media with co-culture gels every 3 days, and viability was tested at day 1 and 14. All values were normalized to the fluorescence value obtained immediately after gel formation (labeled day 0). Fluorescence measurements were conducted using a Synergy H1 microplate reader (BioTek) at 494 nm excitation/521 nm emission. An area scan was performed using a 48 well plate format with a 7X7 matrix, and the average fluorescent intensity was calculated for the entire matrix.

4.6.5. Wet weight, compressive modulus, and biochemical analysis:

On days 1, 7, and 14, hydrogels were removed from culture (n=3), weighed directly on a Mettler Toledo scale to determine the wet weight, and assessed for compressive modulus. Cell-laden constructs were subjected to unconfined compression to 15% strain at a strain rate of 0.5 mm/min to obtain stress-strain curves (MTS Synergie 100, 10N using TestWorks® 4 software). The modulus was estimated as the slope of the linear region of the stress-strain curves. Immediately afterwards, gels were snap frozen in LN₂ and stored at -70°C till biochemical analysis. Hydrogels were digested in 500 μ L enzyme buffer (125 μ g/mL papain [Worthington Biochemical] and 10 mM cysteine) and homogenized using 5 mm steel beads in a TissueLyser (Qiagen) that vibrates at 30 Hz for 10 min. Homogenized samples were digested overnight at 60°C.

Digested constructs were analyzed for biochemical content. DNA content was measured using a Picogreen assay (Life Technologies). Sulfated glycosaminoglycan (sGAG) content was

assessed using a dimethylmethylene blue assay as previously described with results presented in equivalents of chondroitin sulfate.⁵² Collagen content in the gels was measured using a hydroxyproline assay where hydroxyproline is assumed to make up 10% of collagen.⁵³ Additionally, digested acellular gels of either non-degradable or degradable formulations with tethered TGF- β 1 and RGD were assessed by the colorimetric assays using the Synergy H1 microplate reader (BioTek), and the resulting values were subtracted from their respective cell-laden sample values. GAG and collagen content were expressed as a percentage of the wet weight of the respective gels.

4.6.6. Histology and immunofluorescent analysis

On day 14, constructs (n=3) were fixed in 10% formalin for 30 min at RT, then snap frozen and cryosectioned as previously described.⁵⁴ Sections were stained for safranin-O and Masson's trichrome on a Leica autostainer XL and imaged in brightfield (20X objective) on a Nikon (TE-2000) inverted microscope.

For immunostaining, on day 14, sections were blocked with 5% BSA, then analyzed by anti-collagen type II (1:50, US Biologicals) and anti-collagen type I (1:50, Abcam). Sections were pre-treated with appropriate enzymes for 1 h at 37°C: hyaluronidase (2080 U) for collagen II, and pepsin A (4000 U) with Retrieagen A (BD Biosciences) treatment for collagen I to help expose the antigen. Sections were probed with AlexaFluor 555-conjugated secondary antibodies and counterstained with DAPI to reveal cell nuclei. All samples were processed at the same time to minimize sample-to-sample variation. Images were collected on a Zeiss LSM710 scanning confocal microscope with a 20X objective using the same settings and post-processing for all images. The background gain was set to negative controls on blank sections that received the same treatment. Positive controls were performed on porcine hyaline cartilage for collagen type

II and porcine meniscus for collagen type I [Figure 4.S5.]. The amount of cells that stained positive for each type of collagen was quantified by image analysis using Image J software.

4.6.7. Statistical analysis

Data are shown as mean \pm standard deviation. Two-way analysis of variance (ANOVA) with Bonferonni post-test for pairwise comparisons was used to evaluate the statistical significance of the data where the factors were culture time and hydrogel condition. One-way ANOVA was used to assess differences between conditions at specific time points for cases with two and three different groups. $p < 0.05$ was considered to be statistically significant.

4.7. Acknowledgements

The authors acknowledge Kyle Kyburz and Chun Yang for providing MSCs, as well as Amanda Meppelink and Richard Erali for providing knees on which chondrocyte isolations were performed. The authors would also like to acknowledge Emi Tokuda for helping purify the fluorescent peptide sensor as well as Dr. William Wan, Dr. Huan Wang for assistance on experimental design, and Russell Chagolla for help with image analysis. Funding for these studies was provided by the Howard Hughes Medical Institute and Department of Defense award number W81XWH-10-1-0791. The US Army Medical Research Acquisition Activity, 820 Chandler Street, Fort Detrick MD 21702-5014 is the awarding and administering acquisition office.

4.8. Supplementary Figures

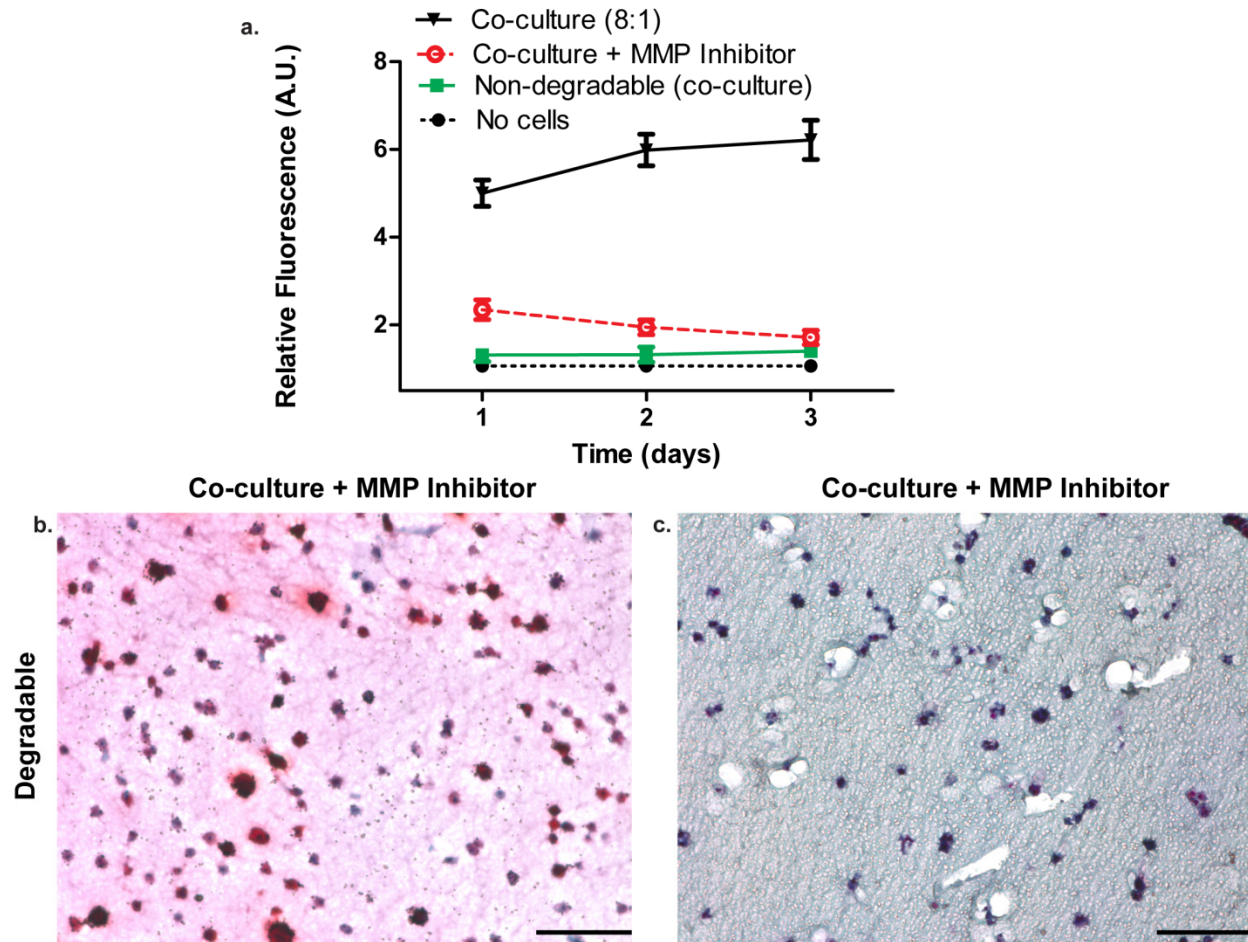
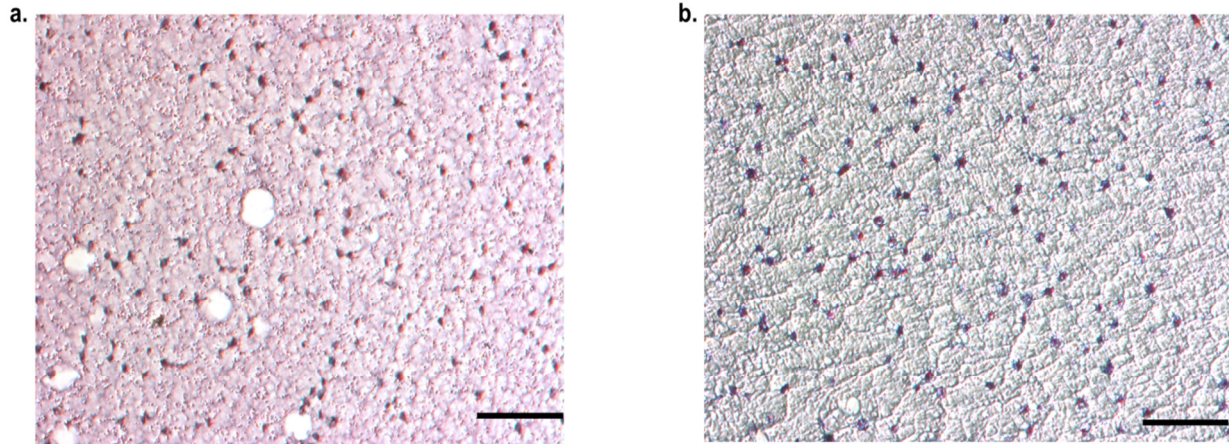
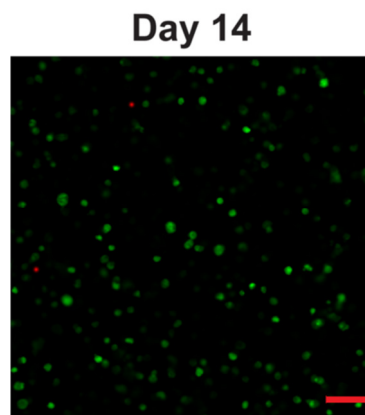


Figure 4.S1. Effect of MMP inhibitor on degradable 8:1 co-culture construct ECM production. (a) Evaluation of MMP cleavage rate reveals that the addition of MMP inhibitor (100 μ M) to co-culture gel media decreases the degradation rate of the degradable gel to a similar fluorescent signal as non-degradable and acellular constructs at day 3. Unadulterated co-culture gels continue to degrade the sequence at a high level. Results are presented as mean \pm SD (n=3). (b) GAG distribution in degradable gel sections treated with MMP inhibitor at day 14 with nuclei stained black and GAGs stained red. (c) Collagen distribution in degradable gel sections treated with MMP inhibitor at day 14 with nuclei stained black and collagen stained blue. Scale bars represent 100 μ m.



Supplementary Figure 4.S2. Early culture time points for matrix deposition of chondrocytes in degradable systems. (a) GAG distribution in degradable gel sections with chondrocytes seeded at 40 million cells/mL at day 7 with nuclei stained black and GAGS stained red. (b) Collagen distribution in degradable gel sections with chondrocytes seeded at 40 million cells/mL at day 7 with nuclei stained black and collagen stained blue. Scale bars represent 100 μ m.



Supplementary Figure 4.S3. Live/dead stain of an 8:1 co-culture degradable gel at day 14 with live cells (green), and dead cells (red). Non-degradable viability results are similar. Cells maintain $96 \pm 2\%$ viability in the degradable gel at day 14 ($n=3$). Scale bars represent 100 μ m.

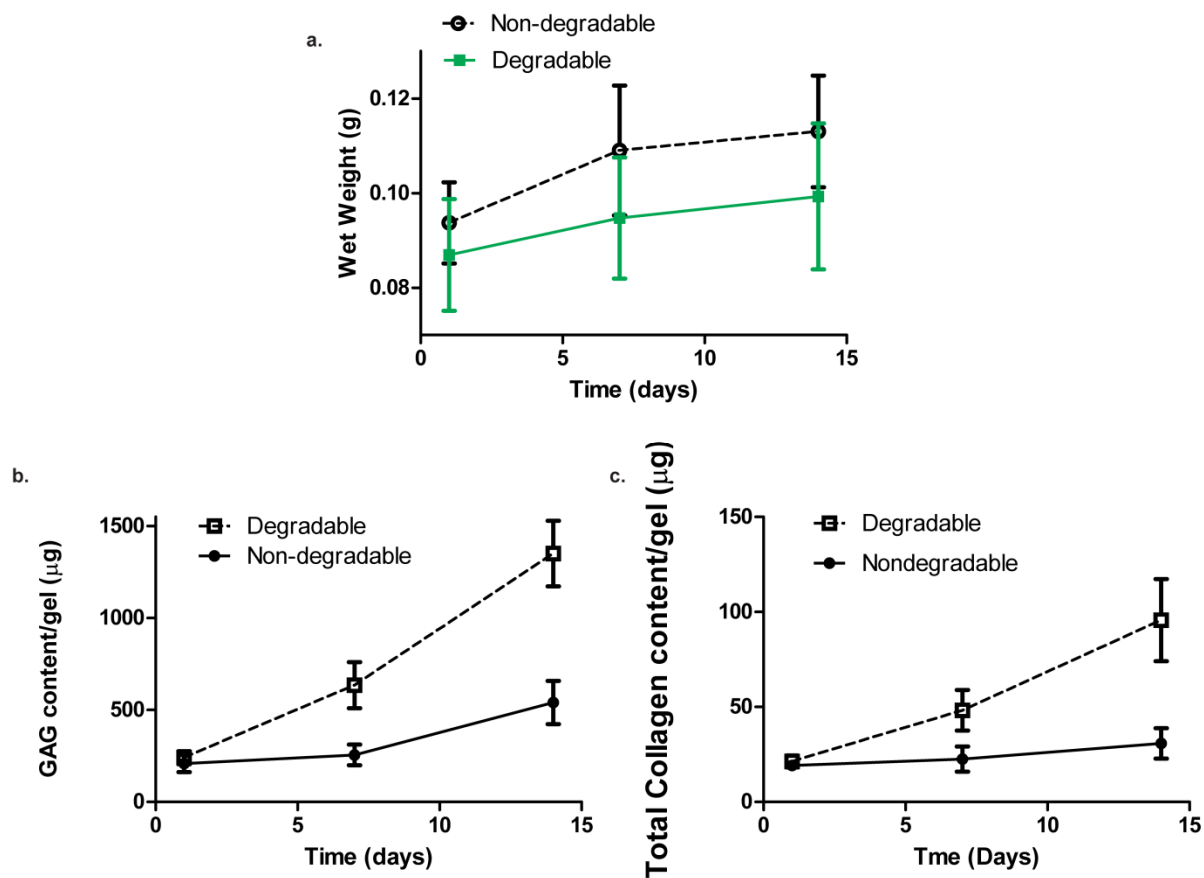


Figure 4.S4. Gel total content as a function of time. (a) Wet weight values shown for non-degradable and degradable 8:1 co-culture constructs at day 1, 7, and 14. Results are presented as mean \pm SD (n=3). (b) GAG content per gel at day 1, 7, and 14 for degradable and non-degradable constructs. (c) Total collagen content at day 1, 7, and 14 for degradable and non-degradable constructs. Results are presented as mean \pm SD (n=3).

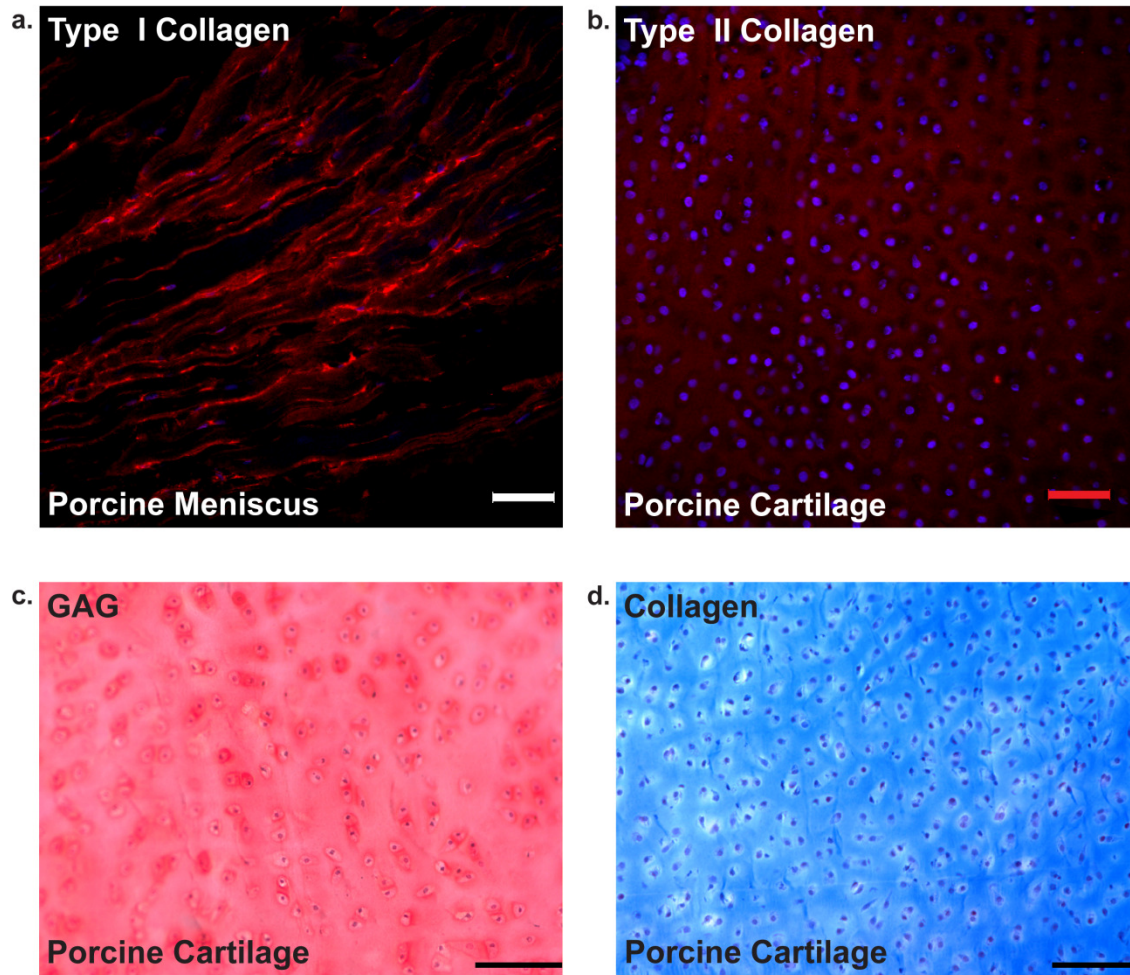


Figure 4.S5. ECM staining of native tissue.(a) Type I collagen (red) distribution in porcine meniscus with cell nuclei counterstained with DAPI (blue) as a positive control to confirm the antibody is working as expected. Scale bars represent 50 μm. (b) Type II collagen (red) distribution in porcine articular cartilage with cell nuclei counterstained with DAPI (blue) as a positive control to confirm the antibody is working as expected. Scale bars represent 50 μm. (c) GAG (red) distribution in porcine articular cartilage with cell nuclei stained black or violet. Scale bars represent 100 μm. (d) Collagen (blue) distribution in porcine meniscus with cell nuclei stained violet or black. Scale bars represent 100 μm.

4.9. References

1. Adolphe, M. *Biological regulation of the chondrocytes*. (CRC Press, 1992).
2. Falah, M., Nierenberg, G., Soudry, M., Hayden, M. & Volpin, G. Treatment of articular cartilage lesions of the knee. *Int. Orthop.* **34**, 621–30 (2010).

3. Kon, E. *et al.* Matrix-assisted autologous chondrocyte transplantation for the repair of cartilage defects of the knee: systematic clinical data review and study quality analysis. *Am. J. Sports Med.* **37**, 1565–665 (2009).
4. Kim, I. L., Mauck, R. L. & Burdick, J. A. Hydrogel design for cartilage tissue engineering: a case study with hyaluronic acid. *Biomaterials* **32**, 8771–82 (2011).
5. Hutson, C. B. *et al.* Synthesis and characterization of tunable poly(ethylene glycol): gelatin methacrylate composite hydrogels. *Tissue Eng. Part A* **17**, 1713–23 (2011).
6. Kock, L., van Donkelaar, C. C. & Ito, K. Tissue engineering of functional articular cartilage: the current status. *Cell Tissue Res.* **347**, 613–27 (2012).
7. Spiller, K. L., Maher, S. A. & Lowman, A. M. Hydrogels for the Repair of Articular Cartilage Defects. *Tissue Eng. Part B* **17**, 281–299 (2011).
8. Forsyth, C. B. *et al.* Increased matrix metalloproteinase-13 production with aging by human articular chondrocytes in response to catabolic stimuli. *J. Gerontol. A. Biol. Sci. Med. Sci.* **60**, 1118–24 (2005).
9. Nicodemus, G. D., Skaalure, S. C. & Bryant, S. J. Gel structure has an impact on pericellular and extracellular matrix deposition, which subsequently alters metabolic activities in chondrocyte-laden PEG hydrogels. *Acta Biomater.* **7**, 492–504 (2011).
10. Bryant, S. J. & Anseth, K. S. Hydrogel properties influence ECM production by chondrocytes photoencapsulated in poly(ethylene glycol) hydrogels. *J. Biomed. Mater. Res.* **59**, 63–72 (2002).
11. Bryant, S. J. & Anseth, K. S. Controlling the spatial distribution of ECM components in degradable PEG hydrogels for tissue engineering cartilage. *J. Biomed. Mater. Res. A* **64**, 70–9 (2003).
12. Zhao, W., Jin, X., Cong, Y., Liu, Y. & Fu, J. Degradable natural polymer hydrogels for articular cartilage tissue engineering. *J. Chem. Technol. Biotechnol.* **88**, 327–339 (2013).
13. Hume, P. S., He, J., Haskins, K. & Anseth, K. S. Strategies to reduce dendritic cell activation through functional biomaterial design. *Biomaterials* **33**, 3615–25 (2012).
14. Deforest, C. A. & Anseth, K. S. Photoreversible Patterning of Biomolecules within Click-Based Hydrogels. *Angew. Chem. Int. Ed. Engl.* **124**, 1852–1855 (2012).
15. Aimetti, A. A., Machen, A. J. & Anseth, K. S. Poly(ethylene glycol) hydrogels formed by thiol-ene photopolymerization for enzyme-responsive protein delivery. *Biomaterials* **30**, 6048–54 (2009).

16. Benton, J. A., Fairbanks, B. D. & Anseth, K. S. Characterization of valvular interstitial cell function in three dimensional matrix metalloproteinase degradable PEG hydrogels. *Biomaterials* **30**, 6593–603 (2009).
17. Fairbanks, B. D. *et al.* A Versatile Synthetic Extracellular Matrix Mimic via Thiol-Norbornene Photopolymerization. *Adv. Mater.* **21**, 5005–5010 (2009).
18. Hoyle, C. E. & Bowman, C. N. Thiol-ene click chemistry. *Angew. Chem. Int. Ed. Engl.* **49**, 1540–73 (2010).
19. Schwartz, M. P. *et al.* A synthetic strategy for mimicking the extracellular matrix provides new insight about tumor cell migration. *Integr. Biol. (Camb)*. **2**, 32–40 (2010).
20. Fairbanks, B. D., Schwartz, M. P., Bowman, C. N. & Anseth, K. S. Photoinitiated polymerization of PEG-diacrylate with lithium phenyl-2,4,6-trimethylbenzoylphosphinate: polymerization rate and cytocompatibility. *Biomaterials* **30**, 6702–7 (2009).
21. Sridhar, B. V., Doyle, N. R., Randolph, M. A. & Anseth, K. S. Covalently tethered TGF- β 1 with encapsulated chondrocytes in a PEG hydrogel system enhances extracellular matrix production. *J. Biomed. Mater. Res. A* **102**, 4464–4472 (2014).
22. Manicourt, D. H., Devogelaer, J. P. & Thonar, E. J. in *Dyn. Bone Cartil. Metab.* (Seibel, M., Robins, S. P. & Bilezikian, J. P.) 421–439 (Elsevier Science, 2006).
23. Lutolf, M. P. & Hubbell, J. A. Synthetic biomaterials as instructive extracellular microenvironments for morphogenesis in tissue engineering. *Nat. Biotechnol.* **23**, 47–55 (2005).
24. Park, Y., Lutolf, M. P., Hubbell, J. A., Hunziker, E. B. & Wong, M. Bovine Primary Chondrocyte Culture in Synthetic Matrix Hydrogels as a Scaffold for Cartilage Repair. *Tissue Eng.* **10**, 515–522 (2004).
25. Chubinskaya, S. Chondrocyte Matrix Metalloproteinase-8. *J. Biol. Chem.* **271**, 11023–11026 (1996).
26. Wu, P., DeLassus, E., Patra, D., Liao, W. & Sandell, L. J. Effects of serum and compressive loading on the cartilage matrix synthesis and spatiotemporal deposition around chondrocytes in 3D culture. *Tissue Eng. Part A* **19**, 1199–208 (2013).
27. Lin, Z., Willers, C., Xu, J. & Zheng, M.-H. The chondrocyte: biology and clinical application. *Tissue Eng.* **12**, 1971–84 (2006).
28. Kyburz, K. A. & Anseth, K. S. Three-dimensional hMSC motility within peptide-functionalized PEG-based hydrogels of varying adhesivity and crosslinking density. *Acta Biomater.* **9**, 6381–92 (2013).

29. Bahney, C. S., Hsu, C.-W., Yoo, J. U., West, J. L. & Johnstone, B. A bioresponsive hydrogel tuned to chondrogenesis of human mesenchymal stem cells. *FASEB J.* **25**, 1486–96 (2011).
30. Bian, L., Zhai, D. Y., Mauck, R. L. & Burdick, J. A. Coculture of Human Mesenchymal Stem Cells and Enhances Functional Properties of Engineered Cartilage Reverse primer. *Tissue Eng. Part A* **17**, 1137–1145 (2011).
31. Steadman, J. R. *et al.* Outcomes of microfracture for traumatic chondral defects of the knee: average 11-year follow-up. *Arthroscopy* **19**, 477–84 (2003).
32. McCall, J. D., Luoma, J. E. & Anseth, K. S. Covalently tethered transforming growth factor beta in PEG hydrogels promotes chondrogenic differentiation of encapsulated human mesenchymal stem cells. *Drug Deliv. Transl. Res.* **2**, 305–312 (2012).
33. Dahlin, R. L. *et al.* Articular chondrocytes and mesenchymal stem cells seeded on biodegradable scaffolds for the repair of cartilage in a rat osteochondral defect model. *Biomaterials* **35**, 7460–7469 (2014).
34. Leight, J. L., Alge, D. L., Maier, A. J. & Anseth, K. S. Direct measurement of matrix metalloproteinase activity in 3D cellular microenvironments using a fluorogenic peptide substrate. *Biomaterials* **34**, 7344–7352 (2013).
35. Silverman, R. P., Passaretti, D., Huang, W., Randolph, M. A. & Yaremchuk, M. J. Injectable tissue-engineered cartilage using a fibrin glue polymer. *Plast. Reconstr. Surg.* **103**, 1809–1818 (1999).
36. Passaretti, D. & Silverman, R.P. Huang, W Kirchhoff, C.H. Ashiku, S. Randolph, M.A. Yaremchuk, M. J. Cultured chondrocytes produce injectable tissue-engineered cartilage in hydrogel polymer. *Tissue Eng.* **7**, 805–15 (2001).
37. Ibusuki, S. *et al.* Engineering Cartilage in a Photochemically Crosslinked Collagen Gel. *J. Knee Surg.* **22**, 72–81 (2010).
38. Anderson, S. B., Lin, C.-C., Kuntzler, D. V & Anseth, K. S. The performance of human mesenchymal stem cells encapsulated in cell-degradable polymer-peptide hydrogels. *Biomaterials* **32**, 3564–74 (2011).
39. Bryant, S. J., Bender, R. J., Durand, K. L. & Anseth, K. S. Encapsulating chondrocytes in degrading PEG hydrogels with high modulus: engineering gel structural changes to facilitate cartilaginous tissue production. *Biotechnol. Bioeng.* **86**, 747–55 (2004).
40. Bryant, S. J., Arthur, J. A. & Anseth, K. S. Incorporation of tissue-specific molecules alters chondrocyte metabolism and gene expression in photocrosslinked hydrogels. *Acta Biomater.* **1**, 243–52 (2005).

41. Coimbra, I. B., Jimenez, S. A., Hawkins, D. F., Piera-Velazquez, S. & Stokes, D. G. Hypoxia inducible factor-1 alpha expression in human normal and osteoarthritic chondrocytes. *Osteoarthritis Cartilage* **12**, 336–45 (2004).
42. Wu, L., Prins, H.-J., Helder, M. N., van Blitterswijk, C. A. & Karperien, M. Trophic effects of mesenchymal stem cells in chondrocyte co-cultures are independent of culture conditions and cell sources. *Tissue Eng. Part A* **18**, 1542–51 (2012).
43. Hall, B. K. Earliest evidence of cartilage and bone development in embryonic life. *Clin. Orthop. Relat. Res.* **225**, 255–72 (1987).
44. Bryant, S. J., Chowdhury, T. T., Lee, D. A., Bader, D. L. & Anseth, K. S. Crosslinking Density Influences Chondrocyte Metabolism in Dynamically Loaded Photocrosslinked Poly(ethylene glycol) Hydrogels. *Ann. Biomed. Eng.* **32**, 407–417 (2004).
45. Hardingham, T. & Fosang, A. Proteoglycans: many forms and many functions. *FASEB J* **6**, 861–870 (1992).
46. Huey, D., Hu, J. & Athanasiou, K. Unlike Bone, Cartilage Regeneration Remains Elusive. *Science (80-.)*. **6933**, 917–921 (2012).
47. Yoo, J. J., Bichara, D. A., Zhao, X., Randolph, M. A. & Gill, T. J. Implant-assisted meniscal repair in vivo using a chondrocyte-seeded flexible PLGA scaffold. *J. Biomed. Mater. Res. A* **99**, 102–8 (2011).
48. Byers, B. A., Mauck, R. L., Chiang, I. E. & Tuan, R. S. Transient exposure to transforming growth factor beta 3 under serum-free conditions enhances the biomechanical and biochemical maturation of tissue-engineered cartilage. *Tissue Eng. Part A* **14**, 1821–34 (2008).
49. Chua, K. H., Aminuddin, B. S., Fuzina, N. H. & Ruszymah, B. H. I. Insulin-transferrin-selenium prevent human chondrocyte dedifferentiation and promote the formation of high quality tissue engineered human hyaline cartilage. *Eur. Cell. Mater.* **9**, 58–67 (2005).
50. Salinas, C. N. & Anseth, K. S. The enhancement of chondrogenic differentiation of human mesenchymal stem cells by enzymatically regulated RGD functionalities. *Biomaterials* **29**, 2370–7 (2008).
51. Villanueva, I., Weigel, C. A. & Bryant, S. J. Cell-matrix interactions and dynamic mechanical loading influence chondrocyte gene expression and bioactivity in PEG-RGD hydrogels. *Acta Biomater.* **5**, 2832–46 (2009).
52. Farndale, R. W., Sayers, C. A. & Barrett, A. J. A direct spectrophotometric microassay for sulfated glycosaminoglycans in cartilage cultures. *Connect. Tissue Res.* **9**, 247–8 (1982).

53. Woessner, J. F. The determination of hydroxyproline in tissue and protein samples containing small proportions of this imino acid. *Arch. Biochem. Biophys.* **93**, 440–7 (1961).
54. Ruan, J.-L. *et al.* An Improved Cryosection Method for Polyethylene Glycol Hydrogels Used in Tissue Engineering. *Tissue Eng. Part C. Methods* **19**, 794–801 (2013).

CHAPTER V

A BIOSYNTHETIC SCAFFOLD THAT FACILITATES CHONDROCYTE-MEDIATED DEGRADATION AND PROMOTES ARTICULAR CARTILAGE EXTRACELLULAR MATRIX DEPOSITION

Submitted to *Regenerative Engineering and Translational Medicine* 2015

5.1. Abstract

Articular cartilage remains a significant clinical challenge to repair because of its limited self-healing capacity. Interest has grown in the delivery of autologous chondrocytes to cartilage defects, and combining cell-based therapies with scaffolds that capture aspects of native tissue and allow cell-mediated remodeling could improve outcomes. Currently, scaffold-based therapies with encapsulated chondrocytes permit matrix production; however, resorption of the scaffold often does not match the rate of matrix production by chondrocytes, which can limit functional tissue regeneration. Here, we designed a hybrid biosynthetic system consisting of poly(ethylene glycol) (PEG) endcapped with thiols and crosslinked by norbornene-functionalized gelatin via a thiol-ene photopolymerization. The protein crosslinker was selected to facilitate chondrocyte-mediated scaffold remodeling and matrix deposition. Gelatin was functionalized with norbornene to varying degrees (~4-17 norbornenes/gelatin), and the shear modulus of the resulting hydrogels was characterized (<0.1-0.5 kPa). Degradation of the crosslinked PEG-gelatin hydrogels by chondrocyte-secreted enzymes was confirmed by gel permeation chromatography. Finally, chondrocytes encapsulated in these biosynthetic scaffolds showed significantly increased glycosaminoglycan deposition over just 14 days of culture, while maintaining high levels of viability and producing a distributed matrix. These results indicate the potential of a hybrid PEG-gelatin hydrogel to permit chondrocyte-mediated remodeling and

promote articular cartilage matrix production. Tunable scaffolds that can easily permit chondrocyte-mediated remodeling may be useful in designing treatment options for cartilage tissue engineering applications.

5.2. Introduction

Articular cartilage has limited self-healing properties, which can necessitate clinical interventions to heal tissue defects. Chondrocytes, the sole, differentiated resident cells found in mature articular cartilage are responsible for the generation and maintenance of tissue extracellular matrix (ECM).¹ When combined with encapsulated chondrocytes, biofunctional scaffolds can facilitate cartilage ECM production and deposition. A variety of natural and synthetic materials have been examined as potential cell carriers and as therapeutic solutions for cartilage repair.^{2,3,4,5}

A limitation with many of the currently studied chondrocyte scaffold carriers is that their resorption rates do not match the rate of matrix deposition by encapsulated cells as found in native tissue.⁶ Synthetic hydrogel carriers often limit deposition of chondrocyte-secreted matrix molecules to the space around the cell (i.e., the pericellular space).^{7,8} To overcome this issue, hydrogels have been engineered to hydrolytically degrade at physiologic pH, and while bulk degradation can be readily controlled, numerous material properties are highly coupled to this degradation. For example, high extents of degradation must occur before an ECM protein, like collagen, can assemble throughout hydrogel scaffolds, but this often coincides with a precipitous drop in gel mechanics.^{7,9} Alternatively, natural ECM proteins (e.g., collagen, hyaluronan) can form fibrillar hydrogel networks and provide numerous biological cues to guide tissue deposition by encapsulated cells.¹⁰ These ECM proteins can also be easily degraded by encapsulated cells, which leads to a cell-mediated, local degradation mechanism.¹¹ However, natural protein-derived

scaffold are often mechanically weak, and it is difficult to control their reproducibility and degradation, which can necessitate synthetic modification to these materials to control their time varying properties as well as facilitate the cell encapsulation process.^{12,13,14} As a result, recent efforts in the field have included a focus on hybrid synthetic ECM-mimics that have the potential to capture the tunability of synthetic scaffolds while integrating the properties of a cell-dictated degradation.

Previous work in our group demonstrated that cartilage cells encapsulated in poly (ethylene glycol) (PEG) hydrogels crosslinked by a collagen-derived peptide sequence (KCGPQG↓IWGQCK) generated constructs with increased, wide-spread articular cartilage-specific ECM compared to non-degradable gels.¹⁵ These findings supported the hypothesis that local, cell-mediated degradation not only promotes cartilage tissue deposition, but also maintains and in some cases increases scaffold mechanical integrity, in contrast to the decrease in bulk modulus typically found in hydrolytically cleavable scaffolds. However, it was found that enzymes secreted by encapsulated chondrocytes alone could not cleave the collagen-derived peptide linker with appropriate kinetics to enable a wide-spread distribution of matrix macromolecules. In fact, those constructs had the same pericellular matrix deposition pattern found in non-degradable scaffolds. Although previously, the Hubbell group engineered the collagen-derived peptide linker GPQG↓IWGQ to be more responsive to matrix metalloproteinases (MMPs),¹⁶ chondrocytes were found to remodel synthetic scaffolds more appropriately in the presence of cartilage progenitor cells, mesenchymal stem cells (MSCs). Only when encapsulated in co-culture with MSCs could the relatively metabolically inactive chondrocytes¹⁷ readily degrade the sequence and then generate ECM throughout the scaffold. Furthermore, others have shown that cell-secreted MMPs are able to cleave a full-length protein

at a greater rate than a peptide derived from that protein.¹⁸ Collectively, these findings motivated the experiments reported herein, where we investigate whether a hybrid scaffold composed of PEG and a full length protein, with a larger amount of collagenase-cleavable sequences per molecule than a peptide, would be responsive to chondrocyte-mediated local degradation and permit wide-spread matrix deposition.

Hybrid scaffolds that combine full-length proteins with synthetic linkers have been widely explored in tissue engineering applications. For example, fibrinogen^{19,20,21} and collagen^{22,23,24} have been chemically modified to allow covalent attachment to PEG by controlled reactions, and thereby facilitate encapsulated cell development and proliferation. Collagen appears to be a good candidate material to use as a scaffold with chondrocytes since degradation of collagen is a rate-limiting step in cartilage remodeling.²⁵ However, collagen is resistant to most proteases and requires special collagenases for its enzyme hydrolysis. On the other hand, gelatin, a natural biomacromolecule derived from denatured collagen, is less antigenic, more cost-effective,²⁶ and susceptible to more proteases than collagen.²⁷ These attributes potentially make gelatin an easier substrate to cleave by chondrocyte-secreted enzymes. Chondrocytes are also known to secrete gelatinases,^{28,29} which can specifically cleave gelatin more efficiently than most proteases. Finally, gelatin has been successfully employed as a scaffold to promote articular cartilage-specific matrix production of encapsulated chondrocytes,^{30,31} and hybrid PEG-gelatin networks have been developed for other tissue engineering applications with high cell viability under photopolymerization conditions.^{32,33,34}

In this work, we report the development of a gelatin network crosslinked with PEG for use with encapsulated chondrocytes and observe that the full-length protein is sensitive to local degradation cues and facilitates wide-spread cartilage-specific ECM deposition. Specifically,

gelatin was modified to contain pendant norbornene functionalities and reacted via a facile thiol-ene photopolymerization with PEG dithiols. The photoinitiated thiol-ene reaction is fast, highly efficient, and permits precise spatial and temporal control of network formation.³⁵

5.3. Materials and Methods

5.3.1. Functionalization of gelatin with norbornene

1 wt% (w/v) Gelatin type A 300 bloom with $M_n \sim 75$ kDa³⁶ (Sigma-Aldrich), which contains around 21 primary amines per molecule, was dissolved in pH 8.5 sodium bicarbonate. 5-norbornene-2-acetic acid succinimidyl ester (Sigma-Aldrich) was added to the gelatin solution (21 molar eq. to gelatin for 1:1 NB:gelatin amine stoichiometric ratio, 10.5 molar eq to gelatin for 0.5:1 NB:gelatin amine ratio, and 5.25 molar eq. to gelatin for 0.25:1 NB:gelatin amine ratio) and reacted with free amines on the gelatin molecule at 37°C for 1 h. The functionalized gelatin was dialyzed against pH 8.5 sodium bicarbonate for 4 h at RT exchanging buffer every hour, using Slide-A-Lyzer™ G2 dialysis cassette MW 10 kDa (Thermo scientific). After dialysis, solutions were frozen, lyophilized, and stored at -20°C until use.

The degree of functionalization of gelatin with norbornene was quantified as previously described.³² Briefly, the lysyl residue modification of gelatin was evaluated via the trinitrobenzenesulfonic acid assay (TNBSA, Thermo Scientific), which is a colorimetric assay that involves reacting TNBSA with primary amines on proteins for 2 h at 37°C, stopping the reaction with 10% SDS and 1 N HCl, then reading the absorbance at $\lambda=335$ nm using a Synergy H1 microplate reader (BioTek). The functionalization efficiency was calculated using

$$\left(1 - \frac{[\text{amines}] \text{ after gelatin modification}}{[\text{amines}] \text{ before gelatin modification}}\right) \times 100\%.$$

5.3.2. Characterization of degradation of the functionalized gelatin

To assess enzymatic cleavage of the norbornene-functionalized gelatin, 0.2 wt% gelatin solutions with varying extents of functionalization (1:1, 0.5:1, 0.25:1 NB:gelatin amine molar ratios, or unmodified gelatin) were dissolved in 0.1 M sodium nitrate (Sigma Aldrich) and 0.1 M sodium dibasic phosphate (Sigma Aldrich), so that the resulting solution could be assessed using aqueous mobile phase gel permeation chromatography (GPC) as previously described.³⁷ The gelatin solutions were incubated with either 20 units/mL (~0.1 mg/mL) type II collagenase (Worthington Biochemical) or chondrocyte-conditioned media from cells cultured for 3 days. The enzyme solutions were reacted with the functionalized gelatin for 1 h at 37°C. GPC was performed using a Waters HPLC pump and refractive index detector, Polymer Standard Service Suprema columns (3000 Å and 100 Å), and a linear PEG standard. All samples for GPC were prepared at a concentration of 0.2 wt% and filtered through a 0.4 µm filter. A mobile phase of 0.1 M sodium nitrate and 0.1 M sodium dibasic phosphate, injection volume of 25 µL and flow rate of 0.5 mL/min were used for all samples.

5.3.3. PEG-Gelatin network formation and mechanical measurements

The photoinitiator lithium phenyl-2,4,6-trimethylbenzoylphosphine oxide (LAP) was synthesized as previously described.³⁸ 2 wt% (w/v) gelatin functionalized with varying amounts of norbornene was prepared in PBS. We used 2 wt% solutions since this is the critical chain overlap concentration above which gelatin can form physical gels at room temperature.³⁹ The gelatin macromolecules were crosslinked by 0.1 wt% (0.3 mM) 3.5 kDa PEG dithiol (JenKem Technology) via a photoinitiated thiolene polymerization with 0.05 wt% (1.7 mM) LAP and light

($I_0 \sim 3.5 \text{ mW/cm}^2$, $\lambda = 365 \text{ nm}$) for 30 s. For all experiments, 40 μL cylindrical gels (O.D. $\sim 5 \text{ mm}$, height $\sim 2 \text{ mm}$) were formed in the cut end of a 1 mL syringe (BD Medical).

The various gels were placed in cell culture media to swell overnight and weighed the next day. The volume swelling ratio Q was calculated by first solving for the mass swelling ratio q , which involved dividing the measured swollen mass by the theoretical dry mass (data not shown) and assuming the density of the polymer was similar to that of its solvent. Parallel plate rheometry was performed on crosslinked gels that were formed with varied norbornene functionalization on the gelatin using an Ares 4400 DHR-3 shear rheometer (TA instruments) with 10% strain frequency sweep and a 10 rad s^{-1} strain sweep. The shear modulus (G) of the constructs was determined when the gels were in the linear viscoelastic regime for both the frequency and the strain sweep. The final network crosslinking density ρ_{xL} was calculated from rubber elastic theory⁴⁰ where $\rho_{\text{xL}} = GQ^{1/3}(RT)^{-1}$.

5.3.4. Cell harvest and expansion

Primary chondrocytes were isolated from articular cartilage of the femoral-patellar groove of 6-month old Yorkshire swine as detailed previously.⁴¹ Cells were grown in a T-75 culture flask with media as previously described.⁴² Briefly, chondrocytes were grown in growth medium (high glucose DMEM supplemented with ITS+ Premix 1 % v/v (BD Biosciences), 50 mg/mL L-ascorbic acid 2-phosphate, 40 $\mu\text{g/mL}$ L-proline, 0.1 μM dexamethasone, 110 $\mu\text{g/mL}$ pyruvate, and 1% penicillin-streptomycin-fungizone) with the addition of 10 ng/mL insulin-like growth factor (IGF-1) (Peprotech) to maintain cells in a de-differentiated state. ITS was used because it can promote formation of articular cartilage from chondrocytes.⁴³ Cultures were maintained at 5% CO_2 and 37°C .

5.3.5. Chondrocyte encapsulation and viability assessment

Chondrocytes were encapsulated at 40 million cells/ mL in 40 μ L cylindrical PEG-gelatin gels using gels formed from the 1:1 NB:gelatin amine synthesis conditions (~4.5 mM norbornene per gelatin chain). This macromolecule formulation degraded readily in response to chondrocyte-secreted enzymes. Cell-laden gels were immediately placed in 1 mL DMEM growth medium in 48-well nontreated tissue culture plates. Media was changed every 3 days. At day 1, 7, and 14 cell viability, and cellularity was assessed using a LIVE/DEAD® (Life Technologies) membrane integrity assay and confocal microscopy with ImageJ (NIH) for assessment of cell circularity.

5.3.6. Biochemical analysis of cell-hydrogel constructs

On days 1, 7, and 14, gels were removed from culture (n=3), weighed directly to determine the wet weight, snap frozen in LN₂ and stored at -70°C prior to biochemical analysis. Hydrogels were digested in 500 μ L enzyme buffer (125 μ g/mL papain [Worthington Biochemical] and 10 mM cysteine) and homogenized using 5 mm steel beads in a TissueLyser (Qiagen). Homogenized samples were digested overnight at 60°C.

Digested constructs were analyzed for biochemical content. DNA content, as an indicator of cell number, was measured using a Picogreen assay (Life Technologies). Sulfated glycoasaminoglycan (sGAG) content was assessed using a dimethylmethylene blue assay as previously described with results presented in equivalents of chondroitin sulfate.⁴⁴ As a cell-free control, digested acellular gels were assessed by the colorimetric assays, and the resulting values were subtracted from their respective cell-laden sample values. GAG content was expressed as a percentage of the wet weight of the respective gels.

5.3.7. Histology and immunofluorescence analysis

On day 14, constructs (n=3) were fixed in 10% formalin for 30 min at RT, then snap frozen and cryosectioned to 20 μ m sections as previously described.⁴⁵ At day 14, sections were stained for safranin-O and Masson's trichrome on a Leica autostainer XL and imaged in brightfield (20X objective) on a Nikon (TE-2000) inverted microscope.

For immunostaining, on day 14, sections were blocked with 5% BSA, then analyzed by anti-type II collagen (1:50, US Biologicals) and anti-type I collagen (1:50, Abcam). Sections were pre-treated with appropriate enzymes for 1 hr at 37°C: hyaluronidase (2080 U) for type II collagen, and Pepsin A (4000 U) with Retrieval A (BD Biosciences) treatment for type I collagen to help expose the antigen. Sections were probed with AlexaFluor 555-conjugated secondary antibodies (1:200, Life Technologies) and counterstained with DAPI to reveal cell nuclei. All samples were processed at the same time to minimize sample-to-sample variation. Images were collected on a Zeiss LSM710 scanning confocal microscope with a 20X objective using a z-stack maximum intensity projection of 4 x 5 μ m slices of the 20 μ m section using the same settings and post-processing for all the images. The background gain was set to negative controls on acellular sections that received the same treatment. Positive controls were performed on porcine hyaline cartilage for type II collagen and porcine meniscus for type I collagen (Figure 5.S2.a,b).

5.3.8. Statistical analysis

Data are shown as mean \pm standard deviation. One-way ANOVA with a two-tailed Bonferroni's multiple comparison posttest was used to assess differences in experimental outputs at different culture time points, since means of three samples are being compared

simultaneously. $\alpha=0.05$ was used for all analysis. Statistical calculations were performed on GraphPad Prism[®]. $p<0.05$ was considered to be statistically significant.

5.4. Results

5.4.1. *Modifying PEG-gelatin network properties*

By varying the extent of norbornene functionalization of gelatin, we aimed to tune the crosslinking density of the final network, and therefore the macroscopic properties of the resulting hydrogel. Figure 5.1.a contains a schematic of gelatin functionalization with norbornene, along with the estimated amount of norbornenes attached to each gelatin molecule (based on calculations). Figure 5.1.b depicts the photopolymerization between 2 wt% NB-functionalized gelatin with varying amounts of norbornene and 0.1 wt% PEG dithiol along with the concentrations of norbornene and thiol.

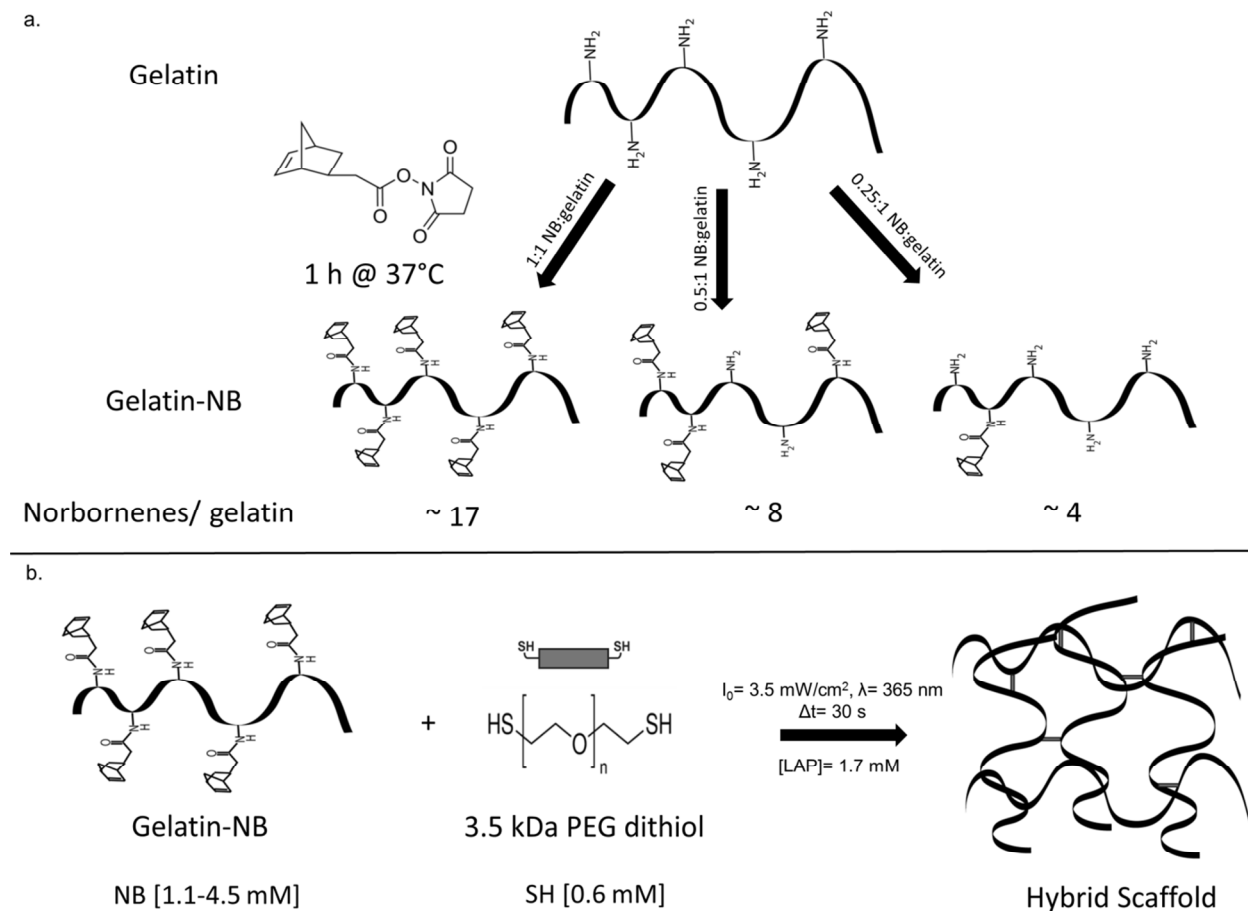


Figure 5.1. Gelatin functionalization with norbornene and photopolymerization with PEG. a) Depiction of the reaction of gelatin with varying molar amounts of norbornene succinimidyl ester. The reaction proceeded for 1 h at 37°C and the amount of functionalization on the product was measured by TNBSA. The estimated amount of norbornenes per gelatin molecule is shown below based on functionalization efficiency calculations. b) Photopolymerization scheme between 2 wt% norbornene-functionalized gelatin with varying amounts of norbornene [1.1-4.5 mM] and 0.1 wt% 3.5 kDa PEG dithiol with [0.6 mM] thiol to form a covalently-crosslinked hybrid scaffold.

We characterized the efficiency of lysine modification on gelatin by the 5-norbornene-2-acetic acid succinimidyl ester reaction using the TNBSA assay, with data shown in Table 5.1. (n=5). The 1:1 norbornene:gelatin amine condition led to $75 \pm 6\%$ functionalization efficiency, which is similar to that observed with other studies using similar amine modifying

techniques.^{32,33} Lower stoichiometric ratios (0.5:1 and 0.25:1 norbornene:gelatin amine) led to corresponding decreases in the functionalization efficiency, $36 \pm 5\%$ and $19 \pm 5\%$, respectively. The unmodified gelatin was measured to have ~ 21 amine groups per molecule, which was also confirmed by other studies,^{32,36} and suggests that the synthesized gelatin macromolecules have on average ~17 (75%), 8 (36%), and 4 (19%) norbornene pendent groups per molecule for crosslinking. The swollen shear modulus of the resulting acellular constructs was measured, and the crosslinking density of the scaffold was calculated. Consistent with the expected crosslinking reaction, both values increased with increasing amount of norbornene functionalization as shown in Table 5.1. (n=5).

Table 5.1. Material properties of acellular hybrid scaffolds (n=5)

Molar ratio of norbornene succinimidyl ester reacted with gelatin amines	Norbornene Functionalization Efficiency^a (%)	Calculated amount of norbornene on gelatin chain^b (mM)	Thiol concentration (mM)	Swollen Shear Modulus G (kPa)	Crosslinking Density^c ρ_{XL} (mM)
0.25:1 Norbornene:gelatin amines	$19 \pm 5\%$	~1.1	0.6	<0.1	<0.18
0.5:1 Norbornene: gelatin amines	$36 \pm 5\%$	~2.2	0.6	0.2 ± 0.1	0.36 ± 0.04
1:1 Norbornene:gelatin amines	$75 \pm 6\%$	~4.5	0.6	0.5 ± 0.1	0.90 ± 0.05

a. Norbornene functionalization efficiency was calculated using $\{1 - \frac{[\text{amines}]_{\text{after modification}}}{[\text{amines}]_{\text{before modification}}}\} \times 100\%$

b. Norbornene concentration per gelatin molecule was calculated by accounting for the amount of amines on type A gelatin (~21) and the norbornene functionalization efficiency for each condition assuming only norbornenes replaced the gelatin amines.

c. Crosslinking density was calculated from rubber elastic theory: $\rho_{XL} = GQ^{1/3} (RT)^{-1}$

5.4.2. Verification of degradation of modified gelatin by chondrocyte-secreted enzymes

Modification of proteins can alter their structure and change their susceptibility to enzymatic degradation, since altered lysines may affect the way an enzyme binds to its site to initiate cleavage. To verify that the modified gelatin could degrade in the response to chondrocyte-secreted enzymes, we performed a solution based assay, and tested the degradability of various modified gelatin macromolecules when exposed to either collagenase or chondrocyte-conditioned media. We chose chondrocyte-conditioned media that was collected after 3 days of culture, since we have previously observed that the secreted enzymes can cleave a collagen-derived peptide sequence during that time frame.¹⁵ After incubation of the modified gelatin with enzymes, GPC was used to monitor the degradation of both unmodified and norbornene-substituted gelatin. The unmodified gelatin peak elutes at 18 min and is clearly distinguished from a large system peak at 20 min that occurs as a consequence of a small dissimilarity in composition, and thus a refractive index difference, between the injected buffer and the mobile phase. A substitution of 0.25:1 or 0.5:1 NB:gelatin amine resulted in no significant change in retention time compared to the unmodified gelatin, while the 1:1 NB:gelatin amine showed a distinguishable, yet slightly shifted and significantly smaller peak. We hypothesize that this may be due to the formation of a slightly more hydrophobic macromolecule that may be more susceptible to interaction with the column stationary phase than the unmodified gelatin. When collagenase was added to each gelatin sample, the peak at 18 min completely disappears, indicating degradation of gelatin into smaller molecular weight fragments. A lower MW shoulder appears on the system peak, which corresponds to the gelatin degradation products. Finally, chondrocyte-conditioned media was added to each gelatin sample to assess degradation in the presence of cell-secreted enzymes. Similar to treatment with

collagenase, the gelatin peak was shifted to the low molecular weight shoulder, indicating that the norbornene-functionalized gelatin can be degraded by chondrocyte-secreted enzymes. Results are summarized in Figure 5.S1., while Figure 5.2. shows the effect of adding collagenase or chondrocyte-secreted enzymes to the most highly substituted gelatin (i.e., reacted at 1:1 NB:gelatin amines).

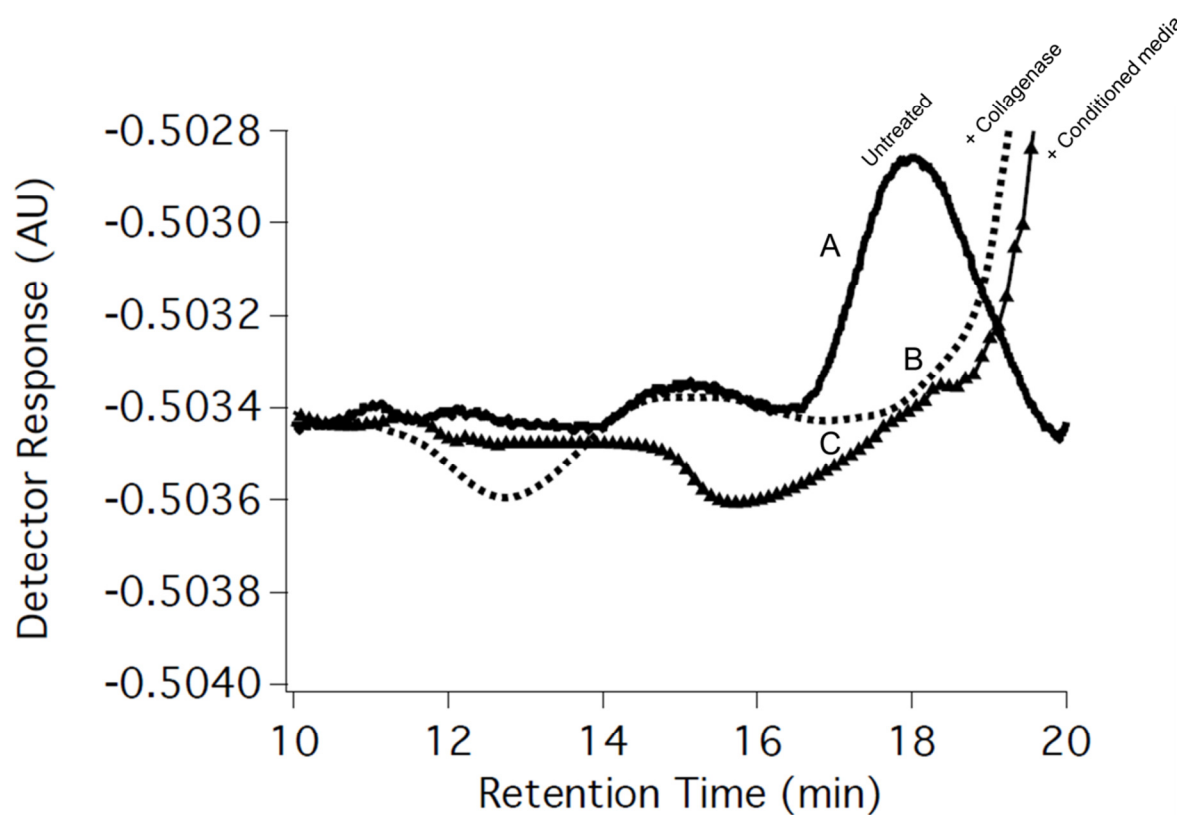


Figure 5.2. GPC chromatogram of gelatin functionalized with norbornene at 1:1 NB:gelatin amine that is either untreated (A), treated with 20 U/mL collagenase for 1 h at 37°C (B) or treated with day 3 chondrocyte-conditioned media for 1 h at 37°C (C). The untreated gelatin peak that is found at 18 min elution disappears after treatment with either collagenase or chondrocyte-conditioned media suggesting degradation of gelatin to smaller byproducts by the enzymes.

5.4.3. Chondrocyte viability, cellularity, and morphology

Gelatin amines that were reacted at a 1:1 molar ratio with norbornene was used in all subsequent cell encapsulation experiments, since this formulation contained a higher amount of covalent crosslinks and thus could retain a gel structure for a longer period of time for the slow-growing chondrocytes. We chose a chondrocyte seeding density of 40 million cells/mL, as chondrocytes have been studied at this density for cartilage tissue engineering experiments using 3D scaffolds and shown to secrete an elaborate ECM at this concentration.^{46,47,48} After chondrocytes were encapsulated, their viability, cellularity, and morphology were assessed at day 1, 7, and 14. In Figure 5.3.a, the chondrocytes retained a spherical morphology at day 1 and begin to spread as observed on days 7 and 14, which suggests that the chondrocytes are able to locally remodel the environment. Image processing reveals that the circularity of the chondrocytes decreases from day 1 to day 7 and day 14 as shown in Figure 5.3.b, further corroborating the results seen in Figure 5.3.a.

Additionally, the cells retain a high viability (calculated to be >95%) at all the time points and appear to proliferate over time, as there are many more cells in the constructs at day 14 than there are at day 1. This increase in cellularity was quantified by the Picogreen analysis that measures DNA content and shows a significant increase in cell number between day 1 and day 14 ($p=0.01$) (Figure 5.3.c). Collectively, these results suggest that chondrocytes can thrive, proliferate, and remodel their environment in this scaffold system.

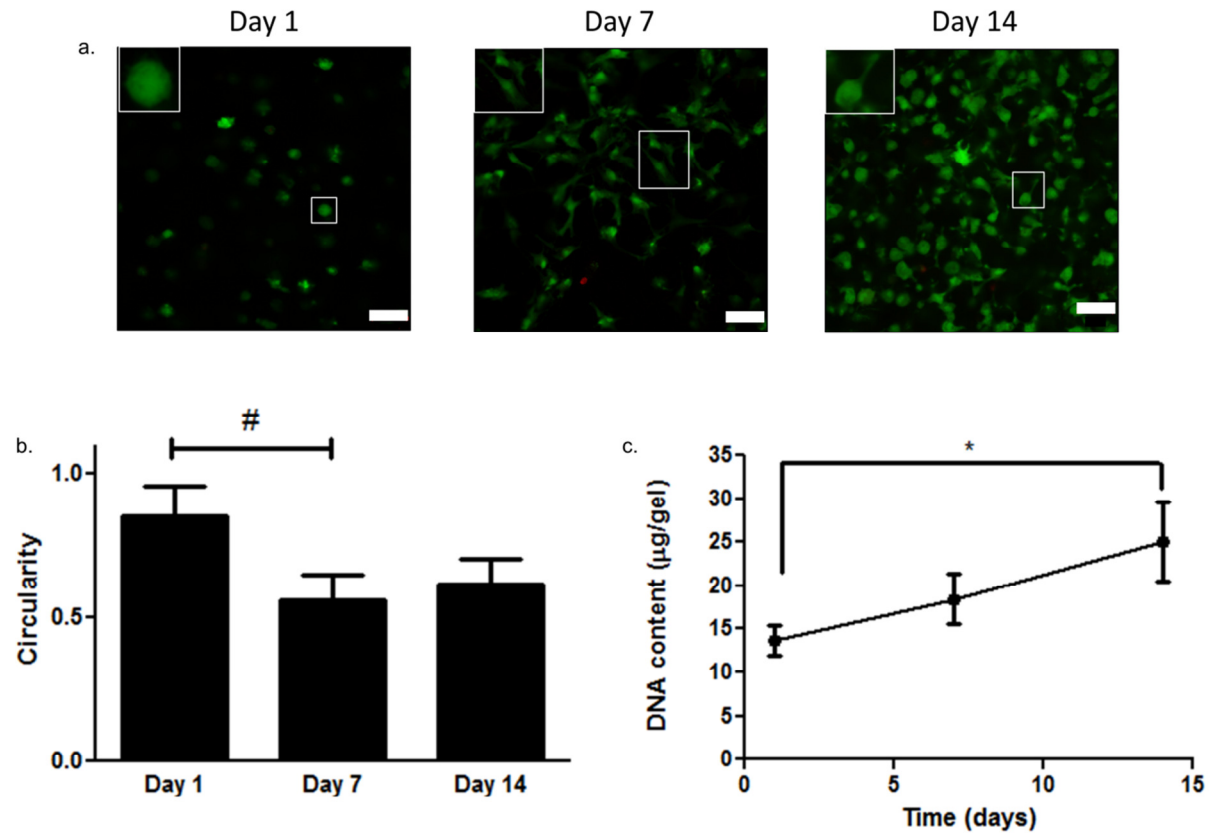


Figure 5.3. Viability, morphology, and cellularity of 1:1 NB:gelatin amine hybrid scaffold. a) Live(green)/dead (red) stains of encapsulated chondrocytes. Viability is calculated to be greater than 95% at all the time points. Insets highlight single cells changing in morphology from rounded to more spread over time. Scale bars represent 50 μm. b) Degree of circularity between 0 (not rounded) and 1(rounded) of the encapsulated cells. # with a line indicates a statistically significant difference in circularity value between day 1 and day 7 ($p=0.02$). Results are presented as mean \pm SD ($n=3$). c) DNA content (μg/gel) as measured by Picogreen assay over 14 days. * with a line indicates a statistically significant difference between day 1 and day 14 in DNA content ($p=0.01$). Results are presented as mean \pm SD ($n=3$).

5.4.4. ECM production and deposition in scaffolds

GAG content was assessed biochemically at days 1,7, and 14, and the distribution of secreted matrix molecules was examined by staining sections with Safranin-O (GAG) and

Masson's trichrome (collagen). Measured quantities of the matrix molecules were normalized to the wet weight of each construct. As Figure 5.4.a shows, at day 14, GAGs (red) were extensively distributed throughout the gel. Staining of an acellular construct revealed low background staining (Figure 5.4.b), indicating that staining was primarily from macromolecules secreted by the resident chondrocytes. Not only do the GAG molecules appear to be elaborated throughout the scaffold, quantitative analysis, as shown in Figure 5.4.c, supports the conclusion that the amount of sGAG deposition increased significantly from day 1 to day 14 ($p=0.0004$). A similar distribution pattern is observed with collagen (dark blue) as seen in Figure 5.5.a and Figure 5.5.b. Figure 5.5.e depicts the scaffold as optically opaque, with a cartilaginous appearance after 14 days of culture, much more than either the acellular (Figure 5.5.c) or day 1 time point (Figure 5.5.d), further suggesting wide-spread ECM distribution in the scaffold⁴⁹. This versatile PEG-crosslinked gelatin system appears to provide a scaffold that is readily degraded by chondrocytes and can support matrix deposition over time.

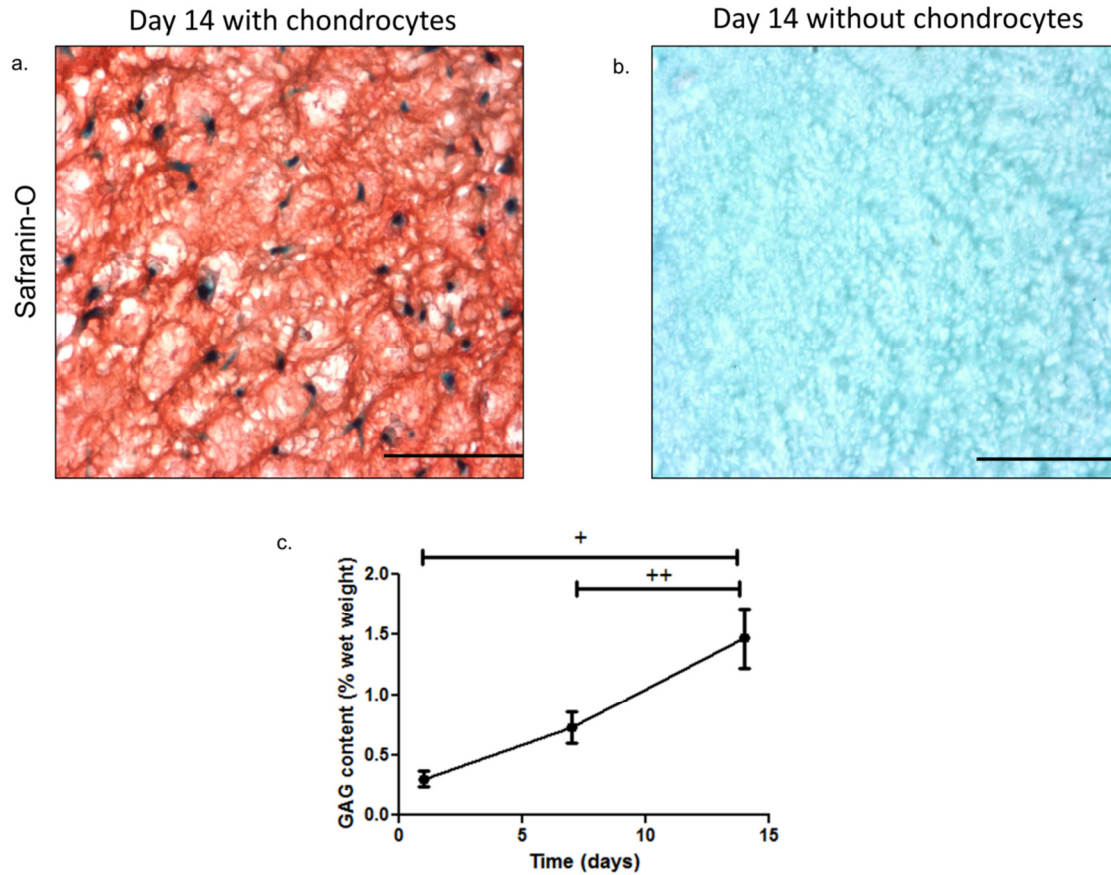


Figure 5.4. Glycosaminoglycan distribution and production in a 1:1 NB:gelatin amine hybrid scaffold. a) Section with encapsulated chondrocytes at day 14 stained for GAGs with nuclei stained black and GAGs stained red. b) Acellular section stained for GAGs at day 14. Scale bars represent 100 μm . c) Total GAG content expressed as a percentage of the respective construct wet weight assessed at day 1, 7, and 14. + with a line indicates a statistically significant difference in GAG content between day 1 and day 14 ($p=0.0004$), and ++ with a line indicates a statistically significant difference in GAG content between day 7 and day 14 ($p=0.001$). Results are presented as mean \pm SD ($n=3$).

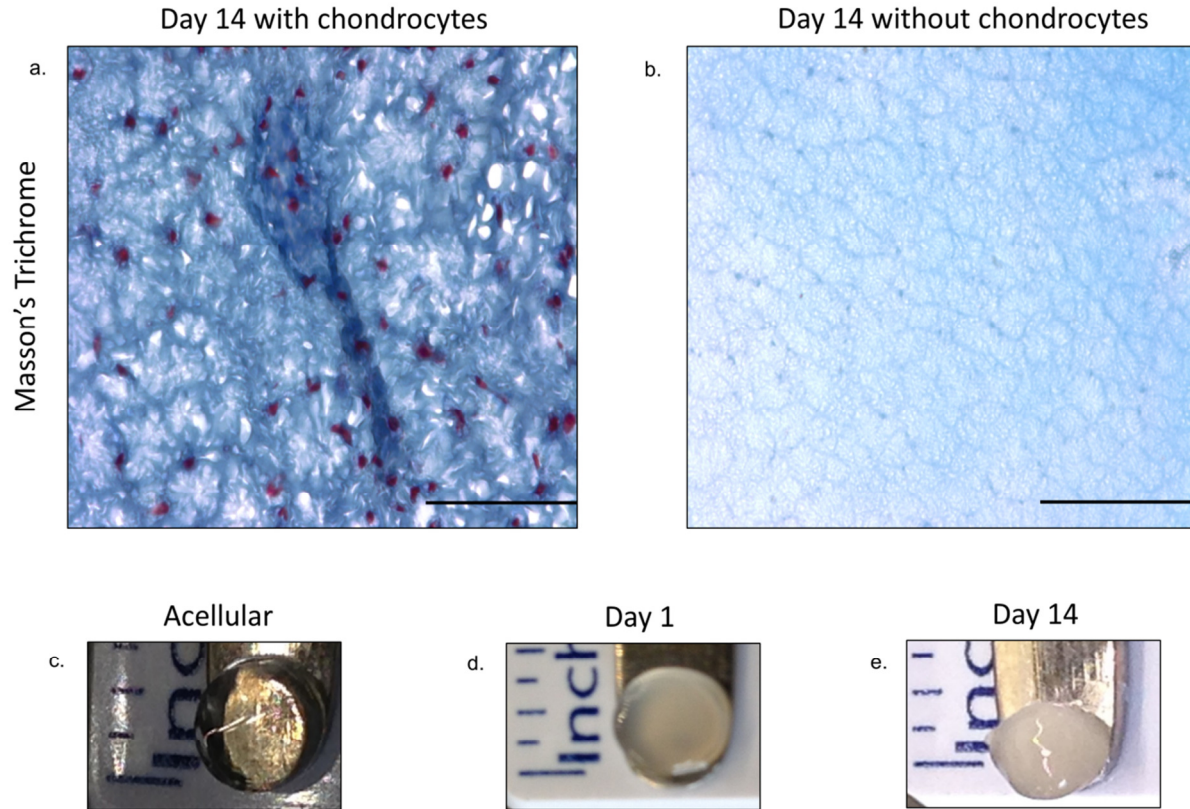


Figure 5.5. Collagen and ECM distribution in a 1:1 NB:gelatin amine hybrid scaffold. a) Section with encapsulated chondrocytes at day 14 stained for collagen with nuclei stained violet and collagen stained blue. b) Acellular section stained for collagen at day 14. Scale bars represent 100 μm . c) Gross image of a transparent acellular scaffold at day 1. d) Gross image of a translucent scaffold with encapsulated chondrocytes at day 1. e) Gross image of an opaque scaffold with encapsulated chondrocytes at day 14 that has a cartilaginous appearance.

5.4.5. *Quality of collagen generated by chondrocytes in the scaffold*

To verify that the collagen generated by the chondrocytes had an articular cartilage phenotype, we qualitatively assessed the ratio of type II collagen to type I collagen on gel immunostained sections. Images revealed that at day 14, negligible type I collagen (red) was observed, but robust type II collagen (red) was observed throughout the scaffold as seen in Figure 5.6.

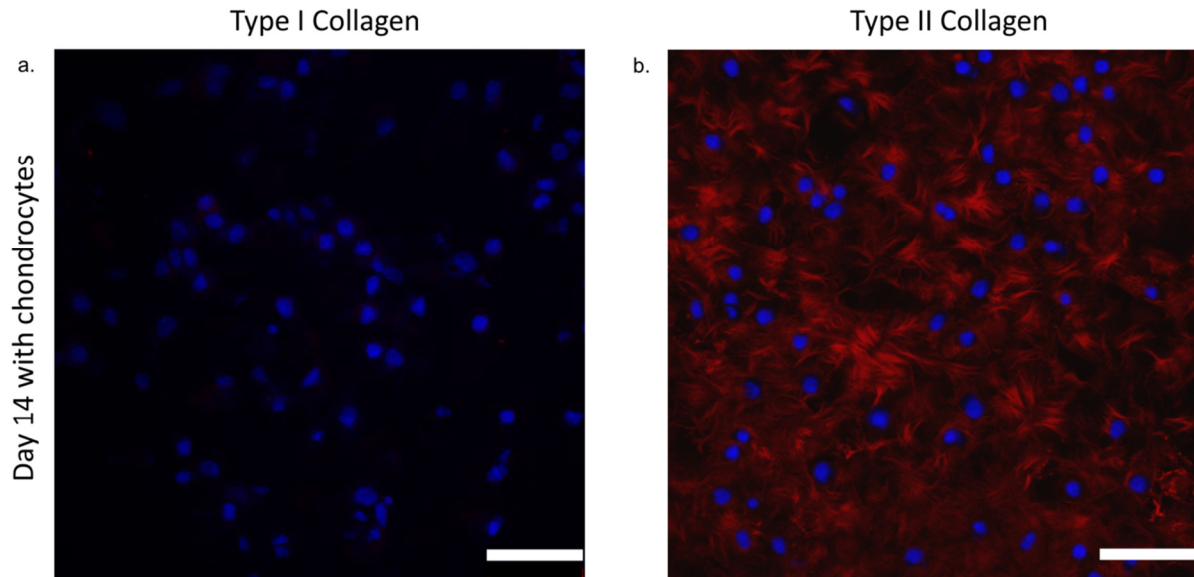


Figure 5.6. Type I collagen versus type II collagen distribution assessed by immunofluorescence in a 1:1 NB:gelatin amine hybrid construct with encapsulated chondrocytes at day 14. a) Gel section stained for type I collagen. b) Gel section stained for type II collagen. Sections were stained for both anti-collagen type I and anti-collagen type II antibodies (red) and were counterstained with DAPI (blue) for cell nuclei. Scale bars represent 50 μm .

5.5. Discussion

Engineering a clinically viable scaffold to promote cartilage regeneration is challenging. By using a novel, tunable hybrid biologic-synthetic system, we have shown quantitatively and qualitatively, *in vitro*, that encapsulated chondrocytes generate highly distributed cartilage-specific ECM molecules. We showed that chondrocyte-secreted enzymes can degrade norbornene-functionalized gelatin and further demonstrated that cells are viable when embedded in the hydrogel formulation. The chondrocytes appear to spread throughout the scaffold, suggesting that encapsulated cells are locally remodeling their environment, and, facilitates the eventual deposition of matrix throughout the scaffold. Future investigations with this scaffold could prove useful in designing a cell carrier system to promote cartilage regeneration *in vivo*.

Modulus studies confirmed that these PEG-gelatin scaffolds could be tuned to adjust their crosslinking density and macroscopic properties that depend on this parameter (Table 5.1.). In general, it can be more difficult to change material properties of pure protein-based gels, so covalent crosslinking can lead to higher mechanical properties.²² If the crosslinking density can be adjusted by the user, it can also alter the amount of tissue deposition.^{9,50} Gel properties, degradation and ECM deposition might be further tuned by changing the network connectivity using different molecular weight PEG crosslinkers or multiarm PEG crosslinkers depending on whether a more tightly or loosely crosslinked network is desired.

We confirmed that chondrocyte-secreted enzymes could degrade norbornene-functionalized gelatin by visualizing the degradation products with GPC (Figure 5.2.). GPC data suggests that norbornene-functionalized gelatin is degraded to smaller molecular weight products in the presence of chondrocyte-conditioned media. This confirms that norbornene-functionalized gelatin is a viable platform for the formation of chondrocyte-specific cellularly degradable hydrogels. We demonstrated these results in a solution-based assay, but a complementary study has shown that functionalized, and crosslinked gelatin can be degraded by cell-secreted enzymes as well.⁵¹ Here, we observe this indirectly by changes in the chondrocyte morphology (Figure 3a); however, there are alternate ways to design systems that might respond to chondrocyte-secreted enzymes. One idea would be to include an aggrecanase-based cleavable peptide linker.⁵² We selected the full-length protein gelatin for this study, as we hypothesized that its multiple MMP-cleavable sites would lead to more facile cleavage by chondrocytes than small peptide sequences as suggested by other groups.¹⁸ In fact, the gelatin molecule contains about 6 MMP-sensitive sequences per molecule,²⁷ which appears to be readily cleaved by chondrocyte-secreted enzymes at the cell density studied.

Viability results revealed that chondrocytes thrive and proliferate in the hybrid network. Cellularity in the gel quantitatively increased, which was confirmed by Picogreen, and the cells spread over time (Figure 5.3.). Part of the reason for this change in cell morphology is likely because the chondrocytes are binding to adhesion factors present on the protein.²⁶ Another explanation is that the cells are degrading the network by a cell-mediated mechanism and spreading,⁵¹ which could facilitate the observed wide-spread matrix deposition. Future studies could focus on improving methods to verify that local degradation is occurring, which could include monitoring the cell-based degradation using microrheological techniques, such as microparticle tracking.⁵³

Cartilage-specific matrix produced by chondrocytes was distributed throughout the entire scaffold as it was in other cell-mediated degradable scaffolds¹⁵ (Figure 5.4.a & Figure 5.5.a). Additionally, the GAG production from this scaffold was comparable to what was seen in a cellularly degradable cartilage tissue engineering scaffold with a similar cell seeding density;¹⁵ however, this system did not need to tether a growth factor, such as TGF- β , to the network in order to elicit a response from chondrocytes. A possible explanation for the robust secretory properties might relate to the fact that gelatin can bind to growth factors released by cells and perhaps present them to embedded chondrocytes in a local and sustained manner.¹

The encapsulated chondrocytes have a lower circularity at day 14, which can be suggestive of a hypertrophic phenotype that generate higher amounts of type I collagen and functionally inferior cartilage tissue.⁵⁴ Interestingly, the collagen produced by the encapsulated cells maintained a higher quality articular cartilage phenotype, as indicated by the collagen typing result with a high type II collagen: type I collagen ratio (Figure 5.6.).

In a potential clinical application as a scaffold, this system could be advantageous since it is easy to tune formation of this network. Currently, collagen-based materials are used as scaffolds in the clinic and have yielded variable success, partly due to high variations in network formation.⁵⁵ This hybrid system can form a chondrocyte-laden hydrogel *in situ* with consistent and tunable material properties. Furthermore, the cell-mediated degradation allows for the widespread elaboration of cartilage-specific ECM molecules over a short period of time and without the need for including growth factors in the scaffold. It would be interesting to see how matrix production is affected as the length of culture time is extended, especially in an *in vivo* environment where the presence of macrophages could help stimulate chondrocyte gelatinase secretion.²⁸

5.6. Conclusion

In summary, a novel hydrogel system based on crosslinking a full-length protein gelatin by PEG was designed to increase control over network formation and permit local chondrocyte-mediated degradation for cartilage tissue engineering applications. The hydrogel increases chondrocyte cellularity, and facilitates cartilage ECM production via cell-mediated degradation in a manner that promotes widespread matrix deposition in just 14 days. The materials approach was to modify gelatin with norbornene functionalities that were crosslinked with PEG dithiols via a photoinitiated thiol-ene reaction. Results confirmed that the final PEG-gelatin gel properties could be altered by modifying the amount of norbornene functionalization, while maintaining susceptibility to enzymatic degradation. Culture of chondrocyte-laden hydrogel scaffolds led to ECM molecules distributed throughout the construct and resembled articular cartilage with respect to collagen typing (high type II collagen: type I collagen ratio). This

biosynthetic system may prove useful in clinical applications as a scaffold to promote cartilage regeneration.

5.7. Acknowledgments

The authors acknowledge Amanda Meppelink for providing knees on which chondrocyte isolations were performed as well as Kathryn Morrissey for help with setting up GPC experiments. The authors would also like to thank Jason Silver, Dr. William Wan, and Dr. Malar Azagarsamy for assistance on experimental design. Funding for these studies was provided by the Howard Hughes Medical Institute, National Institutes of Health (R01 DE016523-10) and Department of Defense (W81XWH-10-1-0791). The US Army Medical Research Acquisition Activity, 820 Chandler Street, Fort Detrick, MD 21702-5014 is the awarding and administering acquisition office. The authors have no conflicts of interest to declare.

5.8. Supplementary Figures

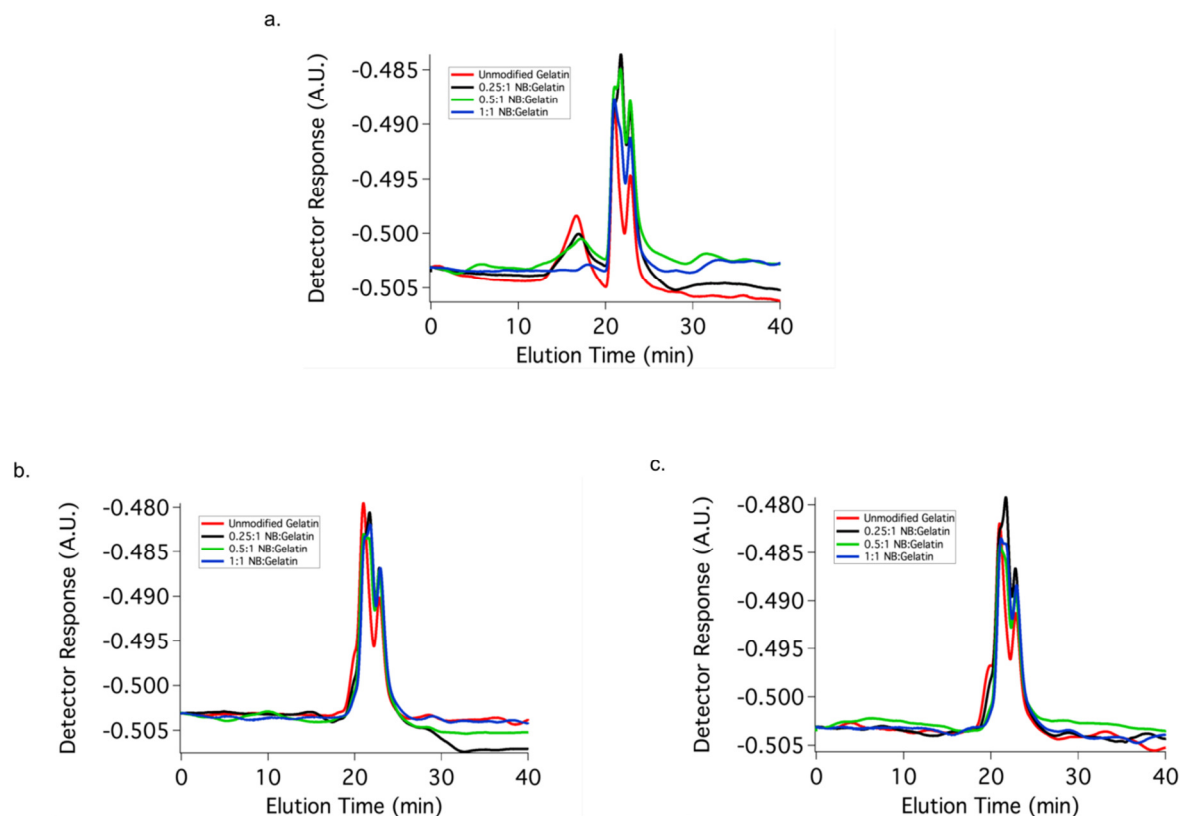


Figure 5.S1. Gel permeation chromatography chromatograms to assess degradation of gelatin functionalized with norbornene. a) GPC chromatogram of unmodified and gelatin functionalized with varying ratios of norbornene in buffer. b) Unmodified and functionalized gelatin treated with 20 U/mL collagenase type II for 1 h at 37°C with disappearance of peak found at 18 min. c) Unmodified and functionalized gelatin treated with chondrocyte-conditioned medium for 1 h at 37°C with disappearance of peak at 18 min.

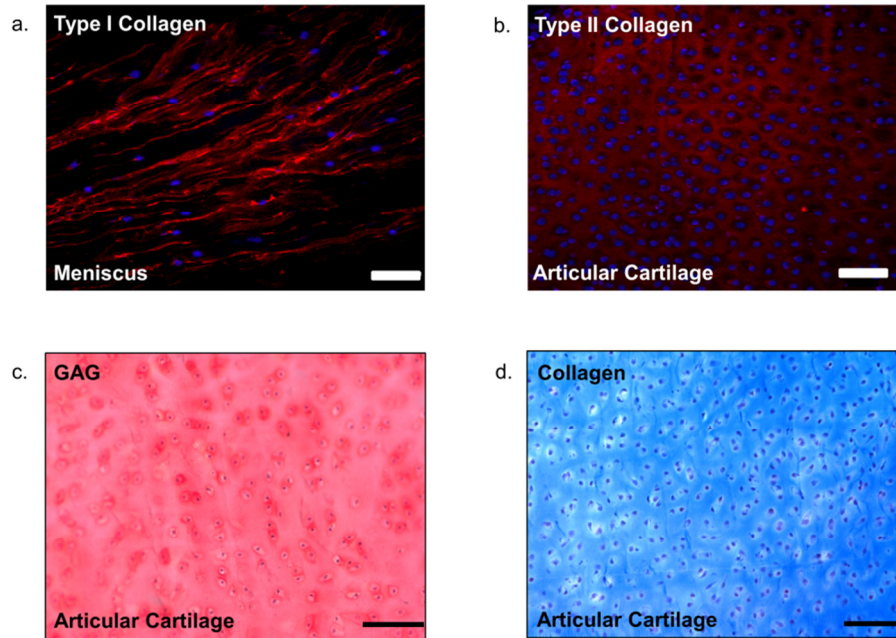


Figure 5.S2. Staining of native tissue. a) Type I collagen (red) distribution in porcine meniscus with cell nuclei counterstained with DAPI (blue) as a positive control to confirm the antibody is working as expected. Scale bar represents 50 μm . b) Type II collagen (red) distribution in porcine articular cartilage with cell nuclei counterstained with DAPI (blue) as a positive control to confirm the antibody is working as expected. Scale bar represents 50 μm . c) GAG (red) distribution in porcine articular cartilage with cell nuclei stained black and GAGs stained red. Scale bar represents 100 μm . d) Collagen (blue) distribution in porcine cartilage with cell nuclei stained violet and collagen stained blue. Scale bar represents 100 μm .

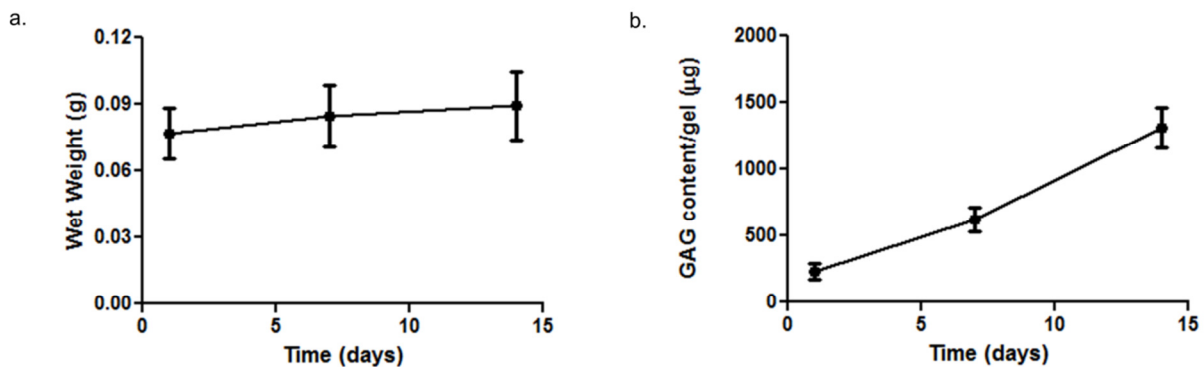


Figure 5.S3. a) Wet weight values (g) shown for 1:1 NB: gelatin amine hybrid scaffold collected at day 1, 7, and 14. Results are presented as mean \pm SD (n=3). b) GAG content per gel (μg) at day 1, 7, and 14 for constructs with encapsulated chondrocytes. Results are presented as mean \pm SD (n=3).

5.9. References

1. Adolphe, M. *Biological regulation of the chondrocytes*. (CRC Press, 1992).
2. Kim, I. L., Mauck, R. L. & Burdick, J. A. Hydrogel design for cartilage tissue engineering: a case study with hyaluronic acid. *Biomaterials* **32**, 8771–82 (2011).
3. Hutson, C. B. *et al.* Synthesis and characterization of tunable poly(ethylene glycol): gelatin methacrylate composite hydrogels. *Tissue Eng. Part A* **17**, 1713–23 (2011).
4. Kock, L., van Donkelaar, C. C. & Ito, K. Tissue engineering of functional articular cartilage: the current status. *Cell Tissue Res.* **347**, 613–27 (2012).
5. Spiller, K. L., Maher, S. A. & Lowman, A. M. Hydrogels for the Repair of Articular Cartilage Defects. *Tissue Eng. Part B* **17**, 281–299 (2011).
6. Forsyth, C. B. *et al.* Increased matrix metalloproteinase-13 production with aging by human articular chondrocytes in response to catabolic stimuli. *J. Gerontol. A. Biol. Sci. Med. Sci.* **60**, 1118–24 (2005).
7. Nicodemus, G. D., Skaalure, S. C. & Bryant, S. J. Gel structure has an impact on pericellular and extracellular matrix deposition, which subsequently alters metabolic activities in chondrocyte-laden PEG hydrogels. *Acta Biomater.* **7**, 492–504 (2011).
8. Sridhar, B. V, Doyle, N. R., Randolph, M. A. & Anseth, K. S. Covalently tethered TGF- β 1 with encapsulated chondrocytes in a PEG hydrogel system enhances extracellular matrix production. *J. Biomed. Mater. Res. A* **102**, 4464–4472 (2014).
9. Bryant, S. J. & Anseth, K. S. Hydrogel properties influence ECM production by chondrocytes photoencapsulated in poly(ethylene glycol) hydrogels. *J. Biomed. Mater. Res. A* **59**, 63–72 (2002).
10. Lee, K. Y. & Mooney, D. J. Hydrogels for Tissue Engineering. *Chem. Rev.* **101**, 1869–1880 (2001).
11. Lutolf, M. P. & Hubbell, J. A. Synthetic biomaterials as instructive extracellular microenvironments for morphogenesis in tissue engineering. *Nat. Biotechnol.* **23**, 47–55 (2005).
12. Bryant, S. J. & Anseth, K. S. Controlling the spatial distribution of ECM components in degradable PEG hydrogels for tissue engineering cartilage. *J. Biomed. Mater. Res. A* **64**, 70–9 (2003).
13. Zhao, W., Jin, X., Cong, Y., Liu, Y. & Fu, J. Degradable natural polymer hydrogels for articular cartilage tissue engineering. *J. Chem. Technol. Biotechnol.* **88**, 327–339 (2013).

14. Kretlow, J. D. & Mikos, A. G. From Material to Tissue: Biomaterial Development, Scaffold Fabrication, and Tissue Engineering. *AIChE J.* **54**, 3048–3067 (2008).
15. Sridhar, B. V *et al.* Development of a Cellularly Degradable PEG Hydrogel to Promote Articular Cartilage Extracellular Matrix Deposition. *Adv. Healthc. Mater.* **4**, 635–781 (2015).
16. Patterson, J. & Hubbell, J. A. Enhanced proteolytic degradation of molecularly engineered PEG hydrogels in response to MMP-1 and MMP-2. *Biomaterials* **31**, 7836–45 (2010).
17. Lin, Z., Willers, C., Xu, J. & Zheng, M.-H. The chondrocyte: biology and clinical application. *Tissue Eng.* **12**, 1971–84 (2006).
18. Fields, G. B., Wart, H. E. Van & Birkedal-hansen, H. Sequence Specificity of Human Skin Fibroblast Collagenase: Evidence for the role of collagen structure in determining the collagenase cleavage site. *J. Biol. Chem.* **262**, 6221–6226 (1987).
19. Schmidt, O., Mizrahi, J., Elisseeff, J. & Seliktar, D. Immobilized fibrinogen in PEG hydrogels does not improve chondrocyte-mediated matrix deposition in response to mechanical stimulation. *Biotechnol. Bioeng.* **95**, 1061–9 (2006).
20. Almany, L. & Seliktar, D. Biosynthetic hydrogel scaffolds made from fibrinogen and polyethylene glycol for 3D cell cultures. *Biomaterials* **26**, 2467–77 (2005).
21. Mironi-Harpaz, I., Wang, D. Y., Venkatraman, S. & Seliktar, D. Photopolymerization of cell-encapsulating hydrogels: crosslinking efficiency versus cytotoxicity. *Acta Biomater.* **8**, 1838–48 (2012).
22. Gonen-Wadmany, M., Oss-Ronen, L. & Seliktar, D. Protein-polymer conjugates for forming photopolymerizable biomimetic hydrogels for tissue engineering. *Biomaterials* **28**, 3876–86 (2007).
23. Appelman, T. P., Mizrahi, J., Elisseeff, J. H. & Seliktar, D. The influence of biological motifs and dynamic mechanical stimulation in hydrogel scaffold systems on the phenotype of chondrocytes. *Biomaterials* **32**, 1508–16 (2011).
24. Singh, R. K., Seliktar, D. & Putnam, A. J. Capillary morphogenesis in PEG-collagen hydrogels. *Biomaterials* **34**, 9331–40 (2013).
25. Manicourt, D. H., Devogelaer, J. P. & Thonar, E. J. in *Dyn. Bone Cartil. Metab.* (Seibel, M., Robins, S. P. & Bilezikian, J. P.) 421–439 (Elsevier Science, 2006).
26. Rice, J. J. *et al.* Engineering the regenerative microenvironment with biomaterials. *Adv. Healthc. Mater.* **2**, 57–71 (2013).

27. Gorgieva, S. & Kokol, V. in *Biomater. Appl. Nanomedicine* (Pignatello, R.) 17–52 (InTech, 2011).
28. Dreier, R., Wallace, S., Fuchs, S., Bruckner, P. & Grassel, S. Paracrine interactions of chondrocytes and macrophages in cartilage degradation: articular chondrocytes provide factors that activate macrophage-derived pro-gelatinase B (pro-MMP-9). *J. Cell Sci.* **114**, 3813–3822 (2001).
29. Mohtai, M. *et al.* Expression of 92-kD type IV collagenase/gelatinase (gelatinase B) in osteoarthritic cartilage and its induction in normal human articular cartilage by interleukin 1. *J. Clin. Invest.* **92**, 179–85 (1993).
30. Wang, C.-C. *et al.* A biomimetic honeycomb-like scaffold prepared by flow-focusing technology for cartilage regeneration. *Biotechnol. Bioeng.* **111**, 2338–48 (2014).
31. Mazaki, T. *et al.* A novel, visible light-induced, rapidly cross-linkable gelatin scaffold for osteochondral tissue engineering. *Sci. Rep.* **4**, 4457 (2014).
32. Fu, Y. *et al.* 3D cell entrapment in crosslinked thiolated gelatin-poly(ethylene glycol) diacrylate hydrogels. *Biomaterials* **33**, 48–58 (2012).
33. Daniele, M. A., Adams, A. A., Naciri, J., North, S. H. & Ligler, F. S. Interpenetrating networks based on gelatin methacrylamide and PEG formed using concurrent thiol click chemistries for hydrogel tissue engineering scaffolds. *Biomaterials* **35**, 1845–56 (2014).
34. Muñoz, Z., Shih, H. & Lin, C.-C. Gelatin hydrogels formed by orthogonal thiol–norbornene photochemistry for cell encapsulation. *Biomater. Sci.* **2**, 1063 (2014).
35. Hoyle, C. E. & Bowman, C. N. Thiol-ene click chemistry. *Angew. Chem. Int. Ed. Engl.* **49**, 1540–73 (2010).
36. Einerson, N. J., Stevens, K. R. & Kao, W. J. Synthesis and physicochemical analysis of gelatin-based hydrogels for drug carrier matrices. *Biomaterials* **24**, 509–523 (2003).
37. Waldeck, H. & Kao, W. J. Effect of the Addition of a Labile Gelatin Component on the Degradation and Solute Release Kinetics of a Stable PEG Hydrogel. *J. Biomater. Sci. Polym. Ed.* **23**, 1595–1611 (2011).
38. Fairbanks, B. D., Schwartz, M. P., Bowman, C. N. & Anseth, K. S. Photoinitiated polymerization of PEG-diacrylate with lithium phenyl-2,4,6-trimethylbenzoylphosphine: polymerization rate and cytocompatibility. *Biomaterials* **30**, 6702–7 (2009).
39. Mohanty, B. & Bohidar, H. B. Microscopic structure of gelatin coacervates. *Int. J. Biol. Macromol.* **36**, 39–46 (2005).

40. Bryant, S. J. & Anseth, K. S. in *Scaffolding Tissue Eng.* (Ma, P. X. & Ellisseeff, J.) 1–45 (CRC Press, 2006).
41. Yoo, J. J., Bichara, D. A., Zhao, X., Randolph, M. A. & Gill, T. J. Implant-assisted meniscal repair in vivo using a chondrocyte-seeded flexible PLGA scaffold. *J. Biomed. Mater. Res. A* **99**, 102–8 (2011).
42. Byers, B. A., Mauck, R. L., Chiang, I. E. & Tuan, R. S. Transient exposure to transforming growth factor beta 3 under serum-free conditions enhances the biomechanical and biochemical maturation of tissue-engineered cartilage. *Tissue Eng. Part A* **14**, 1821–34 (2008).
43. Chua, K. H., Aminuddin, B. S., Fuzina, N. H. & Ruszymah, B. H. I. Insulin-transferrin-selenium prevent human chondrocyte dedifferentiation and promote the formation of high quality tissue engineered human hyaline cartilage. *Eur. Cell. Mater.* **9**, 58–67 (2005).
44. Farndale, R. W., Sayers, C. A. & Barrett, A. J. A direct spectrophotometric microassay for sulfated glycosaminoglycans in cartilage cultures. *Connect. Tissue Res.* **9**, 247–8 (1982).
45. Ruan, J.-L. *et al.* An Improved Cryosection Method for Polyethylene Glycol Hydrogels Used in Tissue Engineering. *Tissue Eng. Part C. Methods* **19**, 794–801 (2013).
46. Silverman, R. P., Passaretti, D., Huang, W., Randolph, M. A. & Yaremchuk, M. J. Injectable tissue-engineered cartilage using a fibrin glue polymer. *Plast. Reconstr. Surg.* **103**, 1809–1818 (1999).
47. Passaretti, D. & Silverman, R.P. Huang, W Kirchhoff, C.H. Ashiku, S. Randolph, M.A. Yaremchuk, M. J. Cultured chondrocytes produce injectable tissue-engineered cartilage in hydrogel polymer. *Tissue Eng.* **7**, 805–15 (2001).
48. Ibusuki, S. *et al.* Engineering Cartilage in a Photochemically Crosslinked Collagen Gel. *J. Knee Surg.* **22**, 72–81 (2010).
49. Gu, Y. *et al.* Chondrogenesis of myoblasts in biodegradable poly-lactide-co-glycolide scaffolds. *Mol. Med. Rep.* **7**, 1003–1009 (2013).
50. Bryant, S. J., Chowdhury, T. T., Lee, D. A., Bader, D. L. & Anseth, K. S. Crosslinking Density Influences Chondrocyte Metabolism in Dynamically Loaded Photocrosslinked Poly(ethylene glycol) Hydrogels. *Ann. Biomed. Eng.* **32**, 407–417 (2004).
51. Benton, J. A., DeForest, C. A., Vivekanandan, V. & Anseth, K. S. Photocrosslinking of gelatin macromers to synthesize porous hydrogels that promote valvular interstitial cell function. *Tissue Eng. Part A* **15**, 3221–30 (2009).

52. Skaalure, S. C., Chu, S. & Bryant, S. J. An Enzyme-Sensitive PEG Hydrogel Based on Aggrecan Catabolism for Cartilage Tissue Engineering. *Adv. Healthc. Mater.* **4**, 420–431 (2014).
53. Schultz, K. M. & Anseth, K. S. Monitoring degradation of matrix metalloproteinases-cleavable PEG hydrogels via multiple particle tracking microrheology. *Soft Matter* **9**, 1570 (2013).
54. Huey, D., Hu, J. & Athanasiou, K. Unlike Bone, Cartilage Regeneration Remains Elusive. *Science*. **6933**, 917–921 (2012).
55. Kon, E. *et al.* Matrix-assisted autologous chondrocyte transplantation for the repair of cartilage defects of the knee: systematic clinical data review and study quality analysis. *Am. J. Sports Med.* **37**, 1565–665 (2009).

6.1. Conclusions

The research in this thesis advances approaches in biofunctional hydrogel scaffold design to promote cartilage-specific tissue matrix production of encapsulated cells, which can ultimately be adopted to repair focal cartilage defects in patients. Native articular cartilage does not intrinsically have the ability to repair, primarily because it lacks vasculature and innervation.¹ Chondrocytes, the sole differentiated resident cells found in mature articular cartilage, are capable of regenerating and maintaining the tissue in a healthy state, but without biological cues from nerves or blood vessels they are not able to achieve their regenerative potential in a diseased state.^{2,3} Therefore, many cartilage regeneration therapies have focused on properly triggering the regenerative capacity of chondrocytes.

Currently, cutting edge strategies to treat cartilage defects utilize chondrocytes or their progenitor cells, mesenchymal stem cells (MSCs) as cell-based therapies.⁴ A common treatment option combines the use of a three-dimensional scaffold network with autologous chondrocytes to mimic native cartilage and facilitate tissue development. This technique is also known as matrix-assisted autologous chondrocyte transplantation (MACT), and has been employed with varying degrees of success in the clinic.^{5,6} However, current MACT therapies typically use natural-protein derived scaffolds (e.g., collagen), which help promote cartilage tissue formation with a nurturing environment,⁷ but lack facile control over network formation and can have high batch-to-batch variation.⁸ Hence, in an effort to improve upon the design of current MACT scaffolds, this thesis has focused on engineering hydrogels, based on a widely used synthetic polymer used in human medicine, poly-(ethylene glycol) (PEG) to create a stimulative

environment to encapsulated chondrocytes. Synthetic PEG based materials allow easy control of the gelation reaction, minimize variation between batches, and provides for facile control of the final material properties.⁹ In this thesis, we used a photoinitiated thiol-norbornene step-growth mediated click reaction since it provides precise temporal and spatial control over hydrogel formation under cytocompatible conditions¹⁰ while also permitting covalent attachment of biological motifs.¹¹ The ultimate goal of this project was to create a biofunctional hydrogel platform to stimulate the secretory properties of and matrix deposition by encapsulated cells, through the introduction of environmental cues that are relevant in cartilage tissue.

To investigate whether a PEG scaffold could be engineered to introduce biological signals to enhance chondrocyte matrix production, we modified TGF- β 1 so that it could be covalently tethered to the synthetic network and present a local signal to encapsulated cells (Chapter 3). TGF- β 1 is a good target protein to use for cartilage tissue engineering purposes since it has been shown to positively influence ECM production of chondrocytes.¹² We modified TGF- β 1 to contain thiol functionalities without a statistically significant change in its bioactivity,^{13,14} so that it could participate in a thiol-ene reaction and be conjugated to the norbornene functionalized PEG macromers. The resultant macromer solution was then crosslinked by a non-degradable PEG dithiol linker to form a hydrogel. Non-degradable hydrogels were selected in these studies to investigate the effects of a persistent TGF- β 1 signal on chondrocyte properties, and eliminate complexities that arise when the gel simultaneously degrades and releases the signal.

Results verified that TGF- β 1 was not only covalently attached, but also homogeneously distributed throughout the network using a section ELISA technique. We further confirmed that the tethered protein retained its bioactivity and signaled to encapsulated cells by using a PE-25

luciferase reporter assay. Longer term culture of chondrocyte-laden constructs showed an increase in cellularity, as well as GAG and collagen production over a 28 days period in the presence of the tethered TGF- β 1 compared to doses that were delivered solubly or control scaffolds with no TGF- β 1. Of further note, for a potential clinical application, the tethered TGF- β 1 hydrogels utilized a lower total protein dosage than hydrogels where the growth factor was solubly delivered, yet still promoted higher levels of ECM production from the chondrocytes. Moreover, chondrocytes maintained a spherical morphology with high viability and a phenotype that resembled articular cartilage (e.g., high type II collagen and low type I collagen levels). Collectively, these results demonstrate the feasibility of delivering bioactive protein signals in a 3-D PEG culture platform to enhance matrix production of chondrocytes.

Through these experiments, we identified a system with a high degree of user control of polymer formation that could deliver bioactive signals to encapsulated chondrocytes; however, in a non-degradable matrix, chondrocyte-secreted ECM molecules are limited to the pericellular space. Once we demonstrated the ability to introduce growth factors and influence secretory properties of local cells, we next sought to study and develop a degradable scaffold. Matrix distribution is important for cartilage regeneration, as heterogeneities lead to scaffolds with inferior biochemical and biomechanical properties.^{15,16} Furthermore, non-degradable systems can also lead to catabolic expression in chondrocytes, which can lead to tissue destruction.¹⁷ Mature cartilage tissue undergoes a homeostasis of matrix anabolism and catabolism that is regulated by cell-secreted proteases and is necessary to transport ECM molecules from the chondrocyte pericellular space to the extracellular space and replace the resultant void with newer matrix molecules.¹⁸ Hence, to exploit the thiol-click reaction and to introduce multiple functionalities, we designed a biofunctional hydrogel that contained tethered TGF β -1, as well as collagen-

derived matrix metalloproteinase (MMP)-sensitive peptide linker sequence (KCGPQG↓IWGQCK) to permit cell-mediated cleavage and remodeling of the network (Chapter 4).

Results confirm that this biofunctional PEG constructs allows local cell degradation, in a manner that promotes wide-spread cartilage-specific ECM production, and ultimately, leads to constructs with improved mechanical properties in just over 14 days. The approach exploited the synergistic effects of co-culture between MSCs and chondrocytes to facilitate degradation of the MMP-degradable peptide linker, as well as to promote cartilage ECM production in the presence of tethered TGF- β 1. Results confirmed that both encapsulated cell types maintained a high viability and a spherical morphology in the gels. Furthermore, the generated ECM resembled articular cartilage with respect to collagen typing by immunofluorescent staining (high type II collagen: type I collagen ratio). Local degradation was shown to play a critical role in matrix elaboration with these PEG tissue engineering constructs, as non-degradable constructs of the same formulation had significantly less ECM production and lower moduli values over 14 days.

Despite the significant benefit of cell-mediated scaffold degradation in promoting the generation of a biofunctional cartilage matrix, our approach employed MSCs to assist with matrix degradation, perhaps by stimulating the metabolic activity of these chondrocytes.¹⁹ While complementary approaches exist to alter the peptide sequence design to make it more specific to chondrocytes, we pursued an alternative approach in Chapter 5. Gelatin, a denatured byproduct of collagen, was modified so that it could be used as a major component of the scaffold; the motivation being that this ECM molecule provides a nurturing environment for chondrocytes and has been used in previous cartilage engineering applications.^{20,21} Gelatin also contains multiple

collagenase-sensitive sequences that can be readily cleaved by chondrocytes,²² which can make it a good scaffold system to promote local chondrocyte-mediated remodeling.

Results in Chapter 5 show that we can reliably attach various amounts of norbornene functional groups to gelatin macromolecules, and form hydrogels by crosslinking the protein with a PEG dithiol using a thiol-ene photopolymerization. We demonstrated that chondrocyte-secreted enzymes could reliably degrade the modified gelatin molecule using gel permeation chromatography. We further showed that encapsulated chondrocytes retained a high viability, increased their cellularity, and were even able to spread through the scaffold over time, suggesting that local degradation had occurred. Matrix production, both qualitatively and quantitatively, was assessed, and both GAG and collagen deposition increased over time with a relatively uniform distribution. We identified that the collagen generated in the constructs was consistent with an articular cartilage phenotype, by visualizing levels of type II collagen and type I collagen using an immunofluorescence assay. Overall, this work illustrates the potential to combine the promotive effects of a natural-based protein, like gelatin, with the engineered properties of synthetic-based PEG to create an environment that not only stimulates chondrocytes, but also respond to cell-mediated degradation to permit ECM elaboration.

In summary, the collective findings of this thesis illustrate the importance of creating a chondrocyte delivery scaffold that can not only introduce bioactive signals, but also degrade in a manner that is responsive to cell-secreted enzymes, thereby permitting robust ECM elaboration. Such scaffolds that allow local degradation to facilitate ECM deposition could diminish the effects of variation in patient-to-patient cells, advance tissue regeneration at the site of transplantation, and also maintain, and in some cases, increase its bulk mechanical properties. All of these attributes are desirable in a useful candidate product for clinical applications. With

respect to these points, this thesis showed significant progress towards the design of chondrocyte scaffolds that 1) tether TGF- β 1 to a PEG hydrogel matrix and enhance ECM production by chondrocytes, 2) locally present a growth factor, but also degrade in response to cell-mediated enzymes and permit increased matrix deposition, 3) integrate a protein matrix component, gelatin, that can be degraded by chondrocytes at physiologically relevant rates to permit high quality cartilage-specific ECM generation. Such scaffolds that can be easily engineered by the user to have specific physical properties, as well as the ability to introduce multiple biological signals, and be remodeled by encapsulated cells should aid in advancement related to cartilage regeneration for use in the clinic to heal joint focal defects in millions of people worldwide.

6.2. Recommendations

This thesis demonstrated the potential of PEG-based scaffolds and their modification to create biofunctional cell carriers for assisting in cartilage matrix deposition by encapsulated chondrocytes. PEG hydrogels were formed by a thiol-norbornene photoclick reaction and this system is quite useful and robust, not only because PEG has been used in cartilage tissue engineering applications,²³ but also because the thiol-norbornene step-growth mediated reaction minimizes radical mediated damage to encapsulated cells compared to commonly used acrylate chain-growth mediated polymerization reactions.^{24,25} While work in this thesis studied and elucidated factors (e.g., TGF- β 1, peptide or protein degradability) that were shown to improve upon cartilage regeneration techniques, there are a multitude of options to further optimize this blueprint so that it can be more easily implemented in clinical practice. Suggestions for improved design strategies and future work related to cartilage tissue engineering scaffolds, based on this thesis and a literature review, are outlined below.

6.2.1. Alternate methods to design scaffolds that locally degrade in response to chondrocyte-secreted enzymes

In this thesis, we demonstrated that local cell-mediated degradation plays a major role on cartilage ECM elaboration (Chapter 4 & 5); however, we found that MSCs were much more efficient alone, and in combination with chondrocytes, in degrading the collagenase sensitive peptide linker. This was also true of the crosslinker composed of a full-length protein, presumably since it contains multiple MMP-sensitive sites. It could be advantageous to engineer sequences or methods that can be readily regulated by chondrocyte-mediated cleavage to optimize ECM deposition.

We focused on peptides and proteins derived from collagen since it is a major component of the cartilage ECM. It is well known that chondrocytes secrete MMP-8²⁶ and MMP-13,²⁷ which are collagenases that specifically cleave collagen. A variety of collagen-derived peptide sequences have been engineered to cleave in response to MMPs at different rates by introducing amino acid point mutations,^{28,29} or introducing synthetic, non-natural amino acids.³⁰ It could be beneficial to investigate how these sequences cleave in response to chondrocyte-secreted enzymes and utilize the peptides that respond well to enzymes as linkers in hydrogel scaffolds for cartilage engineering. Moreover, we found in Chapter 4 that co-culture of MSCs and chondrocytes led to synergistic increase in cleavage of a collagen-derived peptide sequence. It would be interesting to study the cell signaling interaction between MSCs and chondrocytes,³¹ and isolate and use the factors that are stimulating the chondrocytes to degrade that sequence and expedite ECM production. It would also be interesting to track the fate of MSCs in co-culture systems over a longer period of time. Do they become hypertrophic like they are capable of doing in monoculture,³² or can they retain a chondrogenic morphology without expressing type I

collagen³³ in co-culture? Or do they simply provide trophic support and maintain their multipotency or even apoptose long term?

In Chapter 5, we modified gelatin, a denatured byproduct of collagen, so that it could be used in a scaffold to facilitate chondrocyte-mediated degradation of the network. We used gelatin, as the chemistry for modification was somewhat easier than collagen. Future directions might focus on modifying collagen, or fragments of collagen that could be incorporated into a hybrid biosynthetic network to not only strengthen the bulk modulus, but also aid in ECM deposition from chondrocytes.

Beyond collagen-related macromolecules, aggrecan might also be a candidate molecule as it is the next most abundant component of cartilage ECM to collagen. Aggrecan's turnover rate in native cartilage is relatively rapid,^{34,35} so an aggrecan-derived sequence might be a useful linker in a hydrogel that would be more quickly degraded.³⁶ However, some of the problems with this specific sequence are that it requires lipopolysaccharide (LPS) to stimulate degradation and a long culture time period to generate ECM. Finally, engineering aggrecan-based linkers with sequences similar to its interglobular domain (IGD)³⁷ would be another interesting avenue to investigate for aiding chondrocyte-mediated degradation of scaffolds. In following the theme of this thesis, it would be interesting to explore complementary approaches to modify full-length aggrecan or hyaluronic acid to be used in combination with synthetic materials to form scaffolds that can be degraded by cell-mediated mechanisms for cartilage tissue engineering purposes as some studies have shown this is possible.^{38,39,40}

Something not investigated in this thesis is the effect of factors found in the *in vivo* environment on enhancing chondrocyte-mediated degradation and resultant matrix production in

these biofunctional hydrogels. The joint space contains multiple cells ranging from synovial fibroblasts to macrophages, which secrete various growth factors and proteins.⁴¹ Macrophages interact with chondrocytes via paracrine signaling to secrete more MMPs,⁴² which could be helpful in expediting cell-mediated remodeling of the scaffold. In summary, there are a variety of strategies and methods that could be investigated to assist in cell-mediated remodeling and tissue formation in biofunctional scaffolds.

6.2.2. Use of a covalently adaptable network as a biofunctional scaffold for cartilage tissue engineering

Cell-mediated degradation of a hydrogel scaffold leads to more uniform ECM deposition, but an alternate technique in scaffold development could be to exploit covalently adaptable networks. Typically, covalently crosslinked synthetic hydrogels are used in tissue engineering applications because of their robust mechanical properties compared to physically associated gels. However, most of these polymer networks produce a predominantly elastic material; while native tissues are complex viscoelastic structures.⁴³ Furthermore, as mentioned above, in some cases the linkers of these networks need to be engineered to respond better to cell-mediated enzyme degradation. In contrast, covalently adaptable network responds to external stresses by rapidly breaking and reforming elastically active crosslinks while maintaining stable material properties over time.⁴⁴ The viscoelastic properties of the material also affect the way mechanical loads and subsequent signals are distributed throughout the gel, which can further enhance tissue distribution.⁴⁵

We briefly tested the compatibility of this system with encapsulated chondrocytes. We utilized a system composed of 8-arm 10 kDa PEG macromers with aliphatic hydrazine (Hz) end

groups linker with 4-arm 20 kDa PEG macromers with an aliphatic aldehyde (Ald) end group. We formed the gels at a 15:9 Hz:Ald ratio to lower the amount of aldehyde exposed to the cells since it is known to be cytotoxic at higher amounts.⁴⁶ We found that after 49 days, cells in these scaffolds could generate anisotropically organized collagen, which was detected by SHG microscopy as shown in Figure 6.1. Preliminary results suggest that scaffolds composed of covalently adaptable materials warrant further investigation as chondrocyte delivery vehicles.

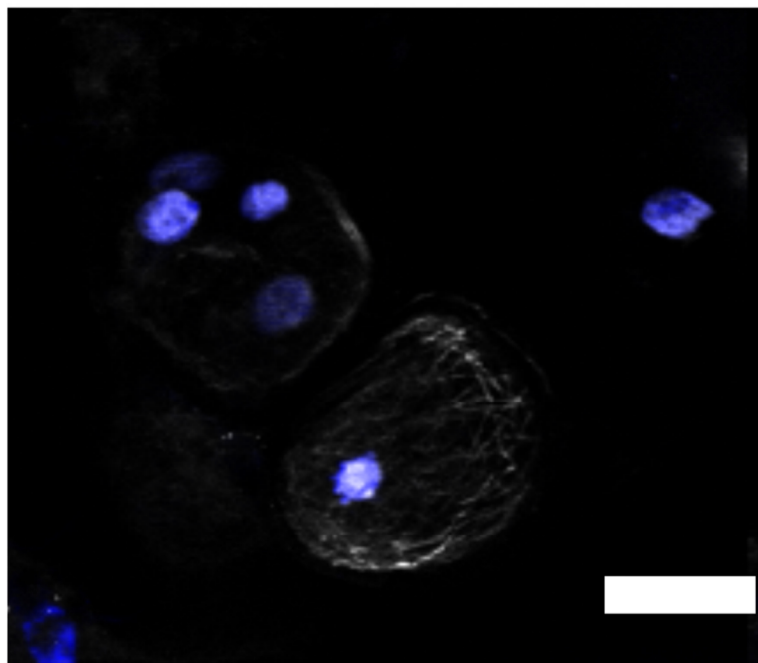


Figure 6.1. Second harmonic generation signal of collagen generated from chondrocytes encapsulated in a covalently adaptable network (15:9 HZ:ALD) after 49 days of culture. This data suggests that covalently adaptable scaffolds could be used to help promote functional tissue production from cells in lieu of cellularly degradable constructs. Blue represents cell nuclei and white fibers represent organized collagen fibers. Scale bar represents 10 μm . Image courtesy of Dr. Magnus Ølderoy.

6.2.3. Alternate cell sources for cartilage tissue engineering

This thesis primarily investigated the use of primary chondrocytes and study their function in biofunctionalized PEG hydrogels. One of the limitations with using autologous chondrocytes in cartilage repair is that they are found in limited supply in the donor joint cartilage and take time to expand in culture,⁴⁷ which could make them difficult to use as a clinical cell source. Induced pluripotent stem cells (iPSCs) derived from the autologous chondrocytes might be a good candidate cell source to investigate in future applications with the biofunctional hydrogel matrices detailed in this thesis. iPSCs would circumvent the issue of a limited supply of chondrocytes, since they can be more easily expanded in culture than their somatic counterparts.⁴⁸ iPSCs have been successfully differentiated into chondrocytes, from both juvenile⁴⁹ and osteoarthritic sources,⁵⁰ but more work needs to be done to determine the quality of the tissue generated and how these cells function in these scaffolds.

Neonatal chondrocytes (NChons) are another intriguing cell source for use in biofunctional scaffolds, since they are not immunogenic and only a small number of them are required to greatly influence chondrocyte secretory properties.⁵¹ In fact, studies have been shown that when used in co-culture with adult chondrocytes, NChons greatly influence the resultant matrix deposition.⁵²

6.2.4. *In vivo studies with hydrogel matrices*

To more rigorously test whether the scaffolds designed in this thesis can be used in patients, they need to be implanted *in vivo* to observe if that environment permits the same results seen *in vitro*. First, implanting these gels subcutaneously into nude mice would give insights into whether the encapsulated cells maintain a high viability and deposit cartilage ECM even in the presence of various other growth factors present in the animal.⁵³

As a next step, the porcine knee seems to be a good model as it withstands large mechanical loads and closely approximates that of a human knee in shape and movement.^{54,55} Because the biofunctional scaffold can be polymerized to fit the shape of the defect, cell-laden materials could easily be studied in pre-formed defects in the knee. A potential problem with implanting these biofunctional scaffolds in the joint defect is that their bulk modulus is low, which is not a limitation of the materials themselves, as higher moduli are easily attainable. The problem relates to the fact that more densely crosslinked, higher modulus materials prevent uniform matrix elaboration and deposition.⁵⁶ Until challenges are resolved in designing cellularly degraded materials that are remodeled in a local manner, mechanical damage to the scaffolds could be circumvented by implanting the gel deep into the defect, or shouldering it between the healthy pieces of cartilage tissue, so it does not have to interact with opposing knee. Further, the hydrogel could be secured into the defect using a fibrin polymer glue that has been shown to affix tissue engineered cartilage to native tissue *in vivo*.⁵⁷ To see if the scaffolds designed in this thesis can withstand the variety of forces (e.g., immunologic, mechanical, etc...) witnessed in a patient joint, they would need to successfully generate tissue in a large animal, such as the porcine model without major issues.

6.3. References

1. Sophia Fox, A. J., Bedi, A. & Rodeo, S. A. The basic science of articular cartilage: structure, composition, and function. *Sports Health* **1**, 461–8 (2009).
2. Adolphe, M. *Biological regulation of the chondrocytes*. (CRC Press, 1992).
3. Ateshian, G. A. & Hung, C. T. in *Funct. Tissue Eng.* (Guliak, F Butler, DL Goldstein, SA Mooney, D.) 46–68 (Springer-Verlag, 2003).
4. Perera, J. R., Gikas, P. D. & Bentley, G. The present state of treatments for articular cartilage defects in the knee. *Ann. R. Coll. Surg. Engl.* **94**, 381–7 (2012).

5. Kon, E. *et al.* Matrix-assisted autologous chondrocyte transplantation for the repair of cartilage defects of the knee: systematic clinical data review and study quality analysis. *Am. J. Sports Med.* **37**, 1565–665 (2009).
6. Bartlett, W. *et al.* Autologous chondrocyte implantation versus matrix-induced autologous chondrocyte implantation for osteochondral defects of the knee: a prospective, randomised study. *J. Bone Joint Surg. Br.* **87**, 640–5 (2005).
7. Behrens, P., Bitter, T., Kurz, B. & Russlies, M. Matrix-associated autologous chondrocyte transplantation/implantation (MACT/MACI)--5-year follow-up. *Knee* **13**, 194–202 (2006).
8. Zhao, W., Jin, X., Cong, Y., Liu, Y. & Fu, J. Degradable natural polymer hydrogels for articular cartilage tissue engineering. *J. Chem. Technol. Biotechnol.* **88**, 327–339 (2013).
9. Zhu, J. Bioactive modification of poly(ethylene glycol) hydrogels for tissue engineering. *Biomaterials* **31**, 4639–56 (2010).
10. Hoyle, C. E. & Bowman, C. N. Thiol-ene click chemistry. *Angew. Chem. Int. Ed. Engl.* **49**, 1540–73 (2010).
11. Fairbanks, B. D. *et al.* A Versatile Synthetic Extracellular Matrix Mimic via Thiol-Norbornene Photopolymerization. *Adv. Mater.* **21**, 5005–5010 (2009).
12. Li, T., O’Keefe, R. & Chen, D. TGF- β signaling in chondrocytes. *Front. Biosci.* 681–688 (2005).
13. Hume, P. S., He, J., Haskins, K. & Anseth, K. S. Strategies to reduce dendritic cell activation through functional biomaterial design. *Biomaterials* **33**, 3615–25 (2012).
14. McCall, J. D., Luoma, J. E. & Anseth, K. S. Covalently tethered transforming growth factor beta in PEG hydrogels promotes chondrogenic differentiation of encapsulated human mesenchymal stem cells. *Drug Deliv. Transl. Res.* **2**, 305–312 (2012).
15. Park, Y., Lutolf, M. P., Hubbell, J. A., Hunziker, E. B. & Wong, M. Bovine Primary Chondrocyte Culture in Synthetic Matrix Hydrogels as a Scaffold for Cartilage Repair. *Tissue Eng.* **10**, 515–522 (2004).
16. Roberts, J. J., Nicodemus, G. D., Greenwald, E. C. & Bryant, S. J. Degradation improves tissue formation in (un)loaded chondrocyte-laden hydrogels. *Clin. Orthop. Relat. Res.* **469**, 2725–34 (2011).
17. Nicodemus, G. D., Skaalure, S. C. & Bryant, S. J. Gel structure has an impact on pericellular and extracellular matrix deposition, which subsequently alters metabolic activities in chondrocyte-laden PEG hydrogels. *Acta Biomater.* **7**, 492–504 (2011).

18. Forsyth, C. B. *et al.* Increased matrix metalloproteinase-13 production with aging by human articular chondrocytes in response to catabolic stimuli. *J. Gerontol. A. Biol. Sci. Med. Sci.* **60**, 1118–24 (2005).
19. Lin, Z., Willers, C., Xu, J. & Zheng, M.-H. The chondrocyte: biology and clinical application. *Tissue Eng.* **12**, 1971–84 (2006).
20. Wang, C.-C. *et al.* A biomimetic honeycomb-like scaffold prepared by flow-focusing technology for cartilage regeneration. *Biotechnol. Bioeng.* **111**, 2338–48 (2014).
21. Mazaki, T. *et al.* A novel, visible light-induced, rapidly cross-linkable gelatin scaffold for osteochondral tissue engineering. *Sci. Rep.* **4**, 4457 (2014).
22. Gorgieva, S. & Kokol, V. in *Biomater. Appl. Nanomedicine* (Pignatello, R.) 17–52 (InTech, 2011).
23. Sharma, B. *et al.* Human cartilage repair with a photoreactive adhesive-hydrogel composite. *Sci. Transl. Med.* **5**, 167–173 (2013).
24. Roberts, J. J. & Bryant, S. J. Comparison of photopolymerizable thiol-ene PEG and acrylate-based PEG hydrogels for cartilage development. *Biomaterials* (2013).
25. Lin, C.-C., Raza, A. & Shih, H. PEG hydrogels formed by thiol-ene photo-click chemistry and their effect on the formation and recovery of insulin-secreting cell spheroids. *Biomaterials* **32**, 9685–95 (2011).
26. Chubinskaya, S. Chondrocyte Matrix Metalloproteinase-8. *J. Biol. Chem.* **271**, 11023–11026 (1996).
27. Liacini, A. *et al.* Induction of matrix metalloproteinase-13 gene expression by TNF- α is mediated by MAP kinases, AP-1, and NF- κ B transcription factors in articular chondrocytes. *Exp. Cell Res.* **288**, 208–217 (2003).
28. Patterson, J. & Hubbell, J. A. Enhanced proteolytic degradation of molecularly engineered PEG hydrogels in response to MMP-1 and MMP-2. *Biomaterials* **31**, 7836–45 (2010).
29. Nagase, H. & Fields, G. B. Human matrix metalloproteinase specificity studies using collagen sequence-based synthetic peptides. *Biopolymers* **40**, 399–416 (1996).
30. Nagase, H., Fields, C. & Fields, G. Design and characterization of a fluorogenic substrate selectively hydrolyzed by stromelysin 1 (matrix metalloproteinase-3). *J. Biol. Chem.* **269**, 20952–20957 (1994).
31. Wu, L., Prins, H.-J., Helder, M. N., van Blitterswijk, C. A. & Karperien, M. Trophic effects of mesenchymal stem cells in chondrocyte co-cultures are independent of culture conditions and cell sources. *Tissue Eng. Part A* **18**, 1542–51 (2012).

32. Koga, H., Engebretsen, L., Brinchmann, J. E., Muneta, T. & Sekiya, I. Mesenchymal stem cell-based therapy for cartilage repair: a review. *Knee Surg. Sports Traumatol. Arthrosc.* **17**, 1289–97 (2009).
33. Steck, E. *et al.* Induction of intervertebral disc-like cells from adult mesenchymal stem cells. *Stem Cells* **23**, 403–11 (2005).
34. Knudson, C. B. & Knudson, W. Cartilage proteoglycans. *Semin. Cell Dev. Biol.* **12**, 69–78 (2001).
35. Mok, S. S., Masuda, K., Hauselmann, H. J., Aydelotte, M. B. & Thonar, E. J. M. A. Aggrecan Synthesized by Mature Bovine Chondrocytes Suspended in Alginate associated matrix and the further removed matrix. *J. Biol. Chem.* **269**, 33021–33027 (1994).
36. Skaalure, S. C., Chu, S. & Bryant, S. J. An Enzyme-Sensitive PEG Hydrogel Based on Aggrecan Catabolism for Cartilage Tissue Engineering. *Adv. Healthc. Mater.* (2014). doi:10.1002/adhm.201400277
37. Ilic, M. Z., Handley, C. J., Robinson, H. C. & Mok, M. T. Mechanism of catabolism of aggrecan by articular cartilage. *Arch. Biochem. Biophys.* **294**, 115–122 (1992).
38. Yamane, S. *et al.* Feasibility of chitosan-based hyaluronic acid hybrid biomaterial for a novel scaffold in cartilage tissue engineering. *Biomaterials* **26**, 611–9 (2005).
39. Kim, I. L., Mauck, R. L. & Burdick, J. A. Hydrogel design for cartilage tissue engineering: a case study with hyaluronic acid. *Biomaterials* **32**, 8771–82 (2011).
40. Chung, C., Beecham, M., Mauck, R. L. & Burdick, J. A. The influence of degradation characteristics of hyaluronic acid hydrogels on in vitro neocartilage formation by mesenchymal stem cells. *Biomaterials* **30**, 4287–96 (2009).
41. Inui, A., Iwakura, T. & Reddi, A. H. Human Stem Cells and Articular Cartilage Regeneration. *Cell* **1**, 994–1009 (2012).
42. Dreier, R., Wallace, S., Fuchs, S., Bruckner, P. & Grassel, S. Paracrine interactions of chondrocytes and macrophages in cartilage degradation: articular chondrocytes provide factors that activate macrophage-derived pro-gelatinase B (pro-MMP-9). *J. Cell Sci.* **114**, 3813–3822 (2001).
43. Deng, G., Tang, C., Li, F., Jiang, H. & Chen, Y. Covalent Cross-Linked Polymer Gels with Reversible Sol–Gel Transition and Self-Healing Properties. *Macromolecules* **43**, 1191–1194 (2010).
44. McKinnon, D. D., Domaille, D. W., Cha, J. N. & Anseth, K. S. Biophysically Defined and Cytocompatible Covalently Adaptable Networks as Viscoelastic 3D Cell Culture Systems. *Adv. Mater.* 1–8 (2013).

45. Liu, F. *et al.* Rheological Images of Dynamic Covalent Polymer Networks and Mechanisms behind Mechanical and Self-Healing Properties. *Macromolecules* **45**, 1636–1645 (2012).
46. Bassi, A. M., Penco, S., Canuto, R. A., Muzio, G. & Ferro, M. Comparative evaluation of cytotoxicity and metabolism of four aldehydes in two hepatoma cell lines. *Drug Chem. Toxicol.* **20**, 173–87 (1997).
47. Barbero, A. *et al.* Age related changes in human articular chondrocyte yield, proliferation and post-expansion chondrogenic capacity. *Osteoarthr. Cartil.* **12**, 476–84 (2004).
48. Yu, J. *et al.* Induced pluripotent stem cell lines derived from human somatic cells. *Science* (80-.). **318**, 1917–20 (2007).
49. Diekman, B. O. *et al.* Cartilage tissue engineering using differentiated and purified induced pluripotent stem cells. *Proc. Natl. Acad. Sci.* **109**, (2012).
50. Wei, Y. *et al.* Chondrogenic differentiation of induced pluripotent stem cells from osteoarthritic chondrocytes in alginate matrix. *Eur. Cell. Mater.* **23**, 1–12 (2012).
51. Saha, S., Kirkham, J., Wood, D., Curran, S. & Yang, X. Comparative study of the chondrogenic potential of human bone marrow stromal cells, neonatal chondrocytes and adult chondrocytes. *Biochem. Biophys. Res. Commun.* **401**, 333–8 (2010).
52. Lai, J. H., Kajiyama, G., Smith, R. L., Maloney, W. & Yang, F. Stem cells catalyze cartilage formation by neonatal articular chondrocytes in 3D biomimetic hydrogels. *Sci. Rep.* **3**, 1–9 (2013).
53. Silverman, R. P., Passaretti, D., Huang, W., Randolph, M. A. & Yaremchuk, M. J. Injectable tissue-engineered cartilage using a fibrin glue polymer. *Plast. Reconstr. Surg.* **103**, 1809–1818 (1999).
54. Li, W.-J. *et al.* Evaluation of articular cartilage repair using biodegradable nanofibrous scaffolds in a swine model: a pilot study. *J. Tissue Eng. Regen. Med.* **3**, 1–10 (2009).
55. Peretti, G. M. *et al.* Review of injectable cartilage engineering using fibrin gel in mice and swine models. *Tissue Eng.* **12**, 1151–68 (2006).
56. Bryant, S. J., Bender, R. J., Durand, K. L. & Anseth, K. S. Encapsulating chondrocytes in degrading PEG hydrogels with high modulus: engineering gel structural changes to facilitate cartilaginous tissue production. *Biotechnol. Bioeng.* **86**, 747–55 (2004).
57. Silverman, R. P., Bonassar, L. J., Passaretti, D., Randolph, M. A. & Yaremchuk, M. J. Adhesion of tissue-engineered cartilage to native cartilage. *Plast. Reconstr. Surg.* **105**, 1393–1398 (2000).

CHAPTER VII

REFERENCES

7.1. CHAPTER I

1. Manicourt, D. H., Devogelaer, J. P. & Thonar, E. J. in *Dyn. Bone Cartil. Metab.* (Seibel, M., Robins, S. P. & Bilezikian, J. P.) 421–439 (Elsevier Science, 2006).
2. Buckwalter, J. A. *et al.* Soft-tissue aging and musculoskeletal function. *J. Bone Joint Surg. Am.* **75**, 1533–48 (1993).
3. Robins, S. P. in *Dyn. Bone Cartil. Metab.* (Seibel, Markus J. Robins, Simon P, Bilezikian, J. P.) 41–51 (Elsevier Science, 2006).
4. Ross, M. & Wojciech, P. *Histology: A Text and Atlas.* (Lippincott, Williams, & Wilkins, 2010).
5. Mueller, Michael B. Tuan, R. S. Anabolic/Catabolic Balance in Pathogenesis of Osteoarthritis: Identifying Molecular Targets. *PM&R* **3**, S3–S11 (2011).
6. Hootman, J. M. & Helmick, C. G. Projections of US prevalence of arthritis and associated activity limitations. *Arthritis Rheum.* **54**, 226–9 (2006).
7. Hunziker, E. B. Articular cartilage repair: basic science and clinical progress. A review of the current status and prospects. *Osteoarthr. Cartil.* **10**, 432–63 (2002).
8. Hall, B. K. Earliest evidence of cartilage and bone development in embryonic life. *Clin. Orthop. Relat. Res.* 255–72 (1987).
9. Moore, K. L., Persaud, T. V. N. & Torchia, M. G. in *Dev. Hum. Clin. Oriented Embryol.* (Elsevier, 2011).
10. Yin, H., Price, F. & Rudnicki, M. A. Satellite cells and the muscle stem cell niche. *Physiol. Rev.* **93**, 23–67 (2013).
11. Athanasiou, K., Darling, E. & Hu, J. Articular Cartilage Tissue Engineering. *Synth. Lect. Tissue Eng.* **1**, 1–182 (2009).
12. Ateshian, G. A. & Hung, C. T. in *Funct. Tissue Eng.* (Guliak, F Butler, DL Goldstein, SA Mooney, D.) 46–68 (Springer-Verlag, 2003).
13. Erggelet, C. & Mandelbaum, B. R. in *Princ. Cartil. Repair* 1–5 (Springer-Verlag, 2008).

14. Coimbra, I. B., Jimenez, S. A., Hawkins, D. F., Piera-Velazquez, S. & Stokes, D. G. Hypoxia inducible factor-1 alpha expression in human normal and osteoarthritic chondrocytes. *Osteoarthritis Cartilage* **12**, 336–45 (2004).
15. Ng, S. S. *et al.* Biomechanical study of the edge outgrowth phenomenon of encapsulated chondrocytic isogenous groups in the surface layer of hydrogel scaffolds for cartilage tissue engineering. *Acta Biomater.* **8**, 244–52 (2012).
16. Archer, C., McDowell, J., Bayliss, M., Stephens, M. & Bentley, G. Phenotypic modulation in sub-populations of human articular chondrocytes in vitro. *J. Cell Sci.* **97**, 361–371 (1990).
17. Mansour, J. M. in *Kinesiol. Mech. Pathomechanics Hum. Mov.* (Oatis, C. A.) 66–75 (Lippincott, Williams, & Wilkins, 2003).
18. Ateshian, G. A., Lai, W. M., Zhu, W. B. & Mow, V. C. An asymptotic solution for the contact of two biphasic cartilage layers. *J. Biomech.* **27**, 1347–1360 (1994).
19. Sabatini, M., Pastoureau, P. & Ceuninck De, F. *Cartilage and Osteoarthritis*. (Humana Press, 2004).
20. Guilak, F., Setton, L. & Kraus, V. in *Princ. Pract. Orthop. Sport. Med.* (Garrett, W., Speer, K. & Kirkendall, D.) 1057–1064 (Lippincott, Williams, & Wilkins, 2000).
21. Sophia Fox, A. J., Bedi, A. & Rodeo, S. A. The basic science of articular cartilage: structure, composition, and function. *Sports Health* **1**, 461–8 (2009).
22. Martel-Pelletier, J., Boileau, C., Pelletier, J.-P. & Roughley, P. J. Cartilage in normal and osteoarthritis conditions. *Best Pract. Res. Clin. Rheumatol.* **22**, 351–84 (2008).
23. Hardingham, T. & Fosang, A. Proteoglycans: many forms and many functions. *FASEB J* **6**, 861–870 (1992).
24. Boskey, A. L., Wright, T. M. & Blank, R. D. Collagen and bone strength. *J. Bone Miner. Res.* **14**, 330–5 (1999).
25. Bruckner, P. & van der Rest, M. Structure and function of cartilage collagens. *Microsc. Res. Tech.* **28**, 378–84 (1994).
26. Eyre, D. Collagen of articular cartilage. *Arthritis Res.* **4**, 30–5 (2002).
27. Von der Mark, K. & Sorokin, L. M. in *Connect. Tissue its Heritable Disord.* (Royce, P. M. & Steinmann, B.) 293–328 (Wiley-Liss, 2002).

28. Berg, R. A. & Prockop, D. J. The thermal transition of a non-hydroxylated form of collagen. Evidence for a role for hydroxyproline in stabilizing the triple-helix of collagen. *Biochem. Biophys. Res. Commun.* **52**, 115–120 (1973).
29. Kivirikko, K. I. & Myllyharju, J. Prolyl 4-hydroxylases and their protein disulfide isomerase subunit. *Matrix Biol.* **16**, 357–368 (1998).
30. Edwards, C. A. & O'Brien, W. D. Modified assay for determination of hydroxyproline in a tissue hydrolyzate. *Clin. Chim. Acta* **104**, 161–167 (1980).
31. Smith-Mungo, L. I. & Kagan, H. M. Lysyl oxidase: Properties, regulation and multiple functions in biology. *Matrix Biol.* **16**, 387–398 (1998).
32. Tuderman, L. & Prockop, D. J. Procollagen N-Proteinase. Properties of the Enzyme Purified from Chick Embryo Tendons. *Eur. J. Biochem.* **125**, 545–549 (1982).
33. Olsen, B. R. in *Cell Biol. Extracell. Matrix* (Hay, E. D.) 139–177 (Plenum Press, 1981).
34. Mayne, R. Cartilage collagens. What Is Their Function, and Are They Involved in Articular Disease? *Arthritis Rheum.* **32**, 241–246 (1989).
35. Byers, P. H. Molecular genetics of chondrodysplasias, including clues to development, structure, and function. *Curr. Opin. Rheumatol.* **6**, 345–350 (1994).
36. Von der Mark, K. Localization of collagen types in tissues. *Int. Rev. Connect. Tissue Res.* **9**, 265–324 (1981).
37. De Visser, S. K. *et al.* Anisotropy of collagen fibre alignment in bovine cartilage: comparison of polarised light microscopy and spatially resolved diffusion-tensor measurements. *Osteoarthritis Cartilage* **16**, 689–97 (2008).
38. Zipfel, W. R. *et al.* Live tissue intrinsic emission microscopy using multiphoton-excited native fluorescence and second harmonic generation. *Proc. Natl. Acad. Sci. U. S. A.* **100**, 7075–80 (2003).
39. Guilak, F. *et al.* The pericellular matrix as a transducer of biomechanical and biochemical signals in articular cartilage. *Ann. N. Y. Acad. Sci.* **1068**, 498–512 (2006).
40. Aigner, T. *et al.* Type X collagen expression in osteoarthritic and rheumatoid articular cartilage. *Virchows Arch. B Cell Pathol. Incl. Mol. Pathol.* **63**, 205–211 (1993).
41. Von der Mark, K. in *Dyn. Bone Cartil. Metab.* (Seibel, M. ., Robins, S. P. & Bilezikian, J. P.) 3–40 (Elsevier, 2006).
42. Hay, E. D. in *Cell Biol. Extracell. Matrix* (Hay, E. D.) 379–409 (Plenum Press, 1981).

43. Mandelbaum, B. R. *et al.* Articular Cartilage Lesions of the Knee. *Am. J. Sport. Med.* **26**, 853–861 (1998).
44. Aigner, T., Bertling, W., Stöss, H., Weseloh, G. & von der Mark, K. Independent expression of fibril-forming collagens I, II, and III in chondrocytes of human osteoarthritic cartilage. *J. Clin. Invest.* **91**, 829–37 (1993).
45. Heinegard, D., Lorenzo, P. & Saxne, T. in *Dyn. Bone Cartil. Metab.* (Seibel, M., Robins, S. P. & Bilezikian, J. P.) 71–73 (Elsevier, 2006).
46. Mow, V. & Setton, L. in *Osteoarthritis* (Brandt, K. D., Doherty, M. & Lohmander, L. S.) 108–122 (Oxford University Press Inc., 1998).
47. Hall, A., Horwitz, E. & Wilkins, R. The cellular physiology of articular cartilage. *Exp Physiol* **81**, 535–545 (1996).
48. Knudson, C. B. & Knudson, W. Cartilage proteoglycans. *Semin. Cell Dev. Biol.* **12**, 69–78 (2001).
49. Buckwalter, J. A. & Rosenberg, L. C. Electron Microscopic Studies of Cartilage Proteoglycans. *J. Biol. Chem.* 9830–9839 (1981).
50. Knudson, C. B. Hyaluronan Receptor-Directed Assembly of Chondrocyte Pericellular Matrix. *J. Cell Biol.* 825–834 (1993).
51. Forsyth, C. B. *et al.* Increased matrix metalloproteinase-13 production with aging by human articular chondrocytes in response to catabolic stimuli. *J. Gerontol. A. Biol. Sci. Med. Sci.* **60**, 1118–24 (2005).
52. Mok, S. S., Masuda, K., Hauselmann, H. J., Aydelotte, M. B. & Thonar, E. J. M. A. Aggrecan Synthesized by Mature Bovine Chondrocytes Suspended in Alginate associated matrix and the further removed matrix. *J. Biol. Chem.* **269**, 33021–33027 (1994).
53. Häuselmann, H. J. *et al.* Adult human chondrocytes cultured in alginate form a matrix similar to native human articular cartilage. *Am. J. Physiol.* **271**, C742–52 (1996).
54. Grimshaw, M. J. & Mason, R. M. Modulation of bovine articular chondrocyte gene expression in vitro by oxygen tension. *Osteoarthritis Cartilage* **9**, 357–64 (2001).
55. Nesic, D. *et al.* Cartilage tissue engineering for degenerative joint disease. *Adv. Drug Deliv. Rev.* **58**, 300–22 (2006).
56. Clark, I. M. & Murphy, G. in *Dyn. Bone Cartil. Metab.* (Seibel, M. J., Robins, S. P. & Bilezikian, J. P.) 181–198 (Elsevier, 2006).

57. Wu, W. *et al.* Sites of collagenase cleavage and denaturation of type II collagen in aging and osteoarthritic articular cartilage and their relationship to the distribution of matrix metalloproteinase 1 and matrix metalloproteinase 13. *Arthritis Rheum.* **46**, 2087–94 (2002).
58. Knauper, V., Lopez-Otin, C., Smith, B., Knight, G. & Murphy, G. Biochemical Characterization of Human Collagenase-3. *J. Biol. Chem.* **271**, 1544–1550 (1996).
59. Mehraban, F., Lark, M. W., Ahmed, F. N., Xu, F. & Moskowitz, R. W. Increased secretion and activity of matrix metalloproteinase-3 in synovial tissues and chondrocytes from experimental osteoarthritis. *Osteoarthritis Cartilage* **6**, 286–94 (1998).
60. Chubinskaya, S. Chondrocyte Matrix Metalloproteinase-8. *J. Biol. Chem.* **271**, 11023–11026 (1996).
61. Stanton, H., Ung, L. & Fosang, A. The 45 kDa collagen-binding fragment of fibronectin induces matrix metalloproteinase-13 synthesis by chondrocytes and aggrecan degradation by aggrecanases. *Biochem. J.* **364**, 181–190 (2002).
62. Baker, A. H., Edwards, D. R. & Murphy, G. Metalloproteinase inhibitors: biological actions and therapeutic opportunities. *J. Cell Sci.* 3719–3727 (2002).
63. Goldberg, G. I., Strongin, A., Collier, I. E., Genrich, L. T. & Marmer, B. L. Interaction of 92-kDa type IV collagenase with the tissue inhibitor of metalloproteinases prevents dimerization, complex formation with interstitial collagenase, and activation of the proenzyme with stromelysin. *J. Biol. Chem.* **267**, 4583–4591 (1992).
64. Murphy, G. *et al.* The N-terminal domain of tissue inhibitor of metalloproteinases retains metalloproteinase inhibitory activity. *Biochemistry* **30**, 8097–8102 (1991).
65. Edwards, D. R. *et al.* in *Inhib. Met. Dev. Dis.* (Hawkes, S. P., Edwards, D. R. & Khokha, R.) 13–25 (Harwood Academic Press, 2000).
66. Poole, A. *et al.* Proteolysis of the collagen fibril in osteoarthritis. *Biochem. Soc. Symp.* 115–123 (2003).
67. Hashimoto, S., Ochs, R. L., Komiya, S. & Lotz, M. Linkage of chondrocyte apoptosis and cartilage degradation in human osteoarthritis. *Arthritis Rheum.* **41**, 1632–8 (1998).
68. Billingham, R. C., Mwale, F., Hollander, A., Ionescu, M. & Poole, A. R. Immunoassays for collagens in chondrocyte and cartilage explant cultures. *Methods Mol. Med.* **100**, 251–74 (2004).
69. Eyre, D. R. *et al.* in *Chem. Biol. Miner. Tissues* (Goldber, M., Boskey, A. & Robinson, C.) 347–350 (American Academy of Orthopedic Surgeons, 2000).

70. Gómez-Guillén, M. C. *et al.* Fish gelatin: a renewable material for developing active biodegradable films. *Trends Food Sci. Technol.* **20**, 3–16 (2009).
71. Cole, B. Gelatin. *Encycl. Food Sci. Technol.* (1999).
72. Masters, K. S. Covalent growth factor immobilization strategies for tissue repair and regeneration. *Macromol. Biosci.* **11**, 1149–63 (2011).
73. Darling, E. M. & Athanasiou, K. A. in *Biomed. Technol. devices handbook*. (Moore, J. E. & Zouridakis, G.) (CRC Press, 2004).
74. Reddi, A. H. Role of morphogenetic proteins in skeletal tissue engineering and regeneration. *Nat. Biotechnol.* **16**, 247–52 (1998).
75. Takigawa, M., Kimura, Y. & Takahashi, K. The basic effect of IGF on chondrocytes. *Clin. Pediatr. Endocrinol.* (1997).
76. Vanosch, G., Vandenberg, W., Hunziker, E. & Hausselmann, H. Differential effects of IGF-1 and TGFbeta-2 on the assembly of proteoglycans in pericellular and territorial matrix by cultured bovine articular chondrocytes. *Osteoarthr. Cartil.* **6**, 187–195 (1998).
77. Hulley, P., Russell, G. & Croucher, P. in *Dyn. Bone Cartil. Metab.* (Seibel, M. J., Robins, S. P. & Bilezikian, J. P.) 99–107 (Elsevier, 2006).
78. Lyons, R. M. Mechanism of activation of latent recombinant transforming growth factor beta 1 by plasmin. *J. Cell Biol.* **110**, 1361–1367 (1990).
79. Bassing, C. *et al.* A transforming growth factor beta type I receptor that signals to activate gene expression. *Science (80-.)*. **263**, 87–89 (1994).
80. Alevizopoulos, A. & Mermoud, N. Transforming growth factor-beta: the breaking open of a black box. *Bioessays* **19**, 581–91 (1997).
81. Nakao, A. *et al.* TGF-beta receptor-mediated signalling through Smad2, Smad3 and Smad4. *EMBO J.* **16**, 5353–62 (1997).
82. Derynck, R. *et al.* Human transforming growth factor-beta complementary DNA sequence and expression in normal and transformed cells. *Nature* **316**, 701–5 (1985).
83. Zhou, S., Eid, K. & Glowacki, J. Cooperation between TGF-beta and Wnt pathways during chondrocyte and adipocyte differentiation of human marrow stromal cells. *J. Bone Miner. Res.* **19**, 463–70 (2004).
84. Scharstuhl, A., Vitters, E. L., van der Kraan, P. M. & van den Berg, W. B. Reduction of osteophyte formation and synovial thickening by adenoviral overexpression of

- transforming growth factor beta/bone morphogenetic protein inhibitors during experimental osteoarthritis. *Arthritis Rheum.* **48**, 3442–51 (2003).
85. Li, T., O’Keefe, R. & Chen, D. TGF- β signaling in chondrocytes. *Front. Biosci.* 681–688 (2005).
 86. Buckwalter, J. A. Articular Cartilage Injuries. *Clin. Orthop. Relat. Res.* 21–37 (2002).
 87. Erggelet, C. & Mandelbaum, B. R. in *Princ. Cartil. Repair* 7–17 (Springer-Verlag, 2008).
 88. Reddy, A. S. & Frederick, R. W. Evaluation of the Intraosseous and Extraosseous Blood Supply to the Distal Femoral Condyles. *Am. J. Sport. Med.* **26**, 415–419 (1998).
 89. Furukawa, T., Eyre, D. R., Koide, S. & Glimcher, M. J. Biochemical Studies on Repair Cartilage Resurfacing Experimental Defects in the Rabbitt Knee. *J. Bone Jt. Surgery-American Vol.* **1**, 79–89 (1980).
 90. Buckwalter, J. A., Mankin, H. J. & Grodzinsky, A. J. Articular cartilage and osteoarthritis. in *AAOS Instr. Course Lect.* 465–480 (2005).
 91. Gelber, A. C. Joint Injury in Young Adults and Risk for Subsequent Knee and Hip Osteoarthritis. *Ann. Intern. Med.* **133**, 321 (2000).
 92. Dean, D. D., Martel-Pelletier, J., Pelletier, J. P., Howell, D. S. & Woessner, J. F. Evidence for metalloproteinase and metalloproteinase inhibitor imbalance in human osteoarthritic cartilage. *J. Clin. Invest.* **84**, 678–85 (1989).
 93. Lawrence, R. C. *et al.* Estimates of the prevalence of arthritis and selected musculoskeletal disorders in the United States. *Arthritis Rheum.* **41**, 778–99 (1998).
 94. O’Driscoll, S. W. The healing and regeneration of articular cartilage. *J. Bone Joint Surg. Am.* **80**, 1795–812 (1998).
 95. Oei, E. H. G., van Tiel, J., Robinson, W. H. & Gold, G. E. Quantitative radiological imaging techniques for articular cartilage composition: Towards early diagnosis and development of disease-modifying therapeutics for osteoarthritis. *Arthritis Care Res. (Hoboken)*. (2014). doi:10.1002/acr.22316
 96. Gomoll, A. H. *et al.* Surgical treatment for early osteoarthritis. Part I: cartilage repair procedures. *Knee Surg. Sports Traumatol. Arthrosc.* **20**, 450–66 (2012).
 97. Rambani, R. & Venkatesh, R. Current concepts in articular cartilage repair. *J. Arthrosc. Jt. Surg.* (2014). doi:10.1016/j.jajs.2014.06.003
 98. Pascual-Garrido, C., Moran, C. J., Green, D. W. & Cole, B. J. Osteochondritis dissecans of the knee in children and adolescents. *Curr. Opin. Pediatr.* 46–51 (2013).

99. Erggelet, C. & Mandelbaum, B. R. in *Princ. Cartil. Repair* 29–36 (Springer-Verlag, 2008).
100. Goldberg, V. M. & Buckwalter, J. A. Hyaluronans in the treatment of osteoarthritis of the knee: evidence for disease-modifying activity. *Osteoarthritis Cartilage* **13**, 216–24 (2005).
101. Lu, Y. *et al.* Thermal chondroplasty with bipolar and monopolar radiofrequency energy. *Arthrosc. J. Arthrosc. Relat. Surg.* **18**, 779–788 (2002).
102. Levy, A. S., Lohnes, J., Sculley, S., LeCroy, M. & Garrett, W. Chondral Delamination of the Knee in Soccer Players. *Am. J. Sports Med.* **24**, 634–639 (1996).
103. Mollon, B., Kandel, R., Chahal, J. & Theodoropoulos, J. The clinical status of cartilage tissue regeneration in humans. *Osteoarthritis Cartilage* 1–10 (2013).
104. Marcacci, M. *et al.* Arthroscopic autologous osteochondral grafting for cartilage defects of the knee: prospective study results at a minimum 7-year follow-up. *Am. J. Sports Med.* **35**, 2014–21 (2007).
105. Wood, J. J. *et al.* Autologous cultured chondrocytes: adverse events reported to the United States Food and Drug Administration. *J. Bone Joint Surg. Am.* **88**, 503–7 (2006).
106. Vanlauwe, J. *et al.* Repair of symptomatic cartilage lesions of the knee: the place of autologous chondrocyte implantation. *Acta Orthop. Belgium* 145–158 (2007).
107. Pridie, K. & Gordon, G. A method of resurfacing osteoarthritic knee joints. *J. Bone Jt. Surgery-British Vol.* **41**, 618–9 (1959).
108. Steadman, J. R. *et al.* Outcomes of microfracture for traumatic chondral defects of the knee: average 11-year follow-up. *Arthroscopy* **19**, 477–84 (2003).
109. Mithoefer, K., McAdams, T., Williams, R. J., Kreuz, P. C. & Mandelbaum, B. R. Clinical efficacy of the microfracture technique for articular cartilage repair in the knee: an evidence-based systematic analysis. *Am. J. Sports Med.* **37**, 2053–63 (2009).
110. Hoemann, C. D. *et al.* Chitosan-glycerol phosphate/blood implants improve hyaline cartilage repair in ovine microfracture defects. *J. Bone Joint Surg. Am.* **87**, 2671–86 (2005).
111. Erggelet, C. *et al.* Formation of cartilage repair tissue in articular cartilage defects pretreated with microfracture and covered with cell-free polymer-based implants. *J. Orthop. Res.* **27**, 1353–60 (2009).
112. Fortin, P. R. *et al.* Outcomes of total hip and knee replacement: preoperative functional status predicts outcomes at six months after surgery. *Arthritis Rheum.* **42**, 1722–8 (1999).

113. McNickle, A., Provencher, M. & Cole, B. Overview of existing cartilage repair technology. *Sports Med. Arthrosc.* **4**, 196–201 (2008).
114. Liao, I.-C., Moutos, F. T., Estes, B. T., Zhao, X. & Guilak, F. Tissue Engineering: Composite Three-Dimensional Woven Scaffolds with Interpenetrating Network Hydrogels to Create Functional Synthetic Articular Cartilage. *Adv. Funct. Mater.* **23**, 5825–5825 (2013).
115. Gomoll, A. H. *et al.* Surgical treatment for early osteoarthritis. Part II: allografts and concurrent procedures. *Knee Surg. Sports Traumatol. Arthrosc.* **20**, 468–86 (2012).
116. Richardson, J. B., Caterson, B., Evans, E. H., Ashton, B. A. & Roberts, S. Repair of human articular cartilage after implantation of autologous chondrocytes. *J Bone Jt. Surg Br* **81-B**, 1064–1068 (1999).
117. Gillogly, S. D. & Myers, T. H. Treatment of full-thickness chondral defects with autologous chondrocyte implantation. *Orthop. Clin. North Am.* **36**, 433–46 (2005).
118. Brittberg, M. & Lindahl, A. Treatment of deep cartilage defects in the knee with autologous chondrocyte transplantation. *N. Engl. J. Med.* **331**, 889–895 (1994).
119. Roberts, S., McCall, I. & Darby, A. Autologous chondrocyte implantation for cartilage repair: monitoring its success by magnetic resonance imaging and histology. *Arthritis Res. Ther.* **5**, 60–73 (2003).
120. Kurkijärvi, J. E. *et al.* Evaluation of cartilage repair in the distal femur after autologous chondrocyte transplantation using T2 relaxation time and dGEMRIC. *Osteoarthritis Cartilage* **15**, 372–8 (2007).
121. Peterson, L., Brittberg, M., Kiviranta, I., Akerlund, E. L. & Lindahl, A. Autologous Chondrocyte Transplantation: Biomechanics and Long-Term Durability. *Am. J. Sport. Med.* **30**, 2–12 (2002).
122. Huey, D., Hu, J. & Athanasiou, K. Unlike Bone, Cartilage Regeneration Remains Elusive. *Science (80-.)*. **6933**, 917–921 (2012).
123. Worthen, J., Waterman, B. R., Davidson, P. A. & Lubowitz, J. H. Limitations and sources of bias in clinical knee cartilage research. *Arthroscopy* **28**, 1315–25 (2012).
124. Adkisson, H. D. *et al.* The potential of human allogeneic juvenile chondrocytes for restoration of articular cartilage. *Am. J. Sports Med.* **38**, 1324–33 (2010).
125. Marlovits, S., Zeller, P., Singer, P., Resinger, C. & Vécsei, V. Cartilage repair: generations of autologous chondrocyte transplantation. *Eur. J. Radiol.* **57**, 24–31 (2006).

126. Barbero, A. *et al.* Age related changes in human articular chondrocyte yield, proliferation and post-expansion chondrogenic capacity. *Osteoarthr. Cartil.* **12**, 476–84 (2004).
127. Schnabel, M. *et al.* Dedifferentiation-associated changes in morphology and gene expression in primary human articular chondrocytes in cell culture. *Osteoarthr. Cartil.* **10**, 62–70 (2002).
128. Tuan, R. S. Stemming cartilage degeneration: adult mesenchymal stem cells as a cell source for articular cartilage tissue engineering. *Arthritis Rheum.* **54**, 3075–8 (2006).
129. Mauck, R. L., Byers, B. A., Yuan, X. & Tuan, R. S. Regulation of cartilaginous ECM gene transcription by chondrocytes and MSCs in 3D culture in response to dynamic loading. *Biomech. Model. Mechanobiol.* **6**, 113–25 (2007).
130. Erickson, I. E. *et al.* Differential maturation and structure-function relationships in mesenchymal stem cell- and chondrocyte-seeded hydrogels. *Tissue Eng. Part A* **15**, 1041–52 (2009).
131. Steck, E. *et al.* Induction of intervertebral disc-like cells from adult mesenchymal stem cells. *Stem Cells* **23**, 403–11 (2005).
132. Koga, H., Engebretsen, L., Brinchmann, J. E., Muneta, T. & Sekiya, I. Mesenchymal stem cell-based therapy for cartilage repair: a review. *Knee Surg. Sports Traumatol. Arthrosc.* **17**, 1289–97 (2009).
133. Richardson, S. M. *et al.* Mesenchymal stem cells in regenerative medicine: opportunities and challenges for articular cartilage and intervertebral disc tissue engineering. *J. Cell. Physiol.* **222**, 23–32 (2010).
134. Guilak, F., Awad, H. A., Fermor, B., Leddy, H. A. & Gimple, J. A. Adipose-derived adult stem cells for cartilage tissue engineering. *Biorheology* 389–399 (2004).
135. Koay, E. J., Hoben, G. M. B. & Athanasiou, K. A. Tissue engineering with chondrogenically differentiated human embryonic stem cells. *Stem Cells* **25**, 2183–90 (2007).
136. Drukker, M. & Benvenisty, N. The immunogenicity of human embryonic stem-derived cells. *Trends Biotechnol.* **22**, 136–41 (2004).
137. Diekman, B. O. *et al.* Cartilage tissue engineering using differentiated and purified induced pluripotent stem cells. *Proc. Natl. Acad. Sci.* **109**, (2012).
138. Saha, S., Kirkham, J., Wood, D., Curran, S. & Yang, X. Comparative study of the chondrogenic potential of human bone marrow stromal cells, neonatal chondrocytes and adult chondrocytes. *Biochem. Biophys. Res. Commun.* **401**, 333–8 (2010).

139. Bian, L., Zhai, D. Y., Mauck, R. L. & Burdick, J. A. Coculture of Human Mesenchymal Stem Cells and Enhances Functional Properties of Engineered Cartilage Reverse primer. *Tissue Eng. Part A* **17**, 1137–1145 (2011).
140. Tsuchiya, K., Chen, G., Ushida, T., Matsuno, T. & Tateishi, T. The effect of coculture of chondrocytes with mesenchymal stem cells on their cartilaginous phenotype in vitro. *Mater. Sci. Eng. C* **24**, 391–396 (2004).
141. Dahlin, R. L. *et al.* Articular chondrocytes and mesenchymal stem cells seeded on biodegradable scaffolds for the repair of cartilage in a rat osteochondral defect model. *Biomaterials* **35**, 7460–7469 (2014).
142. Hubka, K. M., Dahlin, R. L., Meretoja, V. V., Kasper, K. & Mikos, A. G. Enhancing Chondrogenic Phenotype for Cartilage Tissue Engineering: Monoculture and Co-culture of Articular Chondrocytes and Mesenchymal Stem Cells. *Tissue Eng. Part B* 1–50 (2014).
143. Lai, J. H., Kajiya, G., Smith, R. L., Maloney, W. & Yang, F. Stem cells catalyze cartilage formation by neonatal articular chondrocytes in 3D biomimetic hydrogels. *Sci. Rep.* **3**, 1–9 (2013).
144. Darling, E. M. & Athanasiou, K. A. Retaining zonal chondrocyte phenotype by means of novel growth environments. *Tissue Eng.* **11**, 395–403 (2005).
145. Hunter, C. Dynamic compression of chondrocyte-seeded fibrin gels: effects on matrix accumulation and mechanical stiffness. *Osteoarthr. Cartil.* **12**, 117–130 (2004).
146. Liu, Y., Shu, X. Z. & Prestwich, G. D. Osteochondral defect repair with autologous bone marrow-derived mesenchymal stem cells in an injectable, in situ, cross-linked synthetic extracellular matrix. *Tissue Eng.* **12**, 3405–16 (2006).
147. Nehrer, S. *et al.* Canine chondrocytes seeded in type I and type II collagen implants investigated in vitro. *J. Biomed. Mater. Res.* **38**, 95–104 (1997).
148. Omobono, M. A. *et al.* Enhancing the stiffness of collagen hydrogels for delivery of encapsulated chondrocytes to articular lesions for cartilage regeneration. *J. Biomed. Mater. Res. Part A* 1–7 (2014). doi:10.1002/jbm.a.35266
149. Zhao, W., Jin, X., Cong, Y., Liu, Y. & Fu, J. Degradable natural polymer hydrogels for articular cartilage tissue engineering. *J. Chem. Technol. Biotechnol.* **88**, 327–339 (2013).
150. Nicodemus, G. D. & Bryant, S. J. Cell encapsulation in biodegradable hydrogels for tissue engineering applications. *Tissue Eng. Part B. Rev.* **14**, 149–65 (2008).
151. Burdick, J. A., Chung, C., Jia, X., Randolph, M. A. & Langer, R. Controlled degradation and mechanical behavior of photopolymerized hyaluronic acid networks. *Biomacromolecules* **6**, 386–91 (2005).

152. Buschmann, M. D., Gluzband, Y. A., Grodzinsky, A. J., Kimura, J. H. & Hunziker, E. B. Chondrocytes in agarose culture synthesize a mechanically functional extracellular matrix. *J. Orthop. Res.* **10**, 745–58 (1992).
153. Augst, A. D., Kong, H. J. & Mooney, D. J. Alginate hydrogels as biomaterials. *Macromol. Biosci.* **6**, 623–33 (2006).
154. Hong, Y. *et al.* Covalently crosslinked chitosan hydrogel: properties of in vitro degradation and chondrocyte encapsulation. *Acta Biomater.* **3**, 23–31 (2007).
155. Burdick, J. A. & Prestwich, G. D. Hyaluronic acid hydrogels for biomedical applications. *Adv. Mater.* **23**, H41–56 (2011).
156. Mauck, R. L. *et al.* Functional Tissue Engineering of Articular Cartilage Through Dynamic Loading of Chondrocyte-Seeded Agarose Gels. *J. Biomech. Eng.* **122**, 252–260 (2000).
157. Kelly, T.-A. N., Ng, K. W., Wang, C. C.-B., Ateshian, G. A. & Hung, C. T. Spatial and temporal development of chondrocyte-seeded agarose constructs in free-swelling and dynamically loaded cultures. *J. Biomech.* **39**, 1489–97 (2006).
158. Athanasiou, K. Sterilization, toxicity, biocompatibility and clinical applications of polylactic acid/ polyglycolic acid copolymers. *Biomaterials* **17**, 93–102 (1996).
159. Athanasiou, K., Agrawal, C., Barber, F. & Burkhart, S. Orthopaedic applications for PLA-PGA biodegradable polymers. *Arthrosc. J. Arthrosc. Relat. Surg.* **14**, 726–737 (1998).
160. Yoon, D. . & Fisher, J. P. Chondrocyte signaling and artificial matrices for articular cartilage engineering. *Adv. Exp. Med. Biol.* **585**, 67–86 (2006).
161. Chen, G. *et al.* The use of a novel PLGA fiber/collagen composite web as a scaffold for engineering of articular cartilage tissue with adjustable thickness. *J. Biomed. Mater. Res. A* **67**, 1170–80 (2003).
162. Slaughter, B. V, Khurshid, S. S., Fisher, O. Z., Khademhosseini, A. & Peppas, N. A. Hydrogels in regenerative medicine. *Adv. Mater.* **21**, 3307–29 (2009).
163. Ifkovits, J. L. & Burdick, J. A. Review: photopolymerizable and degradable biomaterials for tissue engineering applications. *Tissue Eng.* **13**, 2369–85 (2007).
164. Bryant, S. J., Durand, K. L. & Anseth, K. S. Manipulations in hydrogel chemistry control photoencapsulated chondrocyte behavior and their extracellular matrix production. *J. Biomed. Mater. Res. A* **67**, 1430–6 (2003).

165. Bryant, S. J. & Anseth, K. S. Hydrogel properties influence ECM production by chondrocytes photoencapsulated in poly(ethylene glycol) hydrogels. *J. Biomed. Mater. Res.* **59**, 63–72 (2002).
166. Azagarsamy, M. A. & Anseth, K. S. Bioorthogonal Click Chemistry: An Indispensable Tool to Create Multifaceted Cell Culture Scaffolds. *ACS Macro Lett.* **2**, 5–9 (2013).
167. Sanborn, T. J., Messersmith, P. B. & Barron, A. E. In situ crosslinking of a biomimetic peptide-PEG hydrogel via thermally triggered activation of factor XIII. *Biomaterials* **23**, 2703–2710 (2002).
168. Lutolf, M. P. & Hubbell, J. A. Synthesis and physicochemical characterization of end-linked poly(ethylene glycol)-co-peptide hydrogels formed by Michael-type addition. *Biomacromolecules* **4**, 713–22 (2003).
169. Lin, C.-C., Sawicki, S. M. & Metters, A. T. Free-radical-mediated protein inactivation and recovery during protein photoencapsulation. *Biomacromolecules* **9**, 75–83 (2008).
170. Nguyen, K. T. & West, J. L. Photopolymerizable hydrogels for tissue engineering applications. *Biomaterials* **23**, 4307–14 (2002).
171. Nuttelman, C. R. *et al.* Macromolecular Monomers for the Synthesis of Hydrogel Niches and Their Application in Cell Encapsulation and Tissue Engineering. *Prog. Polym. Sci.* **33**, 167–179 (2008).
172. Kloxin, A. M., Kloxin, C. J., Bowman, C. N. & Anseth, K. S. Mechanical properties of cellularly responsive hydrogels and their experimental determination. *Adv. Mater.* **22**, 3484–94 (2010).
173. Fairbanks, B. D. *et al.* A Versatile Synthetic Extracellular Matrix Mimic via Thiol-Norbornene Photopolymerization. *Adv. Mater.* **21**, 5005–5010 (2009).
174. Roberts, J. J. & Bryant, S. J. Comparison of photopolymerizable thiol-ene PEG and acrylate-based PEG hydrogels for cartilage development. *Biomaterials* (2013).
175. Lynn, A. D., Blakney, A. K., Kyriakides, T. R. & Bryant, S. J. Temporal progression of the host response to implanted poly(ethylene glycol)-based hydrogels. *J. Biomed. Mater. Res. A* **96**, 621–31 (2011).
176. Nicodemus, G. D., Skaalure, S. C. & Bryant, S. J. Gel structure has an impact on pericellular and extracellular matrix deposition, which subsequently alters metabolic activities in chondrocyte-laden PEG hydrogels. *Acta Biomater.* **7**, 492–504 (2011).
177. Bryant, S. J., Bender, R. J., Durand, K. L. & Anseth, K. S. Encapsulating chondrocytes in degrading PEG hydrogels with high modulus: engineering gel structural changes to facilitate cartilaginous tissue production. *Biotechnol. Bioeng.* **86**, 747–55 (2004).

178. Metters, A. T., Anseth, K. S. & Bowman, C. N. Fundamental studies of a novel, biodegradable PEG-b-PLA hydrogel. *Polymer (Guildf)*. **41**, 3993–4004 (2000).
179. Anseth, K. S. *et al.* In situ forming degradable networks and their application in tissue engineering and drug delivery. *J. Control. Release* **78**, 199–209 (2002).
180. West, J. L. & Hubbell, J. A. Polymeric Biomaterials with Degradation Sites for Proteases Involved in Cell Migration. *Macromolecules* **32**, 241–244 (1999).
181. Lutolf, M. P. *et al.* Synthetic matrix metalloproteinase-sensitive hydrogels for the conduction of tissue regeneration: engineering cell-invasion characteristics. *Proc. Natl. Acad. Sci. U. S. A.* **100**, 5413–8 (2003).
182. Lutolf, M. P., Raeber, G. P., Zisch, A. H., Tirelli, N. & Hubbell, J. A. Cell-Responsive Synthetic Hydrogels. *Adv. Mater.* **15**, 888–892 (2003).
183. Park, Y., Lutolf, M. P., Hubbell, J. A., Hunziker, E. B. & Wong, M. Bovine Primary Chondrocyte Culture in Synthetic Matrix Hydrogels as a Scaffold for Cartilage Repair. *Tissue Eng.* **10**, 515–522 (2004).
184. Patterson, J. & Hubbell, J. A. Enhanced proteolytic degradation of molecularly engineered PEG hydrogels in response to MMP-1 and MMP-2. *Biomaterials* **31**, 7836–45 (2010).
185. Mironi-Harpaz, I., Wang, D. Y., Venkatraman, S. & Seliktar, D. Photopolymerization of cell-encapsulating hydrogels: crosslinking efficiency versus cytotoxicity. *Acta Biomater.* **8**, 1838–48 (2012).
186. Gonen-Wadmany, M., Oss-Ronen, L. & Seliktar, D. Protein-polymer conjugates for forming photopolymerizable biomimetic hydrogels for tissue engineering. *Biomaterials* **28**, 3876–86 (2007).
187. Singh, R. K., Seliktar, D. & Putnam, A. J. Capillary morphogenesis in PEG-collagen hydrogels. *Biomaterials* **34**, 9331–40 (2013).
188. Appelman, T. P., Mizrahi, J., Elisseeff, J. H. & Seliktar, D. The influence of biological motifs and dynamic mechanical stimulation in hydrogel scaffold systems on the phenotype of chondrocytes. *Biomaterials* **32**, 1508–16 (2011).
189. Almany, L. & Seliktar, D. Biosynthetic hydrogel scaffolds made from fibrinogen and polyethylene glycol for 3D cell cultures. *Biomaterials* **26**, 2467–77 (2005).
190. Ito, A. *et al.* Transglutaminase-mediated gelatin matrices incorporating cell adhesion factors as a biomaterial for tissue engineering. *J. Biosci. Bioeng.* **95**, 196–199 (2003).

191. Lien, S.-M., Ko, L.-Y. & Huang, T.-J. Effect of pore size on ECM secretion and cell growth in gelatin scaffold for articular cartilage tissue engineering. *Acta Biomater.* **5**, 670–9 (2009).
192. Mazaki, T. *et al.* A novel, visible light-induced, rapidly cross-linkable gelatin scaffold for osteochondral tissue engineering. *Sci. Rep.* **4**, 4457 (2014).
193. Daniele, M. A., Adams, A. A., Naciri, J., North, S. H. & Ligler, F. S. Interpenetrating networks based on gelatin methacrylamide and PEG formed using concurrent thiol click chemistries for hydrogel tissue engineering scaffolds. *Biomaterials* **35**, 1845–56 (2014).
194. Byers, B. A., Mauck, R. L., Chiang, I. E. & Tuan, R. S. Transient exposure to transforming growth factor beta 3 under serum-free conditions enhances the biomechanical and biochemical maturation of tissue-engineered cartilage. *Tissue Eng. Part A* **14**, 1821–34 (2008).
195. Park, H., Temenoff, J. S., Holland, T. A., Tabata, Y. & Mikos, A. G. Delivery of TGF-beta1 and chondrocytes via injectable, biodegradable hydrogels for cartilage tissue engineering applications. *Biomaterials* **26**, 7095–103 (2005).
196. Salinas, C. N. & Anseth, K. S. The influence of the RGD peptide motif and its contextual presentation in PEG gels on human mesenchymal stem cell viability. *J. Tissue Eng. Regen. Med.* **2**, 296–304 (2008).
197. Salinas, C. N. & Anseth, K. S. The enhancement of chondrogenic differentiation of human mesenchymal stem cells by enzymatically regulated RGD functionalities. *Biomaterials* **29**, 2370–7 (2008).
198. McCall, J. D., Luoma, J. E. & Anseth, K. S. Covalently tethered transforming growth factor beta in PEG hydrogels promotes chondrogenic differentiation of encapsulated human mesenchymal stem cells. *Drug Deliv. Transl. Res.* **2**, 305–312 (2012).
199. Sridhar, B. V, Doyle, N. R., Randolph, M. A. & Anseth, K. S. Covalently tethered TGF- β 1 with encapsulated chondrocytes in a PEG hydrogel system enhances extracellular matrix production. *J. Biomed. Mater. Res. A* **102**, 4464–4472 (2014).
200. Lin, C.-C. & Anseth, K. S. Controlling Affinity Binding with Peptide-Functionalized Poly(ethylene glycol) Hydrogels. *Adv. Funct. Mater.* **19**, 2325 (2009).
201. Lin, C.-C. & Anseth, K. S. PEG hydrogels for the controlled release of biomolecules in regenerative medicine. *Pharm. Res.* **26**, 631–43 (2009).
202. Bryant, S. J., Chowdhury, T. T., Lee, D. A., Bader, D. L. & Anseth, K. S. Crosslinking Density Influences Chondrocyte Metabolism in Dynamically Loaded Photocrosslinked Poly(ethylene glycol) Hydrogels. *Ann. Biomed. Eng.* **32**, 407–417 (2004).

203. Chung, C., Beecham, M., Mauck, R. L. & Burdick, J. A. The influence of degradation characteristics of hyaluronic acid hydrogels on in vitro neocartilage formation by mesenchymal stem cells. *Biomaterials* **30**, 4287–96 (2009).
204. Eyrich, D. *et al.* In vitro and in vivo cartilage engineering using a combination of chondrocyte-seeded long-term stable fibrin gels and polycaprolactone-based polyurethane scaffolds. *Tissue Eng.* **13**, 2207–18 (2007).
205. Miot, S. *et al.* Cartilage tissue engineering by expanded goat articular chondrocytes. *J. Orthop. Res.* **24**, 1078–85 (2006).
206. Villanueva, I., Klement, B. J., von Deutsch, D. & Bryant, S. J. Cross-linking density alters early metabolic activities in chondrocytes encapsulated in poly(ethylene glycol) hydrogels and cultured in the rotating wall vessel. *Biotechnol. Bioeng.* **102**, 1242–50 (2009).
207. Kisiday, J. D., Jin, M., DiMicco, M. A., Kurz, B. & Grodzinsky, A. J. Effects of dynamic compressive loading on chondrocyte biosynthesis in self-assembling peptide scaffolds. *J. Biomech.* **37**, 595–604 (2004).
208. Roberts, J. J., Nicodemus, G. D., Giunta, S. & Bryant, S. J. Incorporation of biomimetic matrix molecules in PEG hydrogels enhances matrix deposition and reduces load-induced loss of chondrocyte-secreted matrix. *J. Biomed. Mater. Res. A* **97**, 281–91 (2011).
209. Kon, E. *et al.* Matrix-assisted autologous chondrocyte transplantation for the repair of cartilage defects of the knee: systematic clinical data review and study quality analysis. *Am. J. Sports Med.* **37**, 1565–665 (2009).
210. Sharma, B. *et al.* Human cartilage repair with a photoreactive adhesive-hydrogel composite. *Sci. Transl. Med.* **5**, 167–173 (2013).

7.2. CHAPTER II

1. Bentley, G. *et al.* A prospective, randomized comparison of autologous chondrocyte implantation versus mosaicplasty for osteochondral defects in the knee. *J. Bone Jt. Surg.* **85**, 223–230 (2003).
2. Behrens, P., Bitter, T., Kurz, B. & Russlies, M. Matrix-associated autologous chondrocyte transplantation/implantation (MACT/MACI)--5-year follow-up. *Knee* **13**, 194–202 (2006).
3. Malafaya, P. B., Silva, G. A. & Reis, R. L. Natural-origin polymers as carriers and scaffolds for biomolecules and cell delivery in tissue engineering applications. *Adv. Drug Deliv. Rev.* **59**, 207–33 (2007).

4. Nguyen, K. T. & West, J. L. Photopolymerizable hydrogels for tissue engineering applications. *Biomaterials* **23**, 4307–14 (2002).
5. Elisseeff, J. *et al.* Photoencapsulation of chondrocytes in poly(ethylene oxide)-based semi-interpenetrating networks. *J. Biomed. Mater. Res.* **51**, 164–71 (2000).
6. Hunziker, E. B. Articular cartilage repair: basic science and clinical progress. A review of the current status and prospects. *Osteoarthr. Cartil.* **10**, 432–63 (2002).
7. Hume, P. S., He, J., Haskins, K. & Anseth, K. S. Strategies to reduce dendritic cell activation through functional biomaterial design. *Biomaterials* **33**, 3615–25 (2012).
8. Aimetti, A. A., Machen, A. J. & Anseth, K. S. Poly(ethylene glycol) hydrogels formed by thiol-ene photopolymerization for enzyme-responsive protein delivery. *Biomaterials* **30**, 6048–54 (2009).
9. Lee, S. J. Cytokine delivery and tissue engineering. *Yonsei Med. J.* **41**, 704–719 (2000).
10. Park, H., Temenoff, J. S., Holland, T. A., Tabata, Y. & Mikos, A. G. Delivery of TGF- β 1 and chondrocytes via injectable, biodegradable hydrogels for cartilage tissue engineering applications. *Biomaterials* **26**, 7095–103 (2005).
11. Li, T., O’Keefe, R. & Chen, D. TGF- β signaling in chondrocytes. *Front. Biosci.* 681–688 (2005).
12. Forsyth, C. B. *et al.* Increased matrix metalloproteinase-13 production with aging by human articular chondrocytes in response to catabolic stimuli. *J. Gerontol. A. Biol. Sci. Med. Sci.* **60**, 1118–24 (2005).
13. Nicodemus, G. D., Skaalure, S. C. & Bryant, S. J. Gel structure has an impact on pericellular and extracellular matrix deposition, which subsequently alters metabolic activities in chondrocyte-laden PEG hydrogels. *Acta Biomater.* **7**, 492–504 (2011).
14. Bryant, S. J. & Anseth, K. S. Hydrogel properties influence ECM production by chondrocytes photoencapsulated in poly(ethylene glycol) hydrogels. *J. Biomed. Mater. Res.* **59**, 63–72 (2002).
15. Leight, J. L., Alge, D. L., Maier, A. J. & Anseth, K. S. Direct measurement of matrix metalloproteinase activity in 3D cellular microenvironments using a fluorogenic peptide substrate. *Biomaterials* **34**, 7344–7352 (2013).
16. Kyburz, K. A. & Anseth, K. S. Three-dimensional hMSC motility within peptide-functionalized PEG-based hydrogels of varying adhesivity and crosslinking density. *Acta Biomater.* **9**, 6381–92 (2013).

17. Anderson, S. B., Lin, C.-C., Kuntzler, D. V & Anseth, K. S. The performance of human mesenchymal stem cells encapsulated in cell-degradable polymer-peptide hydrogels. *Biomaterials* **32**, 3564–74 (2011).
18. Zhao, W., Jin, X., Cong, Y., Liu, Y. & Fu, J. Degradable natural polymer hydrogels for articular cartilage tissue engineering. *J. Chem. Technol. Biotechnol.* (2012).
19. Fu, Y. *et al.* 3D cell entrapment in crosslinked thiolated gelatin-poly(ethylene glycol) diacrylate hydrogels. *Biomaterials* **33**, 48–58 (2012).
20. Daniele, M. A., Adams, A. A., Naciri, J., North, S. H. & Ligler, F. S. Interpenetrating networks based on gelatin methacrylamide and PEG formed using concurrent thiol click chemistries for hydrogel tissue engineering scaffolds. *Biomaterials* **35**, 1845–56 (2014).
21. Gorgieva, S. & Kokol, V. in *Biomater. Appl. Nanomedicine* (Pignatello, R.) 17–52 (InTech, 2011).

7.3. CHAPTER III

1. Hunziker, E. B. Articular cartilage repair: basic science and clinical progress. A review of the current status and prospects. *Osteoarthr. Cartil.* **10**, 432–63 (2002).
2. Holland, T. A. & Mikos, A. G. Advances in drug delivery for articular cartilage. *J. Control. Release* **86**, 1–14 (2003).
3. Chen, F. H., Rousche, K. T. & Tuan, R. S. Technology Insight: adult stem cells in cartilage regeneration and tissue engineering. *Nat. Clin. Pract. Rheumatol.* **2**, 373–82 (2006).
4. Jackson, D. W. & Simon, T. M. Tissue engineering principles in orthopaedic surgery. *Clin. Orthop. Relat. Res.* S31–45 (1999).
5. Masters, K. S. Covalent growth factor immobilization strategies for tissue repair and regeneration. *Macromol. Biosci.* **11**, 1149–63 (2011).
6. Tayalia, P. & Mooney, D. J. Controlled growth factor delivery for tissue engineering. *Adv. Mater.* **21**, 3269–85 (2009).
7. Zhao, W., Jin, X., Cong, Y., Liu, Y. & Fu, J. Degradable natural polymer hydrogels for articular cartilage tissue engineering. *J. Chem. Technol. Biotechnol.* **88**, 327–339 (2013).
8. Kock, L., van Donkelaar, C. C. & Ito, K. Tissue engineering of functional articular cartilage: the current status. *Cell Tissue Res.* **347**, 613–27 (2012).

9. Spiller, K. L., Maher, S. A. & Lowman, A. M. Hydrogels for the Repair of Articular Cartilage Defects. *Tissue Eng. Part B* **17**, 281–299 (2011).
10. Bryant, S. J. & Anseth, K. S. Hydrogel properties influence ECM production by chondrocytes photoencapsulated in poly(ethylene glycol) hydrogels. *J. Biomed. Mater. Res.* **59**, 63–72 (2002).
11. Sharma, B. *et al.* Human cartilage repair with a photoreactive adhesive-hydrogel composite. *Sci. Transl. Med.* **5**, 167–173 (2013).
12. Lee, S. J. Cytokine delivery and tissue engineering. *Yonsei Med. J.* **41**, 704–719 (2000).
13. Park, H., Temenoff, J. S., Holland, T. A., Tabata, Y. & Mikos, A. G. Delivery of TGF- β 1 and chondrocytes via injectable, biodegradable hydrogels for cartilage tissue engineering applications. *Biomaterials* **26**, 7095–103 (2005).
14. Hume, P. S., He, J., Haskins, K. & Anseth, K. S. Strategies to reduce dendritic cell activation through functional biomaterial design. *Biomaterials* **33**, 3615–25 (2012).
15. Deforest, C. A. & Anseth, K. S. Photoreversible Patterning of Biomolecules within Click-Based Hydrogels. *Angew. Chem. Int. Ed. Engl.* **124**, 1852–1855 (2012).
16. Aimetti, A. A., Machen, A. J. & Anseth, K. S. Poly(ethylene glycol) hydrogels formed by thiol-ene photopolymerization for enzyme-responsive protein delivery. *Biomaterials* **30**, 6048–54 (2009).
17. Benton, J. A., Fairbanks, B. D. & Anseth, K. S. Characterization of valvular interstitial cell function in three dimensional matrix metalloproteinase degradable PEG hydrogels. *Biomaterials* **30**, 6593–603 (2009).
18. Fairbanks, B. D. *et al.* A Versatile Synthetic Extracellular Matrix Mimic via Thiol-Norbornene Photopolymerization. *Adv. Mater.* **21**, 5005–5010 (2009).
19. Fairbanks, B. D., Schwartz, M. P., Bowman, C. N. & Anseth, K. S. Photoinitiated polymerization of PEG-diacrylate with lithium phenyl-2,4,6-trimethylbenzoylphosphine: polymerization rate and cytocompatibility. *Biomaterials* **30**, 6702–7 (2009).
20. McCall, J. D., Luoma, J. E. & Anseth, K. S. Covalently tethered transforming growth factor β 1 in PEG hydrogels promotes chondrogenic differentiation of encapsulated human mesenchymal stem cells. *Drug Deliv. Transl. Res.* **2**, 305–312 (2012).
21. McCall, J. D. & Anseth, K. S. Thiol-ene photopolymerizations provide a facile method to encapsulate proteins and maintain their bioactivity. *Biomacromolecules* **13**, 2410–7 (2012).

22. Huey, D., Hu, J. & Athanasiou, K. Unlike Bone, Cartilage Regeneration Remains Elusive. *Science* (80-.). **6933**, 917–921 (2012).
23. Roberts, J. J. & Bryant, S. J. Comparison of photopolymerizable thiol-ene PEG and acrylate-based PEG hydrogels for cartilage development. *Biomaterials* (2013).
24. Li, T., O’Keefe, R. & Chen, D. TGF- β signaling in chondrocytes. *Front. Biosci.* 681–688 (2005).
25. Clarke, D. C., Brown, M. L., Erickson, R. A., Shi, Y. & Liu, X. Transforming growth factor beta depletion is the primary determinant of Smad signaling kinetics. *Mol. Cell. Biol.* **29**, 2443–55 (2009).
26. Yoo, J. J., Bichara, D. A., Zhao, X., Randolph, M. A. & Gill, T. J. Implant-assisted meniscal repair in vivo using a chondrocyte-seeded flexible PLGA scaffold. *J. Biomed. Mater. Res. A* **99**, 102–8 (2011).
27. Byers, B. A., Mauck, R. L., Chiang, I. E. & Tuan, R. S. Transient exposure to transforming growth factor beta 3 under serum-free conditions enhances the biomechanical and biochemical maturation of tissue-engineered cartilage. *Tissue Eng. Part A* **14**, 1821–34 (2008).
28. Chua, K. H., Aminuddin, B. S., Fuzina, N. H. & Ruszymah, B. H. I. Insulin-transferrin-selenium prevent human chondrocyte dedifferentiation and promote the formation of high quality tissue engineered human hyaline cartilage. *Eur. Cell. Mater.* **9**, 58–67 (2005).
29. Ruan, J.-L. *et al.* An Improved Cryosection Method for Polyethylene Glycol Hydrogels Used in Tissue Engineering. *Tissue Eng. Part C. Methods* **19**, 794–801 (2013).
30. Kim, Y.-J., Sah, R. L. Y., Doong, J.-Y. H. & Grodzinsky, A. J. Fluorometric assay of DNA in cartilage explants using Hoechst 33258. *Anal. Biochem.* **174**, 168–176 (1988).
31. Farndale, R. W., Sayers, C. A. & Barrett, A. J. A direct spectrophotometric microassay for sulfated glycosaminoglycans in cartilage cultures. *Connect. Tissue Res.* **9**, 247–8 (1982).
32. Woessner, J. F. The determination of hydroxyproline in tissue and protein samples containing small proportions of this imino acid. *Arch. Biochem. Biophys.* **93**, 440–7 (1961).
33. Ballock, R. T. & O’Keefe, R. J. The Biology of the Growth Plate. *J. Bone Jt. Surg.* **85**, 715–726 (2003).
34. Passaretti, D. & Silverman, R.P. Huang, W Kirchhoff, C.H. Ashiku, S. Randolph, M.A. Yaremchuk, M. J. Cultured chondrocytes produce injectable tissue-engineered cartilage in hydrogel polymer. *Tissue Eng.* **7**, 805–15 (2001).

35. Burdick, J. A., Chung, C., Jia, X., Randolph, M. A. & Langer, R. Controlled degradation and mechanical behavior of photopolymerized hyaluronic acid networks. *Biomacromolecules* **6**, 386–91 (2005).
36. Ibusuki, S. *et al.* Engineering Cartilage in a Photochemically Crosslinked Collagen Gel. *J. Knee Surg.* **22**, 72–81 (2010).
37. Zwaagstra, J. C., El-Alfy, M. & O'Connor-McCourt, M. D. Transforming growth factor (TGF)-beta 1 internalization: modulation by ligand interaction with TGF-beta receptors types I and II and a mechanism that is distinct from clathrin-mediated endocytosis. *J. Biol. Chem.* **276**, 27237–45 (2001).
38. Shi, Y. & Massagué, J. Mechanisms of TGF-beta signaling from cell membrane to the nucleus. *Cell* **113**, 685–700 (2003).
39. Derynck, R. *et al.* Human transforming growth factor-beta complementary DNA sequence and expression in normal and transformed cells. *Nature* **316**, 701–5 (1985).
40. Lin, Z., Willers, C., Xu, J. & Zheng, M.-H. The chondrocyte: biology and clinical application. *Tissue Eng.* **12**, 1971–84 (2006).
41. Jin, R. L., Park, S. R., Choi, B. H. & Min, B.-H. Scaffold-free cartilage fabrication system using passaged porcine chondrocytes and basic fibroblast growth factor. *Tissue Eng. Part A* **15**, 1887–95 (2009).
42. Baghaban Eslaminejad, M., Taghiyar, L. & Falahi, F. Quantitative analysis of the proliferation and differentiation of rat articular chondrocytes in alginate 3D culture. *Iran. Biomed. J.* **13**, 153–60 (2009).
43. Skaalure, S. C., Milligan, I. L. & Bryant, S. J. Age impacts extracellular matrix metabolism in chondrocytes encapsulated in degradable hydrogels. *Biomed. Mater.* **7**, 1–13 (2012).
44. Park, Y., Lutolf, M. P., Hubbell, J. A., Hunziker, E. B. & Wong, M. Bovine Primary Chondrocyte Culture in Synthetic Matrix Hydrogels as a Scaffold for Cartilage Repair. *Tissue Eng.* **10**, 515–522 (2004).
45. Roberts, J. J., Nicodemus, G. D., Greenwald, E. C. & Bryant, S. J. Degradation improves tissue formation in (un)loaded chondrocyte-laden hydrogels. *Clin. Orthop. Relat. Res.* **469**, 2725–34 (2011).

7.4. CHAPTER IV

1. Adolphe, M. *Biological regulation of the chondrocytes*. (CRC Press, 1992).

2. Falah, M., Nierenberg, G., Soudry, M., Hayden, M. & Volpin, G. Treatment of articular cartilage lesions of the knee. *Int. Orthop.* **34**, 621–30 (2010).
3. Kon, E. *et al.* Matrix-assisted autologous chondrocyte transplantation for the repair of cartilage defects of the knee: systematic clinical data review and study quality analysis. *Am. J. Sports Med.* **37**, 1565–665 (2009).
4. Kim, I. L., Mauck, R. L. & Burdick, J. A. Hydrogel design for cartilage tissue engineering: a case study with hyaluronic acid. *Biomaterials* **32**, 8771–82 (2011).
5. Hutson, C. B. *et al.* Synthesis and characterization of tunable poly(ethylene glycol): gelatin methacrylate composite hydrogels. *Tissue Eng. Part A* **17**, 1713–23 (2011).
6. Kock, L., van Donkelaar, C. C. & Ito, K. Tissue engineering of functional articular cartilage: the current status. *Cell Tissue Res.* **347**, 613–27 (2012).
7. Spiller, K. L., Maher, S. A. & Lowman, A. M. Hydrogels for the Repair of Articular Cartilage Defects. *Tissue Eng. Part B* **17**, 281–299 (2011).
8. Forsyth, C. B. *et al.* Increased matrix metalloproteinase-13 production with aging by human articular chondrocytes in response to catabolic stimuli. *J. Gerontol. A. Biol. Sci. Med. Sci.* **60**, 1118–24 (2005).
9. Nicodemus, G. D., Skaalure, S. C. & Bryant, S. J. Gel structure has an impact on pericellular and extracellular matrix deposition, which subsequently alters metabolic activities in chondrocyte-laden PEG hydrogels. *Acta Biomater.* **7**, 492–504 (2011).
10. Bryant, S. J. & Anseth, K. S. Hydrogel properties influence ECM production by chondrocytes photoencapsulated in poly(ethylene glycol) hydrogels. *J. Biomed. Mater. Res.* **59**, 63–72 (2002).
11. Bryant, S. J. & Anseth, K. S. Controlling the spatial distribution of ECM components in degradable PEG hydrogels for tissue engineering cartilage. *J. Biomed. Mater. Res. A* **64**, 70–9 (2003).
12. Zhao, W., Jin, X., Cong, Y., Liu, Y. & Fu, J. Degradable natural polymer hydrogels for articular cartilage tissue engineering. *J. Chem. Technol. Biotechnol.* **88**, 327–339 (2013).
13. Hume, P. S., He, J., Haskins, K. & Anseth, K. S. Strategies to reduce dendritic cell activation through functional biomaterial design. *Biomaterials* **33**, 3615–25 (2012).
14. Deforest, C. A. & Anseth, K. S. Photoreversible Patterning of Biomolecules within Click-Based Hydrogels. *Angew. Chem. Int. Ed. Engl.* **124**, 1852–1855 (2012).

15. Aimetti, A. A., Machen, A. J. & Anseth, K. S. Poly(ethylene glycol) hydrogels formed by thiol-ene photopolymerization for enzyme-responsive protein delivery. *Biomaterials* **30**, 6048–54 (2009).
16. Benton, J. A., Fairbanks, B. D. & Anseth, K. S. Characterization of valvular interstitial cell function in three dimensional matrix metalloproteinase degradable PEG hydrogels. *Biomaterials* **30**, 6593–603 (2009).
17. Fairbanks, B. D. *et al.* A Versatile Synthetic Extracellular Matrix Mimic via Thiol-Norbornene Photopolymerization. *Adv. Mater.* **21**, 5005–5010 (2009).
18. Hoyle, C. E. & Bowman, C. N. Thiol-ene click chemistry. *Angew. Chem. Int. Ed. Engl.* **49**, 1540–73 (2010).
19. Schwartz, M. P. *et al.* A synthetic strategy for mimicking the extracellular matrix provides new insight about tumor cell migration. *Integr. Biol. (Camb)*. **2**, 32–40 (2010).
20. Fairbanks, B. D., Schwartz, M. P., Bowman, C. N. & Anseth, K. S. Photoinitiated polymerization of PEG-diacrylate with lithium phenyl-2,4,6-trimethylbenzoylphosphine: polymerization rate and cytocompatibility. *Biomaterials* **30**, 6702–7 (2009).
21. Sridhar, B. V, Doyle, N. R., Randolph, M. A. & Anseth, K. S. Covalently tethered TGF- β 1 with encapsulated chondrocytes in a PEG hydrogel system enhances extracellular matrix production. *J. Biomed. Mater. Res. A* **102**, 4464–4472 (2014).
22. Manicourt, D. H., Devogelaer, J. P. & Thonar, E. J. in *Dyn. Bone Cartil. Metab.* (Seibel, M., Robins, S. P. & Bilezikian, J. P.) 421–439 (Elsevier Science, 2006).
23. Lutolf, M. P. & Hubbell, J. A. Synthetic biomaterials as instructive extracellular microenvironments for morphogenesis in tissue engineering. *Nat. Biotechnol.* **23**, 47–55 (2005).
24. Park, Y., Lutolf, M. P., Hubbell, J. A., Hunziker, E. B. & Wong, M. Bovine Primary Chondrocyte Culture in Synthetic Matrix Hydrogels as a Scaffold for Cartilage Repair. *Tissue Eng.* **10**, 515–522 (2004).
25. Chubinskaya, S. Chondrocyte Matrix Metalloproteinase-8. *J. Biol. Chem.* **271**, 11023–11026 (1996).
26. Wu, P., DeLassus, E., Patra, D., Liao, W. & Sandell, L. J. Effects of serum and compressive loading on the cartilage matrix synthesis and spatiotemporal deposition around chondrocytes in 3D culture. *Tissue Eng. Part A* **19**, 1199–208 (2013).
27. Lin, Z., Willers, C., Xu, J. & Zheng, M.-H. The chondrocyte: biology and clinical application. *Tissue Eng.* **12**, 1971–84 (2006).

28. Kyburz, K. A. & Anseth, K. S. Three-dimensional hMSC motility within peptide-functionalized PEG-based hydrogels of varying adhesivity and crosslinking density. *Acta Biomater.* **9**, 6381–92 (2013).
29. Bahney, C. S., Hsu, C.-W., Yoo, J. U., West, J. L. & Johnstone, B. A bioresponsive hydrogel tuned to chondrogenesis of human mesenchymal stem cells. *FASEB J.* **25**, 1486–96 (2011).
30. Bian, L., Zhai, D. Y., Mauck, R. L. & Burdick, J. A. Coculture of Human Mesenchymal Stem Cells and Enhances Functional Properties of Engineered Cartilage Reverse primer. *Tissue Eng. Part A* **17**, 1137–1145 (2011).
31. Steadman, J. R. *et al.* Outcomes of microfracture for traumatic chondral defects of the knee: average 11-year follow-up. *Arthroscopy* **19**, 477–84 (2003).
32. McCall, J. D., Luoma, J. E. & Anseth, K. S. Covalently tethered transforming growth factor beta in PEG hydrogels promotes chondrogenic differentiation of encapsulated human mesenchymal stem cells. *Drug Deliv. Transl. Res.* **2**, 305–312 (2012).
33. Dahlin, R. L. *et al.* Articular chondrocytes and mesenchymal stem cells seeded on biodegradable scaffolds for the repair of cartilage in a rat osteochondral defect model. *Biomaterials* **35**, 7460–7469 (2014).
34. Leight, J. L., Alge, D. L., Maier, A. J. & Anseth, K. S. Direct measurement of matrix metalloproteinase activity in 3D cellular microenvironments using a fluorogenic peptide substrate. *Biomaterials* **34**, 7344–7352 (2013).
35. Silverman, R. P., Passaretti, D., Huang, W., Randolph, M. A. & Yaremchuk, M. J. Injectable tissue-engineered cartilage using a fibrin glue polymer. *Plast. Reconstr. Surg.* **103**, 1809–1818 (1999).
36. Passaretti, D. & Silverman, R.P. Huang, W Kirchhoff, C.H. Ashiku, S. Randolph, M.A. Yaremchuk, M. J. Cultured chondrocytes produce injectable tissue-engineered cartilage in hydrogel polymer. *Tissue Eng.* **7**, 805–15 (2001).
37. Ibusuki, S. *et al.* Engineering Cartilage in a Photochemically Crosslinked Collagen Gel. *J. Knee Surg.* **22**, 72–81 (2010).
38. Anderson, S. B., Lin, C.-C., Kuntzler, D. V & Anseth, K. S. The performance of human mesenchymal stem cells encapsulated in cell-degradable polymer-peptide hydrogels. *Biomaterials* **32**, 3564–74 (2011).
39. Bryant, S. J., Bender, R. J., Durand, K. L. & Anseth, K. S. Encapsulating chondrocytes in degrading PEG hydrogels with high modulus: engineering gel structural changes to facilitate cartilaginous tissue production. *Biotechnol. Bioeng.* **86**, 747–55 (2004).

40. Bryant, S. J., Arthur, J. A. & Anseth, K. S. Incorporation of tissue-specific molecules alters chondrocyte metabolism and gene expression in photocrosslinked hydrogels. *Acta Biomater.* **1**, 243–52 (2005).
41. Coimbra, I. B., Jimenez, S. A., Hawkins, D. F., Piera-Velazquez, S. & Stokes, D. G. Hypoxia inducible factor-1 alpha expression in human normal and osteoarthritic chondrocytes. *Osteoarthritis Cartilage* **12**, 336–45 (2004).
42. Wu, L., Prins, H.-J., Helder, M. N., van Blitterswijk, C. A. & Karperien, M. Trophic effects of mesenchymal stem cells in chondrocyte co-cultures are independent of culture conditions and cell sources. *Tissue Eng. Part A* **18**, 1542–51 (2012).
43. Hall, B. K. Earliest evidence of cartilage and bone development in embryonic life. *Clin. Orthop. Relat. Res.* **225**, 255–72 (1987).
44. Bryant, S. J., Chowdhury, T. T., Lee, D. A., Bader, D. L. & Anseth, K. S. Crosslinking Density Influences Chondrocyte Metabolism in Dynamically Loaded Photocrosslinked Poly(ethylene glycol) Hydrogels. *Ann. Biomed. Eng.* **32**, 407–417 (2004).
45. Hardingham, T. & Fosang, A. Proteoglycans: many forms and many functions. *FASEB J* **6**, 861–870 (1992).
46. Huey, D., Hu, J. & Athanasiou, K. Unlike Bone, Cartilage Regeneration Remains Elusive. *Science* (80-.). **6933**, 917–921 (2012).
47. Yoo, J. J., Bichara, D. A., Zhao, X., Randolph, M. A. & Gill, T. J. Implant-assisted meniscal repair in vivo using a chondrocyte-seeded flexible PLGA scaffold. *J. Biomed. Mater. Res. A* **99**, 102–8 (2011).
48. Byers, B. A., Mauck, R. L., Chiang, I. E. & Tuan, R. S. Transient exposure to transforming growth factor beta 3 under serum-free conditions enhances the biomechanical and biochemical maturation of tissue-engineered cartilage. *Tissue Eng. Part A* **14**, 1821–34 (2008).
49. Chua, K. H., Aminuddin, B. S., Fuzina, N. H. & Ruszymah, B. H. I. Insulin-transferrin-selenium prevent human chondrocyte dedifferentiation and promote the formation of high quality tissue engineered human hyaline cartilage. *Eur. Cell. Mater.* **9**, 58–67 (2005).
50. Salinas, C. N. & Anseth, K. S. The enhancement of chondrogenic differentiation of human mesenchymal stem cells by enzymatically regulated RGD functionalities. *Biomaterials* **29**, 2370–7 (2008).
51. Villanueva, I., Weigel, C. A. & Bryant, S. J. Cell-matrix interactions and dynamic mechanical loading influence chondrocyte gene expression and bioactivity in PEG-RGD hydrogels. *Acta Biomater.* **5**, 2832–46 (2009).

52. Farndale, R. W., Sayers, C. A. & Barrett, A. J. A direct spectrophotometric microassay for sulfated glycosaminoglycans in cartilage cultures. *Connect. Tissue Res.* **9**, 247–8 (1982).
53. Woessner, J. F. The determination of hydroxyproline in tissue and protein samples containing small proportions of this imino acid. *Arch. Biochem. Biophys.* **93**, 440–7 (1961).
54. Ruan, J.-L. *et al.* An Improved Cryosection Method for Polyethylene Glycol Hydrogels Used in Tissue Engineering. *Tissue Eng. Part C. Methods* **19**, 794–801 (2013).

7.5. CHAPTER V

1. Adolphe, M. *Biological regulation of the chondrocytes*. (CRC Press, 1992).
2. Kim, I. L., Mauck, R. L. & Burdick, J. A. Hydrogel design for cartilage tissue engineering: a case study with hyaluronic acid. *Biomaterials* **32**, 8771–82 (2011).
3. Hutson, C. B. *et al.* Synthesis and characterization of tunable poly(ethylene glycol): gelatin methacrylate composite hydrogels. *Tissue Eng. Part A* **17**, 1713–23 (2011).
4. Kock, L., van Donkelaar, C. C. & Ito, K. Tissue engineering of functional articular cartilage: the current status. *Cell Tissue Res.* **347**, 613–27 (2012).
5. Spiller, K. L., Maher, S. A. & Lowman, A. M. Hydrogels for the Repair of Articular Cartilage Defects. *Tissue Eng. Part B* **17**, 281–299 (2011).
6. Forsyth, C. B. *et al.* Increased matrix metalloproteinase-13 production with aging by human articular chondrocytes in response to catabolic stimuli. *J. Gerontol. A. Biol. Sci. Med. Sci.* **60**, 1118–24 (2005).
7. Nicodemus, G. D., Skaalure, S. C. & Bryant, S. J. Gel structure has an impact on pericellular and extracellular matrix deposition, which subsequently alters metabolic activities in chondrocyte-laden PEG hydrogels. *Acta Biomater.* **7**, 492–504 (2011).
8. Sridhar, B. V, Doyle, N. R., Randolph, M. A. & Anseth, K. S. Covalently tethered TGF- β 1 with encapsulated chondrocytes in a PEG hydrogel system enhances extracellular matrix production. *J. Biomed. Mater. Res. A* **102**, 4464–4472 (2014).
9. Bryant, S. J. & Anseth, K. S. Hydrogel properties influence ECM production by chondrocytes photoencapsulated in poly(ethylene glycol) hydrogels. *J. Biomed. Mater. Res. A* **59**, 63–72 (2002).
10. Lee, K. Y. & Mooney, D. J. Hydrogels for Tissue Engineering. *Chem. Rev.* **101**, 1869–1880 (2001).

11. Lutolf, M. P. & Hubbell, J. A. Synthetic biomaterials as instructive extracellular microenvironments for morphogenesis in tissue engineering. *Nat. Biotechnol.* **23**, 47–55 (2005).
12. Bryant, S. J. & Anseth, K. S. Controlling the spatial distribution of ECM components in degradable PEG hydrogels for tissue engineering cartilage. *J. Biomed. Mater. Res. A* **64**, 70–9 (2003).
13. Zhao, W., Jin, X., Cong, Y., Liu, Y. & Fu, J. Degradable natural polymer hydrogels for articular cartilage tissue engineering. *J. Chem. Technol. Biotechnol.* **88**, 327–339 (2013).
14. Kretlow, J. D. & Mikos, A. G. From Material to Tissue: Biomaterial Development, Scaffold Fabrication, and Tissue Engineering. *AIChE J.* **54**, 3048–3067 (2008).
15. Sridhar, B. V *et al.* Development of a Cellularly Degradable PEG Hydrogel to Promote Articular Cartilage Extracellular Matrix Deposition. *Adv. Healthc. Mater.* **4**, 635–781 (2015).
16. Patterson, J. & Hubbell, J. A. Enhanced proteolytic degradation of molecularly engineered PEG hydrogels in response to MMP-1 and MMP-2. *Biomaterials* **31**, 7836–45 (2010).
17. Lin, Z., Willers, C., Xu, J. & Zheng, M.-H. The chondrocyte: biology and clinical application. *Tissue Eng.* **12**, 1971–84 (2006).
18. Fields, G. B., Wart, H. E. Van & Birkedal-hansen, H. Sequence Specificity of Human Skin Fibroblast Collagenase: Evidence for the role of collagen structure in determining the collagenase cleavage site. *J. Biol. Chem.* **262**, 6221–6226 (1987).
19. Schmidt, O., Mizrahi, J., Elisseeff, J. & Seliktar, D. Immobilized fibrinogen in PEG hydrogels does not improve chondrocyte-mediated matrix deposition in response to mechanical stimulation. *Biotechnol. Bioeng.* **95**, 1061–9 (2006).
20. Almany, L. & Seliktar, D. Biosynthetic hydrogel scaffolds made from fibrinogen and polyethylene glycol for 3D cell cultures. *Biomaterials* **26**, 2467–77 (2005).
21. Mironi-Harpaz, I., Wang, D. Y., Venkatraman, S. & Seliktar, D. Photopolymerization of cell-encapsulating hydrogels: crosslinking efficiency versus cytotoxicity. *Acta Biomater.* **8**, 1838–48 (2012).
22. Gonen-Wadmany, M., Oss-Ronen, L. & Seliktar, D. Protein-polymer conjugates for forming photopolymerizable biomimetic hydrogels for tissue engineering. *Biomaterials* **28**, 3876–86 (2007).
23. Appelman, T. P., Mizrahi, J., Elisseeff, J. H. & Seliktar, D. The influence of biological motifs and dynamic mechanical stimulation in hydrogel scaffold systems on the phenotype of chondrocytes. *Biomaterials* **32**, 1508–16 (2011).

24. Singh, R. K., Seliktar, D. & Putnam, A. J. Capillary morphogenesis in PEG-collagen hydrogels. *Biomaterials* **34**, 9331–40 (2013).
25. Manicourt, D. H., Devogelaer, J. P. & Thonar, E. J. in *Dyn. Bone Cartil. Metab.* (Seibel, M., Robins, S. P. & Bilezikian, J. P.) 421–439 (Elsevier Science, 2006).
26. Rice, J. J. *et al.* Engineering the regenerative microenvironment with biomaterials. *Adv. Healthc. Mater.* **2**, 57–71 (2013).
27. Gorgieva, S. & Kokol, V. in *Biomater. Appl. Nanomedicine* (Pignatello, R.) 17–52 (InTech, 2011).
28. Dreier, R., Wallace, S., Fuchs, S., Bruckner, P. & Grassel, S. Paracrine interactions of chondrocytes and macrophages in cartilage degradation: articular chondrocytes provide factors that activate macrophage-derived pro-gelatinase B (pro-MMP-9). *J. Cell Sci.* **114**, 3813–3822 (2001).
29. Mohtai, M. *et al.* Expression of 92-kD type IV collagenase/gelatinase (gelatinase B) in osteoarthritic cartilage and its induction in normal human articular cartilage by interleukin 1. *J. Clin. Invest.* **92**, 179–85 (1993).
30. Wang, C.-C. *et al.* A biomimetic honeycomb-like scaffold prepared by flow-focusing technology for cartilage regeneration. *Biotechnol. Bioeng.* **111**, 2338–48 (2014).
31. Mazaki, T. *et al.* A novel, visible light-induced, rapidly cross-linkable gelatin scaffold for osteochondral tissue engineering. *Sci. Rep.* **4**, 4457 (2014).
32. Fu, Y. *et al.* 3D cell entrapment in crosslinked thiolated gelatin-poly(ethylene glycol) diacrylate hydrogels. *Biomaterials* **33**, 48–58 (2012).
33. Daniele, M. A., Adams, A. A., Naciri, J., North, S. H. & Ligler, F. S. Interpenetrating networks based on gelatin methacrylamide and PEG formed using concurrent thiol click chemistries for hydrogel tissue engineering scaffolds. *Biomaterials* **35**, 1845–56 (2014).
34. Muñoz, Z., Shih, H. & Lin, C.-C. Gelatin hydrogels formed by orthogonal thiol–norbornene photochemistry for cell encapsulation. *Biomater. Sci.* **2**, 1063 (2014).
35. Hoyle, C. E. & Bowman, C. N. Thiol-ene click chemistry. *Angew. Chem. Int. Ed. Engl.* **49**, 1540–73 (2010).
36. Einerson, N. J., Stevens, K. R. & Kao, W. J. Synthesis and physicochemical analysis of gelatin-based hydrogels for drug carrier matrices. *Biomaterials* **24**, 509–523 (2003).
37. Waldeck, H. & Kao, W. J. Effect of the Addition of a Labile Gelatin Component on the Degradation and Solute Release Kinetics of a Stable PEG Hydrogel. *J. Biomater. Sci. Polym. Ed.* **23**, 1595–1611 (2011).

38. Fairbanks, B. D., Schwartz, M. P., Bowman, C. N. & Anseth, K. S. Photoinitiated polymerization of PEG-diacrylate with lithium phenyl-2,4,6-trimethylbenzoylphosphinate: polymerization rate and cytocompatibility. *Biomaterials* **30**, 6702–7 (2009).
39. Mohanty, B. & Bohidar, H. B. Microscopic structure of gelatin coacervates. *Int. J. Biol. Macromol.* **36**, 39–46 (2005).
40. Bryant, S. J. & Anseth, K. S. in *Scaffolding Tissue Eng.* (Ma, P. X. & Ellisseeff, J.) 1–45 (CRC Press, 2006).
41. Yoo, J. J., Bichara, D. A., Zhao, X., Randolph, M. A. & Gill, T. J. Implant-assisted meniscal repair in vivo using a chondrocyte-seeded flexible PLGA scaffold. *J. Biomed. Mater. Res. A* **99**, 102–8 (2011).
42. Byers, B. A., Mauck, R. L., Chiang, I. E. & Tuan, R. S. Transient exposure to transforming growth factor beta 3 under serum-free conditions enhances the biomechanical and biochemical maturation of tissue-engineered cartilage. *Tissue Eng. Part A* **14**, 1821–34 (2008).
43. Chua, K. H., Aminuddin, B. S., Fuzina, N. H. & Ruszymah, B. H. I. Insulin-transferrin-selenium prevent human chondrocyte dedifferentiation and promote the formation of high quality tissue engineered human hyaline cartilage. *Eur. Cell. Mater.* **9**, 58–67 (2005).
44. Farndale, R. W., Sayers, C. A. & Barrett, A. J. A direct spectrophotometric microassay for sulfated glycosaminoglycans in cartilage cultures. *Connect. Tissue Res.* **9**, 247–8 (1982).
45. Ruan, J.-L. *et al.* An Improved Cryosection Method for Polyethylene Glycol Hydrogels Used in Tissue Engineering. *Tissue Eng. Part C. Methods* **19**, 794–801 (2013).
46. Silverman, R. P., Passaretti, D., Huang, W., Randolph, M. A. & Yaremchuk, M. J. Injectable tissue-engineered cartilage using a fibrin glue polymer. *Plast. Reconstr. Surg.* **103**, 1809–1818 (1999).
47. Passaretti, D. & Silverman, R.P. Huang, W Kirchhoff, C.H. Ashiku, S. Randolph, M.A. Yaremchuk, M. J. Cultured chondrocytes produce injectable tissue-engineered cartilage in hydrogel polymer. *Tissue Eng.* **7**, 805–15 (2001).
48. Ibusuki, S. *et al.* Engineering Cartilage in a Photochemically Crosslinked Collagen Gel. *J. Knee Surg.* **22**, 72–81 (2010).
49. Gu, Y. *et al.* Chondrogenesis of myoblasts in biodegradable poly-lactide-co-glycolide scaffolds. *Mol. Med. Rep.* **7**, 1003–1009 (2013).
50. Bryant, S. J., Chowdhury, T. T., Lee, D. A., Bader, D. L. & Anseth, K. S. Crosslinking Density Influences Chondrocyte Metabolism in Dynamically Loaded Photocrosslinked Poly(ethylene glycol) Hydrogels. *Ann. Biomed. Eng.* **32**, 407–417 (2004).

51. Benton, J. A., DeForest, C. A., Vivekanandan, V. & Anseth, K. S. Photocrosslinking of gelatin macromers to synthesize porous hydrogels that promote valvular interstitial cell function. *Tissue Eng. Part A* **15**, 3221–30 (2009).
52. Skaalure, S. C., Chu, S. & Bryant, S. J. An Enzyme-Sensitive PEG Hydrogel Based on Aggrecan Catabolism for Cartilage Tissue Engineering. *Adv. Healthc. Mater.* **4**, 420–431 (2014).
53. Schultz, K. M. & Anseth, K. S. Monitoring degradation of matrix metalloproteinases-cleavable PEG hydrogels via multiple particle tracking microrheology. *Soft Matter* **9**, 1570 (2013).
54. Huey, D., Hu, J. & Athanasiou, K. Unlike Bone, Cartilage Regeneration Remains Elusive. *Science*. **6933**, 917–921 (2012).
55. Kon, E. *et al.* Matrix-assisted autologous chondrocyte transplantation for the repair of cartilage defects of the knee: systematic clinical data review and study quality analysis. *Am. J. Sports Med.* **37**, 1565–665 (2009).

7.6. CHAPTER VI

1. Sophia Fox, A. J., Bedi, A. & Rodeo, S. A. The basic science of articular cartilage: structure, composition, and function. *Sports Health* **1**, 461–8 (2009).
2. Adolphe, M. *Biological regulation of the chondrocytes*. (CRC Press, 1992).
3. Ateshian, G. A. & Hung, C. T. in *Funct. Tissue Eng.* (Guliak, F Butler, DL Goldstein, SA Mooney, D.) 46–68 (Springer-Verlag, 2003).
4. Perera, J. R., Gikas, P. D. & Bentley, G. The present state of treatments for articular cartilage defects in the knee. *Ann. R. Coll. Surg. Engl.* **94**, 381–7 (2012).
5. Kon, E. *et al.* Matrix-assisted autologous chondrocyte transplantation for the repair of cartilage defects of the knee: systematic clinical data review and study quality analysis. *Am. J. Sports Med.* **37**, 1565–665 (2009).
6. Bartlett, W. *et al.* Autologous chondrocyte implantation versus matrix-induced autologous chondrocyte implantation for osteochondral defects of the knee: a prospective, randomised study. *J. Bone Joint Surg. Br.* **87**, 640–5 (2005).
7. Behrens, P., Bitter, T., Kurz, B. & Russlies, M. Matrix-associated autologous chondrocyte transplantation/implantation (MACT/MACI)--5-year follow-up. *Knee* **13**, 194–202 (2006).

8. Zhao, W., Jin, X., Cong, Y., Liu, Y. & Fu, J. Degradable natural polymer hydrogels for articular cartilage tissue engineering. *J. Chem. Technol. Biotechnol.* **88**, 327–339 (2013).
9. Zhu, J. Bioactive modification of poly(ethylene glycol) hydrogels for tissue engineering. *Biomaterials* **31**, 4639–56 (2010).
10. Hoyle, C. E. & Bowman, C. N. Thiol-ene click chemistry. *Angew. Chem. Int. Ed. Engl.* **49**, 1540–73 (2010).
11. Fairbanks, B. D. *et al.* A Versatile Synthetic Extracellular Matrix Mimic via Thiol-Norbornene Photopolymerization. *Adv. Mater.* **21**, 5005–5010 (2009).
12. Li, T., O’Keefe, R. & Chen, D. TGF- β signaling in chondrocytes. *Front. Biosci.* 681–688 (2005).
13. Hume, P. S., He, J., Haskins, K. & Anseth, K. S. Strategies to reduce dendritic cell activation through functional biomaterial design. *Biomaterials* **33**, 3615–25 (2012).
14. McCall, J. D., Luoma, J. E. & Anseth, K. S. Covalently tethered transforming growth factor beta in PEG hydrogels promotes chondrogenic differentiation of encapsulated human mesenchymal stem cells. *Drug Deliv. Transl. Res.* **2**, 305–312 (2012).
15. Park, Y., Lutolf, M. P., Hubbell, J. A., Hunziker, E. B. & Wong, M. Bovine Primary Chondrocyte Culture in Synthetic Matrix Hydrogels as a Scaffold for Cartilage Repair. *Tissue Eng.* **10**, 515–522 (2004).
16. Roberts, J. J., Nicodemus, G. D., Greenwald, E. C. & Bryant, S. J. Degradation improves tissue formation in (un)loaded chondrocyte-laden hydrogels. *Clin. Orthop. Relat. Res.* **469**, 2725–34 (2011).
17. Nicodemus, G. D., Skaalure, S. C. & Bryant, S. J. Gel structure has an impact on pericellular and extracellular matrix deposition, which subsequently alters metabolic activities in chondrocyte-laden PEG hydrogels. *Acta Biomater.* **7**, 492–504 (2011).
18. Forsyth, C. B. *et al.* Increased matrix metalloproteinase-13 production with aging by human articular chondrocytes in response to catabolic stimuli. *J. Gerontol. A. Biol. Sci. Med. Sci.* **60**, 1118–24 (2005).
19. Lin, Z., Willers, C., Xu, J. & Zheng, M.-H. The chondrocyte: biology and clinical application. *Tissue Eng.* **12**, 1971–84 (2006).
20. Wang, C.-C. *et al.* A biomimetic honeycomb-like scaffold prepared by flow-focusing technology for cartilage regeneration. *Biotechnol. Bioeng.* **111**, 2338–48 (2014).
21. Mazaki, T. *et al.* A novel, visible light-induced, rapidly cross-linkable gelatin scaffold for osteochondral tissue engineering. *Sci. Rep.* **4**, 4457 (2014).

22. Gorgieva, S. & Kokol, V. in *Biomater. Appl. Nanomedicine* (Pignatello, R.) 17–52 (InTech, 2011).
23. Sharma, B. *et al.* Human cartilage repair with a photoreactive adhesive-hydrogel composite. *Sci. Transl. Med.* **5**, 167–173 (2013).
24. Roberts, J. J. & Bryant, S. J. Comparison of photopolymerizable thiol-ene PEG and acrylate-based PEG hydrogels for cartilage development. *Biomaterials* (2013).
25. Lin, C.-C., Raza, A. & Shih, H. PEG hydrogels formed by thiol-ene photo-click chemistry and their effect on the formation and recovery of insulin-secreting cell spheroids. *Biomaterials* **32**, 9685–95 (2011).
26. Chubinskaya, S. Chondrocyte Matrix Metalloproteinase-8. *J. Biol. Chem.* **271**, 11023–11026 (1996).
27. Liacini, A. *et al.* Induction of matrix metalloproteinase-13 gene expression by TNF- α is mediated by MAP kinases, AP-1, and NF- κ B transcription factors in articular chondrocytes. *Exp. Cell Res.* **288**, 208–217 (2003).
28. Patterson, J. & Hubbell, J. A. Enhanced proteolytic degradation of molecularly engineered PEG hydrogels in response to MMP-1 and MMP-2. *Biomaterials* **31**, 7836–45 (2010).
29. Nagase, H. & Fields, G. B. Human matrix metalloproteinase specificity studies using collagen sequence-based synthetic peptides. *Biopolymers* **40**, 399–416 (1996).
30. Nagase, H., Fields, C. & Fields, G. Design and characterization of a fluorogenic substrate selectively hydrolyzed by stromelysin 1 (matrix metalloproteinase-3). *J. Biol. Chem.* **269**, 20952–20957 (1994).
31. Wu, L., Prins, H.-J., Helder, M. N., van Blitterswijk, C. A. & Karperien, M. Trophic effects of mesenchymal stem cells in chondrocyte co-cultures are independent of culture conditions and cell sources. *Tissue Eng. Part A* **18**, 1542–51 (2012).
32. Koga, H., Engebretsen, L., Brinchmann, J. E., Muneta, T. & Sekiya, I. Mesenchymal stem cell-based therapy for cartilage repair: a review. *Knee Surg. Sports Traumatol. Arthrosc.* **17**, 1289–97 (2009).
33. Steck, E. *et al.* Induction of intervertebral disc-like cells from adult mesenchymal stem cells. *Stem Cells* **23**, 403–11 (2005).
34. Knudson, C. B. & Knudson, W. Cartilage proteoglycans. *Semin. Cell Dev. Biol.* **12**, 69–78 (2001).

35. Mok, S. S., Masuda, K., Hauselmann, H. J., Aydelotte, M. B. & Thonar, E. J. M. A. Aggrecan Synthesized by Mature Bovine Chondrocytes Suspended in Alginate associated matrix and the further removed matrix. *J. Biol. Chem.* **269**, 33021–33027 (1994).
36. Skaalure, S. C., Chu, S. & Bryant, S. J. An Enzyme-Sensitive PEG Hydrogel Based on Aggrecan Catabolism for Cartilage Tissue Engineering. *Adv. Healthc. Mater.* (2014). doi:10.1002/adhm.201400277
37. Ilic, M. Z., Handley, C. J., Robinson, H. C. & Mok, M. T. Mechanism of catabolism of aggrecan by articular cartilage. *Arch. Biochem. Biophys.* **294**, 115–122 (1992).
38. Yamane, S. *et al.* Feasibility of chitosan-based hyaluronic acid hybrid biomaterial for a novel scaffold in cartilage tissue engineering. *Biomaterials* **26**, 611–9 (2005).
39. Kim, I. L., Mauck, R. L. & Burdick, J. A. Hydrogel design for cartilage tissue engineering: a case study with hyaluronic acid. *Biomaterials* **32**, 8771–82 (2011).
40. Chung, C., Beecham, M., Mauck, R. L. & Burdick, J. A. The influence of degradation characteristics of hyaluronic acid hydrogels on in vitro neocartilage formation by mesenchymal stem cells. *Biomaterials* **30**, 4287–96 (2009).
41. Inui, A., Iwakura, T. & Reddi, A. H. Human Stem Cells and Articular Cartilage Regeneration. *Cell* **1**, 994–1009 (2012).
42. Dreier, R., Wallace, S., Fuchs, S., Bruckner, P. & Grassel, S. Paracrine interactions of chondrocytes and macrophages in cartilage degradation: articular chondrocytes provide factors that activate macrophage-derived pro-gelatinase B (pro-MMP-9). *J. Cell Sci.* **114**, 3813–3822 (2001).
43. Deng, G., Tang, C., Li, F., Jiang, H. & Chen, Y. Covalent Cross-Linked Polymer Gels with Reversible Sol–Gel Transition and Self-Healing Properties. *Macromolecules* **43**, 1191–1194 (2010).
44. McKinnon, D. D., Domaille, D. W., Cha, J. N. & Anseth, K. S. Biophysically Defined and Cytocompatible Covalently Adaptable Networks as Viscoelastic 3D Cell Culture Systems. *Adv. Mater.* 1–8 (2013).
45. Liu, F. *et al.* Rheological Images of Dynamic Covalent Polymer Networks and Mechanisms behind Mechanical and Self-Healing Properties. *Macromolecules* **45**, 1636–1645 (2012).
46. Bassi, A. M., Penco, S., Canuto, R. A., Muzio, G. & Ferro, M. Comparative evaluation of cytotoxicity and metabolism of four aldehydes in two hepatoma cell lines. *Drug Chem. Toxicol.* **20**, 173–87 (1997).

47. Barbero, A. *et al.* Age related changes in human articular chondrocyte yield, proliferation and post-expansion chondrogenic capacity. *Osteoarthr. Cartil.* **12**, 476–84 (2004).
48. Yu, J. *et al.* Induced pluripotent stem cell lines derived from human somatic cells. *Science* (80-.). **318**, 1917–20 (2007).
49. Diekman, B. O. *et al.* Cartilage tissue engineering using differentiated and purified induced pluripotent stem cells. *Proc. Natl. Acad. Sci.* **109**, (2012).
50. Wei, Y. *et al.* Chondrogenic differentiation of induced pluripotent stem cells from osteoarthritic chondrocytes in alginate matrix. *Eur. Cell. Mater.* **23**, 1–12 (2012).
51. Saha, S., Kirkham, J., Wood, D., Curran, S. & Yang, X. Comparative study of the chondrogenic potential of human bone marrow stromal cells, neonatal chondrocytes and adult chondrocytes. *Biochem. Biophys. Res. Commun.* **401**, 333–8 (2010).
52. Lai, J. H., Kajiya, G., Smith, R. L., Maloney, W. & Yang, F. Stem cells catalyze cartilage formation by neonatal articular chondrocytes in 3D biomimetic hydrogels. *Sci. Rep.* **3**, 1–9 (2013).
53. Silverman, R. P., Passaretti, D., Huang, W., Randolph, M. A. & Yaremchuk, M. J. Injectable tissue-engineered cartilage using a fibrin glue polymer. *Plast. Reconstr. Surg.* **103**, 1809–1818 (1999).
54. Li, W.-J. *et al.* Evaluation of articular cartilage repair using biodegradable nanofibrous scaffolds in a swine model: a pilot study. *J. Tissue Eng. Regen. Med.* **3**, 1–10 (2009).
55. Peretti, G. M. *et al.* Review of injectable cartilage engineering using fibrin gel in mice and swine models. *Tissue Eng.* **12**, 1151–68 (2006).
56. Bryant, S. J., Bender, R. J., Durand, K. L. & Anseth, K. S. Encapsulating chondrocytes in degrading PEG hydrogels with high modulus: engineering gel structural changes to facilitate cartilaginous tissue production. *Biotechnol. Bioeng.* **86**, 747–55 (2004).
57. Silverman, R. P., Bonassar, L. J., Passaretti, D., Randolph, M. A. & Yaremchuk, M. J. Adhesion of tissue-engineered cartilage to native cartilage. *Plast. Reconstr. Surg.* **105**, 1393–1398 (2000).